

Receptor concentration affects glucocorticoid action

by
Steven Ernest Robertson

*Dissertation presented for the degree of Doctor of Biochemistry
at the
University of Stellenbosch*



Promoter: Prof. Ann Louw
Co-promoter: Prof. Janet Hapgood
Faculty of Science
Department of Biochemistry

March 2011

Declaration

By submitting this dissertation electronically, I declare that the entirety of the work contained therein is my own, original work, that I am the sole author thereof (save to the extent explicitly stated), that reproduction and publication thereof by Stellenbosch University will not infringe any third party rights and that I have not previously in its entirety or in part submitted it for obtaining any qualification.

March 2011

Abstract

Glucocorticoid receptor (GR) levels, which modulate the response to glucocorticoids (GCs), vary between tissues and individuals and are altered by physiological and pharmacological effectors. In this study we set out to investigate the effects and implications of differences in GR concentration. Firstly, we established conditions that resulted in three statistically different GR populations in transiently transfected COS-1 cells. We demonstrated, using whole cell saturation ligand binding experiments, that high levels of wild type GR, but not of dimerization deficient GR, exhibited positive cooperative ligand binding with a concomitant increased ligand binding affinity. Furthermore, we established, through co-immunoprecipitation and fluorescent resonance energy transfer, that ligand independent dimerization correlates with positive cooperative ligand binding. This is the first time that positive cooperative ligand binding and increased ligand binding affinity have been explicitly correlated and linked to increased ligand independent dimerization of the GR. The downstream consequences of variation in GR concentration and dimerization included modulation of GR import and export rates, as investigated through live cell as well as immunofluorescent analysis. Furthermore, the nuclear distribution of GR was also influenced by GR dimerization. The major function of the GR is as a transcription factor, which mediates the response to GCs via activation or repression of genes. We have revealed direct influences of GR concentration and dimerization in a number of promoter reporter assays as well as in the transactivation of an endogenous gene. Specifically, cooperative ligand binding was found to be responsible for the GR level dependent potency shift in transrepression of an NF κ B containing promoter reporter construct via dexamethasone and the shift in the bio-character of Compound A, a dissociative GR agonist. Transactivation potency of dexamethasone as well as the partial agonist bio-character of medroxyprogesterone and mifepristone via a multiple GRE containing promoter reporter construct were influenced directly by cooperative ligand binding. Dimerization of the GR was shown to be crucial for ligand dependent transactivation of a single GRE containing promoter reporter construct, while ligand independent transactivation of both single and multiple GRE containing constructs was significantly increased due to an increase in GR concentration. The endogenous GC responsive glucocorticoid induced leucine zipper (GILZ) gene demonstrated significant ligand independent transactivation at GR levels, which displayed ligand independent dimerization. An increase in GR concentration resulted in an increase in efficacy through all promoter reporter constructs as well as the endogenous GILZ gene. Positive cooperative binding and the concomitant increase in ligand binding affinity to the GR at high levels may be a crucial factor in determining both the efficacy and potency of the GC response. Considering the significant differences in GR concentrations expressed by different tissues and by individuals within the same tissue, our findings may explain the interindividual as well as tissue specific responses to GC treatment and suggest an

important mechanism of action through which the GR is primed to respond to subsaturating GC concentrations and displays a significant level of ligand independent activity.

Opsomming

Glukokortikoïed reseptor (GR) vlakke, wat die gedrag van glukokortikoïede (GCs) moduleer, wissel tussen weefsels en onder individue en word verander deur fisiologiese en farmakologiese effekte. In hierdie studie ondersoek ons die gevolge en implikasies van verskille in GR konsentrasie. Eerstens het ons die kondisies vasgestel wat benodig word om drie statisties verskillende GR populasies te vestig in kortstondige getransfekteerde COS-1 selle. Ons het getoon, met behulp van die heel sel versadigings ligand bindings eksperimente, dat hoë vlakke van wilde-tipe GR, maar nie van dimeriserings gebrekkige GR, positiewe koöperatiewe ligand binding, met 'n gepaardgaande toename in ligand bindings affiniteit, toon. Verder het ons bevestig, deur ko-immunopresipitasie en fluoressente resonansie energie-oordrag, dat ligand onafhanklike dimerisering korreleer met positiewe koöperatiewe ligand binding. Dit is die eerste keer dat positiewe koöperatiewe ligand binding en verhoogde ligand bindings affiniteit uitdruklik gekorreleer en gekoppel word aan verhoogde ligand onafhanklike dimerisering van die GR. Die daarop nagevolge van variasie in GR konsentrasie en dimerisering sluit in modulasie van die invoer en uitvoer tempo van die GR, soos ondersoek deur lewendige sel sowel as immunofluorescente analise. Verder is die verspreiding van die GR in die kern ook beïnvloed deur GR dimerisering. Die belangrikste funksie van die GR is as 'n transkripsie faktor, wat die respons van GCS bemiddel via aktivering of onderdrukking van gene. Ons het die direkte invloed van GR konsentrasie en dimerisering in 'n aantal promotor verslaggewer essays sowel as in die transaktivering van 'n endogene gene onthul. Spesifiek, is gevind dat koöperatiewe ligand binding verantwoordelik is vir die GR vlak afhanklike verskuiwing in transrepressie potensie van 'n NFκB bevattende promotor verslaggewer konstruk via deksametasoon en die verskuiwing van die bio-karakter van verbinding A, 'n dissosiatiewe GR agonis. Transaktiverings potensie van deksametasoon, asook die gedeeltelike agonis bio-karakter van medroksie-progesteron en mifepristoon, via 'n veelvoudige GRE bevattende promotor verslaggewer konstruk is direk beïnvloed deur koöperatiewe ligand binding. Dimerisering van die GR is getoon om deurslaggewend vir ligand afhanklike transaktivering van 'n enkele GRE bevattende promotor verslaggewer konstruk te wees, terwyl ligand onafhanklike transaktivering van beide enkel-en veelvoudige GRE bevattende konstrunkte aansienlik toegeneem het as gevolg van 'n toename in GR konsentrasie. Die endogene GC responsiewe glukokortikoïed geïnduseerde leusien rits (GILZ) gene het beduidende ligand onafhanklike transaktivering gedemonstreer op GR vlakke wat ligand onafhanklike dimerisering toon. 'n toename in GR konsentrasie het gelei tot 'n toename in die effektiwiteit van al die promotor verslaggewer konstrunkte, sowel as die endogene GILZ gene. Positiewe koöperatiewe ligand binding en die gepaardgaande toename in ligand bindings affiniteit van die GR by hoë vlakke kan 'n belangrike faktor wees in die bepaling van sowel die effektiwiteit as die potensie van die GC respons.

As die aansienlike verskille in GR konsentrasies van verskillende weefsels en tussen verskillende individue in dieselfde weefsel in ag geneem word, kan ons bevindings die inter-individuele sowel as weefsel spesifieke response op GC behandeling verduidelik en stel dit 'n belangrike meganisme van aksie voor waardeur die GR voorberei word om op sub-versadigings konsentrasies van GC te reageer deur 'n beduidende vlak van ligand onafhanklike aktiwiteit te toon.

Acknowledgements

Scientific research does not take place in a vacuum and I am indebted to the many individuals whose research has formed the foundation of my own. I feel that the pursuit of understanding is an altruistic act, which is best carried out in a moral and egoless fashion. In that vain I would like to personally thank a number of individuals whose support and collaboration have contributed greatly to this project.

Prof. Johann Rohwer, what started as an enlightened observation was followed through with consummate skill. I am extremely grateful for your assistance in creating the mathematic model based on our FRET data as well as the two-state GR dimerization model which appears in the discussion. Your willingness to collaborate is inspiring.

Prof. Janet Hapgood, thank-you for the constructive critique and for expressing your confidence in me and my research. It is much appreciated.

Dr. Ben Loos for excellent technical assistance, delivered in a consistently courteous and efficient manner. It has been a pleasure working with you.

Carmen Langeveld, who week in and week out delivered world class tissue culture maintenance and administration of our laboratory. Your contribution to every experiment in this document was crucial and greatly appreciated.

Billy Robertson, thanks to you I have been able to focus myself completely on this task. You have lifted the burden of worry from my shoulders time and time again. You are the root of my ambition and it is my privilege to call you my father.

Prof. Ann Louw, I could not have asked for a more proficient and challenging supervisor. I have always admired you as a scientist and as an individual. It is because of this respect that I have found it possible to lay my ego aside and will myself towards achieving your expectations. In the spirit of accuracy, which you have instilled in me, I wholly acknowledge the instrumental role you have played in this doctorate and in my own development.

National Research Foundation, for funding over the time period 2005-2009, which fell under the project FA2005040500031.

Abbreviations

11 β -HSD2	11 β -hydroxysteroid dehydrogenase type 2
11 β -HSD	11 β -hydroxysteroid dehydrogenase type 1
ACTH	adrenocorticotrophic hormone
AF1	activation function 1
AIDS	acquired immune deficiency syndrome
ANOVA	one way analysis of variance
AP-1	activator protein-1
AR	androgen receptor
CBG	corticosteroid-binding globulin
CFP	cyan fluorescent protein
CNS	central nervous system
CpdA	Compound A
CRH	corticotrophin-releasing hormone
Cyp40	cyclosporine A-binding protein
D-loop	dimerization loop
DAC	deacylcortivazol
DBD	DNA binding domain
DEX	dexamethasone
Dex-Mes	dexamethasone-21-mesylate
DR	dietary restriction
E	efficiency
ER	estrogen receptor
ERE	estrogen response element
F	cortisol
FHDC	first-order Hill dose-response curve
FKBP51	FK506 binding protein 51
FKBP52	FK506-binding protein 52
FRET	fluorescent resonance energy transfer
GC	glucocorticoid
GFP-GR	green fluorescent protein-glucocorticoid receptor
GILZ	glucocorticoid induced zipper
GR	glucocorticoid receptor
GRE	glucocorticoid response element

GRIP	glucocorticoid receptor-interacting protein
HPA	hypothalamic-pituitary-adrenal
HRE	hormone response element
HSP	heat shock protein
I κ B	inhibitory protein κ B
K	lysine
L	leucine
LBD	ligand binding domain
M	methionine
MMTV	mouse mammary tumour virus
MPA	medroxyprogesterone
MR	mineralocorticoid receptor
NCoR	nuclear receptor corepressor
NF κ B	nuclear factor- κ B
nGRE	negative glucocorticoid response element
NL1	nuclear localization 1
NLS	nuclear localization signal
NR	nuclear receptor
NRS	nuclear retention signal
PBMC	peripheral blood mononuclear cells
Pgp	P-glycoprotein
PNMT	phenylethanolamine <i>N</i> -methyltransferase
PP5	protein phosphatase 5
PR	progesterone receptor
Prog	progesterone
R	arginine
ROI	region of interest
RU486	mifepristone
SMRT	silencing mediator of retinoid and thyroid hormone receptor
SRC	p160 steroid receptor coactivators
STAT5	signal transduction and activation of transcription-5
SUMO-1	small ubiquitin-related modifier-1
$t_{1/2}$	half-time
TAT	tyrosine amino transferase
TIF2	transcription intermediary factor 2
TNF- α	cytokine tumour necrosis factor- α

TPR	tertratricopeptide repeat domain protein
TSS	transcription start site
Ubc9	ubiquitin-conjugating enzyme 9
YFP	yellow fluorescent protein

Table of contents

Chapter 1

Literature review.....	1
1.1 Glucocorticoids.....	2
1.1.1 Endogenous glucocorticoids are secreted in a circadian and ultradian pattern	
1.1.2 Synthetic glucocorticoids are administered at a single dosage	
1.1.3 Pharmacological uses of glucocorticoids	
1.2 The glucocorticoid receptor.....	9
1.2.1 Overview of the mechanism of glucocorticoid receptor action	
1.2.1.1 Ligand binding and nuclear import	
1.2.1.2 Ligand induced dimerization of the glucocorticoid receptor	
1.2.1.3 How the glucocorticoid receptor functions as a transcription factor	
1.2.1.4 Degradation or nuclear export	
1.2.2 Glucocorticoid receptor functional domains	
1.3 Overview of factors that modulate glucocorticoid response.....	16
1.3.1 Ligand availability	
1.3.2 Glucocorticoid receptor concentration	
1.3.3 Varying glucocorticoid receptor isoforms, polymorphisms and post translational modification	
1.3.4 Coregulating and comodulating factors	
1.3.4.1 Coactivators	
1.3.4.2 Corepressors	
1.3.4.3 Comodulators	
1.4 Physiological glucocorticoid receptor concentrations.....	26
1.4.1 Increased glucocorticoid receptor concentrations	
1.4.2 Decreased glucocorticoid receptor concentrations	
1.5 The cellular affects of glucocorticoid receptor concentration.....	28
1.5.1 Ligand binding affinity and positive cooperative ligand binding	
1.5.2 Nuclear mobility	
1.5.3 Transcription by the glucocorticoid receptor	
1.6 Dimerization of the glucocorticoid receptor	32
1.6.1 Homodimerization and heterodimerization of the glucocorticoid receptor	
1.6.2 The D-loop and ligand binding domain	
1.6.3 Dimerization deficient glucocorticoid receptor	
1.6.4 CpdA abrogates dimerization	

1.7 Summary, hypothesis and aims.....	36
1.7.1 Summary	
1.7.2 Hypothesis	
1.7.3 Aims	
1.8 Bibliography.....	40
Chapter 2	
Materials, methods and model.....	57
2.1 Materials and methods.....	58
2.1.1 Reagents	
2.1.2 Plasmids	
2.1.3 Cell culture and DEAE-dextran transfection	
2.1.4 Whole cell binding to determine the expression levels of the GR plasmids	
2.1.5 Time course to ligand binding equilibrium	
2.1.6 Whole cell saturation binding	
2.1.7 Competitive whole cell binding.	
2.1.8 Co-immunoprecipitation (Co-IP)	
2.1.9 Fluorescence resonance energy transfer (FRET)	
2.1.10 Live cell nuclear import	
2.1.11 Live cell nuclear export	
2.1.12 Nuclear distribution	
2.1.13 Immunofluorescent analysis of nuclear import	
2.1.14 Immunofluorescent analysis of nuclear export	
2.1.15 β -Galactosidase assay	
2.1.16 Promoter reporter transactivation assays	
2.1.17 Promoter reporter transrepression assays	
2.1.18 Real time PCR quantification of endogenous gene expression	
2.1.19 Converting Bmax to mol GR/cell, GR/cell and M GR	
2.1.20 Statistical analysis	
2.2 Mathematical model to calculate percentage monomers from FRET data.....	68
2.3 Bibliography.....	70
Chapter 3	
Results: Positive cooperative ligand binding and increased ligand binding affinity at high glucocorticoid receptor wild type concentrations	72

3.1 Establishing a viable model in which to compare the effects of glucocorticoid receptor concentrations.....	76
3.2 Saturation binding was used to designate low, medium and high glucocorticoid receptor concentrations.....	80
3.3 Positive cooperative ligand binding is glucocorticoid receptor concentration and dimerization dependent.....	83
3.4 Bibliography.....	86

Chapter 4

Results: Ligand independent dimerization of the glucocorticoid receptor	89
4.1 Demonstrating ligand independent dimerization using Co-IP.....	91
4.1.1 Co-IP studies show GFP-GR pull down independent of stimulation which increases as GRwt levels do.	
4.1.2 DEX increases dimerization at the low GRwt concentration while CpdA addition abrogates dimerization at the medium and high GRwt concentrations	
4.2 Demonstrating ligand independent dimerization using FRET.....	97
4.2.1 Ligand independent dimerization of the GR occurs in the cytoplasm at high GR concentrations	
4.2.2 The fold induction of DEX induced maximal FRET decreases as GR levels increase	
4.3 Bibliography.....	105

Chapter 5

Results: The influence of dimerization on glucocorticoid receptor nuclear import, export and distribution.....	107
5.1 Nuclear import of the glucocorticoid receptor.....	109
5.1.1 The $t_{1/2}$ of live cell nuclear import of GFP-GR decreases as receptor concentrations increase.	
5.1.2 The ability to dimerize influences both maximal nuclear localization as well as the $t_{1/2}$ of nuclear import in immunofluorescent nuclear import assays	
5.2 Nuclear distribution is ligand as well as dimerization dependent.....	116
5.3 Nuclear export of the glucocorticoid receptor.....	119
5.3.1 The $t_{1/2}$ of live cell nuclear export is dimerization dependent	
5.3.2 Increased ligand binding affinity of the medium GRwt concentration results in protracted nuclear retention following the washout of 10^{-6} M DEX	
5.4 Overview of Chapter 5 results.....	125
5.5 Bibliography.....	127

Chapter 6

Results: Transactivation and transrepression of genes is influenced by positive cooperative ligand binding to the glucocorticoid receptor.....	130
6.1 Establishing promoter reporter assay conditions.....	134
6.2 Transrepression of a NFκB containing promoter reporter construct is influenced by cooperative ligand binding to the GR.....	136
6.2.1 Potency of transrepression	
6.2.2 Efficacy of transrepression	
6.2.3 Biocharacter shift of CpdA	
6.3 Transactivation of GRE containing promoter reporters is influenced by ligand independent dimerization as well as the dimerization status of the GR.....	144
6.3.1 Potency of transactivation	
6.3.2 Ligand independent transactivation	
6.3.3 Efficacy, fold induction and biocharacter shift	
6.4 Transactivation of the endogenous GILZ gene.....	162
6.4.1 Ligand independent transactivation of GILZ	
6.4.2 Efficacy of GILZ transactivation	
6.4.2.1 Maximal induction	
6.4.2.2 Fold induction	
6.4.3 Summary of endogenous GILZ transactivation	
6.5 Bibliography.....	168

Chapter 7

Discussion.....	174
7.1 Dimerization generates functional diversity.....	175
7.2 Overview of results.....	177
7.2.1 Chapter 3: Ligand binding affinity increases and cooperative ligand binding occurs at medium and high GRwt concentrations (Table.7.1)	
7.2.2 Chapter 4: Ligand independent dimerization occurs at GR concentrations that display positive cooperative ligand binding (Table.7.1)	
7.2.3 Chapter 5: Nuclear import, export and distribution are influenced by GR dimerization (Table.7.1)	
7.2.4 Chapter 6: Transactivation and transrepression of genes is influenced by positive cooperative ligand binding to the GR (Table.7.2)	

7.3 Implications of positive cooperative ligand binding and enhanced ligand binding affinity at high GR concentrations.....	185
7.3.1 Molecular	
7.3.2 Cellular	
7.3.3 Physiological	
7.4 Future research.....	190
7.4.1 GR dimerization	
7.4.2 Cooperative ligand binding and increased ligand binding affinity	
7.4.3 CpdA	
7.5 Bibliography.....	192
Addendum A	
Abstracts from talks.....	196
Addendum B	
Abrogation of glucocorticoid receptor dimerization correlates with dissociated glucocorticoid behaviour of Compound A. S. Robertson <i>et al.</i>	200

Chapter 1

Literature Review

Introduction

We aim to introduce the reader to the relevance of glucocorticoid receptor (GR) concentration and homodimerization at a physiological and cellular level. This is preceded by a brief discussion of the regulation and secretion of endogenous glucocorticoids (GCs) and the pharmacological administration and uses of exogenous GCs. An overview of the mechanism of GR action will then be presented followed by an overview of the major factors which modulate the response to GCs. Having set the scene, we will analyze the two focal topics of this literature review, namely the effects of GR concentration and homodimerization. Finally we will conclude with our hypothesis and aims.

1.1 Glucocorticoids

In a practical demonstration of nomenclature the name glucocorticoid is derived from a few key features of this class of steroid hormone. Namely, the role they play in the regulation of **glucose** metabolism, the fact that they are synthesized endogenously in the adrenal **cortex** and their **steroidal** structure. GCs are pleiotropic and affect diverse cellular processes including homeostasis, cell growth, development, metabolism, stress response and inflammation. Physiological trauma including inflammation, pain, infection or even mental stress, leads to the activation of the hypothalamic-pituitary-adrenal (HPA) axis. This excitation of the hypothalamus causes it to secrete corticotrophin-releasing hormone (CRH), which acts on the anterior pituitary inducing the synthesis and release of adrenocorticotrophic hormone (ACTH). ACTH in turn stimulates the adrenal cortex to release GC's, such as cortisol in humans, which is synthesized in a stepwise fashion from cholesterol by cytochrome P450-catalyzed reactions.

The HPA axis tightly regulates the synthesis and secretion of GCs by the adrenal cortex and is sensitive to negative feedback by circulating hormones and exogenous GCs (1). The majority of secreted cortisol, 90 percent, is bound to corticosteroid-binding globulin (CBG), a high affinity plasma transport glycoprotein in the blood (2-5). Either free or bound GCs are transported in the blood to the target organs. At target organs, free GCs, due to their highly lipophilic nature, readily diffuse across the cell membrane where they elicit their effects, primarily through the GR (6).

Generally, a GR agonist is defined as a compound which mimics the endogenous ligand and is capable of transcriptional regulation, both transactivation as well as transrepression of genes. In contrast a GR antagonist binds to the GR but is transcriptionally inactive, essentially blocking the GR from activation by agonists (7). The majority of GCs, whether endogenous or exogenous, synthetic or natural, share a similar steroidal structure (Fig.1.1A,B). The structure of synthetic GCs such as

dexamethasone (DEX) mimic that of cortisol, the endogenous GC in humans (Fig.1.1A,B). However, exceptions do exist such as the dissociative GC, Compound A (CpdA) (8) (Fig1.1C). There is considerable variation in the behaviour of GCs, their ability to bind the GR, their capacity to induce dimerization of the GR (Addendum B) (9), the degree of nuclear import, export and nuclear distribution they induce (10, 11) and the degree to which they transactivate or transrepress genes (7).

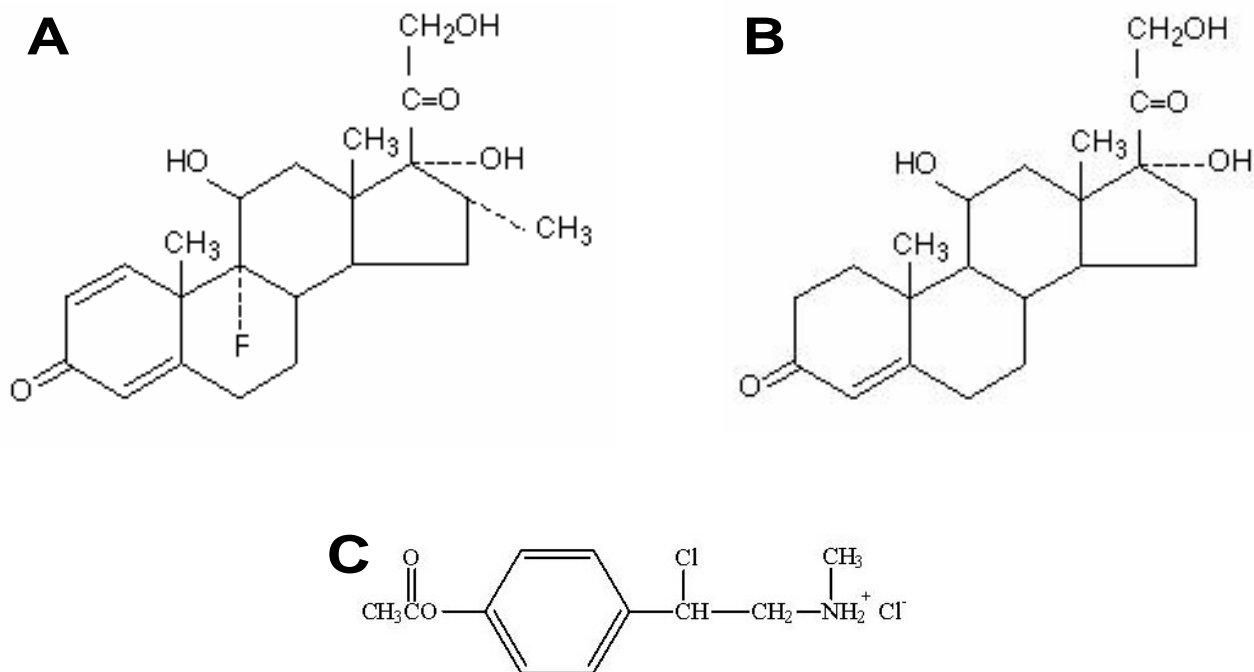


Figure 1.1. **Molecular structure of GCs.** (A) The steroidal synthetic GR agonist, dexamethasone, (B) the endogenous GC agonist, cortisol, and (C) the non-steroidal dissociative synthetic GC, Compound A.

1.1.1 Endogenous glucocorticoids are secreted in a circadian and ultradian pattern

The average non-stressed individual secretes 10 to 20 mg of cortisol daily (1). Cortisol is released in a circadian cycle which is governed by the secretion of ACTH (12) (Fig.1.2). Levels of free serum cortisol, not bound to the high affinity plasma transport glycoprotein, CBG, or the low affinity plasma transport protein, albumin, average 11.0nM daily, peaking at ~18.7nM in the morning and dropping to ~3.3nM at night (13).

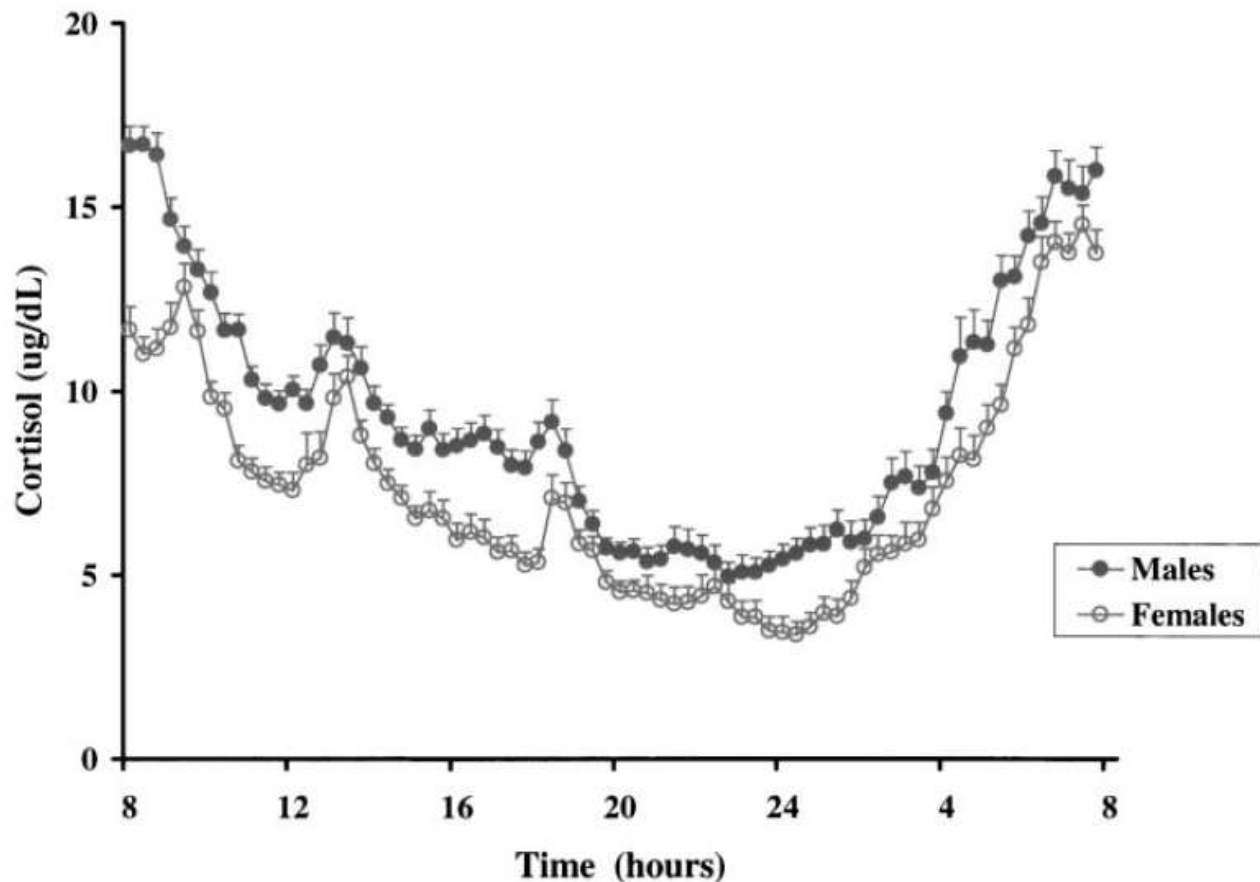


Figure 1.2. **Circadian pattern of total serum cortisol concentration in humans.** Mean total serum cortisol levels ($\mu\text{g/dL}$) in non-stressed male and female humans. (from Charmandari *et al.* (13)).

Although ACTH secretion follows a circadian pattern, which induces a concomitant circadian secretion of cortisol (Fig.1.2), the release of ACTH is not gradual but pulsatile resulting in an ultradian (hourly) pattern of hormone release into the blood stream in both humans and rodents (14),(15, 16) (Fig.1.3). The majority of studies conducted on the pulsatile nature of endogenous GC secretion have been conducted on laboratory rats and mice. We have redrawn a figure from Windle *et al.* (15), which demonstrates this behaviour (Fig.1.3). It is important to note that corticosterone is the primary endogenous GC secreted by rodents, the analog of cortisol in humans. Further more these rodents are nocturnal and their circadian cycle of corticosterone secretion is therefore the inverse of that displayed by humans, peaking at night and dropping to its minimum during the day (Fig.1.3).

Stavreva *et al.* (17) demonstrated that the ultradian cycle of corticosterone release in freely moving rats results in waves of GR activation and transcription followed by GR recycling through the transcription machinery and priming for future reactivation. This form of hormone stimulation is referred to as gene pulsing and is the primary mechanism through which GC exert their basal function endogenously (18).

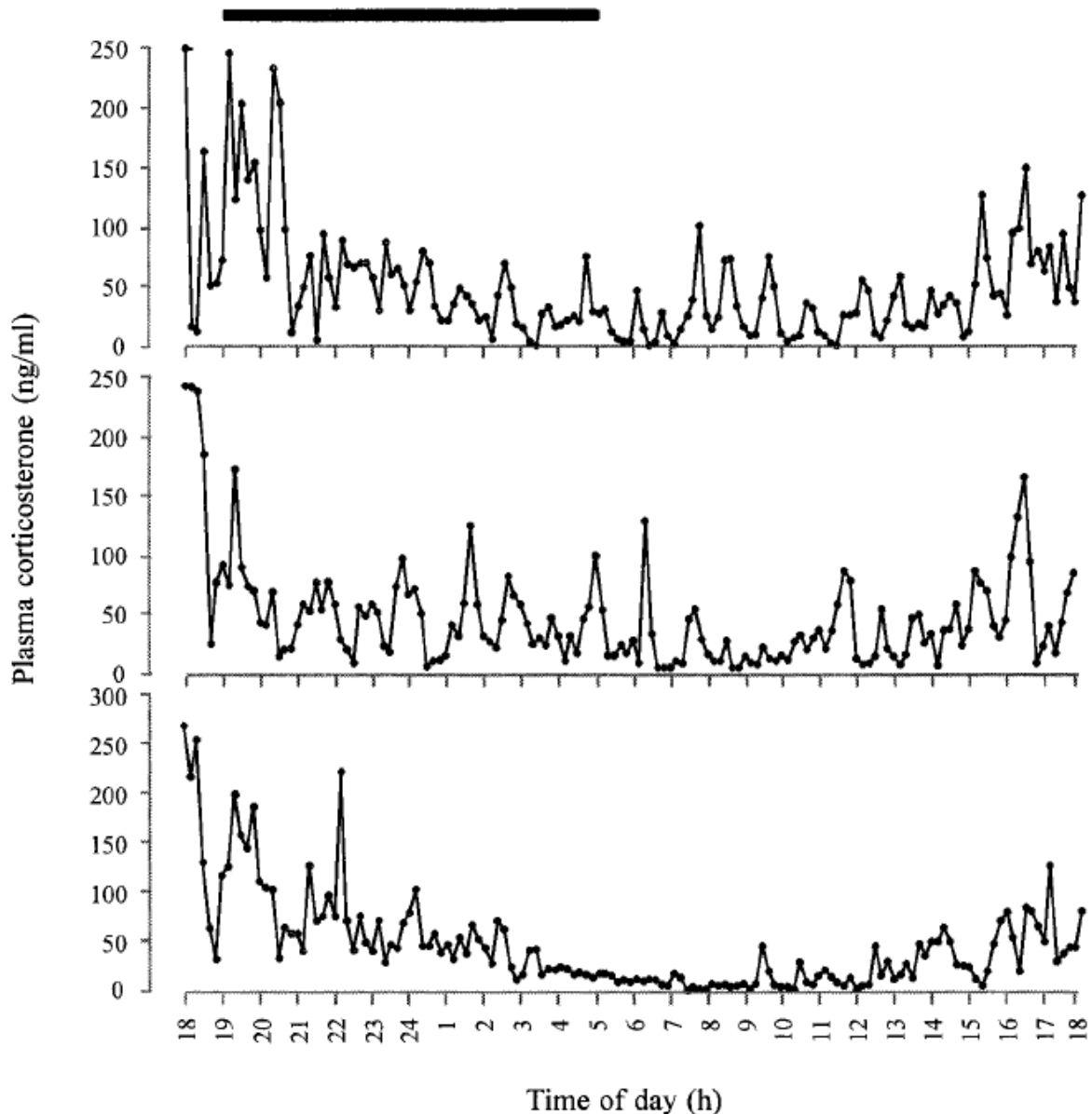


Figure 1.3. **Total plasma corticosterone concentrations of three non-stressed Sprague-Dawley rats.** Blood samples were taken every 10 minutes over a 24 hour period and analyzed for total corticosterone concentration. The 10 hour dark phase of the 24 hour cycle is indicated by the filled bar (from Windle *et al.* (15)).

The transient stress of a 114 decibel noise for 10 minutes caused a significant increase in total corticosterone plasma concentration from 29ng per ml corticosterone in non-stressed rats to a peak of 377ng per ml in stressed rats (Fig.1.4) (15). The maximal response to noise stress was 20 minutes after the initiation of the stress and corticosterone levels decreased to basal levels with in 40 to 50 minutes. This stress response, reflected in the post stress corticosterone peak, resulted in a significantly extended interpeak period from 51 minutes in non-stressed rats to 95 minutes in post stressed rats.

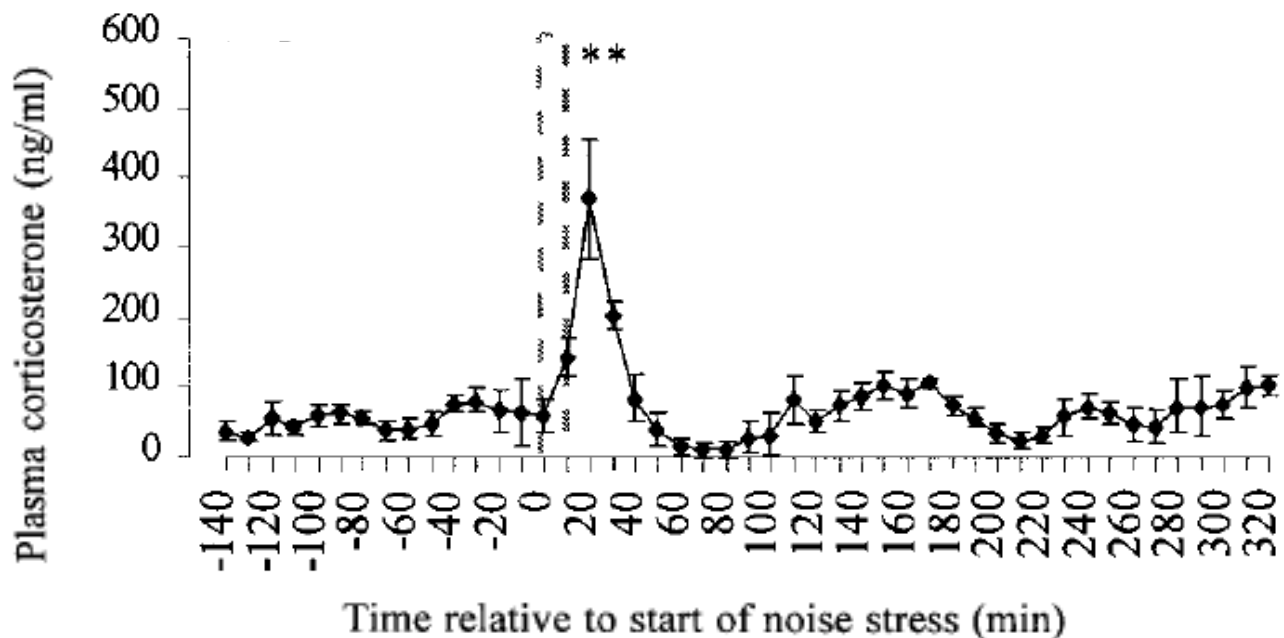


Figure 1.4. **Total plasma corticosterone concentrations of stressed Sprague-Dawley rats.** Noise stress of 114 decibels was administered at 08:20h for 10 minutes and is indicated by the horizontal dashed line bar. Blood samples were taken every 10 minutes before and after the noise stress and analyzed for total corticosterone concentration (\pm SEM, $n=6$) (from Windle *et al.* (15)).

Prolonged stress results in continuously elevated cortisol levels (19, 20). Sarabadjitsingh *et al.* (21) elucidated the effects of prolonged GC exposure on rats implanted with corticosterone releasing pellets. They demonstrated that prolonged exposure to GCs results in significantly decreased levels of GR protein expression in the hippocampal area of the brain. As rats implanted with the corticosterone releasing pellets showed an inability to respond to chronic stress, it was concluded that the pulsatile nature of endogenous GC secretion in non-stressed animals was necessary for the maintenance of the stress response.

1.1.2 Synthetic glucocorticoids are administered at a single dosage

Unlike the daily circadian and hourly pulsatile nature of endogenous GC secretion, synthetic GCs are generally administered once or twice daily, typically in 1 to 2mg daily dosages (22). Following an oral dosage of 1.5mg of DEX, the plasma concentration of the exogenous GC drops from 38nM to 1nM within 24 hours (23). Chriguet *et al.* (24) demonstrated a similar result where subjects exposed to a 1 mg oral dosage of DEX showed plasma DEX levels from 1 to 10 nM, 24 hours after administration. Although the levels of exogenous GC are often lower than those of the endogenous hormones, they are generally more potent due to greater ligand binding affinity (7) and the fact that they display

greater bioavailability. Synthetic GCs, unlike endogenous GCs, are preferentially bound to low affinity albumin and not high affinity CBG in plasma (1), thus increasing their bioavailable component.

As discussed previously, the ultradian cycles of endogenous GC secretion result in the hourly withdrawal of GC stimulation, which leads to the rapid dissociation of GR from DNA, occurring within 10 minutes (18). However, rapid response to ligand withdrawal is only possible through the relatively low affinity endogenous ligands. In the system used by McNally *et al.* (18), the potent synthetic agonist DEX leads to GR association with glucocorticoid response element (GRE) containing promoter arrays, which did not dissociate even after ligand withdrawal, leading to sustained target gene expression (18). Thus, the high affinity of synthetic GCs leads to continuous stimulation of the GR and has been linked to numerous side effects (18). For example, the administration of 0.5mg of the exogenous GC, DEX, leads to negative feed back on the HPA axis, essentially shutting down the secretion of endogenous cortisol secretion within 8 hours of ingestion (25). Thus the long term effects of GC treatment are insidious, leading to, amongst other effects, GR down regulation which in turn may result in GC resistance (26).

1.1.3 Pharmacological uses of glucocorticoids

The ability of GCs to suppress the immune system is of primary interest pharmacologically and has led to GCs becoming the most widely used anti-inflammatory drugs world wide (27). Numerous synthetic GCs are in use, for example, betamethasone, cortisone, DEX, fluprednisone, hydrocortisone, meprednisone, paramethasone and prednisolone. Most of these anti-inflammatory drugs have a chemical structure, which is based on that of the endogenous GC, cortisol (Fig.1.1A,B). Their clinical efficacy stems from their ability to mimic natural GCs in suppressing inflammation and as a result they are administered for the treatment of inflammation and autoimmune diseases such as asthma, inflammatory bowel diseases, systemic lupus erythematosus, sarcoidosis, nephritic syndrome and rheumatoid arthritis (27). GCs also play a role in apoptosis and have as a result found a role in chemotherapeutic regimens (28), while their ability to suppress the immune system means they are commonly administered to transplant patients to reduce the risk of rejection (29).

The secretion of endogenous GCs during times of stress facilitates the 'fight or flight' response, where glucose is mobilized as a readily available source of energy and non-essential functions such as growth are shut down. These influences of GCs are the primary cause of their side effects, notably endogenous or pharmacologically administered GCs lead to an increase in blood glucose levels, stimulate gluconeogenesis in the liver and mobilise amino acids and fatty acids. Furthermore, the effect of GCs in suppressing non-essential functions of the body, promotes bone metabolism. As a

consequence, prolonged high dosages of GCs result in side effects which include HPA-axis depression, diabetes mellitus, adrenal atrophy, growth retardation, muscle atrophy, osteoporosis and hypertension (6). Due to these side effects, which result from high dosage and long-term use of GCs, their usefulness is limited. The prevalence for developing these side effects varies immensely between individuals. One of the great mysteries of GC research is why some patients develop severe side effects following low dose therapy over a short period while others may experience no side effects what so ever, even after prolonged use of GCs at high concentrations (30).

Since the major anti-inflammatory effects of GCs are elicited by transrepression of pro-inflammatory genes (31), while the majority of side-effects are elicited by transactivation of genes involved in metabolism (32), there is much interest in dissociated GCs that selectively transrepress without significant transactivation of GC responsive genes (33). Dissociative GCs may be steroidal or non-steroidal compounds, which display only partial GC effects and are dissociated in their clinical profile. Thus they display a separation between anti-inflammatory effects and certain side effects. Because of this they may be considered as improved therapeutic compounds, exerting many of the anti-inflammatory and immunosuppressive effects of standard GCs, while inducing fewer side effects (34). For example, mifepristone (RU486) better known as a GR antagonist (35), achieves a degree of functional separation in Hela cells transiently transfected with promoter reporters where it shows little ability to transactivate GR dependent transcription, but represses activator protein-1 (AP-1) dependent transcription by 50 to 70 percent of that of DEX (36). However, the behaviour of RU486 has been demonstrated to be cell type specific, achieving a high degree of transactivation of an MMTV promoter in osteosarcoma cells but none in breast cancer cells (37). Intriguingly Zhao *et al.* (35) have shown a GR concentration dependent shift in RU486's ability to repress transcription of an NF- κ B-driven promoter reporter from that of an antagonist at low GR levels to that of a full agonist at high GR levels. Other dissociative GCs include the steroids ZK 216348 (38), RU24782, RU24858, RU40066 (36) and AL-438 (39). Compound A (CpdA), a novel dissociative GC first synthesised by the University of Stellenbosch Biochemistry Department, is an analogue of a compound from the indigenous Southern African shrub *Salsola tuberculatifomis* Botsch. (40). CpdA behaves as a fully dissociative GC in transrepressing, but not transactivating, select GC-responsive genes. As a result it may have potential for pharmacological use in the design of anti-inflammatory drugs with fewer side effects. The dissociative nature of CpdA has recently been linked to its ability to abrogate GR dimerization (9, 41), which we will discuss in more detail in section 1.6.4. However it should be noted that transactivation versus transrepression characteristics are highly cell type and gene specific and that an increasing number of antiinflammatory genes have been characterised which are up-regulated by the GR (42).

1.2 The glucocorticoid receptor

As mentioned above the GR mediates the effects of both endogenous GCs in diverse cellular processes ((43),(44),(45),(46),(47),(48)) as well as natural or synthetic GCs used to treat inflammatory diseases ((49),(42),(1),(27)). The GR is a steroid hormone receptor (SR), a group which comprises the structurally similar progesterone receptor (PR), mineralocorticoid receptor (MR), androgen receptor (AR) and estrogen receptor (ER), which fall under the nuclear receptor (NR) superfamily (50). The GR is a ubiquitous ligand dependent transcription factor and essential for life. Transgenic mice, which express a truncated GR protein because of a disruption in exon 2, were born with severe abnormalities and died a few hours after birth (51, 52).

There are two major isoforms of the GR, namely GR α and GR β . Both originate from the same gene located on chromosome 5 (53) by alternative splicing (Fig.1.5). While the GR α actively binds ligand and is capable of transcription, the GR β is generally inactive (54, 55).

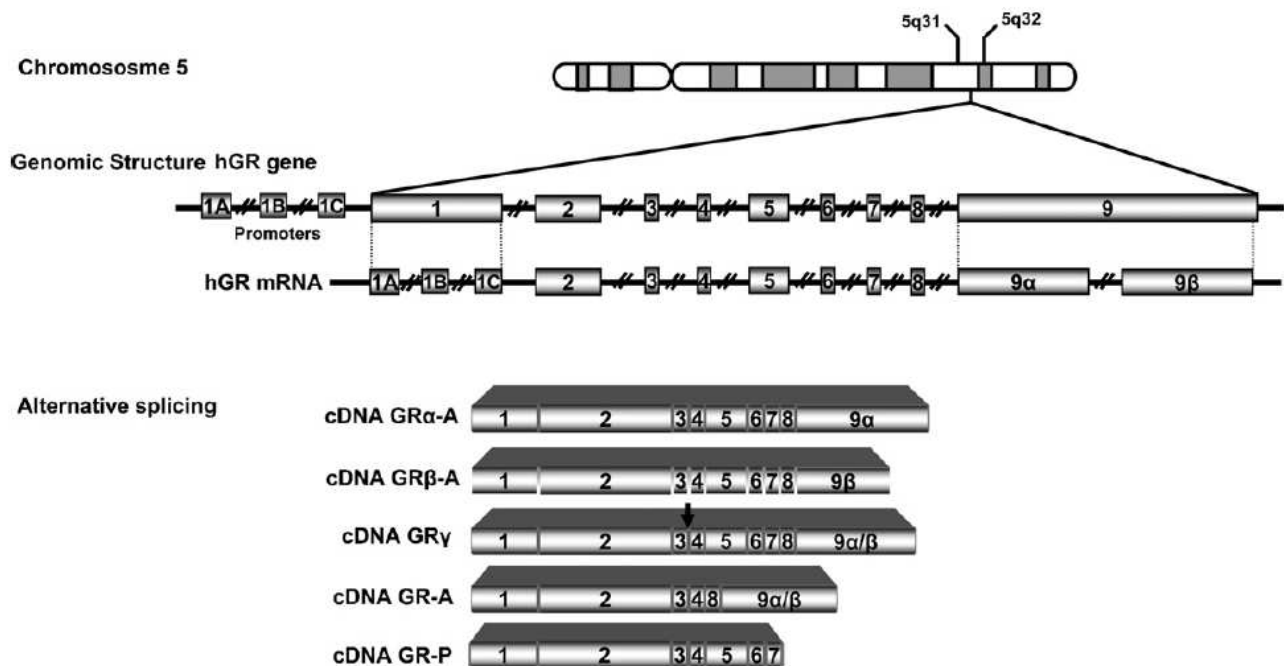


Figure 1.5. **The genomic localization of the GR gene, its structure and major isoforms.** The GR gene is found in chromosome 5 and consists of 9 exons, the numbered boxes. Transcription and translation of the complete 9 exons gives rise to the GR α protein. Splicing of exon 9 results in the truncated GR β . Insertion of an arginine codon between exons 3 and 4 (arrow) results in the GR γ while skipping exons 5 to 7 result in GR-A and deletion of exons 8 and 9 result in GR-P (from Duma *et al.* (56)).

The expression of GR α at both the mRNA, as well as protein, level has been shown to be much higher than that of GR β (54, 55, 57, 58). In fact, although GR β mRNA was found within a number of healthy

tissues, the levels were 400-fold lower than that of GR α and unlike GR α protein, whose presence was ubiquitous, GR β protein was not detected by Pujols *et al.* (59) in any of the ten tissues they examined. Clearly GR α is the predominant isoform of the receptor in healthy tissues having been detected at high concentrations in human brain, liver, nasal mucosa, kidney, lung, muscle, heart, colon, neutrophils and peripheral blood mononuclear cells (PBMC) (59). In addition GR α mRNA was found to be present in all 39 tissues tested in the mouse (60). We will discuss the other 3 GR isoforms as well as GR polymorphisms in greater detail later.

1.2.1 Overview of the mechanism of glucocorticoid receptor action

1.2.1.1 Ligand binding and nuclear import

In the absence of ligand the GR occurs primarily in the cytoplasm in the form of a heteromeric complex consisting of a heat shock protein (Hsp) 90 dimer, Hsp70, the small acidic protein, p23, and one of the tetratricopeptide repeat (TPR)-domain proteins (53). Binding of a GC to the GR produces a conformational change in the GR resulting in a change in the proteins making up the heteromeric complex (61), GR dimerization (62) and active import into the nucleus. Nuclear import of the GR occurs quickly and relies on the association with Hsp90 (63-65), the TPR FK506-binding protein 52 (FKBP52) (66) and importin- α (67). This complex is actively shuttled into the nucleus by dynein (66, 68) along the cytoskeleton (69) through the nuclear pore complex (65, 70, 71). Nuclear import of the GR has been shown to have a half-time ($t_{1/2}$) of 4 to 5 minutes following 10^{-6} M DEX stimulation (10, 63). The unliganded GR, although mostly cytoplasmic, does exist in a dynamic equilibrium where a small proportion of the population is actively shuttled into the nucleus and allowed to diffuse back into the cytoplasm. Upon ligand activation this equilibrium shifts toward a predominantly import driven state, which results in primarily nuclear GR localization (72, 73).

1.2.1.2 Ligand induced dimerization

The ligand bound GR may exist in equilibrium as either a monomer or dimer, although ligand binding shifts the equilibrium toward more dimer (74, 75). Two areas of the GR have been identified as influential in GR dimerization, the dimerization loop (D-loop) of the DNA binding domain (DBD) (76) and the LBD (77). Dimerization of the GR has been demonstrated in the cytoplasm following ligand binding in live cells (62) and through glycerol gradient centrifugation of purified GR (78). Other studies have, however, also indicated that dimerization of the GR occurs via the cooperative association of two GR monomers to the half-sites of the GRE (79). We will discuss this disparity and the influences of GR dimerization in greater detail in section 1.6.

1.2.1.3 How the glucocorticoid receptor functions as a transcription factor

As a ligand activated transcription factor, the primary function of the GR is the transactivation or transrepression of GC responsive genes. In the human U2OS osteosarcoma bone cell line the GR α is directly responsible for the expression of 2978 out of a total of 41079 genes (43), of these, 51 percent were shown to be repressed by the GR, while 49 percent were activated.

In a chromatin immunoprecipitation-microarray study conducted in A549 human lung cancer cells, 68 percent of GC responsive genes demonstrated direct association of the GR with their promoter DNA, which suggests that 32 percent were regulated through tethering of the GR to secondary transcription factors (80). Thus the GR interacts directly with DNA or via other transcription factors and various mechanisms of direct or indirect associations have been demonstrated (31, 81, 82). We present the most common forms of transactivation (via GREs) and transrepression (via negative GREs (nGREs)) in Figure 1.6. To illustrate, the activated GR may bind directly as a dimer to GREs in the promoter regions of GC-responsive genes or alternatively two GR monomers may bind cooperatively to each of the GRE half-sites which constitute a complete GRE (Fig.1.6A), stimulating transcription. Alternatively, in the case of transrepression, the ligand bound GR binds directly to nGREs (Fig.1.6D) or to other transcription factors, such as nuclear factor- κ B (NF κ B) or AP-1 (Fig.1.6F), as either a monomer or a dimer, resulting in repression of gene transcription (80).

Once ligand binding to the GR has occurred, the process of GR nuclear import, dimerization and interaction with GREs occurs rapidly, within 10min (83), while the removal of stimulating ligands results in dissociation of the GR from DNA and reattachment to Hsp90 (84) in the nucleus within 30min (85) (Fig1.7). The interaction of ligand bound GR with GREs has been shown to be a transitory process (86), with the GR binding and dissociating from the DNA within seconds as opposed to remaining attached to the GRE during the course of transcription (83). This dynamic behaviour of the GR was first demonstrated by McNally *et al.* (18) who showed that ligand induced interactions between a green fluorescent protein tagged GR (GFP-GR) and the mouse mammary tumour virus (MMTV) promoter lasted for 10 to 20 seconds at a time before dissociating (18). This transitory association is referred to as the 'hit and run' theory of transcription where transient binding of the GR recruits a secondary set of transcription factors that form a stable complex, which initiates transcription (86-88). Furthermore, it has been shown that the ligand dependent exchange of the GR with its regulatory sites is an active process requiring ATP (83, 86).

Following activation of transcription and before a new round of GRE association can be initiated (89), the GR must first be primed for re-association with the ligand. This is done through the chaperone

cycle which occurs in the nucleus and involves re-chaperoning of the GR with Hsp90 (17) (Fig1.7). Where Hsp90 association with the GR is blocked by the addition of geldanamycin (an Hsp90 inhibitor), GR association with response elements ceases within 5 to 10 minutes even in the continued presence of GC (17). Interaction with Hsp90 has also been demonstrated to be necessary for nuclear retention of the GR (90).

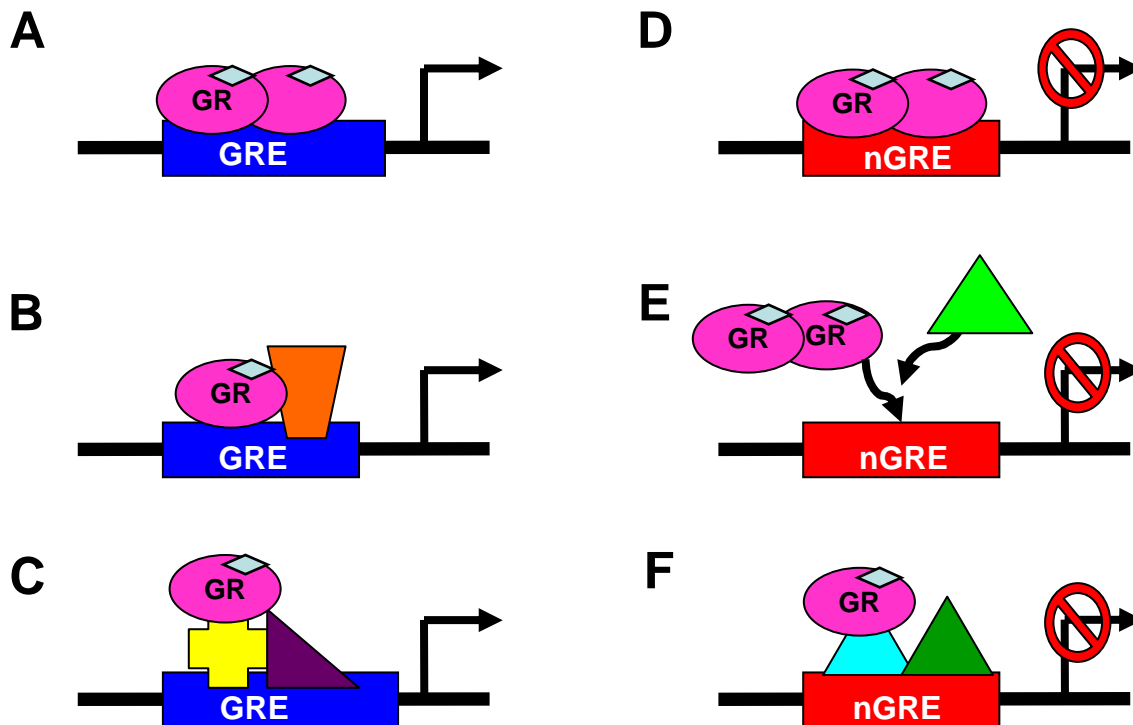


Figure 1.6. **Models of transcriptional regulation by the glucocorticoid receptor.** Transactivation of genes may be initiated by (A) direct binding of a GR dimer to a simple GRE, (B) binding of a GR dimer or monomer as well as a secondary transcription factor to a composite GRE or (C) tethering of the GR to a GRE bound transcription factor. Repression of transcription may be brought about by (D) direct binding of a GR dimer to a nGRE, (E) GR competition for binding to a promoter which blocks its activation by another transcription factor or (F) tethering of the GR to a secondary transcription factor (modified from Newton *et al.* (6)).

The ultradian manner through which the body secretes GCs leads to gene pulsing or cyclic rounds of GR mediated transcriptional regulation (17) (Fig.1.7). The rapid exchange of the activated GR on response elements is followed by reassociation of the receptor with its ligand through the chaperone cycle (17) (Fig1.7), which occurs in the nucleus and does not require transit of the GR through the cytoplasm for the GR to regain functionality (91). The sustained nuclear localization of the GR allows for a dynamic response to the hourly fluctuations in endogenous GC concentration which produces a wave of GR activation that decreases to baseline within 60 minutes of each hormone pulse. In contrast, the pharmacological administration of GCs at a single high dose leads to continuously high levels of GR response (17) as detected by continuous GR induced mRNA production. This behaviour is exacerbated by the fact that potent synthetic GCs, such as DEX, which has a higher affinity for the

GR than the endogenous GC, cortisol (7) take longer to disengage from the GR and have a much longer $t_{1/2}$ in the plasma than endogenous GCs (17) leading to decidedly non-physiological behaviour which increases the risk of side effects.

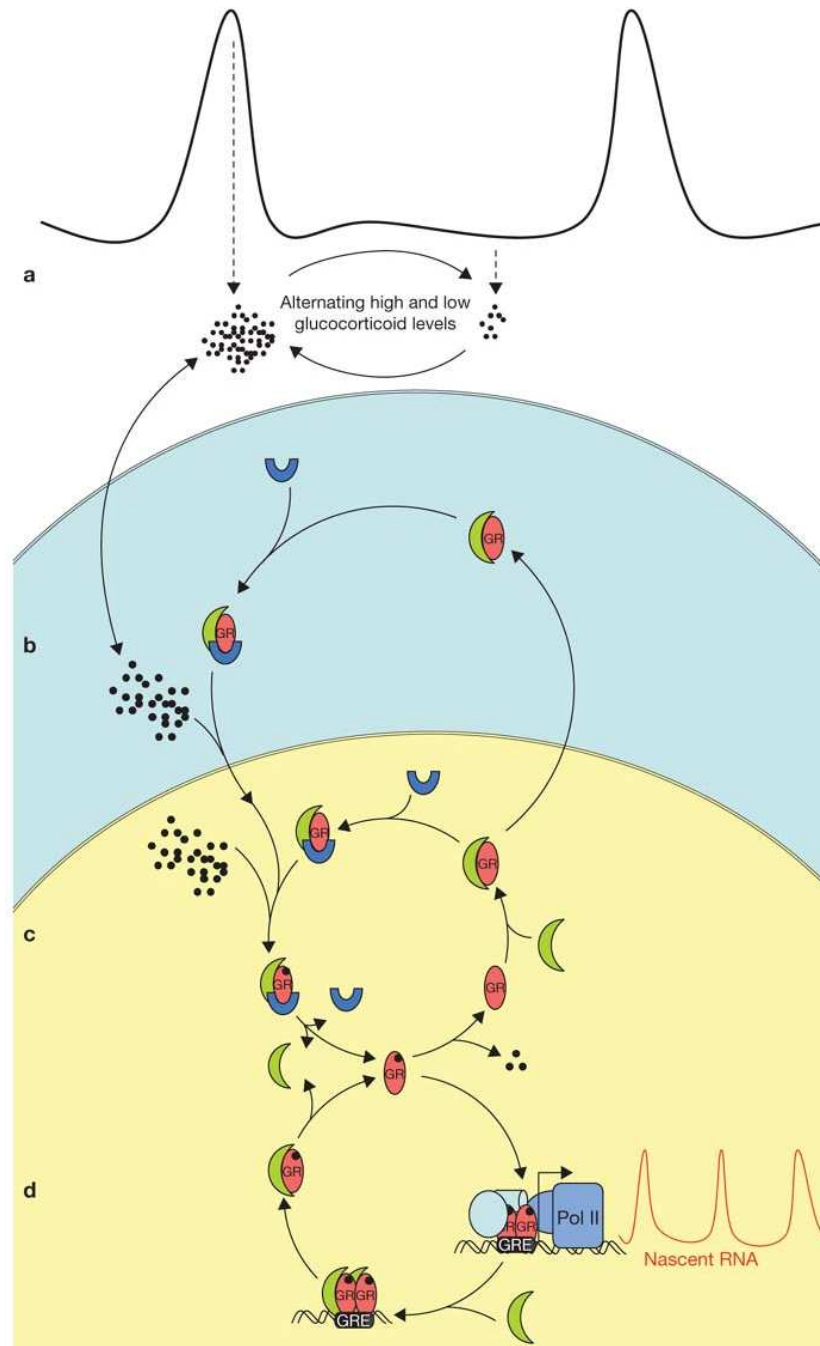


Figure 1.7. **A simplified model of the mechanism of GR action, focusing on the chaperone cycle.** (a) Endogenous GCs vary in concentration due to ultradian hormone pulsing. (b) The GR is chaperoned in the cytoplasm to Hsp90/p23 (green crescent) and Hsp70 (blue half-ring). GC binding induces active nuclear import while nuclear export in the absence of GC is primarily through diffusion. (c) The chaperone cycle in the nucleus, GR re-association with chaperones is necessary for ligand binding. (d) GC activated GR associates with DNA and in so doing dissociates from its chaperones, initiating transcription through the recruitment of cofactors (light blue boxes) and RNA polymerase II (dark blue box) (from Desvergne *et al.* (14)).

1.2.1.4 Degradation or nuclear export

Ligand binding to and the subsequent activation of the GR is the primary cause for its homologous down regulation in most cells types (92, 93), but not all (94). For example, GC treatment has been shown to result in a decrease in GR mRNA levels by 50 to 80 percent (95, 96). While at the protein level, ligand dependent phosphorylation of the GR is responsible for recognition by the ubiquitin and proteosome pathways for degradation of the GR (97). Phosphorylation of the GR allows for recognition by E2 ubiquitin-conjugating enzymes and E3 ubiquitin-ligase enzymes that covalently add the 76-amino acid protein ubiquitin to lysine 426 of the GR (98). Tagging with ubiquitin targets the GR for degradation by the proteosome, a multisubunit protein complex which breaks down proteins into small peptides and amino acids (99, 100)

Ligand dependent phosphorylation of the GR has been shown to occur mainly at serine residues S203, S211 and S226 (101). Furthermore, recent research has demonstrated a correlation between extent of ligand selective phosphorylation at S226 and S211 and the efficacy and potency of transactivation as well as the $t_{1/2}$ of GR degradation. However, the influence of GR phosphorylation on transrepression was inconclusive (102). The same paper revealed a correlation between ligand selective GR $t_{1/2}$ and ligand efficacy in transrepression and transactivation assays (102) and that transcription is not required for DEX mediated GR degradation. Degradation of the GR can occur in both the nucleus and the cytoplasm (103), displaying a $t_{1/2}$ of 44 hours for the unstimulated GR which drops to 10 hours following 10^{-6} M DEX stimulation (102).

After ligand withdrawal the unliganded GR remains nuclear for a considerable amount of time (91), typically 8 to 9 hours following the washout of 10^{-6} M cortisol (63). The retention of the GR in the nucleus is linked to GR association with Hsp90 in the nucleus (90). GR dissociation from DNA following ligand withdrawal occurs rapidly (85) and is followed by the subsequent localization of the GR to transcriptionally inactive areas of the nucleus (91), prior to export of the GR from the nucleus or degradation of the GR by the proteosome. It has been demonstrated that nuclear export of the GR is independent of the exportin 1/CRM1-directed nuclear export pathway (103) and is an inactive process which occurs independently of ATP (91). Considering the slow rate of nuclear export and its inactive nature it is most likely that nuclear export of the GR occurs through passive diffusion.

1.2.2 Glucocorticoid receptor functional domains

The GR protein may be divided into three functional domains, the amino-terminal activation domain, a central DNA binding domain (DBD) and a carboxyl-terminal ligand binding domain (LBD) (Fig.1.8)

(104). The amino or N-terminus contains the hormone-independent activation function 1 (AF1) domain, which is associated with transcriptional activity. The carboxy or C-terminus contains the AF2 domain, which is responsible for hormone binding and hormone-dependent activation. Inactive GR is bound by the C-terminus to Hsp90. Upon hormone binding the receptor undergoes a conformational change and the composition of the Hsp90 tethering complex is altered (105) (Fig.1.8).

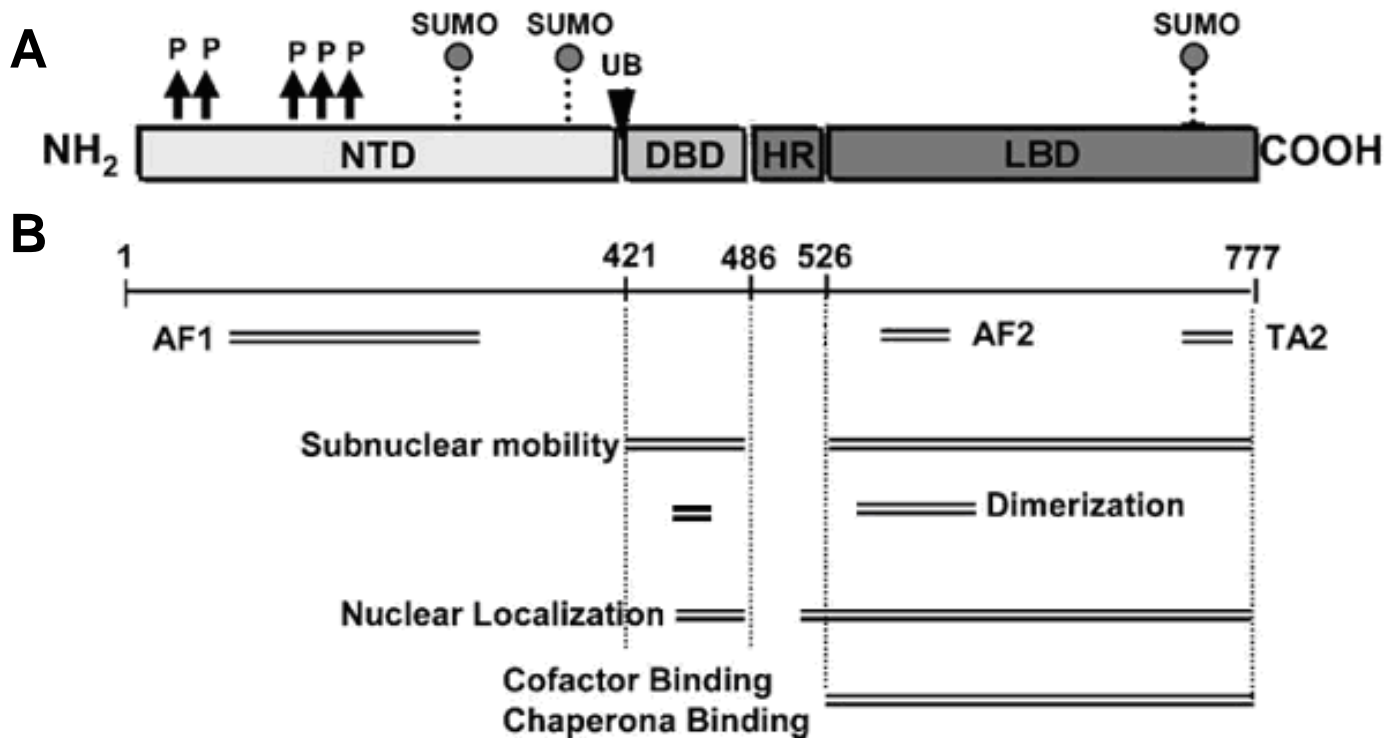


Figure 1.8. **Major functional domains of the GR and positions where post translational modification occurs.** (A) Structural domains of the GR, the N-terminal domain (NTD), DNA binding domain (DBD), hinge region (HR) and ligand binding domain (LBD). Points where post translational modification occur are indicated: phosphorylation sites (P), sumoylation sites (SUMO) and the ubiquitination site (UB). (B) The major functional domains of the GR displaying areas responsible for subnuclear mobility, dimerization, nuclear localization and cofactor/chaperone binding. Transcriptional activation function (AF1), transcriptional activation function 2 (AF2) and an area of additional transcription activity (TA2) are also displayed (redrawn from Duma *et al.* (56)).

Nuclear import of the liganded GR is carried out through the nuclear localization 1 (NL1) sequence, which is situated in the hinge-region of the GR that separates the DBD and the LBD (Fig.1.8). The NL1 is a nuclear localization signal (NLS) that allows for nuclear import of GR through interaction with importin- α and importin 7 (72, 106, 107) (Fig.1.8). A second ligand dependent nuclear localization 2 (NL2) domain that overlaps with the LBD and also plays a role in GR nuclear import (72, 106) has been identified. Comparison with the predominantly nuclear PR has revealed that helices 1 to 5 within the N-terminal of the LBD of the GR are responsible for its cytoplasmic localization when uninduced

(108). Furthermore, a nuclear retention signal (NRS) has been shown to exist in the hinge region of the GR, which actively opposes the nuclear export of GR (109). Homodimerization sequences exist at the C-terminal domain and in the D-loop of the DBD. Both of these are necessary for optimum GR dimer formation (75), however, evidence suggests that the D-loop dimerization signal is more important (75),(110) and we will discuss this in detail in section 1.6.

1.3 Overview of factors that modulate glucocorticoid response

At a specific time point, the concentration of GCs are basically constant throughout the body as they are transported to all cells in the blood plasma and gain entry into the cell by free diffusion across the cellular membrane due to their lipophilic nature. Equally ubiquitous is the GR, which is expressed in all tissues of the human body tested (111). Despite the fact that GC concentration is equal throughout the body at a specific time point and that GR is present in every major tissue there are considerable tissue specific (25), interindividual (25, 112, 113) and diseased compared to healthy tissue (114) differences in GC response. The same can be said for tissue culture experiments where it is common knowledge that GC responses in different cell lines are not always directly comparable (7, 101).

The most widely encountered and clear mechanisms through which GC response is modulated, and which will be discussed in this section, are through availability of the ligand itself (section 1.3.1), concentration of the GR (section 1.3.2), the occurrence of GR isoforms, polymorphisms and post translational modifications (section 1.3.3) and availability of corepressors, coactivators and comodulators (section 1.3.4). In a recent review article De Bosscher *et al.* (49) describe the five most widely accepted modulatory factors of GC response (Fig.1.9), of which our four factors form part. However, the fifth set of factors, which are known to influence the response to GCs, involve interaction with other transcription factors, regulation at RNA level by RNA cofactors and the basal transcription machinery. These influences are more generalized and therefore their effects are not limited to the response to GCs specifically. Thus we will focus on the four more direct mechanisms thought to modulate specificity of GCs.

1.3.2

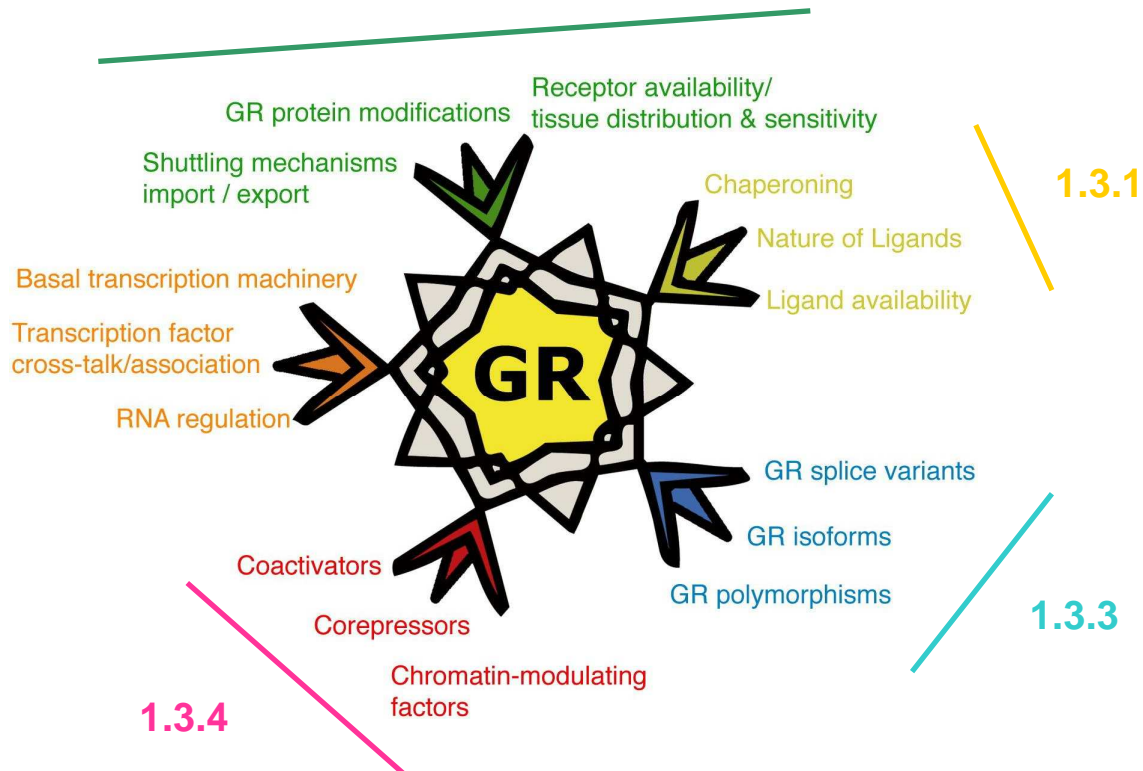


Figure 1.9. **Factors which modulate GR function.** Numbers refer to the subsections under which we discuss the respective modulating factors (from De Bosscher *et al.* (49)).

1.3.1 Ligand availability

The availability of GCs may be influenced at a tissue specific level by the presence of 11 β -hydroxysteroid dehydrogenase type 2 (11 β -HSD2), which catalyzes the conversion of active cortisol to the inactive GC metabolite, cortisone, or 11 β -hydroxysteroid dehydrogenase type 1 (11 β -HSD1), which is responsible for the inverse reaction, namely, the conversion of cortisone to cortisol (48, 115, 116). These enzymes are differentially expressed in order to fine tune tissue specific responses to GCs. For example, 11 β -HSD1 is found in the GC responsive metabolic tissues of the liver, fat, lung and central nervous system (117), while 11 β -HSD2 is predominantly expressed in the mineralocorticoid responsive cells of the kidney (117). In addition, 11 β -HSD1 is highly expressed in the hippocampus of the brain and other tissues of the central nervous system (CNS) and has been shown to amplify the action of GCs in these tissues (118). In contrast, 11 β -HSD2 is expressed most frequently in tissues which are required to display a high level of aldosterone specificity as the primary steroid receptor for aldosterone, the MR, has a high affinity for cortisol and 11 β -HSD2 thus effectively

removes the competing ligand (119, 120). The levels of 11β -HSD1 and 11β -HSD2 enzymes in tissues may thus directly influence the intracellular availability of GCs in a tissue specific manner (115).

Another factor that is responsible for limiting the availability of GCs to specific tissues is the efflux transporter P-glycoprotein (Pgp), which is a member of the ABC-transporter protein family (121). The Pgp is a transmembrane protein, which has been shown to export the synthetic GCs, DEX and prednisolone, as well as endogenous cortisol, from the intracellular compartment to the extracellular space (122). As Pgp is expressed in the capillary endothelial cells of the blood-brain barrier (123) it has been linked to the 6-fold lower levels of cortisol found in the brain as compared to in the blood (124).

Finally, the concentration of CBG, the high affinity plasma transport glycoprotein in the blood, that is primarily produced by the liver may influence the interindividual and tissue specific availability of GCs (4, 5). Intriguingly, the enzyme elastase expressed by neutrophils has been shown to cleave the CBG protein resulting in the localized release of GCs. As elastase is expressed on the surface of these cells it is suggested that interaction with CBG is a mechanism for the delivery of large amounts of GCs to the activated neutrophil and sites of inflammation (4).

1.3.2 GR concentration

Physiologically, the concentration of expressed GR varies considerably between tissues, ranging from 4.1 fmol GR per mg protein in PBMCs (24) to as high as 893 fmol GR per mg protein in the skin (125) (Table.1.1). Considerable interindividual variation, within the same tissue type, has also been reported, primarily in cancerous tissues (Table.1.1, Table.1.2). In an extensive study, which characterized the mRNA expression of 49 NRs in 39 different mouse tissues, GR mRNA was detected in all the tissues tested (60), however, the levels of GR mRNA varied by at least 20-fold (60).

A useful model in which to appreciate the effects of interindividual differences in GR concentration are transgenic mice that contain two additional copies of the GR gene (126). Their expression of GR mRNA was shown to be elevated by 20 to 60 percent in various tissues, while in the one tissue analyzed for GR protein levels, the hippocampus, GR concentration was found to be 50 percent above that of wild-type mice (126). These GR knock-in mice are therefore a tool through which to study the physiological consequences of GR concentration. GR knock-in mice display significantly reduced basal levels of ACTH and consequently levels of corticosterone which are 4 times lower than in wild-type mice. Their response to restraint stress was also reduced indicating a better capacity to handle psychological stress. This may be linked to studies that demonstrate a decrease in the capacity to handle psychological stress in mice, which display reduced hippocampal GR expression, due to

exposure to postnatal stress (127). GC treatment is known to induce thymocyte apoptosis, which the GR knock-in mice have an increased sensitivity to, in fact despite expressing only 1.5-fold more GR than wild type mice, the potency of GC induced thymocyte apoptosis is 10-fold greater in the knock-in mice. Finally, increased GR concentration enhances the ability of knock-in mice to resist inflammation as displayed by their heightened resistance to cytokine induced endotoxic shock (126). Thus, an increased expression of GR allows these mice to cope better with stress and inflammation.

Table 1.1. **GR concentrations of various human cell lines and tissue biopsies.**

Cell Line or tissue biopsy	fmol GR/mg protein	GR/cell	Reference
Cell lines:			
LMCAT (fibroblast)	151.8	-	(128)
MCF-7 (breast cancer)	-	29995	(129)
K562 (bone marrow cancer)	-	32450	(130)
SiHa (uterine cervical cancer)	-	81000	(130)
Hep3B (hepatoma)	-	43000	(130)
Healthy tissue biopsies:			
brain	30	-	(131)
bone marrow	-	1106 to 27000	(112)
lung	30.3 to 84.9	-	(132)
cytotrophoblasts (epithelial stem cells)	16200	-	(133)
lymphocyte (white blood cell)	-	2248 to 79364	(28)
monocyte (white blood cell)	-	4834 to 17734	(28)
PBMC	4.1	-	(24)
mononuclear leukocytes (white blood cell)	191	-	(12)
skin fibroblasts	-	133400	(125)
skin	893	-	(125)
AIDS patient biopsy:			
skin	2777	-	(125)
Cancerous tissue biopsies:			
skin (AIDS patient Kaposi's sarcoma tumour)	4663	-	(125)
skin	-	52000	(113)
brain	142	-	(131)
lung	-	5230 to 36500	(134)
lung	56.5 to 87.8	-	(132)

Table 1.2 Interindividual variances in GR expression within the same tissue type.

Tissue	Variance [GR] (GR/cell)	Fold difference	Population	Ref.
Leukemia	1433 to 26858	19	18	(112)
Leukemia	2248 to 79364	35	174	(28)
PBMC	1391 to 15133	11	54	(135)
Lung cancer	1100 to 314000	285	49	(136)
Lung cancer	5230 to 36500	7	43	(134)

The most widely encountered phenomena of GR concentration change is the down regulation of GR protein and mRNA brought about by prolonged GC treatment (26). A decrease in GR concentration has been directly linked to GC resistance in rheumatoid arthritis (137, 138), systemic lupus erythematosus (139), and bronchial asthma (140).

GCs are capable of inducing apoptosis and are used in conjunction with chemotherapeutic regimes in the treatment of hematological cancers such as Hodgkin's lymphoma, acute lymphoblastic leukemia and myelomas (141). The administration of GCs along with chemotherapeutic agents are an effective means of treating lymphoblastic leukemias as high doses of GCs promote the cytolysis of these cells. However, only 70 percent of patients respond to this therapy (141). A significant correlation has been demonstrated between the clinical responsiveness to the GC prednisone, with or without co-administration of the chemotherapeutic agent vincristine, and GR levels (112). Of the patients studied, all 11 that demonstrated low levels of GR (< 5000 GR per cell) were resistant to the treatment. Conversely, 13 of the 20 patients with GR levels between 5000 and 15000 GRs per cell, responded readily to prednisone alone or to the combination of prednisone and vincristine (112). Another study of leukemia patients, demonstrated that those with GR levels below 16000 GR per cell were shown to have a higher risk of relapse following chemotherapeutic treatment (28). Furthermore, a direct correlation was found between GR concentration and survival rates of patients with advanced non-small cell lung cancer (NSCLC), with increased GR expression in tumours resulting in a beneficial outcome to GC and chemotherapeutic treatment (134). In addition, primary cancer tissue cell lines treated with high dosages of DEX displayed inhibition of cell growth if expressing high levels of GR (> 19400 GR per cell) (130). Unusually, human leukemia cells demonstrated increased GR expression as a result of prolonged GC treatment. This is one of the few cases of GC induced auto-induction of GR and facilitates GC induced apoptosis of this cancer (142). Thus increased GR concentration imparts heightened GC induced apoptosis in a variety of cancerous tissues.

The concentration of GR varies widely between individuals and tissues. Furthermore, within the same individual and the same tissue the concentration of GR may differ due to a diseased state such as cancer. A low GR concentration has been directly linked to decreased GC response while heightened GR concentrations may result in increased GC response. We will discuss the factors which influence GR concentration in more detail in section 1.4 and explain the influence of GR concentration at a cellular level.

1.3.3 Varying glucocorticoid receptor isoforms, polymorphisms and post translational modification

Multiple isoforms of the GR are generated from a single gene, through alternative RNA splicing and translation initiation, while mutations in the GR gene itself result in a number of GR polymorphisms. Additionally, each isoform may be modified post-translationally through phosphorylation, sumoylation and ubiquitination (56).

As mentioned before, there are two major isoforms of the human GR namely, GR α and GR β (Fig.1.5). They are identical up to amino acid 727 where their sequences diverge. The ligand binding GR α is made up of the full 777 amino acids coded for by the GR gene, while the 50 carboxy terminal amino acids of the GR α have been replaced by 15 non-homogenous amino acids to form the 724 amino acid GR β (143). Pujols *et al.* (59) detected GR β mRNA in healthy human tissue but found that it occurred at a level that was 400 times lower than that of GR α mRNA, while their Western blots for GR protein detected GR α , but no GR β protein was found in any of the 12 healthy human tissues tested due to its low level of expression.

It has been suggested that the GR β , which is largely incapable of binding GCs and displays a greatly reduced capacity for transcriptional activation (58), acts as a dominant negative inhibitor of GR α mediated transcription through heterodimerization with the GR α (144). Gougat *et al.* (145) have shown that the GR β isoform, when overexpressed in A549 cells, is constitutively nuclear and that when transfected at a 5-fold excess to GR α in COS-1 cells results in a 40 percent inhibition of DEX stimulated transactivation. As a result of the tendency of GR β to repress the response of GR α it has been implicated in tissue specific GC resistance in several diseases (146, 147). Furthermore, exposure of human skeletal myoblasts to increasing concentrations of cortisol resulted in a dose dependent decrease in GR α expression and a dose dependent increase in GR β expression (148). In similar studies, GC exposure has been demonstrated to increase the ratio of GR β /GR α expression in PBMCs leading to generalized GC resistance (149) and in tuberculin induced inflammatory lesions resulting in steroid resistant asthma (146). In addition, studies in epithelial and lymphoid cells have demonstrated

that stimulation with the cytokine, tumour necrosis factor (TNF)- α , lead to the disproportionate increase in GR β over GR α , which again may contribute to GC resistance in this cell line and possibly in other tissues that are exposed to high levels of TNF α (150). Apart from the more common GR α and GR β isoforms, the rare splice variants GR ρ and GR λ (Fig.1.5) have been identified in GC resistant myeloma patients (151, 152) and are thought to be the cause of their reduced response to GCs. Finally GR γ has been detected in childhood acute lymphoblastic leukemia (153). The GR α isoforms GR α , GR α -A, GR α -B, GR α -C and GR α -D have a unique capacity to transactivate and transrepress genes and as a result their varied expression levels in tissues may contribute to tissue specific responses, for example, only GR α influences the BCL10 gene, only GR α -A the BMF gene, only GR α -B the BCL2L14 gene, only GR α -C the GADD45A gene and only GR α -D the EPO (43).

Not much work has been done on the tissue specific levels of GR phosphorylation. However, it has been suggested that at a cellular level hyperphosphorylation of GR during the G2/M phase may account for GC resistance reported during this period of the cell cycle (154). Furthermore, an increase in the ligand dependent phosphorylation of the GR at serine residues S211 and S226 has been correlated with an increased ability to activate transcription (102) (Fig.1.8A). Although the phosphorylation status of the GR has been shown to be ligand dependent (102), results from investigations of tissue specific differences due to the phosphorylation status of the GR are inconclusive (155).

Another form of post translational modification of the GR is the attachment of ubiquitin to lysine 426 of the GR (Fig.1.8A), which marks it for degradation by the proteasome (98). Finally, the process of sumoylation involves the covalent attachment of a small ubiquitin-related modifier-1 (SUMO-1) to lysine residues of the target protein (156). Sumoylation of the GR at K277, K293 and/or K703 is involved in the regulation of protein stability, localization and activity (Fig.1.8A). Over expression of SUMO-1 as well as GR in COS-1 cells has been demonstrated to result in a 5-fold increase in ligand induced transactivation through a promoter reporter (157) though once again no tissue specific responses have been described.

GC hypersensitivity, as defined by the inability of a patient's endogenous cortisol levels to recover 8 hours after the administration of a potent synthetic GC, DEX (called the overnight DEX suppression test), has been linked to two single nucleotide polymorphisms of the GR gene (158). The N363S polymorphism, which occurs in ~4 percent of the population (159), has been linked to increased sensitivity to GCs with a physiological profile that closely resembles the side effects of prolonged GC exposure namely, lower bone mineral density and increased body mass index (160). *BclI* a restriction fragment length polymorphism, which results from a C/G substitution in intron 2, 646 nucleotides

downstream from exon 2, also displays increased sensitivity to GCs (161) and is associated with an increased risk of cardiovascular disease (162).

A mouse model used to investigate GC hypersensitivity is based on an artificial mutant human GR that contains a leucine (L) substitution for methionine (M) at residue 604 in the LBD. The artificial human GR mutant does not correspond to any known human polymorphisms and is activated by 5 to 10-fold lower corticosterone concentrations than the GR wild type (163). The mouse analog has the same substitution at residue 610 and is termed GR_{M610L}. GR_{M610L} knock-in mice were created that express this gain in function GR as opposed to wild type GR and their response to GCs was studied (164). Similarly to the mice which over express GR (discussed in section 1.3.2), these gain in function GR mice displayed decreased corticosterone and ACTH levels, both basally as well as in response to psychological stress. A response which is linked to enhanced down-regulation of the HPA axis. In addition, these mutant mice responded to a 10-fold lower concentration of DEX as compared to the wild type mice, displaying a DEX induced rise in blood pressure following the administration of 1mg per litre DEX in their drinking water, while a similar effect was only seen at 10mg per litre DEX in the wild type population (164). This model demonstrates that an increase in GR sensitivity to GCs has an influence on the physiological response to endogenous as well as exogenous GCs.

GR polymorphisms associated with GC insensitivity have also been found. An arginine (R) to lysine (K) amino acid mutation at position 23 (R23K) in the N terminus results in the ER22/23EK polymorphism, which has been detected in ~3 percent of the population (159). ER22/23EK displays reduced transcriptional activity in promoter reporter assays and of endogenous genes when compared to the wild type receptor (165). Carriers of this polymorphism display phenotypes which are associated with GC insensitivity such as lower total cholesterol levels, lower fasting insulin concentrations and increased insulin sensitivity (160). Furthermore, a polymorphism of the GR β , A3669G, results in enhanced expression of the dominant negative GR β protein (166) and homozygous carriers display reduced immunosuppression reflected by increased incidences of rheumatoid arthritis (167).

1.3.4 Coregulating and comodulating factors

Transactivation of GRE driven genes by the ligand activated GR is modulated by multiple proteins with coactivating or corepressing influences on transcription. They are generally referred to as coregulators and are subdivided into coactivators and corepressors (168). Furthermore, the behaviour of the GR is also influenced by factors which influence events upstream from transcription. These proteins are called comodulators.

1.3.4.1 Coactivators

The over expression of coactivators results in nonspecific up regulation of promoter reporter transactivation by various SRs. Due to this tendency, the specificity of coactivators was initially unclear, however, it was subsequently demonstrated that the combination of coactivators interacting with the PR or GR on a single promoter varied (169). For example, the p160 steroid receptor coactivators (SRCs) interact differently with steroid receptors and have tissue specific expression patterns (170). It is therefore likely that the combination of coactivators which act on a given steroid receptor and their tissue specific expression confers tissue as well as steroid receptor specific activation (47, 171). The SRC family make up the most prominent group of coactivators that interact with the GR and consist of three genes that code for related proteins, namely, SRC-1 (protein: NCoA-1), SRC-2 (proteins: NCoA-2, TIF2 or GRIP1) and SRC-3 (proteins: NCoA-3 or pCIP/ACTR/AIB1/RAC3/TRAM1) (172).

The majority of coactivators bind to the LBD of the GR via nuclear receptor boxes such as LXXLL motifs (173, 174). They promote transactivation either through direct interaction with the basal transcription machinery or by the induction of local chromatin remodeling, which serves to activate promoters (47, 175, 176). The coactivators, transcription intermediary factor 2 (TIF2)/GR-interacting protein (GRIP), SRC-1 and AIB1/pCIP/ACTR/RAC3/TRAM1, have all been shown to increase transactivation potency and partial agonist activity of antagonists (177, 178). In addition, a recent paper by Ronacher *et al.* (7) demonstrated that GRIP-1 and SRC-1a interaction with the GR leads to an increase in both potency and efficacy of transactivation via GREs in a ligand specific manner. They found that in general, agonist bound GR has a higher affinity for these coactivators than antagonist bound GR.

An example of tissue specific expression of coactivators comes from the SRC-1 gene, which has two splice variants SRC-1a and SRC-1e. These two variants interact differently with the LDB of the GR (179) and influence the behaviour of the GR differentially (171). SRC-1a mRNA was detected at much higher levels than SRC-1e mRNA in hypothalamic nuclei (180). Additionally, SRC-3 also demonstrates tissue specific expression in sub fields of the hippocampus, while knock-out of the SRC-3 gene in mice resulted in numerous detrimental phenotypes (181).

1.3.4.2 Corepressors

Corepressors, such as nuclear receptor corepressor (NCoR) and silencing mediator of the retinoid and thyroid hormone receptor (SMRT), have histone deacetyl transferase activity, which catalyzes the

deacetylation of chromatin and may recruit additional components of corepressor complexes. Traditionally, it was thought that corepressors only functioned in the absence of ligand or in the presence of antagonists, to repress transcription (47, 182). However, it is now accepted that corepressors are capable of interacting with agonist as well as partial agonist bound GR in transactivation as well as transrepression assays (7, 183).

Their capacity to prevent access of the GR to GREs and nGREs results in a reduction in transcription (184) as has been demonstrated in experiments over expressing SMRT which result in a decrease in DEX induced potency and efficacy at subsaturating concentrations of ligand in transactivation assays (177). Szapary *et al.* (177) have shown that the coactivator TIF2 and the corepressor SMRT were mutually antagonistic and that SMRT over expression reversed the increase in potency and efficacy brought about by an increase in GR concentration (177). This implies that the level of corepressors influences the effect of increased GR concentrations on transactivation. Thus the ratio of corepressors versus coactivators affects the extent of GC induced gene expression (185) and therefore tissue specific differences in the expression of either of these coregulatory protein groups would result in differences in the response to GCs.

1.3.4.3 Comodulators

Whether bound to a ligand or unliganded, the cytoplasmic GR occurs in a complex consisting of an Hsp90 dimer, Hsp70, the cochaperone p23 and one of the TPR proteins, also called immunophilins (186). The four TPRs are FKBP52, FK506 binding protein 51 (FKBP51), cyclosporine A-binding protein (Cyp40) and protein phosphatase 5 (PP5). They are known to associate indirectly to the GR via binding to the C-terminal TPR acceptor site of the Hsp90 dimer (187-189), which can bind to any of the four TPR proteins. FKBP51, FKBP52 and PP5 have been shown to have profound influences on the ligand binding affinity of the GR, while FKBP51 and FKBP52 are known to influence the localization of the GR (66, 128).

Ligand binding to the GR results in a shift from FKBP51 to FKBP52 association with Hsp90, which in turn stimulates nuclear import of the GR, Hsp90 and FKBP52 complex by dynein (66). Interestingly, WCL2 cells, which have a high concentration of FKBP52, display a high degree of ligand independent nuclear localization of the GR (190). Neither Cyp40 nor PP5 influence GR nuclear localization (61).

Over expression of FKBP52 resulted in an increase in GR ligand binding affinity for [³H]-DEX, reflected in a decrease in the equilibrium dissociation constant (K_d) from 32.6nM to 10.1nM (128). Association of PP5 increased [³H]-DEX binding affinity from 32.6nM to 15.6nM, while Cyp40 had no effect on the

ligand binding affinity of the GR (128). FKBP51 over expression reduces the ligand binding affinity of the GR (191-193). Thus, it is possible that cells which over express FKBP52 would display enhanced GC responsiveness relative to cells over expressing FKBP51.

TPR expression levels have also been demonstrated to vary between cell lines. For example, WCL2 cells (a Chinese hamster ovary cell line) have more FKBP52 than L929 (a murine fibrosarcoma cell line) and COS-1 (monkey kidney fibroblast cells), while L929 cells have the highest FKBP51 expression amongst these three cell lines. COS-1 and WCL2 cell lines have similar Cyp40 and PP5 expression levels, both of which are lower than L929 cells (61). The difference in expression levels of these comodulators between cell lines results in tissue specific behaviour, for example, GR in L929 cells was found predominantly in the cytoplasm in a complex containing PP5 and FKBP51, while the GR of WCL2 cells was predominantly nuclear and complexed with PP5 and FKBP52 (61).

Intriguingly, Cho *et al.* (194) have shown that GR concentration influences the behaviour of the comodulator, ubiquitin-conjugating enzyme 9 (Ubc9) in DEX stimulated promoter reporter transactivation assays. At low GR concentrations, increased Ubc9 expression raises efficacy significantly but has no influence on potency. However, at high GR concentrations, increased Ubc9 has a reduced effect on efficacy, but increases potency significantly. As GR concentrations differ dramatically between tissues, the GR concentration dependent influence of Ubc9 may lead to further separation of tissue specific response above that which is already elicited by differences in GR concentration.

Finally, it is not immediately clear from the literature whether each of the two Hsp90 dimers which is found in association with the dimerized cytoplasmic GR are associated with TPRs. However, recent research by Banerjee *et al.* (61) demonstrated association of both PP5 and FKBP52 in the nuclear unliganded GR complex and PP5 and FKBP51 in the cytoplasmic unliganded GR complex, which suggests that both Hsp90 chaperone complexes are capable of binding a TPR while in association with GR. Furthermore this evidence suggests ligand independent dimerization of the GR.

1.4 Physiological glucocorticoid receptor concentrations

We have established that GR concentration has a profound effect on the physiological response to GCs and have discussed the fact that GR concentrations vary between tissue types (12, 59, 60, 114, 195, 196) (Table.1.1) and individuals (28, 112, 135) (Table.1.2). However, we have focused on only a few of the causes for differences in GR concentration, notably down regulation due to GC exposure (21, 148, 197-199). There are a wide variety of other influences that affect GR concentration and we

will now elaborate on these in terms of influences that increase or decrease physiological GR concentrations.

1.4.1 Increased glucocorticoid receptor concentrations

High levels of GR have been detected in a number of cancers (28, 130). For example, while the average concentration of GR in healthy human brain varies from 32 to 67 fmol GR per mg protein, depending on the specific tissue, the concentration of GR in brain tumours is significantly higher, ranging from 99 to 171 fmol GR per mg protein (131). Furthermore acquired immune deficiency syndrome (AIDS) exacerbates the phenomena of increased GR in cancerous cells. For example, although healthy skin has one of the highest GR concentrations of all tissues at 893 fmol GR per mg protein (Table.1.1), this rises 3-fold in the healthy skin of AIDS sufferers and peaks at a 5-fold increase in GR expression in Kaposi's sarcoma of AIDS sufferers (125).

Following an extreme mechanical injury to skeletal muscle tissue, sepsis is known to develop. Sepsis involves the catabolic breakdown of damaged muscle through proteolysis (200). The level of GR expression increases 2-fold in septic muscle, despite dramatically increased plasma corticosterone levels in rats (114). It has been suggested that under septic conditions the up regulation of GR and GCs facilitate the catabolism of the damaged muscle tissue (201).

Adrenalectomy involves the surgical removal of the adrenal glands and results in virtually undetectable plasma corticosterone levels 4 days after the operation in rats (202). This dramatic decrease in circulating GCs results in tissue specific up regulation of GR expression. GR concentration in the rat hippocampus increased 3-fold 4 days after adrenalectomy, while the increase was a less dramatic 2-fold in the prefrontal cortex (202).

Dietary restriction (DR) without malnutrition has been much lauded as a means of delaying aging and has been shown to protect rodents from diabetes, impaired tissue growth and reproductive senescence (203). It also results in a 37 percent increase in the GR expression of mouse liver. Mice subjected to DR demonstrated an increase in GR concentration from 122 to 167 fmol GR per mg protein compared to mice that were fed *ad libitum* (204). Although DR mice displayed a similar age dependent percentage decrease in GR concentration as the mice fed *ad libitum*, their GR levels in old age were statistically the same as young *ad libitum* fed mice. The relatively increased GR levels in old DR mice may allow them to maintain basal and stress-related homeostasis better than old *ad libitum* fed mice.

1.4.1 Decreased glucocorticoid receptor concentrations

A ubiquitous cause of down regulation of GR expression is aging. For example, an inverse correlation has been demonstrated between GR concentration in PBMCs and age in human subjects (205), while cortisol levels remained unchanged. Levels of GR mRNA in the human prefrontal cortex have also been shown to decrease in subjects greater than 77 years of age (195). Studies in rats indicated a similar trend, showing significant decreases in GR levels in the liver of older animals (> 20 months old) ranging from 19 to 25 percent decrease in GR expression, depending on the study (198, 204). The loss of GR in the liver of aging rats was associated with decreased GC responsiveness and may contribute to impaired metabolic function (198).

Ironically exercise has also been linked to a significant decrease in GR expression levels of PBMCs in humans. The strenuous training of athletes is reflected in an increased plasma cortisol level compared to sedentary individuals, which in turn results in greater down regulation of GR expression (205).

The body draws little distinction between its physiological response to physical or psychological stress. In animal studies, psychological stress results in a down regulation of GR in the muscle, liver and hippocampus and prefrontal cortex of the brain (196, 206, 207). These lowered GR levels, particularly in the hippocampus, are associated with heightened resting as well as stress induced GC levels (196, 206, 207). For example, the psychological stress of maternal separation of rat pups within the first 3 weeks of life results in permanently lowered hippocampal GR expression, which causes a lack of negative feedback of GCs to the HPA axis and therefore to massively elevated endogenous GC levels in response to stress. This is associated with depressive-like behaviour and a general inability to cope with psychological stress (206). Human depressives also display elevated cortisol levels in the brain and GC resistance consistent with the results found in rodents (208).

To summarize, the concentration of GR in tissues can be upregulated following adrenalectomy, due to the environmental influence of DR and in diseased states such as cancers, AIDS and in muscle sepsis. Factors which have been shown to result in a decrease in tissue GR concentration, other than aging, are generally linked to an increase in the stress response for example, strenuous exercise and psychological stress.

1.5 The cellular effects of glucocorticoid receptor concentration

The influence of GR concentration on GC response has been explored in a number of tissue culture studies, which focus on the modulation of GC response at a cellular level. Where as clinical

observations of patients broadly reveal hypersensitivity to GCs brought about by increased GR levels or GC resistance at reduced GR levels, molecular biological investigation suggests the cause of these symptoms. We will focus on the effects of altered GR concentration on ligand binding and transcription. Additionally, as it has been revealed that the nuclear mobility of activated AR is receptor concentration dependent (209), we will discuss these findings as well.

1.5.1 Ligand binding affinity and positive cooperative ligand binding

Ligand binding affinity is quantified in terms of K_d (210-213). The K_d is calculated by dividing the dissociation constant by the association constant (211). In the case of receptor ligand binding, K_d is defined as the concentration of ligand required to bind to half of the available binding sites (213). Although counter intuitive an increase in ligand binding affinity is reflected in a decrease in K_d . Physiologically a 4.3-fold decrease in GR concentration brought about by the tumour promoter, phorbol 12-myristate 13-acetate (PMA), in mice resulted in a 5.2-fold decrease in DEX binding affinity (199). Furthermore, cytosolic fractions from human mononuclear leukocytes demonstrate a 2-fold increase in ligand binding affinity at high GR concentrations (12). However, 48 hour treatment of the human monocytic cell line, U937, with tumor necrosis factor α (TNF α), a pro-inflammatory cytokine, resulted in a 2.4-fold decrease in GR concentration (from 11709 to 4834 GR per cell) but no significant change in ligand binding affinity (214). There are only a handful of studies which explore the link between GR concentration and ligand binding affinity and their findings are not definitive. This is an issue which begs further analysis.

Ligand binding behaviour may also be quantified in terms of the amount of ligand required to shift receptor occupancy from 10 to 90 percent (215). The slope of the ligand binding curve between 10 and 90 percent receptor occupancy by ligand is termed the Hill slope (Fig.3.2). Where an 81-fold increase in ligand is required to shift receptor occupancy from 10 to 90 percent a Hill slope of 1 is generated and ligand binding is considered non-cooperative. When less than an 81-fold difference in ligand concentration is required to shift the receptor occupancy from 10 to 90 percent a Hill slope of greater than 1 is generated. A Hill slope greater than 1 is indicative of positive cooperative ligand binding, which implies an increase in the ligand binding affinity by the receptor. A Hill slope of 1 reflects a single binding site on the receptor or receptor complex, while a Hill slope greater than 1 can only be achieved where more than one binding site exists. The Hill slope indicates the minimal number of binding sites possible. Therefore, a Hill slope between 1 and 2 suggests the existence of 2 binding sites. Changes in receptor concentration have been directly linked to shifts in Hill slope. Notides *et al.* (216) demonstrated a relationship between the concentration of the ER and Hill slope, where increasing ER levels brought about an increase in the Hill slope. A shift from non-cooperative ligand

binding at low ER concentrations to positive cooperative ligand binding at high ER concentrations was ascribed to dimerization of the ER. At high concentrations of ER (above 2 nM ER in cytosolic preparations) the Hill slope of [³H]-estradiol binding to the ER was 1.68, however, preincubation with low levels of the enzyme trypsin decreased the Hill slope to ~1. The level of trypsin used over the 1 hour co-incubation with [³H]-estradiol at 0°C was shown to result in ER monomers without affecting the number of binding sites significantly. Thus the authors concluded that the loss of positive cooperative ligand binding was not as a result of enzymatic degradation of the ER by trypsin but as a result of the loss in ER dimerization.

In a recent paper, which explored the influence of GR concentration on [³H]-DEX binding, it was found that, similarly to the ER, an increase in GR concentration resulted in a shift from non-cooperative (Hill slope of 0.995) to positive cooperative ligand binding (Hill slope of 1.479) (194). Once again this phenomenon was ascribed to receptor dimerization, as a GR mutant, which displayed an enhanced capacity to homodimerize, retained the capacity for positive cooperative ligand binding at concentrations where the wild type receptor displayed non-cooperative ligand binding.

The increase in ligand affinity at high GR concentrations, reflected by the shift to positive cooperative ligand binding and a decrease in the K_d , could explain the hypersensitivity to GCs displayed by tissues with high GR concentrations. Less ligand would be required to shift GR occupancy from 10 to 90 percent, while 50 percent of receptor occupancy would occur at a lower ligand concentration, implying greater sensitivity to both endogenous as well as exogenous GCs.

1.5.2 Nuclear mobility

Although we have found no studies where the influence of GR concentration on GR nuclear mobility has been analysed, receptor concentration has been demonstrated to influence the nuclear mobility of ER and AR. Marcelli *et al.* (209) demonstrated, in fluorescent recovery after photobleaching (FRAP) studies, that the nuclear mobility of agonist bound GFP tagged AR is related to AR concentration. Increasing AR levels in transiently transfected HeLa cells lead to a 5-fold decrease in the rate of nuclear mobility. Over expression of GFP-ER has been shown to behave in a similar manner (217). The nuclear localization of agonist bound AR and ER results in discrete foci at areas of transcription. It is suggested that increased levels of these receptors allow for greater association with slow moving components of the transcription machinery and DNA resulting in a decrease in nuclear mobility (209, 217).

1.5.3 Transcription by the glucocorticoid receptor

The GR mediated transcriptional response to GCs is influenced by GR concentrations (46). It is an accepted fact that increasing the concentration of a transcription factor, like the GR, will enhance its maximal efficacy, however, this does not imply an increase in potency or the amount of partial agonist activity produced by antagonists (44). In order to affect the concentration of agonist required to elicit 50 percent of the maximal gene expression or repression (potency) a mechanistic change must occur, which facilitates greater sensitivity to ligand. The shift towards greater ligand affinity reflected by a decrease in K_d or positive cooperative ligand binding at high GR concentrations is one such mechanism. Facilitating greater GR occupancy at lower ligand concentrations should result in an increase in transcription potency. Similarly a mechanistic change must also occur in order for an antagonist or weak agonist to display a shift to full agonist behaviour.

Maximal GC dependent (218) as well as GC independent (145) transrepression, referred to as efficacy, increases as GR levels are increased. Furthermore, Zhao *et al.* (35) demonstrated an increase in both the potency ($\log EC_{50}$) and efficacy (maximal response) of DEX induced transrepression by increasing the concentration of transfected GR in promoter reporter assays. They also revealed a biocharacter shift in the transrepression profile of RU486, which shifted from behaving as an antagonist of DEX at low GR concentrations to full agonist behaviour at high GR concentrations.

Similarly, increased GR concentrations cause an increase in the potency and efficacy of GC induced transactivation of promoter reporters (177, 194, 219-221). An increase in the efficacy of ligand independent transactivation has also been reported (145). Furthermore, increased GR concentration also leads to a biocharacter shift from weak agonist to partial agonist behaviour by RU486 (222), dexamethasone-21-mesylate (Dex-Mes) (220) and progesterone (Prog) (219, 220) in transactivation assays. It has been observed that the effects of increased GR concentration on both potency and efficacy are saturable. Voss *et al.* (223) have suggested that at increasingly high GR concentrations the cofactors required to facilitate GR action may become limiting.

Although GR concentration changes have been shown to result in clear shifts in efficacy, potency and biocharacter of partial agonists, none of the above studies have defined the specific GR concentrations at which shifts occur nor have they compared or attempted to correlate the changes in GR induced transcription with a change in K_d or shift from non-cooperative ligand binding to positive cooperative ligand binding.

1.6 Dimerization of the glucocorticoid receptor

1.6.1 Homodimerization and heterodimerization of the glucocorticoid receptor

Upon ligand binding the GR is known to homodimerize (62, 75, 78, 110, 224), a characteristic shared with other members of the SR family, including the ER, PR, MR and AR (224).

Savory *et al.* (62) demonstrated that DEX- as well as RU486-stimulated nuclear import of a nuclear import defective GR mutant was facilitated by over expression of the wild type GR. This cotransport from the cytoplasm into the nucleus of the nuclear import defective mutant GR through interaction with the wild type GR is strong evidence that homodimerization of the GR occurs in the cytoplasm. However, other studies suggest that NR dimerization occurs on the DNA following the sequential binding of two receptor monomers. Dahlman-Wright *et al.* (79) demonstrated using the DBD of the GR that occupancy of the low binding affinity half-site of the GRE is dependent on the initial binding of the GR to the high binding affinity half-site. Similarly, it has been shown that the binding of the DBD of the retinoid-X-receptor to DNA induces conformational changes in the receptor monomer which facilitate dimerization of the receptor at direct repeat recognition elements (225). *In vitro* evidence has also been brought to light which shows ER binding to DNA as either a monomer or a dimer (226). Tellingly, it has been shown that the GRE has a greater affinity for the GR dimer than for the GR monomer. Binding of the GR dimer to the imperfect palindromic GRE of the tyrosine amino transferase (TAT) gene (**TGTACA**gga**TGTTCT**) has a K_d of 2.56nM, while association of the GR monomer to one site of this GRE has a K_d of 62nM (75). Similarly, Drouin *et al.* (74) demonstrated a 5-fold decrease in GRE affinity through GR monomer binding than through dimer binding. Furthermore, they revealed that activated GR binds to DNA as a preformed dimer and not in a stepwise fashion. When increasing concentrations of purified GR were added to a fixed concentration of GRE probe and run in an electrophoretic mobility shift assay (EMSA) a singleband representing GR dimers associated to the GRE was revealed (74). This result is consistent with the finding that the GR monomer displays a lower affinity for the GRE than the GR dimer (75),(74) as the GR dimer binds preferentially to the GRE. These studies present strong evidence that the activated GR is capable of DNA independent dimerization and that ligand induced DNA binding of the GR occurs primarily through the dimer.

Dimerization of the GR to other SRs has also been observed. GR heterodimerization to the MR (227), as well as to the AR (228), occurs in the nucleus only and is believed to require monomeric receptor binding to the half-sites of hormone response elements (HRE) in order for dimerization to be achieved. To clarify the SRs, AR, MR, PR and GR display similar binding affinity for many promoters and the terms HRE and GRE are often used interchangeably, it is thus possible for the association of a GR as

well as either an MR or AR on the two half-sites of an HRE. Heterodimerization of the GR with MR or AR can result in heterodimer specific transactivation via HREs (227, 228), while GR heterodimerization with the MR leads to impaired transactivation via GREs (229). Thus, these interactions may play a part in tissue specific GC responses in tissues where these receptors are co-expressed. However, dimerization of the GR favours homodimerization. Where as heterodimerization appears to be limited to the nucleus (62, 227), homodimerization occurs both independently of (78) and dependently on (79) DNA binding. Furthermore, although co-immunoprecipitation (Co-IP) as well as fluorescent resonance energy transfer (FRET) experiments have revealed a high degree of ligand independent homodimerization of the GR in transiently transfected cells over expressing the GR (9, 41), no ligand independent heterodimerization has been reported. As GR homodimerization is the primary form of GR dimerization, we will refer to it as dimerization and refer to heterodimerization specifically when discussing GR dimerization to other SRs.

1.6.2 The D-loop and ligand binding domain

As mentioned earlier the GR has two dimerization domains, one within the LBD and one in the DBD. Both of these are necessary for optimal dimer formation (Fig.1.8) (75). Dahlman-Wright *et al.* (76) identified 5 amino acids (amino acids 458 to 462 in the human GR) within the second zinc finger of the DBD, which when mutated abolished high affinity GR binding to the DNA as defined by a significant increase in the K_d of GR binding to DNA. As GR dimerization is required to elicit high affinity DNA binding it was concluded that these 5 amino acids play a significant role in the dimerization of the GR. These 5 amino acids have subsequently been termed the D-loop (Fig.1.10).

Although crystallographic studies of the GR LBD consisting of amino acids 521 to 777, which does not include the DBD, have shown that ligand dependent dimerization of the LBD alone is also possible, the interaction is relatively weak displaying a K_d for dimerization of 1.5 μ M (110). In comparison Segard-Maurel *et al.* (75) determined the K_d of activated and non-truncated GR dimerization independent of DNA binding as 3.9nM in cell cytosol. The affinity for GR dimerization is therefore 385-fold higher in the whole protein than for the LBD alone. Dimerization of a truncated GR mutant that does not contain the LBD has also been demonstrated, further supporting the importance of the D-loop in dimerization (62). It is therefore likely that the activated GR exists in equilibrium as either a monomer or a dimer where increased GR concentrations shift the balance towards a higher concentration of dimerized receptor (194).

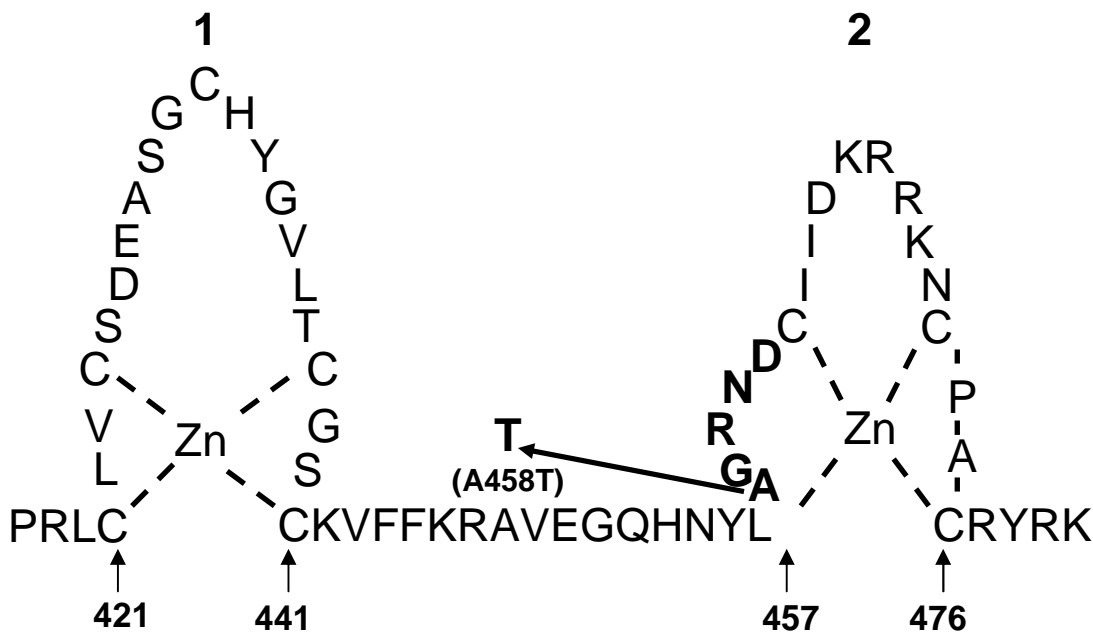


Figure 1.10. **The amino acid sequence of the two zinc fingers of the human GR.** Zinc fingers one and two are labelled while the 5 amino acids which make up the D-loop are indicated in bold type. The A to T mutation that results in the dimerization defective mutation at position 458 is indicated.

1.6.3 Dimerization deficient glucocorticoid receptor

Based on work by Kaspar *et al.* (230) in the AR, which demonstrated inhibition of dimerization due to a single amino acid exchange in the D-loop, Heck *et al.* (231) created a dimerization deficient GR mutant, through the exchange of alanine to threonine at position 458, in the human GR. We will henceforth refer to GR which contains this amino acid substitution in the D-loop and which is characterized by impaired dimerization as the GRdim. It was demonstrated in gel mobility shift experiments on whole cell extracts of COS-7 cells expressing GRdim and exposed to DEX stimulation that unlike the GR wild type (GRwt), the GRdim did not associate with radio-labelled GRE, suggesting a reduced ability to bind directly to DNA. In DEX induced promoter reporter assays GRdim was also shown to have a greatly reduced capacity to transactivate via a single GRE (GRE-tk-CAT) as well as via a multiple GRE (MMTV-CAT). However, GRdim displayed the same capacity to repress an AP-1 driven promoter reporter as the GRwt (231). This study concluded that GR dimerization is required for DNA binding, that transactivation occurs primarily through the GR dimer and that transrepression of the AP-1 transcription factor is as efficient through the GR monomer as the GR dimer. Dimerization of the GR has been linked to high affinity binding of the receptor to DNA (54), which is prevented through mutation of the D-loop (76). Although GRdim has been demonstrated to have a reduced affinity for DNA it does not prove that dimerization was abrogated by this mutation. Despite the ubiquitous use of this dimerization deficient mutant its ability to dimerize has never actually been reported. Numerous

other dimerization reduced GR mutants exist (232) but the GRdim is the most widely characterised and as a result it is the one we will focus on.

Subsequent research supports the theory that GRdim can not transactivate through a single GRE, however, its capacity to transactivate via multiple GRE containing promoter reporters has been revealed to be greater than that of the GRwt (232, 233). Specifically, Adams *et al.* (232) demonstrate that the GRdim can in fact bind to the promoter of the GR regulated phenylethanolamine N-methyltransferase (PNMT) gene, which contains multiple GREs, although with a slightly reduced affinity than the GRwt, and that it is capable of inducing 3-fold higher levels of transcription via a PNMT promoter driven reporter. Work with endogenous genes reveals that differences in promoter architecture results in varied transcriptional response through both the GRwt as well as the GRdim (234). Of the 10 GR responsive genes studied by Rogatsky *et al.* (234), 3 were induced to at least 50 percent of the GRwt levels by the GRdim, while 1 was more responsive to the GRdim. These findings were supported by the work of Meijsing *et al.* (235) who showed that the GRdim was capable of 30 percent of the GRwt's TAT transactivation capacity and enhanced transactivation through a number of GR responsive gene promoters such as glucocorticoid induced zipper (GILZ), Cgt, Sgk and Pal.

Transgenic mice which express the GRdim as opposed to the wild type receptor display similar properties, namely, a lack of GR binding to DNA and greatly reduced transactivation of GRE containing promoter reporters (197). Furthermore, injection of these mice with DEX did not influence mRNA levels of the GRE containing TAT gene (236). In contrast, tissue from GRdim mice has an equal capacity as that of wild type mice for DEX stimulated down regulation of AP-1 induced collagenase-3 mRNA expression. Reichardt *et al.* (31) went on to prove that these mice retain the ability to repress the inflammatory response of locally irritated skin, the metabolic response to lipopolysaccharides and that repression of NFkB driven transcription is also possible through the GRdim. A recent study which explored the influence of the synthetic GC, prednisolone, on the expression of liver genes in wild type and GRdim mice demonstrated a greatly reduced transcriptional response in the GRdim mice (237). Where as prednisolone treatment influenced the regulation of 518 genes (347 upregulated and 171 down regulated) in GR wild type mice, only 34 genes (29 upregulated and 5 down regulated) were influenced in the GRdim mice (237). Of the genes, which were regulated by both the GRwt and the GRdim, there was on average a two thirds reduction in the response through the GRdim. Clearly GR dimerization is a factor in the ability of the GR to regulate transcription, and that this influence is more pronounced in the physiological system of the transgenic mouse model than in promoter reporter assays.

1.6.4 CpdA abrogates dimerization

A possible mechanism through which CpdA achieves its dissociative behaviour (238-240) has been revealed in two recent articles by Dewint *et al.* (41) and Robertson *et al.* (Addendum B (9)). Unlike DEX, which induces maximal dimerization of the GR, addition of CpdA results in abrogation of GR dimerization as displayed in Co-IP (41) as well as fluorescent resonance energy transfer (FRET) (9) and nuclear immunofluorescence studies of nuclear localization deficient GR (9) experiments. It was found that the action of DEX through the GRdim was similar to that of CpdA through the GRwt in nuclear import, nuclear export and transactivation as well as transrepression assays (9). This offers a strong argument that the loss of dimerization of GR brought about by CpdA results in the dissociated behaviour of the compound. Intriguingly, these studies utilized tissue culture cell lines over expressing GR and display a high degree of ligand independent dimerization of the GR. Ligand independent dimerization ranges from 40 percent to 90 percent of the maximal DEX induced dimerization in the FRET (9) and Co-IP (41) experiments, respectively.

1.7 Summary, hypothesis and aims

1.7.1 Summary

Analysis of the literature has confirmed the influence of GR concentration on ligand binding affinity as well as the response to GCs at a physiological level as well as in tissue culture experiments. Increased GR concentrations result in GC hypersensitivity in individuals and in an increase in the efficacy, potency and biocharacter of partial agonists in promoter reporter assays. Low GR levels are associated with GC hyposensitivity in patients and reduced response in promoter reporter assays. It is clear that there is a vast difference in the level of GR expression between tissues as well as between individuals within the same tissue. Furthermore, GR concentration may differ in the same tissue type in the same individual due to diseases such as cancer or physiological trauma such as muscle sepsis. This variance in GR concentration has been directly linked to GC hypersensitivity in the case of GR over expression and GC resistance in the case of GR suppression.

The increased ligand binding affinity and shift to positive cooperative ligand binding as well as increased potency and shift in biocharacter of partial agonists in both transactivation as well as transrepression due to increased GR concentrations suggest the involvement of a mechanistic alteration in GR conformation at heightened GR levels. A mechanistic alteration implies a change in the conformation of the receptor itself most probably the ligand binding site, which facilitates cooperative ligand binding and an increase in ligand binding affinity. A direct influence of a GR

concentration dependent mechanistic change in GR is illustrated by studies, which have shown an increase in ligand binding affinity and a shift from non-cooperative ligand binding to positive cooperative ligand binding at high GR concentrations. Dimerization of the GR has been implicated in the shift from non-cooperative to positive cooperative ligand binding at high GR concentrations, however, no attempt has been made to correlate this with ligand binding affinity.

1.7.2 Hypothesis

As reviewed in this Chapter, a number of studies have shown that GR concentration has a direct influence on the ligand binding behaviour of the GR, affecting both K_d and Hill slope. GR concentration has also been shown to affect the potency of agonists and the biocharacter of partial agonists. Unfortunately, none of the studies reviewed have quantified the concentrations of GR required to elicit these shifts in behaviour so inter experimental comparison is speculative. Nonetheless it is highly plausible that increases in GR concentration result in a GR dimerization dependent increase in ligand binding affinity that facilitates an increase in transcriptional potency.

It has been reported that positive cooperative ligand binding to the GR at high GR concentrations demonstrates a Hill slope of ~ 1.5 , which can only be achieved through ligand association to a receptor or receptor complex containing 2 binding sites, the GR dimer. Ligand independent dimerization of the GR could account for the shift from non-cooperative to positive cooperative ligand binding to the GR as this protein-protein interaction creates a GR complex containing two binding sites.

The canonical model of ligand binding to the GR monomer is non-cooperative (Fig.1.11A). We propose that ligand independent dimerization of the GR occurs at high GR concentrations (Fig.1.11B), which allows for positive cooperative ligand binding to the two ligand binding sites on the GR dimer. If our assumption is correct high concentrations of GRdim will continue to display non-cooperative ligand binding due to this mutant's impaired ability to dimerize (Fig.1.11C). Furthermore, the use of GRdim may provide insight into the influence of GR dimerization on the down stream behaviour of the GR.

An increase in ligand binding affinity at high GR concentrations would allow for an increase in transcriptional potency and biocharacter shift in partial agonists. At a physiological level differences in biological response at differing GR concentrations may be due to cooperative ligand binding and an increase in ligand binding affinity at high GR concentrations. Therefore we hypothesize that:

Ligand independent dimerization of the GR at high concentrations facilitates positive cooperative ligand binding and a concomitant increase in ligand binding affinity, which may affect down stream signalling events such as nuclear localization and transcription.

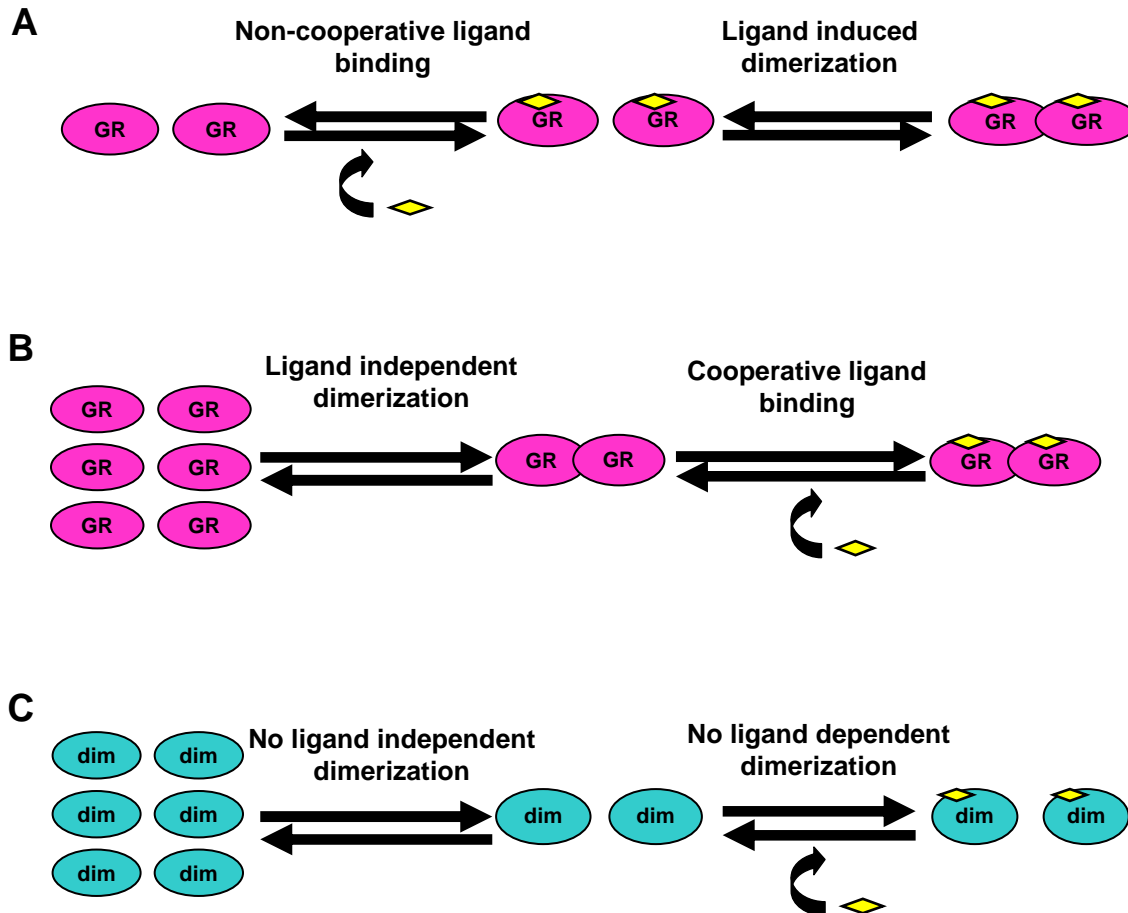


Figure 1.11. **Theoretical models of ligand binding to the GRwt and GRdim.** (A) At low GRwt levels non-cooperative ligand binding to GR monomers results in dimerization of the GR. (B) High GR levels result in ligand independent dimerization of the GR, which allows for positive cooperative ligand binding. (C) At high levels the GRdim remains monomeric resulting in non-cooperative ligand binding after which it does not dimerize.

1.7.3 Aims

Our four major aims are each investigated in a separate results chapter. In this section we will present an overview of the methodology and objectives which underpin each of these chapters. For ease of reference, we will present the over arching aim of each results chapter in a separate paragraph.

Aim 1: Establish GR concentrations that display cooperative and non-cooperative ligand binding as well as a significant difference in K_d

Central to our hypothesis is the establishment of GR concentrations in transiently transfected COS-1 cells which display either non-cooperative or positive cooperative ligand binding. Using whole cell saturation ligand binding assays, we will define three levels of GR concentration which we will term low, medium and high, respectively. Saturation ligand binding generates both a Hill slope as well as a K_d , which makes it possible for us to identify the shift from non-cooperative to positive cooperative ligand binding as well as to quantify a change in ligand binding affinity. In addition, we will include the GRdim mutant in our saturation ligand binding studies in order to investigate the influence of dimerization on the two ligand binding parameters investigated. Results are reported in Chapter 3.

Aim 2: Confirm that ligand independent dimerization of the GR occurs at GR concentrations that display cooperative ligand binding and increased ligand binding affinity

In order for cooperative ligand binding to occur we hypothesize that ligand independent dimerization of the GR must occur. In Chapter 4 we make use of Co-IP and FRET techniques in order to test whether ligand independent dimerization of the GR correlates with an increase in ligand binding affinity and cooperative ligand binding. Co-IP of low, medium and high GR concentrations will be employed to demonstrate the level of GFP-GRwt or GFP-GRdim dimerization to Flag-GRwt. We will examine the levels of ligand independent GR dimerization as well as the level of dimerization brought about by stimulation with DEX and by the dimerization abrogating compound, CpdA. While Co-IP will be carried out on cell lysates, FRET relies on live cells expressing low, medium and high levels of cyan fluorescent protein (CFP) tagged GR and yellow fluorescent protein (YFP) tagged GR. Dimerization of CFP-GR and YFP-GR will be quantified as an increase in the level of corrected FRET signal, which will be measured prior to DEX induction and for 30 minutes afterwards. Ligand independent dimerization of the GR will be quantified as either the fold ligand induced maximal FRET response or through mathematical modelling of the FRET results.

Aim 3: Determine the influence of positive cooperative ligand binding and increased ligand binding affinity, GR concentration and GR dimerization on glucocorticoid receptor nuclear import, export and distribution

In Chapter 5, live cell nuclear import and export studies will be conducted on cells expressing medium and high levels of GFP-GRwt or GFP-GRdim. The nuclear import rate will be measured following stimulation with a range of test compounds, while export will be measured following the washout of DEX. Cells expressing medium and high GFP-GRwt or GFP-GRdim will be stimulated with either DEX or CpdA prior to being permeabilized and fixed. Nuclear distribution of the GFP tagged receptors will be quantified and related directly to random or non-random nuclear distribution. An indirect method for fluorescence labelling of the GR, termed immunofluorescence, will also be employed to determine the nuclear import and export rates of low and medium GRwt or GRdim concentrations. The nuclear

import rate following DEX or CpdA stimulation will be tested in order to elucidate the effect of dimerization on nuclear import in the GRwt. The use of GFP-GRdim or GRdim in the live cell or immunofluorescence assays, respectively, will allow insight into the influence dimerization may have on the rate of nuclear import and export as well as the pattern of nuclear distribution.

Aim 4: Establish the influence cooperative ligand binding and increased ligand binding affinity has on GR mediated transcription

Finally, the major function of the GR, namely its ability to induce transcription both dependent and independent of ligand binding, will be put under the spot light in Chapter 6. We will examine the influence of GR concentration, the ability to dimerize and positive cooperative ligand binding on transrepression of a promoter reporter as well as transactivation through a single and multiple GRE containing promoter reporter and the endogenous GILZ gene. Potency ($\log EC_{50}$), efficacy (maximal induction or repression) and the biocharacter of a range of ligands relative to DEX will be determined in order to quantify transcription. Transrepression of an NF κ B promoter containing construct will be tested at varying GRwt and GRdim concentrations stimulated by DEX or CpdA in order to elucidate the influence of GR dimerization, cooperative ligand binding and an increase in ligand binding affinity. A similar methodology will be applied to the investigation of transactivation through a single as well as a multiple GRE containing promoter reporter construct and the endogenous GC responsive GILZ gene. Use of varying GRwt concentrations allows for the elucidation of cooperative ligand binding and an increase in ligand binding affinity on transcription, while the behaviour of the same concentrations of GRdim reveal the influence of dimerization.

1.8 Bibliography

1. Lu NZ, *et al* (2006) International union of pharmacology. LXV. the pharmacology and classification of the nuclear receptor superfamily: Glucocorticoid, mineralocorticoid, progesterone, and androgen receptors. *Pharmacol Rev* 58: 782-797.
2. Torpy DJ & Ho JT (2007) Corticosteroid-binding globulin gene polymorphisms: Clinical implications and links to idiopathic chronic fatigue disorders. *Clin Endocrinol (Oxf)* 67: 161-167.
3. Lin HY, Muller YA & Hammond GL (2010) Molecular and structural basis of steroid hormone binding and release from corticosteroid-binding globulin. *Mol Cell Endocrinol* 316: 3-12.
4. Hammond GL, Smith CL & Underhill DA (1991) Molecular studies of corticosteroid binding globulin structure, biosynthesis and function. *J Steroid Biochem Mol Biol* 40: 755-762.
5. Siiteri PK, *et al* (1982) The serum transport of steroid hormones. *Recent Prog Horm Res* 38: 457-510.

6. Newton R (2000) Molecular mechanisms of glucocorticoid action: What is important?. *Thorax* 55: 603-613.
7. Ronacher K, *et al* (2009) Ligand-selective transactivation and transrepression via the glucocorticoid receptor: Role of cofactor interaction. *Mol Cell Endocrinol* 299: 219-231.
8. Louw A, Swart P, de Kock SS & van der Merwe KJ (1997) Mechanism for the stabilization in vivo of the aziridine precursor 2-(4-acetoxyphenyl)-2-chloro-N-methyl-ethylammonium chloride by serum proteins. *Biochem Pharmacol* 53: 189-197.
9. Robertson S, *et al* (2010) Abrogation of glucocorticoid receptor dimerization correlates with dissociated glucocorticoid behavior of compound a. *J Biol Chem* 285: 8061-8075.
10. Vicent GP, Pecci A, Ghini A, Piwien-Pilipuk G & Galigniana MD (2002) Differences in nuclear retention characteristics of agonist-activated glucocorticoid receptor may determine specific responses. *Exp Cell Res* 276: 142-154.
11. Schaaf MJ & Cidlowski JA (2003) Molecular determinants of glucocorticoid receptor mobility in living cells: The importance of ligand affinity. *Mol Cell Biol* 23: 1922-1934.
12. Chrousos GP, *et al* (1982) Primary cortisol resistance in man. A glucocorticoid receptor-mediated disease. *J Clin Invest* 69: 1261-1269.
13. Charmandari E, *et al* (2001) Joint growth hormone and cortisol spontaneous secretion is more asynchronous in older females than in their male counterparts. *J Clin Endocrinol Metab* 86: 3393-3399.
14. Desvergne B & Heligon C (2009) Steroid hormone pulsing drives cyclic gene expression. *Nat Cell Biol* 11: 1051-1053.
15. Windle RJ, Wood SA, Shanks N, Lightman SL & Ingram CD (1998) Ultradian rhythm of basal corticosterone release in the female rat: Dynamic interaction with the response to acute stress. *Endocrinology* 139: 443-450.
16. Droste SK, *et al* (2008) Corticosterone levels in the brain show a distinct ultradian rhythm but a delayed response to forced swim stress. *Endocrinology* 149: 3244-3253.
17. Stavreva DA, *et al* (2009) Ultradian hormone stimulation induces glucocorticoid receptor-mediated pulses of gene transcription. *Nat Cell Biol* 11: 1093-1102.
18. McNally JG, Muller WG, Walker D, Wolford R & Hager GL (2000) The glucocorticoid receptor: Rapid exchange with regulatory sites in living cells. *Science* 287: 1262-1265.
19. Herman JP, Ostrander MM, Mueller NK & Figueiredo H (2005) Limbic system mechanisms of stress regulation: Hypothalamo-pituitary-adrenocortical axis. *Prog Neuropsychopharmacol Biol Psychiatry* 29: 1201-1213.
20. Dedovic K, Duchesne A, Andrews J, Engert V & Pruessner JC (2009) The brain and the stress axis: The neural correlates of cortisol regulation in response to stress. *Neuroimage* 47: 864-871.
21. Sarabdjitsingh RA, *et al* (2010) Disrupted corticosterone pulsatile patterns attenuate responsiveness to glucocorticoid signaling in rat brain. *Endocrinology* 151: 1177-1186.

22. Katzung BG (2004) *Basic and clinical pharmacology*
23. Loew D, Schuster O & Graul EH (1986) Dose-dependent pharmacokinetics of dexamethasone. *Eur J Clin Pharmacol* 30: 225-230.
24. Chriguier RS, *et al* (2005) Glucocorticoid sensitivity in young healthy individuals: In vitro and in vivo studies. *J Clin Endocrinol Metab* 90: 5978-5984.
25. Ebrecht M, *et al* (2000) Tissue specificity of glucocorticoid sensitivity in healthy adults. *J Clin Endocrinol Metab* 85: 3733-3739.
26. Pretorius E, Wallner B & Marx J (2006) Cortisol resistance in conditions such as asthma and the involvement of 11beta-HSD-2: A hypothesis. *Horm Metab Res* 38: 368-376.
27. Cosio BG, Torrego A & Adcock IM (2005) Molecular mechanisms of glucocorticoids. *Arch Bronconeumol* 41: 34-41.
28. Costlow ME, Pui CH & Dahl GV (1982) Glucocorticoid receptors in childhood acute lymphocytic leukemia. *Cancer Res* 42: 4801-4806.
29. Roberts IS, Stratopoulos C, Zilvetti M, Reddy S & Friend PJ (2009) Impact of immunosuppression on the incidence of early subclinical renal allograft rejection: Implications for protocol biopsy policy. *Transpl Int* 22: 831-836.
30. Huizenga NA, *et al* (1998) A polymorphism in the glucocorticoid receptor gene may be associated with and increased sensitivity to glucocorticoids in vivo. *J Clin Endocrinol Metab* 83: 144-151.
31. Reichardt HM, *et al* (2001) Repression of inflammatory responses in the absence of DNA binding by the glucocorticoid receptor. *EMBO J* 20: 7168-7173.
32. Schacke H, Docke WD & Asadullah K (2002) Mechanisms involved in the side effects of glucocorticoids. *Pharmacol Ther* 96: 23-43.
33. Resche-Rigon M & Gronemeyer H (1998) Therapeutic potential of selective modulators of nuclear receptor action. *Curr Opin Chem Biol* 2: 501-507.
34. Schacke H, *et al* (2002) SEGRAs: A novel class of anti-inflammatory compounds. *Ernst Schering Res found Workshop* (40): 357-371.
35. Zhao Q, Pang J, Favata MF & Trzaskos JM (2003) Receptor density dictates the behavior of a subset of steroid ligands in glucocorticoid receptor-mediated transrepression. *Int Immunopharmacol* 3: 1803-1817.
36. Vayssiere BM, *et al* (1997) Synthetic glucocorticoids that dissociate transactivation and AP-1 transrepression exhibit antiinflammatory activity in vivo. *Mol Endocrinol* 11: 1245-1255.
37. Fryer CJ, Kinyamu HK, Rogatsky I, Garabedian MJ & Archer TK (2000) Selective activation of the glucocorticoid receptor by steroid antagonists in human breast cancer and osteosarcoma cells. *J Biol Chem* 275: 17771-17777.

38. Schacke H, *et al* (2004) Dissociation of transactivation from transrepression by a selective glucocorticoid receptor agonist leads to separation of therapeutic effects from side effects. *Proc Natl Acad Sci U S A* 101: 227-232.
39. Coghlan MJ, *et al* (2003) A novel antiinflammatory maintains glucocorticoid efficacy with reduced side effects. *Mol Endocrinol* 17: 860-869.
40. Louw A & Swart P (1999) *Salsola tuberculiformis* *botschantzev* and an aziridine precursor analog mediates the in vivo increase in free corticosterone and decrease in corticosteroid-binding globulin in female wistar rats. *Endocrinology* 140: 2044-2053.
41. Dewint P, *et al* (2008) A plant-derived ligand favoring monomeric glucocorticoid receptor conformation with impaired transactivation potential attenuates collagen-induced arthritis. *J Immunol* 180: 2608-2615.
42. De Bosscher K & Haegeman G (2009) Minireview: Latest perspectives on antiinflammatory actions of glucocorticoids. *Mol Endocrinol* 23: 281-291.
43. Lu NZ, Collins JB, Grissom SF & Cidlowski JA (2007) Selective regulation of bone cell apoptosis by translational isoforms of the glucocorticoid receptor. *Mol Cell Biol* 27: 7143-7160.
44. Stoney Simons S, Jr (2003) The importance of being varied in steroid receptor transactivation. *Trends Pharmacol Sci* 24: 253-259.
45. Simons SS, Jr (2008) What goes on behind closed doors: Physiological versus pharmacological steroid hormone actions. *Bioessays* 30: 744-756.
46. Newton R, Leigh R & Giembycz MA (2010) Pharmacological strategies for improving the efficacy and therapeutic ratio of glucocorticoids in inflammatory lung diseases. *Pharmacol Ther* 125: 286-327.
47. Heitzer MD, Wolf IM, Sanchez ER, Witchel SF & DeFranco DB (2007) Glucocorticoid receptor physiology. *Rev Endocr Metab Disord* 8: 321-330.
48. Gross KL & Cidlowski JA (2008) Tissue-specific glucocorticoid action: A family affair. *Trends Endocrinol Metab* 19: 331-339.
49. De Bosscher K, Van Craenenbroeck K, Meijer OC & Haegeman G (2008) Selective transrepression versus transactivation mechanisms by glucocorticoid receptor modulators in stress and immune systems. *Eur J Pharmacol* 583: 290-302.
50. Robinson-Rechavi M, Carpentier AS, Duffraisse M & Laudet V (2001) How many nuclear hormone receptors are there in the human genome?. *Trends Genet* 17: 554-556.
51. Cole TJ, *et al* (1995) Targeted disruption of the glucocorticoid receptor gene blocks adrenergic chromaffin cell development and severely retards lung maturation. *Genes Dev* 9: 1608-1621.
52. Mittelstadt PR & Ashwell JD (2003) Disruption of glucocorticoid receptor exon 2 yields a ligand-responsive C-terminal fragment that regulates gene expression. *Mol Endocrinol* 17: 1534-1542.
53. Pujols L, Mullol J, Torrego A & Picado C (2004) Glucocorticoid receptors in human airways. *Allergy* 59: 1042-1052.

54. Hecht K, *et al* (1997) Evidence that the beta-isoform of the human glucocorticoid receptor does not act as a physiologically significant repressor. *J Biol Chem* 272: 26659-26664.
55. Oakley RH, Sar M & Cidlowski JA (1996) The human glucocorticoid receptor beta isoform. expression, biochemical properties, and putative function. *J Biol Chem* 271: 9550-9559.
56. Duma D, Jewell CM & Cidlowski JA (2006) Multiple glucocorticoid receptor isoforms and mechanisms of post-translational modification. *J Steroid Biochem Mol Biol* 102: 11-21.
57. Dahia PL, *et al* (1997) Expression of glucocorticoid receptor gene isoforms in corticotropin-secreting tumors. *J Clin Endocrinol Metab* 82: 1088-1093.
58. Oakley RH, Webster JC, Sar M, Parker CR, Jr & Cidlowski JA (1997) Expression and subcellular distribution of the beta-isoform of the human glucocorticoid receptor. *Endocrinology* 138: 5028-5038.
59. Pujols L, *et al* (2002) Expression of glucocorticoid receptor alpha- and beta-isoforms in human cells and tissues. *Am J Physiol Cell Physiol* 283: C1324-31.
60. Bookout AL, *et al* (2006) Anatomical profiling of nuclear receptor expression reveals a hierarchical transcriptional network. *Cell* 126: 789-799.
61. Banerjee A, *et al* (2008) Control of glucocorticoid and progesterone receptor subcellular localization by the ligand-binding domain is mediated by distinct interactions with tetratricopeptide repeat proteins. *Biochemistry* 47: 10471-10480.
62. Savory JG, *et al* (2001) Glucocorticoid receptor homodimers and glucocorticoid-mineralocorticoid receptor heterodimers form in the cytoplasm through alternative dimerization interfaces. *Mol Cell Biol* 21: 781-793.
63. Hache RJ, Tse R, Reich T, Savory JG & Lefebvre YA (1999) Nucleocytoplasmic trafficking of steroid-free glucocorticoid receptor. *J Biol Chem* 274: 1432-1439.
64. Caamano CA, Morano MI, Dalman FC, Pratt WB & Akil H (1998) A conserved proline in the hsp90 binding region of the glucocorticoid receptor is required for hsp90 heterocomplex stabilization and receptor signaling. *J Biol Chem* 273: 20473-20480.
65. Pemberton LF & Paschal BM (2005) Mechanisms of receptor-mediated nuclear import and nuclear export. *Traffic* 6: 187-198.
66. Davies TH, Ning YM & Sanchez ER (2002) A new first step in activation of steroid receptors: Hormone-induced switching of FKBP51 and FKBP52 immunophilins. *J Biol Chem* 277: 4597-4600.
67. Tanaka M, Nishi M, Morimoto M, Sugimoto T & Kawata M (2003) Yellow fluorescent protein-tagged and cyan fluorescent protein-tagged imaging analysis of glucocorticoid receptor and importins in single living cells. *Endocrinology* 144: 4070-4079.
68. Harrell JM, *et al* (2004) Evidence for glucocorticoid receptor transport on microtubules by dynein. *J Biol Chem* 279: 54647-54654.
69. Galigniana MD, *et al* (1998) Heat shock protein 90-dependent (geldanamycin-inhibited) movement of the glucocorticoid receptor through the cytoplasm to the nucleus requires intact cytoskeleton. *Mol Endocrinol* 12: 1903-1913.

70. Echeverria PC & Picard D (2010) Molecular chaperones, essential partners of steroid hormone receptors for activity and mobility. *Biochim Biophys Acta* 1803: 641-649.
71. Echeverria PC, *et al* (2009) Nuclear import of the glucocorticoid receptor-hsp90 complex through the nuclear pore complex is mediated by its interaction with Nup62 and importin beta. *Mol Cell Biol* 29: 4788-4797.
72. Savory JG, *et al* (1999) Discrimination between NL1- and NL2-mediated nuclear localization of the glucocorticoid receptor. *Mol Cell Biol* 19: 1025-1037.
73. Defranco DB, *et al* (1995) Nucleocytoplasmic shuttling of steroid receptors. *Vitam Horm* 51: 315-338.
74. Drouin J, *et al* (1992) Homodimer formation is rate-limiting for high affinity DNA binding by glucocorticoid receptor. *Mol Endocrinol* 6: 1299-1309.
75. Segard-Maurel I, *et al* (1996) Glucocorticosteroid receptor dimerization investigated by analysis of receptor binding to glucocorticosteroid responsive elements using a monomer-dimer equilibrium model. *Biochemistry* 35: 1634-1642.
76. Dahlman-Wright K, Wright A, Gustafsson JA & Carlstedt-Duke J (1991) Interaction of the glucocorticoid receptor DNA-binding domain with DNA as a dimer is mediated by a short segment of five amino acids. *J Biol Chem* 266: 3107-3112.
77. De Kloet ER, Vreugdenhil E, Oitzl MS & Joels M (1998) Brain corticosteroid receptor balance in health and disease. *Endocr Rev* 19: 269-301.
78. Wrangé O, Eriksson P & Perlmann T (1989) The purified activated glucocorticoid receptor is a homodimer. *J Biol Chem* 264: 5253-5259.
79. Dahlman-Wright K, Siltala-Roos H, Carlstedt-Duke J & Gustafsson JA (1990) Protein-protein interactions facilitate DNA binding by the glucocorticoid receptor DNA-binding domain. *J Biol Chem* 265: 14030-14035.
80. Hayashi R, Wada H, Ito K & Adcock IM (2004) Effects of glucocorticoids on gene transcription. *Eur J Pharmacol* 500: 51-62.
81. De Bosscher K, Vanden Berghe W & Haegeman G (2003) The interplay between the glucocorticoid receptor and nuclear factor-kappaB or activator protein-1: Molecular mechanisms for gene repression. *Endocr Rev* 24: 488-522.
82. Meijsing SH, Elbi C, Luecke HF, Hager GL & Yamamoto KR (2007) The ligand binding domain controls glucocorticoid receptor dynamics independent of ligand release. *Mol Cell Biol* 27: 2442-2451.
83. Stavreva DA, Muller WG, Hager GL, Smith CL & McNally JG (2004) Rapid glucocorticoid receptor exchange at a promoter is coupled to transcription and regulated by chaperones and proteasomes. *Mol Cell Biol* 24: 2682-2697.
84. Elbi C, *et al* (2004) Molecular chaperones function as steroid receptor nuclear mobility factors. *Proc Natl Acad Sci U S A* 101: 2876-2881.

85. Reik A, Schutz G & Stewart AF (1991) Glucocorticoids are required for establishment and maintenance of an alteration in chromatin structure: Induction leads to a reversible disruption of nucleosomes over an enhancer. *EMBO J* 10: 2569-2576.
86. Nagaich AK, *et al* (2004) Subnuclear trafficking and gene targeting by steroid receptors. *Ann N Y Acad Sci* 1024: 213-220.
87. George AA, Schiltz RL & Hager GL (2009) Dynamic access of the glucocorticoid receptor to response elements in chromatin. *Int J Biochem Cell Biol* 41: 214-224.
88. Hager GL, Nagaich AK, Johnson TA, Walker DA & John S (2004) Dynamics of nuclear receptor movement and transcription. *Biochim Biophys Acta* 1677: 46-51.
89. Freeman BC & Yamamoto KR (2002) Disassembly of transcriptional regulatory complexes by molecular chaperones. *Science* 296: 2232-2235.
90. Tago K, Tsukahara F, Naruse M, Yoshioka T & Takano K (2004) Regulation of nuclear retention of glucocorticoid receptor by nuclear Hsp90. *Mol Cell Endocrinol* 213: 131-138.
91. Yang J, Liu J & DeFranco DB (1997) Subnuclear trafficking of glucocorticoid receptors in vitro: Chromatin recycling and nuclear export. *J Cell Biol* 137: 523-538.
92. Silva CM, *et al* (1994) Regulation of the human glucocorticoid receptor by long-term and chronic treatment with glucocorticoid. *Steroids* 59: 436-442.
93. Burnstein KL, Bellingham DL, Jewell CM, Powell-Oliver FE & Cidlowski JA (1991) Autoregulation of glucocorticoid receptor gene expression. *Steroids* 56: 52-58.
94. Pedersen KB, Geng CD & Vedeckis WV (2004) Three mechanisms are involved in glucocorticoid receptor autoregulation in a human T-lymphoblast cell line. *Biochemistry* 43: 10851-10858.
95. Dong Y, Poellinger L, Gustafsson JA & Okret S (1988) Regulation of glucocorticoid receptor expression: Evidence for transcriptional and posttranslational mechanisms. *Mol Endocrinol* 2: 1256-1264.
96. Burnstein KL, Jewell CM, Sar M & Cidlowski JA (1994) Intragenic sequences of the human glucocorticoid receptor complementary DNA mediate hormone-inducible receptor messenger RNA down-regulation through multiple mechanisms. *Mol Endocrinol* 8: 1764-1773.
97. Webster JC, *et al* (1997) Mouse glucocorticoid receptor phosphorylation status influences multiple functions of the receptor protein. *J Biol Chem* 272: 9287-9293.
98. Wallace AD & Cidlowski JA (2001) Proteasome-mediated glucocorticoid receptor degradation restricts transcriptional signaling by glucocorticoids. *J Biol Chem* 276: 42714-42721.
99. Lee DH & Goldberg AL (1998) Proteasome inhibitors: Valuable new tools for cell biologists. *Trends Cell Biol* 8: 397-403.
100. DeMartino GN & Slaughter CA (1999) The proteasome, a novel protease regulated by multiple mechanisms. *J Biol Chem* 274: 22123-22126.

101. Avenant C, Kotitschke A & Hapgood JP (2010) Glucocorticoid receptor phosphorylation modulates transcription efficacy through GRIP-1 recruitment. *Biochemistry* 49: 972-985.
102. Avenant C, Ronacher K, Stubrud E, Louw A & Hapgood JP (2010) Role of ligand-dependent GR phosphorylation and half-life in determination of ligand-specific transcriptional activity. *Mol Cell Endocrinol* 327: 72-88.
103. Liu J & DeFranco DB (2000) Protracted nuclear export of glucocorticoid receptor limits its turnover and does not require the exportin 1/CRM1-directed nuclear export pathway. *Mol Endocrinol* 14: 40-51.
104. Xu M, Chakraborti PK, Garabedian MJ, Yamamoto KR & Simons SS (1996) Modular structure of glucocorticoid receptor domains is not equivalent to functional independence. stability and activity of the steroid binding domain are controlled by sequences in separate domains. *J Biol Chem* 271: 21430-21438.
105. Adcock IM (2000) Molecular mechanisms of glucocorticosteroid actions. *Pulm Pharmacol Ther* 13: 115-126.
106. Freedman ND & Yamamoto KR (2004) Importin 7 and importin alpha/importin beta are nuclear import receptors for the glucocorticoid receptor. *Mol Biol Cell* 15: 2276-2286.
107. Jewell CM, *et al* (1995) Immunocytochemical analysis of hormone mediated nuclear translocation of wild type and mutant glucocorticoid receptors. *J Steroid Biochem Mol Biol* 55: 135-146.
108. Wan Y, Coxe KK, Thackray VG, Housley PR & Nordeen SK (2001) Separable features of the ligand-binding domain determine the differential subcellular localization and ligand-binding specificity of glucocorticoid receptor and progesterone receptor. *Mol Endocrinol* 15: 17-31.
109. Carrigan A, *et al* (2007) An active nuclear retention signal in the glucocorticoid receptor functions as a strong inducer of transcriptional activation. *J Biol Chem* 282: 10963-10971.
110. Bledsoe RK, *et al* (2002) Crystal structure of the glucocorticoid receptor ligand binding domain reveals a novel mode of receptor dimerization and coactivator recognition. *Cell* 110: 93-105.
111. Ballard PL, Baxter JD, Higgins SJ, Rousseau GG & Tomkins GM (1974) General presence of glucocorticoid receptors in mammalian tissues. *Endocrinology* 94: 998-1002.
112. Ho AD, Stojakowits S, Pralle H, Dorner M & Hunstein W (1983) Glucocorticoid receptor level, terminal deoxynucleotidyl transferase activity and initial responsiveness to prednisone and vincristine in leukemia. *Klin Wochenschr* 61: 455-459.
113. Paoletti P, *et al* (1990) Characteristics and biological role of steroid hormone receptors in neuroepithelial tumors. *J Neurosurg* 73: 736-742.
114. Sun X, Fischer DR, Pritts TA, Wray CJ & Hasselgren PO (2002) Expression and binding activity of the glucocorticoid receptor are upregulated in septic muscle. *Am J Physiol Regul Integr Comp Physiol* 282: R509-18.
115. Seckl JR & Walker BR (2001) Minireview: 11beta-hydroxysteroid dehydrogenase type 1- a tissue-specific amplifier of glucocorticoid action. *Endocrinology* 142: 1371-1376.

116. Low SC, *et al* (1994) Sexual dimorphism of hepatic 11 beta-hydroxysteroid dehydrogenase in the rat: The role of growth hormone patterns. *J Endocrinol* 143: 541-548.
117. Walker BR & Andrew R (2006) Tissue production of cortisol by 11beta-hydroxysteroid dehydrogenase type 1 and metabolic disease. *Ann N Y Acad Sci* 1083: 165-184.
118. Moisan MP, Seckl JR & Edwards CR (1990) 11 beta-hydroxysteroid dehydrogenase bioactivity and messenger RNA expression in rat forebrain: Localization in hypothalamus, hippocampus, and cortex. *Endocrinology* 127: 1450-1455.
119. Robson AC, Leckie CM, Seckl JR & Holmes MC (1998) 11 beta-hydroxysteroid dehydrogenase type 2 in the postnatal and adult rat brain. *Brain Res Mol Brain Res* 61: 1-10.
120. Edwards CR, *et al* (1988) Localisation of 11 beta-hydroxysteroid dehydrogenase--tissue specific protector of the mineralocorticoid receptor. *Lancet* 2: 986-989.
121. Borst P & Elferink RO (2002) Mammalian ABC transporters in health and disease. *Annu Rev Biochem* 71: 537-592.
122. Karszen AM, *et al* (2002) The role of the efflux transporter P-glycoprotein in brain penetration of prednisolone. *J Endocrinol* 175: 251-260.
123. Schinkel AH (1999) P-glycoprotein, a gatekeeper in the blood-brain barrier. *Adv Drug Deliv Rev* 36: 179-194.
124. Karszen AM, *et al* (2001) Multidrug resistance P-glycoprotein hampers the access of cortisol but not of corticosterone to mouse and human brain. *Endocrinology* 142: 2686-2694.
125. Guo WX, *et al* (1996) Expression and cytokine regulation of glucocorticoid receptors in kaposi's sarcoma. *Am J Pathol* 148: 1999-2008.
126. Reichardt HM, Umland T, Bauer A, Kretz O & Schutz G (2000) Mice with an increased glucocorticoid receptor gene dosage show enhanced resistance to stress and endotoxic shock. *Mol Cell Biol* 20: 9009-9017.
127. Reul JM, *et al* (1994) Prenatal immune challenge alters the hypothalamic-pituitary-adrenocortical axis in adult rats. *J Clin Invest* 93: 2600-2607.
128. Davies TH, Ning YM & Sanchez ER (2005) Differential control of glucocorticoid receptor hormone-binding function by tetratricopeptide repeat (TPR) proteins and the immunosuppressive ligand FK506. *Biochemistry* 44: 2030-2038.
129. Voutsas IF, *et al* (2007) A novel quantitative flow cytometric method for measuring glucocorticoid receptor (GR) in cell lines: Correlation with the biochemical determination of GR. *J Immunol Methods* 324: 110-119.
130. Lu YS, *et al* (2005) Effects of glucocorticoids on the growth and chemosensitivity of carcinoma cells are heterogeneous and require high concentration of functional glucocorticoid receptors. *World J Gastroenterol* 11: 6373-6380.
131. Yu ZY, *et al* (1981) A study of glucocorticoid receptors in intracranial tumors. *J Neurosurg* 55: 757-760.

132. Beattie CW, Hansen NW & Thomas PA (1985) Steroid receptors in human lung cancer. *Cancer Res* 45: 4206-4214.
133. Driver PM, *et al* (2001) Expression of 11 beta-hydroxysteroid dehydrogenase isozymes and corticosteroid hormone receptors in primary cultures of human trophoblast and placental bed biopsies. *Mol Hum Reprod* 7: 357-363.
134. Lu YS, *et al* (2006) Glucocorticoid receptor expression in advanced non-small cell lung cancer: Clinicopathological correlation and in vitro effect of glucocorticoid on cell growth and chemosensitivity. *Lung Cancer* 53: 303-310.
135. Elakovic I, Perisic T, Cankovic-Kadijevic M & Matic G (2007) Correlation between glucocorticoid receptor binding parameters, blood pressure, and body mass index in a healthy human population. *Cell Biochem Funct* 25: 427-431.
136. Kaiser U, *et al* (1996) Steroid-hormone receptors in cell lines and tumor biopsies of human lung cancer. *Int J Cancer* 67: 357-364.
137. Chikanza IC, Petrou P, Kingsley G, Chrousos G & Panayi GS (1992) Defective hypothalamic response to immune and inflammatory stimuli in patients with rheumatoid arthritis. *Arthritis Rheum* 35: 1281-1288.
138. Schlaghecke R, Kornely E, Wollenhaupt J & Specker C (1992) Glucocorticoid receptors in rheumatoid arthritis. *Arthritis Rheum* 35: 740-744.
139. Tanaka H, Akama H, Ichikawa Y, Makino I & Homma M (1992) Glucocorticoid receptor in patients with lupus nephritis: Relationship between receptor levels in mononuclear leukocytes and effect of glucocorticoid therapy. *J Rheumatol* 19: 878-883.
140. Wilkinson JR, Crea AE, Clark TJ & Lee TH (1989) Identification and characterization of a monocyte-derived neutrophil-activating factor in corticosteroid-resistant bronchial asthma. *J Clin Invest* 84: 1930-1941.
141. Henderson ES (1969) Treatment of acute leukemia. *Semin Hematol* 6: 271-319.
142. Ramdas J, Liu W & Harmon JM (1999) Glucocorticoid-induced cell death requires autoinduction of glucocorticoid receptor expression in human leukemic T cells. *Cancer Res* 59: 1378-1385.
143. Encio IJ & Detera-Wadleigh SD (1991) The genomic structure of the human glucocorticoid receptor. *J Biol Chem* 266: 7182-7188.
144. Oakley RH, Jewell CM, Yudt MR, Bofetiado DM & Cidlowski JA (1999) The dominant negative activity of the human glucocorticoid receptor beta isoform. specificity and mechanisms of action. *J Biol Chem* 274: 27857-27866.
145. Gougat C, *et al* (2002) Overexpression of the human glucocorticoid receptor alpha and beta isoforms inhibits AP-1 and NF-kappaB activities hormone independently. *J Mol Med* 80: 309-318.
146. Hamid QA, *et al* (1999) Increased glucocorticoid receptor beta in airway cells of glucocorticoid-insensitive asthma. *Am J Respir Crit Care Med* 159: 1600-1604.

147. Sousa AR, Lane SJ, Cidlowski JA, Staynov DZ & Lee TH (2000) Glucocorticoid resistance in asthma is associated with elevated in vivo expression of the glucocorticoid receptor beta-isoform. *J Allergy Clin Immunol* 105: 943-950.
148. Whorwood CB, Donovan SJ, Wood PJ & Phillips DI (2001) Regulation of glucocorticoid receptor alpha and beta isoforms and type I 11beta-hydroxysteroid dehydrogenase expression in human skeletal muscle cells: A key role in the pathogenesis of insulin resistance?. *J Clin Endocrinol Metab* 86: 2296-2308.
149. Shahidi H, *et al* (1999) Imbalanced expression of the glucocorticoid receptor isoforms in cultured lymphocytes from a patient with systemic glucocorticoid resistance and chronic lymphocytic leukemia. *Biochem Biophys Res Commun* 254: 559-565.
150. Webster JC, Oakley RH, Jewell CM & Cidlowski JA (2001) Proinflammatory cytokines regulate human glucocorticoid receptor gene expression and lead to the accumulation of the dominant negative beta isoform: A mechanism for the generation of glucocorticoid resistance. *Proc Natl Acad Sci U S A* 98: 6865-6870.
151. Krett NL, Pillay S, Moalli PA, Greipp PR & Rosen ST (1995) A variant glucocorticoid receptor messenger RNA is expressed in multiple myeloma patients. *Cancer Res* 55: 2727-2729.
152. Moalli PA, Pillay S, Krett NL & Rosen ST (1993) Alternatively spliced glucocorticoid receptor messenger RNAs in glucocorticoid-resistant human multiple myeloma cells. *Cancer Res* 53: 3877-3879.
153. Beger C, *et al* (2003) Expression and structural analysis of glucocorticoid receptor isoform gamma in human leukaemia cells using an isoform-specific real-time polymerase chain reaction approach. *Br J Haematol* 122: 245-252.
154. Ismaili N & Garabedian MJ (2004) Modulation of glucocorticoid receptor function via phosphorylation. *Ann N Y Acad Sci* 1024: 86-101.
155. Hoeck W & Groner B (1990) Hormone-dependent phosphorylation of the glucocorticoid receptor occurs mainly in the amino-terminal transactivation domain. *J Biol Chem* 265: 5403-5408.
156. Gill G (2005) Something about SUMO inhibits transcription. *Curr Opin Genet Dev* 15: 536-541.
157. Le Drean Y, Mincheneau N, Le Goff P & Michel D (2002) Potentiation of glucocorticoid receptor transcriptional activity by sumoylation. *Endocrinology* 143: 3482-3489.
158. Longui CA & Faria CD (2009) Evaluation of glucocorticoid sensitivity and its potential clinical applicability. *Horm Res* 71: 305-309.
159. Derijk RH & de Kloet ER (2008) Corticosteroid receptor polymorphisms: Determinants of vulnerability and resilience. *Eur J Pharmacol* 583: 303-311.
160. van Rossum EF & Lamberts SW (2004) Polymorphisms in the glucocorticoid receptor gene and their associations with metabolic parameters and body composition. *Recent Prog Horm Res* 59: 333-357.

161. van Rossum EF, *et al* (2003) Identification of the BclI polymorphism in the glucocorticoid receptor gene: Association with sensitivity to glucocorticoids in vivo and body mass index. *Clin Endocrinol (Oxf)* 59: 585-592.
162. Koeijvoets KC, *et al* (2008) Two common haplotypes of the glucocorticoid receptor gene are associated with increased susceptibility to cardiovascular disease in men with familial hypercholesterolemia. *J Clin Endocrinol Metab* 93: 4902-4908.
163. Zhang J, Simisky J, Tsai FT & Geller DS (2005) A critical role of helix 3-helix 5 interaction in steroid hormone receptor function. *Proc Natl Acad Sci U S A* 102: 2707-2712.
164. Zhang J, *et al* (2009) Characterization of a novel gain of function glucocorticoid receptor knock-in mouse. *J Biol Chem* 284: 6249-6259.
165. Russcher H, *et al* (2005) Two polymorphisms in the glucocorticoid receptor gene directly affect glucocorticoid-regulated gene expression. *J Clin Endocrinol Metab* 90: 5804-5810.
166. Syed AA, *et al* (2006) Association of glucocorticoid receptor polymorphism A3669G in exon 9beta with reduced central adiposity in women. *Obesity (Silver Spring)* 14: 759-764.
167. van den Akker EL, *et al* (2006) Staphylococcus aureus nasal carriage is associated with glucocorticoid receptor gene polymorphisms. *J Infect Dis* 194: 814-818.
168. Rosenfeld MG & Glass CK (2001) Coregulator codes of transcriptional regulation by nuclear receptors. *J Biol Chem* 276: 36865-36868.
169. Szapary D, Song LN, He Y & Simons SS, Jr (2008) Differential modulation of glucocorticoid and progesterone receptor transactivation. *Mol Cell Endocrinol* 283: 114-126.
170. Meijer OC (2002) Coregulator proteins and corticosteroid action in the brain. *J Neuroendocrinol* 14: 499-505.
171. Meijer OC, Karssen AM & de Kloet ER (2003) Cell- and tissue-specific effects of corticosteroids in relation to glucocorticoid resistance: Examples from the brain. *J Endocrinol* 178: 13-18.
172. Wu RC, *et al* (2002) Regulation of SRC-3 (pCIP/ACTR/AIB-1/RAC-3/TRAM-1) coactivator activity by I kappa B kinase. *Mol Cell Biol* 22: 3549-3561.
173. Darimont BD, *et al* (1998) Structure and specificity of nuclear receptor-coactivator interactions. *Genes Dev* 12: 3343-3356.
174. Heery DM, Kalkhoven E, Hoare S & Parker MG (1997) A signature motif in transcriptional co-activators mediates binding to nuclear receptors. *Nature* 387: 733-736.
175. Jenster G, *et al* (1997) Steroid receptor induction of gene transcription: A two-step model. *Proc Natl Acad Sci U S A* 94: 7879-7884.
176. Spencer TE, *et al* (1997) Steroid receptor coactivator-1 is a histone acetyltransferase. *Nature* 389: 194-198.

177. Szapary D, Huang Y & Simons SS,Jr (1999) Opposing effects of corepressor and coactivators in determining the dose-response curve of agonists, and residual agonist activity of antagonists, for glucocorticoid receptor-regulated gene expression. *Mol Endocrinol* 13: 2108-2121.
178. He Y, Szapary D & Simons SS,Jr (2002) Modulation of induction properties of glucocorticoid receptor-agonist and -antagonist complexes by coactivators involves binding to receptors but is independent of ability of coactivators to augment transactivation. *J Biol Chem* 277: 49256-49266.
179. Ding XF, *et al* (1998) Nuclear receptor-binding sites of coactivators glucocorticoid receptor interacting protein 1 (GRIP1) and steroid receptor coactivator 1 (SRC-1): Multiple motifs with different binding specificities. *Mol Endocrinol* 12: 302-313.
180. Meijer OC, Steenbergen PJ & De Kloet ER (2000) Differential expression and regional distribution of steroid receptor coactivators SRC-1 and SRC-2 in brain and pituitary. *Endocrinology* 141: 2192-2199.
181. Xu J, *et al* (2000) The steroid receptor coactivator SRC-3 (p/CIP/RAC3/AIB1/ACTR/TRAM-1) is required for normal growth, puberty, female reproductive function, and mammary gland development. *Proc Natl Acad Sci U S A* 97: 6379-6384.
182. Glass CK & Rosenfeld MG (2000) The coregulator exchange in transcriptional functions of nuclear receptors. *Genes Dev* 14: 121-141.
183. Wang D, Wang Q, Awasthi S & Simons SS,Jr (2007) Amino-terminal domain of TIF2 is involved in competing for corepressor binding to glucocorticoid and progesterone receptors. *Biochemistry* 46: 8036-8049.
184. Privalsky ML (2004) The role of corepressors in transcriptional regulation by nuclear hormone receptors. *Annu Rev Physiol* 66: 315-360.
185. Wang Q, *et al* (2004) Equilibrium interactions of corepressors and coactivators with agonist and antagonist complexes of glucocorticoid receptors. *Mol Endocrinol* 18: 1376-1395.
186. Pratt WB, Galigniana MD, Harrell JM & DeFranco DB (2004) Role of hsp90 and the hsp90-binding immunophilins in signalling protein movement. *Cell Signal* 16: 857-872.
187. Radanyi C, Chambrud B & Baulieu EE (1994) The ability of the immunophilin FKBP59-HBI to interact with the 90-kDa heat shock protein is encoded by its tetratricopeptide repeat domain. *Proc Natl Acad Sci U S A* 91: 11197-11201.
188. Russell LC, Whitt SR, Chen MS & Chinkers M (1999) Identification of conserved residues required for the binding of a tetratricopeptide repeat domain to heat shock protein 90. *J Biol Chem* 274: 20060-20063.
189. Scheufler C, *et al* (2000) Structure of TPR domain-peptide complexes: Critical elements in the assembly of the Hsp70-Hsp90 multichaperone machine. *Cell* 101: 199-210.
190. Sanchez ER, *et al* (1990) Hormone-free mouse glucocorticoid receptors overexpressed in chinese hamster ovary cells are localized to the nucleus and are associated with both hsp70 and hsp90. *J Biol Chem* 265: 20123-20130.

191. Reynolds PD, Ruan Y, Smith DF & Scammell JG (1999) Glucocorticoid resistance in the squirrel monkey is associated with overexpression of the immunophilin FKBP51. *J Clin Endocrinol Metab* 84: 663-669.
192. Denny WB, Valentine DL, Reynolds PD, Smith DF & Scammell JG (2000) Squirrel monkey immunophilin FKBP51 is a potent inhibitor of glucocorticoid receptor binding. *Endocrinology* 141: 4107-4113.
193. Cheung-Flynn J, Roberts PJ, Riggs DL & Smith DF (2003) C-terminal sequences outside the tetratricopeptide repeat domain of FKBP51 and FKBP52 cause differential binding to Hsp90. *J Biol Chem* 278: 17388-17394.
194. Cho S, Kagan BL, Blackford JA, Jr, Szapary D & Simons SS, Jr (2005) Glucocorticoid receptor ligand binding domain is sufficient for the modulation of glucocorticoid induction properties by homologous receptors, coactivator transcription intermediary factor 2, and Ubc9. *Mol Endocrinol* 19: 290-311.
195. Perlman WR, Webster MJ, Herman MM, Kleinman JE & Weickert CS (2007) Age-related differences in glucocorticoid receptor mRNA levels in the human brain. *Neurobiol Aging* 28: 447-458.
196. Smith C, Wilson NW, Louw A & Myburgh KH (2007) Illuminating the interrelated immune and endocrine adaptations after multiple exposures to short immobilization stress by in vivo blocking of IL-6. *Am J Physiol Regul Integr Comp Physiol* 292: R1439-47.
197. Ramakrishnan R, DuBois DC, Almon RR, Pyszczynski NA & Jusko WJ (2002) Fifth-generation model for corticosteroid pharmacodynamics: Application to steady-state receptor down-regulation and enzyme induction patterns during seven-day continuous infusion of methylprednisolone in rats. *J Pharmacokinetic Pharmacodyn* 29: 1-24.
198. Vujcic MT, Velickovic N & Ruzdijic S (2007) Dexamethasone treatment affects nuclear glucocorticoid receptor and glucocorticoid response element binding activity in liver of rats (*rattus norvegicus*) during aging. *Comp Biochem Physiol B Biochem Mol Biol* 148: 463-469.
199. Davidson KA & Slaga TJ (1983) Glucocorticoid receptor levels in mouse skin after repetitive applications of 12-O-tetradecanoylphorbol-13-acetate and mezerein. *Cancer Res* 43: 3847-3851.
200. Abcouwer SF, Bode BP & Souba WW (1995) Glucocorticoids regulate rat glutamine synthetase expression in a tissue-specific manner. *J Surg Res* 59: 59-65.
201. Tiao G, *et al* (1996) Energy-ubiquitin-dependent muscle proteolysis during sepsis in rats is regulated by glucocorticoids. *J Clin Invest* 97: 339-348.
202. O'Donnell D, Francis D, Weaver S & Meaney MJ (1995) Effects of adrenalectomy and corticosterone replacement on glucocorticoid receptor levels in rat brain tissue: A comparison between western blotting and receptor binding assays. *Brain Res* 687: 133-142.
203. Frame LT, Hart RW & Leakey JE (1998) Caloric restriction as a mechanism mediating resistance to environmental disease. *Environ Health Perspect* 106 Suppl 1: 313-324.
204. Dutta D & Sharma R (2004) Age-dependent dietary regulation of glucocorticoid receptors in the liver of mice. *Biogerontology* 5: 177-184.

205. Grasso G, Lodi L, Lupo C & Muscettola M (1997) Glucocorticoid receptors in human peripheral blood mononuclear cells in relation to age and to sport activity. *Life Sci* 61: 301-308.
206. Aisa B, Tordera R, Lasheras B, Del Rio J & Ramirez MJ (2007) Cognitive impairment associated to HPA axis hyperactivity after maternal separation in rats. *Psychoneuroendocrinology* 32: 256-266.
207. Little HJ, *et al* (2008) Selective increases in regional brain glucocorticoid: A novel effect of chronic alcohol. *Neuroscience* 156: 1017-1027.
208. Carvalho LA, *et al* (2008) Clomipramine in vitro reduces glucocorticoid receptor function in healthy subjects but not in patients with major depression. *Neuropsychopharmacology* 33: 3182-3189.
209. Marcelli M, *et al* (2006) Quantifying effects of ligands on androgen receptor nuclear translocation, intranuclear dynamics, and solubility. *J Cell Biochem* 98: 770-788.
210. Borgna JL (2005) Requirements for reliable determination of binding affinity constants by kinetic approach. *J Steroid Biochem Mol Biol* 96: 141-153.
211. Esmailpour N, Hogger P & Rohdewald P (1998) Binding kinetics of budesonide to the human glucocorticoid receptor. *Eur J Pharm Sci* 6: 219-223.
212. Jones TR & Bell PA (1980) Glucocorticoid--receptor interactions. studies of the negative cooperativity induced by steroid interactions with a secondary, hydrophobic, binding site. *Biochem J* 188: 237-245.
213. Jones TR & Bell PA (1982) Glucocorticoid-receptor interactions. discrimination between glucocorticoid agonists and antagonists by means of receptor-binding kinetics. *Biochem J* 204: 721-729.
214. Franchimont D, *et al* (1999) Tumor necrosis factor alpha decreases, and interleukin-10 increases, the sensitivity of human monocytes to dexamethasone: Potential regulation of the glucocorticoid receptor. *J Clin Endocrinol Metab* 84: 2834-2839.
215. Weiss JN (1997) The hill equation revisited: Uses and misuses. *FASEB J* 11: 835-841.
216. Notides AC, Lerner N & Hamilton DE (1981) Positive cooperativity of the estrogen receptor. *Proc Natl Acad Sci U S A* 78: 4926-4930.
217. Stenoien DL, *et al* (2000) Subnuclear trafficking of estrogen receptor-alpha and steroid receptor coactivator-1. *Mol Endocrinol* 14: 518-534.
218. van der Laan S, Lachize SB, Vreugdenhil E, de Kloet ER & Meijer OC (2008) Nuclear receptor coregulators differentially modulate induction and glucocorticoid receptor-mediated repression of the corticotropin-releasing hormone gene. *Endocrinology* 149: 725-732.
219. Chen S, Sarlis NJ & Simons SS,Jr (2000) Evidence for a common step in three different processes for modulating the kinetic properties of glucocorticoid receptor-induced gene transcription. *J Biol Chem* 275: 30106-30117.
220. Szapary D, Xu M & Simons SS,Jr (1996) Induction properties of a transiently transfected glucocorticoid-responsive gene vary with glucocorticoid receptor concentration. *J Biol Chem* 271: 30576-30582.

221. Sun Y, Tao YG, Kagan BL, He Y & Jr SS (2008) Modulation of transcription parameters in glucocorticoid receptor-mediated repression. *Mol Cell Endocrinol* 295: 59-69.
222. Zhang S, Jonklaas J & Danielsen M (2007) The glucocorticoid agonist activities of mifepristone (RU486) and progesterone are dependent on glucocorticoid receptor levels but not on EC50 values. *Steroids* 72: 600-608.
223. Voss TC, John S & Hager GL (2006) Single-cell analysis of glucocorticoid receptor action reveals that stochastic post-chromatin association mechanisms regulate ligand-specific transcription. *Mol Endocrinol* 20: 2641-2655.
224. Franco R, *et al* (2006) The two-state dimer receptor model: A general model for receptor dimers. *Mol Pharmacol* 69: 1905-1912.
225. Holmbeck SM, Dyson HJ & Wright PE (1998) DNA-induced conformational changes are the basis for cooperative dimerization by the DNA binding domain of the retinoid X receptor. *J Mol Biol* 284: 533-539.
226. Furlow JD, Murdoch FE & Gorski J (1993) High affinity binding of the estrogen receptor to a DNA response element does not require homodimer formation or estrogen. *J Biol Chem* 268: 12519-12525.
227. Nishi M, Tanaka M, Matsuda K, Sunaguchi M & Kawata M (2004) Visualization of glucocorticoid receptor and mineralocorticoid receptor interactions in living cells with GFP-based fluorescence resonance energy transfer. *J Neurosci* 24: 4918-4927.
228. Chen S, Wang J, Yu G, Liu W & Pearce D (1997) Androgen and glucocorticoid receptor heterodimer formation. A possible mechanism for mutual inhibition of transcriptional activity. *J Biol Chem* 272: 14087-14092.
229. Liu W, Wang J, Sauter NK & Pearce D (1995) Steroid receptor heterodimerization demonstrated in vitro and in vivo. *Proc Natl Acad Sci U S A* 92: 12480-12484.
230. Kaspar F, Klocker H, Denninger A & Cato AC (1993) A mutant androgen receptor from patients with reifenstein syndrome: Identification of the function of a conserved alanine residue in the D box of steroid receptors. *Mol Cell Biol* 13: 7850-7858.
231. Heck S, *et al* (1994) A distinct modulating domain in glucocorticoid receptor monomers in the repression of activity of the transcription factor AP-1. *EMBO J* 13: 4087-4095.
232. Adams M, Meijer OC, Wang J, Bhargava A & Pearce D (2003) Homodimerization of the glucocorticoid receptor is not essential for response element binding: Activation of the phenylethanolamine N-methyltransferase gene by dimerization-defective mutants. *Mol Endocrinol* 17: 2583-2592.
233. Liu W, Wang J, Yu G & Pearce D (1996) Steroid receptor transcriptional synergy is potentiated by disruption of the DNA-binding domain dimer interface. *Mol Endocrinol* 10: 1399-1406.
234. Rogatsky I, *et al* (2003) Target-specific utilization of transcriptional regulatory surfaces by the glucocorticoid receptor. *Proc Natl Acad Sci U S A* 100: 13845-13850.
235. Meijsing SH, *et al* (2009) DNA binding site sequence directs glucocorticoid receptor structure and activity. *Science* 324: 407-410.

236. Reichardt HM, *et al* (1998) DNA binding of the glucocorticoid receptor is not essential for survival. *Cell* 93: 531-541.
237. Frijters R, *et al* (2010) Prednisolone-induced differential gene expression in mouse liver carrying wild type or a dimerization-defective glucocorticoid receptor. *BMC Genomics* 11: 359.
238. Wust S, *et al* (2009) Therapeutic and adverse effects of a non-steroidal glucocorticoid receptor ligand in a mouse model of multiple sclerosis. *PLoS One* 4: e8202.
239. Yemelyanov A, *et al* (2008) Novel steroid receptor phyto-modulator compound a inhibits growth and survival of prostate cancer cells. *Cancer Res* 68: 4763-4773.
240. De Bosscher K, *et al* (2005) A fully dissociated compound of plant origin for inflammatory gene repression. *Proc Natl Acad Sci U S A* 102: 15827-15832.

Chapter 2

Materials, methods and model

2.1 Materials and methods

2.1.1 Reagents

Dexamethasone (11 β ,16 α)-9-fluoro-11,17,21-trihydroxy-16-methylpregna-1,4-diene-3,20-dione), hydrocortisone (11 β ,17 α ,21-trihydroxypregn-4-ene-3,20-dione-17-hydroxycorticosterone), progesterone (4-pregnene-3,20-dione), medroxyprogesterone (6 α -methyl-17 α -hydroxyprogesterone acetate), mifepristone (11 β -(4-dimethyl amino)phenyl-17 β -hydroxy-17-(1-propynyl)estra-4,9-dien-3-one), cycloheximide, DEAE-Dextran, chloroquine diphosphate salt (chloroquine) and phorbol 12-myristate 13-acetate (PMA) were purchased from Sigma-Aldrich. Compound A (2(4-acetoxyphenyl)-2-chloro-N-methyl-ethylammonium chloride) was synthesized as described previously (1). The [³H]-DEX (specific activity of 68-85Ci/mmol) was obtained from AEC Amersham Biosciences.

2.1.2 Plasmids

The pGL2-basic (empty vector) was obtained from Promega. The pRS-hGR α (GRwt) was a gift from R. M. Evans (2), pECFP-hGR α (CFP-GR) and pEYFP-hGR α (YFP-GR) were gifts from J. Cidlowski (3). pEFFlaghGR α (Flag-GR, molecular mass, 96 kDa) (4) and pHisGRA477T (GRdim) were gifts from K. De Bosscher (University of Ghent, Belgium). The pEGFP-C2-GR (GFP-GR, molecular mass, 128.5 kDa) was provided by S. Okret (Karolinska Institute, Sweden) (5). The GRE-containing promoter reporter constructs, pTAT-GRE2-Elb-luc was a gift from G. Jenster (6) and p Δ ODLO was a gift from D. Pearce (University of California), while the NF κ B containing IL6-luc promoter reporter construct, p(IL6 $\kappa\beta$)₃50hu.IL6P-luc was a gift from G. Haegeman (University of Ghent, Belgium) (7). The pEGFP-C2-GRA477T (GFP-GRdim) was cloned by excising the wild type GR from pEGFP-C2-GR with the restriction enzymes *Xma*I and *Sal*I and replacing it with the mutated GRdim sequence from pHisGRA477T. The presence of the mutation was confirmed through sequencing (primer, forward 5'-AGC TTC AGG ATG TCA TTA TGG AG-3' and reverse 5'-CCC CCC CCG GGG TTT TGA TGA AAC AGA-3'). All plasmids were verified by restriction enzyme digest.

2.1.3 Cell culture and DEAE-dextran transfection Monkey kidney fibroblast cells (COS-1) purchased from American Type Culture Collection (ATCC) were cultured in high glucose (4.5g/ml) Dulbecco's modified Eagle's medium (DMEM) (Sigma) with 2mM glutamine (Merck), 44mM sodium bicarbonate (Invitrogen), and 1mM sodium pyruvate (Invitrogen) (un-supplemented DMEM) supplemented with 10% fetal calf serum (FCS) (Highveld Biologicals, South Africa), 100IU/ml of penicillin, 100 μ g/ml of streptomycin (Pen/Strep) (Invitrogen). All transfections were done using the DEAE-dextran method (8). Cultured cells were plated to achieve a density of 70% to 80% confluence on the target day of transfection. The transfection mix consisted of 11550ng DNA/10cm plate added to preheated un-supplemented DMEM medium (7,5ml/10cm plate), along with 0.1mM chloroquin and 0.1mg/ml

DEAE-Dextran and incubated on the cells at 37°C for 2 hours followed by a 4 minute 10% DMSO in PBS shock at 37°C. The cells were then rinsed with PBS and finally 15ml complete DMEM (1% Pen/Strep; 10% FCS) was added.

2.1.4 Whole cell binding to determine the expression levels of the GR plasmids COS-1 cells (2×10^6 cells/10cm plate) were DEAE-Dextran transfected with the indicated amounts of plasmid DNA (Fig.3.3) and filled to 15000ng total plasmid DNA/10cm plate with empty vector. Twenty four hours after transfection cells were replated (1×10^5 cells/well in 24-well plates) and serum starved (in order to remove GCs in the medium which may result in GR down regulation and interfere with the response to administered GCs) in medium with 10% dextran-coated charcoal stripped FCS (Highveld Biologicals, South Africa) and 1% Pen/Strep (stripped DMEM). Twenty four hours after replating cells were incubated for 4 hours at 37°C with 10nM [3 H]-DEX (total binding) or [3 H]-DEX and a 500 fold excess of unlabeled DEX (non-specific binding) in unsupplemented DMEM. Cells were then placed on ice and washed three times, for 15 minutes each with ice-cold PBS containing 0.2% (w/v) bovine serum albumin (BSA) (Roche). Cells were lysed with 100 μ l of passive lysis buffer (0.2% (v/v) triton, 10% (v/v) glycerol, 2.8% (v/v) 1M tris-phosphate-EDTA and 0.29% (v/v) 0.5M EDTA) and binding was determined by scintillation counting in a 1900CA TRI-CARB liquid scintillation analyzer (Packard) using FLO-SCINT II (Perkin Elmer). Total binding and non-specific binding were normalized to protein concentration (Bradford assay) (9). Specific binding (total binding - nonspecific binding) was plotted. Ligand depletion (LD) was monitored for all whole cell binding assays to ensure that less than 10 percent of the total [3 H]-DEX was removed from solution by specific and non-specific association. LD fell between 0.5 to 2.5 percent for all experiments implying that binding of the [3 H]-DEX did not significantly alter its concentration.

2.1.5 Time course to ligand binding equilibrium COS-1 cells (2×10^6 cells/10-cm plate) were DEAE-Dextran transfected with GRwt (low (38.5ng), medium (385ng) or high (11550ng)), GRdim (low (385ng) or medium (11550ng)) or GFP-GR (medium (38.5ng) or high (11550ng)) and filled to 11550ng total plasmid DNA/10cm plate with empty vector. Twenty-four hours after transfection cells were replated (1×10^5 cells/well in 24-well plates) in stripped DMEM. Twenty four hours after replating cells were incubated for varying time periods at 37°C with 10nM [3 H]-DEX (total binding) or labeled DEX and a 500 fold excess of unlabeled DEX (non-specific binding) in unsupplemented DMEM. Cells were then placed on ice and washed three times, for 15min each with ice-cold PBS containing 0.2% (w/v) BSA. Cells were lysed with 100 μ l of passive lysis buffer and binding was determined by scintillation counting. Total binding and non-specific binding were normalized to protein concentration (Bradford assay) and specific binding (total binding - nonspecific binding) was plotted against time and curves fit using one phase exponential association.

2.1.6 Whole cell saturation binding COS-1 cells (2×10^6 cells/10-cm plate) were DEAE-Dextran transfected with GRwt (low (38.5ng), medium (385ng) or high (11550ng)), GRdim (low (385ng) or medium (11550ng)) or GFP-GR (medium (38.5ng) or high (11550ng)) and filled to 11550ng total plasmid DNA/10cm plate with empty vector. Twenty-four hours after transfection cells were replated (1×10^5 cells/well in 24-well plates) and serum starved in stripped DMEM. Twenty four hours after replating cells were incubated for 4 hours at 37°C with increasing concentrations of [³H]-DEX (total binding) or [³H]-DEX and a constant concentration of 60µM unlabelled DEX (non-specific binding) in unsupplemented DMEM. Cells were then placed on ice and washed three times, for 15 minutes each with ice-cold PBS containing 0.2% (w/v) BSA. Cells were lysed with 100µl of passive lysis buffer and binding was determined by scintillation counting. Total binding and non-specific binding were normalized to protein concentration (Bradford assay). Specific binding (total binding - nonspecific binding) was determined and fmol GR per mg protein was calculated using a counting efficiency of 43%. Specific binding was plotted against nM [³H]-DEX and curves fit using one site binding hyperbola to obtain K_d and maximal binding (Bmax) values. In addition, specific binding was also plotted against logM [³H]-DEX and curves fit using sigmoidal dose-response (variable slope) to obtain Hill slopes.

2.1.7 Competitive whole cell binding.

COS-1 cells (2×10^6 cells/10-cm plate) were DEAE-Dextran transfected with low (38.5ng), medium (385ng) or high (11550ng) levels of GRwt and filled to 11550ng total plasmid DNA/10cm plate with empty vector. Twenty-four hours after transfection cells were replated (1×10^5 cells/well in 24-well plates) and serum starved in stripped DMEM. Twenty four hours after replating cells were incubated for 4 hours at 37°C in unsupplemented DMEM containing 40nM [³H]-DEX and EtOH or a range (10^{-5} to 10^{-11} M) of unlabelled DEX or CpdA. Cells were then placed on ice and washed three times, for 15 minutes each with ice-cold PBS containing 0.2% (w/v) BSA. Cells were lysed with 100µl of passive lysis buffer and binding was determined by scintillation counting. Total binding was normalized to protein concentration (Bradford assay) and expressed as percentage displacement (bottom plateau for maximal [³H]-DEX displacement designated as 100% displacement and top plateau where no displacement took place as 0% displacement). Sigmoidal dose-response curves were fit to this data which generated maximal displacement results.

2.1.8 Co-immunoprecipitation (Co-IP)

COS-1 cells (2×10^6 cells/10-cm plate) were DEAE-Dextran transfected with low levels (38.5ng) of GR (34.22ng Flag-GR and 4.28ng GFP-GRdim or GFP-GRwt), medium levels (385ng) of GR (342.2ng Flag-GR and 42.8ng GFP-GRdim or GFP-GRwt) or high levels (11550ng) of GR (10266ng Flag-GR and 1284ng GFP-GRdim or GFP-GRwt) and made up to a total of 11550ng plasmid DNA/10cm plate with empty vector. Cells were replated (2.5×10^6 cells/10cm plate) and serum starved 24 hours later in

stripped DMEM and after 24 hours treated with ethanol (control), 10^{-6} M DEX, or 10^{-5} M CpdA for 1 hour. After induction cells were washed twice with PBS before being lysed on ice in Buffer A (10mM Hepes pH7.5 (Invitrogen), 1.5mM $MgCl_2$, 10mM KCl, 0.1% Nonidet P-40 (Roche Applied Science), and Complete Mini protease inhibitor mixture (Roche Applied Science)). After two cycles of freeze-thaw the lysates were centrifuged at $14,000 \times g$ for 15 minutes, and the supernatant collected. Protein concentrations were determined using the Bradford method and 600 μ g of protein from the low GR concentration or 200 μ g of protein from the medium and high GR concentration samples were precipitated with 30 μ l of EZview Red ANTI-FLAG M2 Affinity Gel beads (Sigma), pre-washed 4 times with Buffer A in the presence of 2.5% (w/v) casein protein and Complete Mini protease inhibitor mixture. Buffer A, 2.5% casein protein and Complete Mini protease inhibitor mixture, beads and lysate forming a minimum volume of 400 μ l/sample were rotated for 16 hours at 4 $^{\circ}$ C. Beads were washed four times with 200 μ l of Buffer A supplemented with Complete Mini protease inhibitor mixture, 0.5% Triton X-100 (BDH) and 150mM NaCl. 20 μ l of Laemmli buffer (62.5mM Tris-HCl, pH6.8, 10% (v/v) glycerol, 1.25% (m/v) SDS, 0.00125% (m/v) bromphenol blue, and 2.5% (v/v) β -mercaptoethanol) was then added to beads, which were boiled for 7.5 minutes at 95 $^{\circ}$ C. For Western blotting, immune precipitates (20 μ l) were separated on a 10% SDS-PAGE gel, together with the inputs of total cell lysate (20 μ g). Following electrophoresis, proteins were electroblotted and transferred to Hybond-ECL nitrocellulose membrane (Amersham Biosciences), which was probed for GR (H-300 anti-body (Santa Cruz Biotechnology) diluted 1:1000 in 5% (w/v) casein in TBST buffer for low GR concentrations or 1:3000 dilution for medium and high GR concentrations) and visualized using ECL peroxidase-labeled anti-rabbit anti-body (AEC-Amersham Biosciences) diluted in 5% (w/v) casein in TBST buffer (1:5000 for low GR concentrations and 1:10000 for medium and high GR concentration) and ECL Western blotting detection reagents (GE Healthcare) on Hyperfilm (Amersham Biosciences). Densitometric analysis of the immunoblots was carried out using UN-SCAN-IT gel 6.1 software (Silk Scientific) and GFP-GR pull down was normalized against their respective Flag-GR levels.

2.1.9 Fluorescence resonance energy transfer (FRET)

COS-1 cells (2×10^6 cells/10cm plate) were DEAE-Dextran transfected with low levels (38.5ng) of GR (19.25ng CFP-GR and 19.25ng YFP-GR), medium levels (385ng) of GR (195.5ng CFP-GR and 192.5ng YFP-GR) or high levels (11550ng) of GR (5775ng CFP-GR and 5775ng YFP-GR) and made up to a total of 11550ng plasmid DNA/10cm plate with empty vector. Twenty-four hours after transfection cells were replated (3×10^4 cells/well) into 8-well Lab-Tek chambered coverglass plates (Nunc, Denmark) and serum starved in stripped DMEM. Twenty-four hours after replating cells were analyzed in the temperature-controlled chamber (37 $^{\circ}$ C) of an Olympus Cell system attached to an IX-81 inverted fluorescence microscope (Olympus Corp., Japan) equipped with a F-view-II cooled CCD camera (Soft Imaging Systems) and a 150W Xenon lamp as light source which is part of the MT20

excitation source. An Olympus Plan Apo N 60X/1.4 oil objective lens and the Cell® imaging software were used for image acquisition and analysis. Cells were selected which expressed both CFP-GR and YFP-GR. Cells were induced with 10^{-6} M DEX in unsupplemented DMEM. CFP, YFP and FRET images were taken every minute over a 30min period. FRET fluorescence was detected using a filter set with S430/25x excitation and S535/30m emission. The YFP filter set excites at S500/20x and the emission is detected at S535/30m while the CFP filter set excites at S430/25x and the emission is detected at S470/30m. All filter sets were supplied by Chroma Technology Corporation (Rockingham, USA). An exposure time of 1500ms at 100% light intensity was used and the entire cell area as defined by the cellular membrane was selected as the region of interest. The F-don signal (CPF) was used to select cells for analysis as these F-don values reflect the CFP signal after 30min of DEX stimulation measured in a region of interest in the nucleus of each individual cell. Cells with an F-don emission of 0-600 were selected from the low GR concentration population, F-don signals between 600-1200 from the medium GR concentration population and F-don of >1200 from the high GR concentration population. The signals measured in the FRET channel were corrected for cross-talk from the cyan (CFP) and yellow (YFP) channels using the following equation: $n\text{FRET} = \text{FRETsignal} - (\alpha \times \text{YFP signal}) - (\beta \times \text{CFP signal})$ where n is normalized FRET and α and β were determined by measuring the crossover into the FRET channel of the YFP and CFP signals, respectively, in cells expressing each fusion protein on its own. In our system, 2.6% of the YFP signal (α) and 59% of the CFP signal (β) were detected in the FRET channel (10). Background subtraction was carried out on CPF, YFP and uncorrected FRET signals using an area where no cells were present. The fold increase in FRET response was calculated by normalizing each experiment to its unstimulated FRET signal and fit to a sigmoidal dose-response variable slope curve which generates maximal fold induction of FRET. CFP, YFP and corrected FRET images are captured in grey scale for optimal sensitivity, the images are coloured electronically for ease of differentiation.

2.1.10 Live cell nuclear import

COS-1 cells (2×10^6 cells/10-cm plate) were DEAE-Dextran transfected with GFP-GR (medium (38.5ng) or high (11550ng)) or GFP-GRdim (medium (38.5ng) or high (11550ng)) and filled to 11550ng total plasmid DNA/10cm plate with empty vector. Twenty-four hours after transfection cells were replated (3×10^4 cells/well) into 8-well Lab-Tek chambered coverglass plates and serum starved in stripped DMEM. Twenty four hours after replating cells were analyzed in the temperature-controlled chamber (37°C) of an Olympus Cell system attached to an IX-81 inverted fluorescence microscope equipped with a F-view-II cooled CCD camera and a 150W Xenon lamp as light source which is part of the MT20 excitation source. An Olympus Plan Apo N 60X/1.4 oil objective and the Cell® imaging software were used for image acquisition and analysis. The GFP filter set (U-MGFP/XL, Olympus) excites at 470 nm (BP 460-490) and emission is collected at 506 nm (BA510IF). Cells were selected

which displayed clear cytoplasmic GFP-GR distribution, with cells with low GFP-GR levels selected from the medium population while those with greater than average GFP-GR levels selected from the high population. Cells were induced with 10^{-6} M DEX in unsupplemented DMEM and GFP images were taken every minute over a 60 minute period. Nuclear import was quantified as the increase in GFP fluorescence in the nucleus (region of interest) over the period of stimulation. Fluorescence in the nucleus at the zero time point was subtracted from all time points and a one phase exponential association curve was fit to the data where the generated half time ($t_{1/2}$) represents the time it takes to achieve 50% of maximal GFP nuclear accumulation.

2.1.11 Live cell nuclear export

COS-1 cells were DEAE-Dextran transfected, replated and serum starved as for the live cell nuclear import assay. Twenty four hours after replating cells were induced with 10^{-9} M DEX for 1 hour after which they were rinsed 4 times with sterile PBS and stripped DMEM was added. Cells were selected which displayed clear nuclear GFP-GR distribution, with cells with low GFP levels selected from the medium GR concentration population while those with greater than average GFP levels selected from the high GR concentration population. Nuclear export was analyzed at time points between 0 and 36 hours after DEX washout in the temperature-controlled chamber (37°C) of an IX-81 Olympus Cell system using the same hardware and software as for the live nuclear import assay. Nuclear export was quantified as the ratio of GFP fluorescence in the mid point of the nucleus over that in the midpoint between nuclear membrane and cellular membrane. Data was fit to a one phase exponential decay curve which generates a $t_{1/2}$ to maximal cytoplasmic localization.

2.1.12 Nuclear distribution

COS-1 cells were DEAE-Dextran transfected as for the live cell nuclear import assay. Cells were replated 24 hours later onto coverslips in 6-well plates (3×10^5 cells /well) and serum starved in stripped DMEM. Twenty four hours after replating cells were induced with 10^{-6} M DEX or 10^{-5} M CpdA for 1 hour. After induction cells were fixed and permeabilized by being placed on ice, rinsed with 1ml of -20°C methanol, and incubated at -20°C for 15min with another 1ml of -20°C methanol. Cells were then washed three times with ice-cold PBS plus 0.2% BSA and mounted on glass slides. Cells were analyzed on an IX-81 Olympus Cell system using the same hardware and software as for the live cell nuclear import assay. Cells were selected which displayed clear nuclear GFP-GR distribution, with cells with low GFP levels selected from the medium GR concentration population while those with greater than average GFP levels selected from the high GR concentration population. Z-stack images of the nuclei were taken at various focal planes and used to deconvolute a single nuclear image. As long a line as possible was drawn through each nuclei avoiding nucleoli and the Cell® imaging

software was used to quantify the coefficient of variation (CV) of GFP fluorescence intensity along this line. The lower the percentage CV, the more random the nuclear distribution (11).

2.1.13 Immunofluorescent analysis of nuclear import

COS-1 cells (2×10^6 cells/10cm plate) were DEAE-Dextran transfected with GRwt (low (38.5ng) or medium (385ng)) or GRdim (low (385ng) or medium (11550ng)) and filled to 11550ng total plasmid DNA/10cm plate with empty vector. Cells were replated 24 hours later onto coverslips in 6-well plates (3×10^5 cells /well) and serum starved in stripped DMEM. Twenty four hours after replating cells were induced with 10^{-6} M DEX or 10^{-5} M CpdA at time points ranging from 0 to 60 minutes. After induction cells were fixed and permeabilized as for the nuclear distribution assay and transferred to new 6-well plates containing 2ml of blocking buffer (PBS with 3% (v/v) FCS and 1% (w/v) BSA). Cells were incubated for 1 hour at room temperature and then washed twice with ice-cold PBS plus 0.2% BSA. To visualize GR, cells were incubated with the primary rabbit anti-GR H-300 (diluted 1:1000 in blocking buffer) over night. Cells were then washed three times with ice-cold PBS plus 0.2% BSA and incubated for 1 hour at room temperature with secondary anti-body (Alexa Fluor 488-tagged anti-rabbit anti-body (Molecular Probes)) diluted 1:500 in blocking buffer. Nuclei were visualized using Hoechst 33258 stain (Sigma) according to the manufacturer's instructions. Cells were then washed three times with ice-cold PBS and mounted on glass slides. Cells were analyzed on an IX-81 Olympus Cell system using the same hardware and software as for the live nuclear import assay in a double-blind fashion. Cells were allocated as either nuclear (where there was clear nuclear localization (>60% of signal in nucleus) of the signal) or cytoplasmic and the percentage nuclear of 50 total cells per slide counted was fit to a one phase exponential association curve which generated $t_{1/2}$ to maximal nuclear localization as well as maximal nuclear localization values.

2.1.14 Immunofluorescent analysis of nuclear export

COS-1 cells were transfected, replated and serum starved as for the immunofluorescent nuclear import assay. Twenty four hours after replating cells were induced with 10^{-6} M DEX or 10^{-5} M CpdA for 1 hour, rinsed three times with sterile PBS at 37°C and incubated for time points ranging from 0 to 28 hours in stripped DMEM. At the end of each time point cells were fixed, fluorescently labelled and mounted as for the immunofluorescent import assay. Cells were analyzed on an IX-81 Olympus Cell system using the same hardware and software as the live nuclear import assay in a double-blind fashion. Cells were allocated as either nuclear (where there was > 60% nuclear localization of the signal) or cytoplasmic and the percentage nuclear of 50 total cells counted per slide was fit to a one phase exponential decay curve which generated $t_{1/2}$ to maximal cytoplasmic localization values.

2.1.15 β -Galactosidase assay

COS-1 cells (2×10^6 cells/10cm plate) were DEAE-Dextran transfected with GRwt (low (38.5ng), medium (385ng) or high (11550ng)) or GRdim (low (385ng) or medium (11550ng)) and 900ng pSV- β -gal (Promega) and filled to 12450ng total DNA with empty vector or COS-1 cells (2×10^6 cells/10cm plate) were DEAE-Dextran transfected with GRwt (4500ng, 6000ng, 7500ng or 9000ng) or GFP-GR (6000ng or 7500ng) and 1500ng pCMV- β gal (Invitrogen) and filled to 10500ng total DNA with empty vector. Cells were replated 24 hours later into 96-well plates (4×10^4 cells /well) in stripped DMEM. Twenty four hours after replating cells were lysed with 30 μ l of passive lysis buffer, and subjected to a freeze thaw cycle. β -Galactosidase activity was determined using the Galacto-star kit (Tropix). Light emission was measured in a Veritas microplate luminometer (Turner Biosystems) and was normalized to protein concentration.

2.1.16 Promoter reporter transactivation assays

COS-1 cells (2×10^6 cells/10cm plate) were DEAE-Dextran transfected with GRwt (low (38.5ng), medium (385ng) or high (11550ng)), GRdim (low (385ng) or medium (11550ng)) or GFP-GR (medium (38.5ng) or high (11550ng)) and 3000ng pTAT-GRE2-Elb-luc (2 x GRE promoter reporter) or 3000ng p Δ ODLO (1 x GRE promoter reporter) and filled to 14550ng total plasmid DNA/10cm plate with empty vector. Cells were replated 24 hours later onto 96-well plates (4×10^4 cells /well) and serum starved in stripped DMEM. Twenty four hours after replating cells were induced with EtOH or a range (10^{-5} to 10^{-12} M) of DEX, F, MPA or RU486 in stripped DMEM for 24 hours. Cells were lysed with 30 μ l of passive lysis buffer, and subjected to a freeze thaw cycle. Luciferase activity was determined using a luciferase assay kit (Promega) and light emission measured in a Veritas microplate luminometer. Luciferase relative light units were normalized against protein concentrations (Bradford method). Sigmoidal dose-response curves were fit to the experimental data which generated maximal induction as well as log EC₅₀ values.

2.1.17 Promoter reporter transrepression assays

COS-1 cells (2×10^6 cells/10cm plate) were DEAE-Dextran transfected with GRwt (low (38.5ng), medium (385ng) or high (11550ng)) or GRdim (low (385ng) or high (11550ng)) and 12000ng p(IL6 κ β)₃50hu.IL6P-luc and filled to 23550ng total plasmid DNA/10cm plate with empty vector. Cells were replated 24 hours later into 24-well plates (5×10^4 cells /well) and serum starved in stripped DMEM. Twenty four hours after replating cells were induced with EtOH alone (uninduced), PMA (10ng/ml) and EtOH (maximal induction), or PMA (10ng/ml) plus a range (10^{-5} to 10^{-12} M) of DEX or CpdA in stripped DMEM for 24 hours. Cells were lysed with 50 μ l passive lysis buffer, and subjected to a freeze thaw cycle. Luciferase activity was determined and normalized as for the transactivation assay. The EtOH alone value, representing unstimulated luciferase production, was subtracted from

all data points, and the resultant values expressed as a percentage of the maximal induction. Percentage of maximum induction values were finally subtracted from 100 percent producing percentage repression values. Sigmoidal dose-response curves were fit to the data which generated log EC₅₀ as well as maximal percentage repression values.

2.1.18 Real time PCR quantification of endogenous gene expression

COS-1 cells (2×10^6 cells/10cm plate) were DEAE-Dextran transfected with no GR plasmid, GRwt (low (38.5ng), medium (385ng) or high (11550ng)) or GRdim (low (385ng) or high (11550ng)) and filled to 11550ng total plasmid DNA/10cm plate with empty vector. Cells were replated 24 hours later into 12-well plates (3×10^5 cells /well) and serum starved in stripped DMEM. Twenty four hours after replating cells were induced with either EtOH or 10^{-6} M DEX in stripped DMEM for 8 hours. Cells were then placed on ice and rinsed three times with ice cold PBS before being lysed with 400 μ l Tri Reagent (Sigma) and subjected to a freeze thaw cycle at -80°C . RNA was isolated according to the Tri Reagent manufacturer's guidelines and its integrity checked on a 1 percent agarose gel. 1 μ g of RNA, as determined by spectrophotometry, was reverse transcribed to cDNA using the ImProm-II Reverse Transcription system (Promega). Real time PCR was carried out on 200ng of cDNA using 15 μ l SensiMix SYBR Kit (Quantace) made up to a total volume of 25 μ l with nuclease free water and primers for either the glucocorticoid induced leucine zipper (GILZ) or glyceraldehydes-3-phosphate dehydrogenase (GAPDH), which is a constitutively expressed gene that is not influenced by DEX (12) and was used to normalize GILZ values. The GILZ primers were purchased through QuantiTect primers (Qiagen) and have an amplicon size of 69bp. The GAPDH primers were synthesized by Integrated DNA Technologies (forward, 5'- TGA ACG GGA AGC TCA CTG G-3' and reverse 5'-ATT CGT TGT CAT ACC AGG-3') (13) and have an amplicon size of 307bp. Quantitative PCR was carried out in a Rotor-Gene 6000 (Corbett) with 45 cycles of 10sec at 95°C , 10sec at 55°C and 10sec at 72°C . A melting curve for each gene was constructed by raising the temperature from 50°C to 95°C by 0.2°C per second. Standard curves of GILZ and GAPDH amplification in triplicate at 0.32, 1.6, 8, 40 and 200ng/ μ l cDNA concentrations were generated using Rotor-Gene 6000 Series Software 1.7 (Corbett) to determine primer efficiency. GILZ expression was calculated relative to GAPDH for each condition according to the Pfaffl mathematical model (14) and expressed as either fold induction induced by DEX relative to EtOH for each transfection condition or as maximal DEX induction relative to the no GR transfected EtOH condition. Ligand independent transactivation was calculated as the EtOH induction of each condition relative to the no GR transfected EtOH condition.

2.1.19 Converting Bmax to mol GR/cell, GR/cell and M GR

The GR concentration of COS-1 cells transiently transfected with GRwt, GRdim or GFP-GRwt was derived from saturation binding curves and was converted from maximal binding (Bmax) (Fig.3.6B)

with units of counts per minute (cpm)/mg protein to disintegrations per minute (dpm)/mg protein using the experimentally derived counting efficiency (CE) of 43% (equation 1). The dpm/mg protein value was then converted to Curies (Ci) per mg protein by dividing dpm by the amount of dpm (2.22×10^{12}) in one Curie (equation 2). Finally this was converted to GR concentration in mol GR per mg protein by dividing Ci by the specific activity (SA) in Ci per mmol of the [^3H]-DEX used (equation 3).

$$\text{dpm/mg protein} = \frac{\text{Bmax (cpm/mg protein)}}{\text{CE}} \quad (1)$$

$$\text{Ci/mg protein} = \frac{\text{dpm/mg protein}}{2.22 \times 10^{12}} \quad (2)$$

$$\text{mol GR/mg protein} = \frac{\text{Ci}}{\text{SA}} \quad (3)$$

Moles GR per cell was calculated by multiplying the GR concentration in mol GR per mg protein by the Bradford determination of the average protein concentration of a single COS-1 cell (6.49×10^{-7} mg/cell) (equation 4). The number of GR molecules per cell was then calculated by multiplying the moles of GR per cell by the Avogadro constant (6.02×10^{23}) (equation 5) which represents the number of molecules in a mole. The molar concentration of GR was calculated by dividing the moles of GR per cell by the hematocrite derived average volume of a single COS-1 cell (4.02×10^{-9} ml/cell) (equation 6).

$$\text{mol GR/cell} = \text{mol GR/mg protein} \times 6.49 \times 10^{-7} \text{ mg protein/cell} \quad (4)$$

$$\text{GR/cell} = \text{mol GR/cell} \times 6.02 \times 10^{23} \quad (5)$$

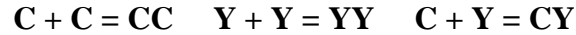
$$\text{M GR} = \frac{\text{mol GR/cell}}{4.02 \times 10^{-9} \text{ ml/cell}} \times 1000 \quad (6)$$

2.1.20 Statistical analysis and curve fitting

Statistical analyses and all curve fitting were carried out using GraphPad Prism 5 software. Statistical analysis was done using one way analysis of variance (ANOVA) with either Bonferroni, Dunnett or Newman-Keuls post-tests or unpaired t tests and carried out on the pooled average \pm SEM of each individual experiment. Statistical significance of differences is indicated in figure legends. Only bars where statistical significance was found are indicated while those left open are non-significant.

2.2 Mathematical model to calculate percentage monomers from FRET data

A derivation carried out on corrected FRET, F-don and F-acc fluorescence from the FRET assay calculates the percentage moles of GR occurring as either monomers or homodimers prior to ligand stimulation. CFP-GR and YFP-GR monomers are defined as C = CFP-GR and Y = YFP-GR, respectively. Receptor dimerization will yield three products:



The equilibrium constants of these reactions are expressed as:

$$K_{eq} = \frac{CY}{C \times Y} = \frac{CC}{C \times C} = \frac{YY}{Y \times Y} \quad (7)$$

The total molar concentration of CFP-GR (C_{tot}) or YFP-GR total (Y_{tot}) in a cell expressing both receptors at the same level consists of a monomeric, heterodimeric and homodimeric fraction.

$$C_{tot} = C + CY + CC \quad (8)$$

$$Y_{tot} = Y + CY + YY \quad (9)$$

From (8) and (9) we can derive the concentrations of the monomers and express their equations as such:

$$C = C_{tot} - CY - CC \quad (10)$$

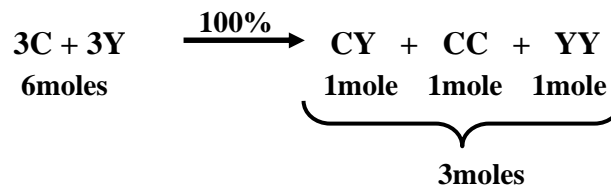
$$Y = Y_{tot} - CY - YY \quad (11)$$

Our FRET experiments generated fluorescence data for total CFP-GR (F-don), total YFP-GR (F-acc) as well as for corrected FRET which represents heterodimer formation. We have defined the terms as C_{tot} = F-don, Y_{tot} = F-acc and CY = FRET. Radioactive binding assays reveal similar expression levels of pCFP-GR, pYFP-GR and pGRwt (Fig.3.3). As equal amounts of CFP-GR and YFP-GR plasmids were transfected we assume that the total average GR content at each receptor level is made up of one half CFP-GR and one half YFP-GR. In order to express the fluorescent signal as a molar concentration we converted fmol GR/mg protein results from saturation binding of the GRwt to nM of GR per cell at low, medium and high GR levels taking into account an experimentally derived average COS-1 cell protein content (6.49×10^{-7} mg/cell) and volume (4.02×10^{-9} ml/cell) (Table 2.1 and Section 2.1.19).

Table 2.1. Average GR concentrations per cell at each GR concentration

	Average GR concentration (nM)		
	Low [GR]	Medium [GR]	High [GR]
GR/cell	10.8	24.6	45.8
Ctot or Ytot/cell	5.4	12.3	22.9
Maximal CY	1.8	4.1	7.6

Assuming 100 percent dimerization following 25 minutes of 10^{-6} M DEX stimulation (Fig.4.8A, (15,16)), one third of all receptor associations will be heterodimeric (equation 8 or 9) consisting of two differentially tagged GR monomers. This results in a maximal heterodimer concentration which is $1/6^{\text{th}}$ of the total monomeric GR concentration (Table 2.1):



We have taken the F-don (CFP-GR) and F-acc (YFP-GR) values at the initial time point (0 minutes) of the FRET experiment to represent Ctot and Ytot, respectively. These values were converted to nM concentrations for each individual cell by dividing them by the average fluorescence for each fluorophore in their population and multiplying the result by the respective Ctot or Ytot/cell concentrations expressed in Table 2.1. The concentration of heterodimer prior to stimulation represents the uninduced (0 minute) FRET signal normalized to the averaged maximal FRET signal consisting of the time points 26 to 30 minutes after DEX induction and multiplied by the maximal molar concentration of CY heterodimer for each respective cell in relation to the average concentration expressed per population in Table 2.1.

Homodimer concentration cannot be measured in this system. However, using equation 7, homodimer concentration may be expressed in terms of the measurable heterodimer (corrected FRET), Ctot and Ytot concentrations. Mathematical derivation of equations (7), (10) and (11) generates C as well as Y monomer concentrations expressed as a function of Ctot (F-don), Ytot (F-acc) and corrected CY (FRET).

$$C = - \frac{3CY^2 + (Y_{tot} + C_{tot})CY - C_{tot}Y_{tot}}{CY + Y_{tot}}$$

$$Y = - \frac{3CY^2 + (Y_{tot} + C_{tot})CY - C_{tot}Y_{tot}}{CY + C_{tot}}$$

Once the concentration of CFP-GR and YFP-GR monomers are derived it is possible to calculate the percentage monomers from the total GR concentration ($C_{tot} + Y_{tot}$):

$$\% \text{ GR monomers} = \left(\frac{C + Y}{C_{tot} + Y_{tot}} \right) 100$$

As the GR exists either as a monomer or a dimer we can calculate the percentage molar concentration of ligand uninduced GR dimers as such:

$$\% \text{ GR dimers} = 100\% - \% \text{ GR monomers}$$

2.3 Bibliography

1. Louw A, Swart P, de Kock SS & van der Merwe KJ (1997) Mechanism for the stabilization in vivo of the aziridine precursor 2(4-acetoxyphenyl)-2-chloro-N-methyl-ethylammonium chloride by serum proteins. *Biochem Pharmacol* 53: 189-197.
2. Yoshikawa N, *et al* (2002) Distinct interaction of cortivazol with the ligand binding domain confers glucocorticoid receptor specificity: Cortivazol is a specific ligand for the glucocorticoid receptor. *J Biol Chem* 277: 5529-5540.
3. Schaaf MJ & Cidlowski JA (2003) Molecular determinants of glucocorticoid receptor mobility in living cells: The importance of ligand affinity. *Mol Cell Biol* 23: 1922-1934.
4. Dewint P, *et al* (2008) A plant-derived ligand favoring monomeric glucocorticoid receptor conformation with impaired transactivation potential attenuates collagen-induced arthritis. *J Immunol* 180: 2608-2615.
5. Tazawa H, *et al* (2003) Regulation of subnuclear localization is associated with a mechanism for nuclear receptor corepression by RIP140. *Mol Cell Biol* 23: 4187-4198.
6. Jenster G, *et al* (1997) Steroid receptor induction of gene transcription: A two-step model. *Proc Natl Acad Sci U S A* 94: 7879-7884.
7. Plaisance S, Vanden Berghe W, Boone E, Fiers W & Haegeman G (1997) Recombination signal sequence binding protein I κ B is constitutively bound to the NF- κ B site of the interleukin-6 promoter and acts as a negative regulatory factor. *Mol Cell Biol* 17: 3733-3743.

8. al-Moslih MI & Dubes GR (1973) The kinetics of DEAE-dextran-induced cell sensitization to transfection. *J Gen Virol* 18: 189-193.
9. Bradford MM (1976) A rapid and sensitive method for the quantitation of microgram quantities of protein utilizing the principle of protein-dye binding. *Anal Biochem* 72: 248-254.
10. Trinkle-Mulcahy L, Sleeman JE & Lamond AI (2001) Dynamic targeting of protein phosphatase 1 within the nuclei of living mammalian cells. *J Cell Sci* 114: 4219-4228.
11. Schaaf MJ, Lewis-Tuffin LJ & Cidlowski JA (2005) Ligand-selective targeting of the glucocorticoid receptor to nuclear subdomains is associated with decreased receptor mobility. *Mol Endocrinol* 19: 1501-1515.
12. Visser K, Smith C & Louw A (2010) Interplay of the inflammatory and stress systems in a hepatic cell line: Interactions between glucocorticoid receptor agonists and interleukin-6. *Endocrinology* 151: 5279-5293
13. Ishibashi H, *et al* (2003) Sex steroid hormone receptors in human thymoma. *J Clin Endocrinol Metab* 88: 2309-2317.
14. Pfaffl MW (2001) A new mathematical model for relative quantification in real-time RT-PCR. *Nucleic Acids Res* 29: e45.
15. Wrangé O, Eriksson P & Perlmann T (1989) The purified activated glucocorticoid receptor is a homodimer. *J Biol Chem* 264: 5253-5259.
16. Segard-Maurel I, *et al* (1996) Glucocorticosteroid receptor dimerization investigated by analysis of receptor binding to glucocorticosteroid responsive elements using a monomer-dimer equilibrium model. *Biochemistry* 35: 1634-1642.

Chapter 3

Results: Positive cooperative ligand binding and increased ligand binding affinity at high glucocorticoid receptor wild type concentrations

Introduction

The basic premise of receptor binding studies involves the association of ligand with a receptor to form a ligand-receptor complex (Fig.3.1). The affinity of a ligand for a receptor is defined by the equilibrium dissociation constant (K_d) which is equal to the concentration of ligand that is required to occupy 50 percent of the receptors and is defined as k_2/k_1 where k_1 is the association rate constant and k_2 is the dissociation rate constant.

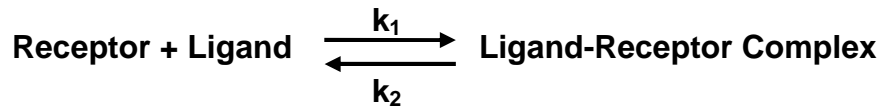


Figure 3.1 **Ligand binding affinity for a receptor is defined as the K_d which is calculated as k_2/k_1 .** The rate of conversion from unbound receptor and ligand to the bound receptor/ligand complex is termed the association rate constant (k_1). The rate of the inverse reaction is termed the dissociation rate constant (k_2).

Plotting the amount of ligand-receptor complex against the log of ligand concentration yields a sigmoidal dose response curve (Fig.3.2). The slope of this curve, also called the Hill slope, is defined as the steepness of the curve between the 10 and 90 percent binding levels (Fig.3.2). A standard binding curve of a ligand to a receptor with only one binding site that follows the laws of mass action has a slope of 1, which implies that an 81-fold increase in ligand concentration will result in an increase of ligand binding from 10 to 90 percent. Positive cooperative ligand binding is defined by a Hill slope which is greater than 1 and not only implies an increase in ligand affinity but also that less ligand is required to shift from 10 to 90 percent of maximal binding. Furthermore, in order for the Hill slope to be greater than one there must be more than one ligand binding site as positive cooperative ligand binding presumes that binding of the ligand to the first binding site results in a conformational change in the second binding site which increases its affinity for the ligand (1).

The ligand binding affinity of a receptor (K_d) has traditionally been thought of as an immutable parameter, however, conformational changes in the GR brought about by mutations in the GR (2) which stimulate dimerization as well as increasing the concentration of certain co-modulators (3) have demonstrated that positive cooperative ligand binding and an increase in ligand binding affinity, respectively, can be achieved. Furthermore, recent results from Cho *et al.*, where decreasing the GR concentration of cytosolic preparations by 3.75-fold resulted in a Hill slope shift from 1.479 to 0.995, indicated positive cooperative DEX binding to the GR at high, but not low, GR concentrations *in vitro* (2). In addition, they demonstrated that positive cooperative ligand binding at high GR concentrations is linked to the dimerization of the GR as a chimeric GAL/GR with enhanced dimerization capacity (4)

retains a Hill slope of 1.39 at low GR concentrations which display non-cooperative ligand binding with the wild type receptor. Due to the positive cooperative nature of ligand binding at low receptor concentrations of the GAL/GR chimera and at high GR wild type (GRwt) concentrations, Cho *et al.* proposed that a shift from intramolecular interactions of GR N- and C-terminal sequences at low GR concentrations to intermolecular interactions at high GR concentrations involving the dimerization sites of the DBD and/or LBD is responsible for positive cooperative ligand binding. The intermolecular interactions proposed by Cho *et al.* (2), which result in positive cooperative ligand binding at high GR concentrations, imply that ligand independent dimerization of the GR occurs at high GR concentrations. The relationship between high concentrations of GR and positive cooperative ligand binding is supported by studies that have shown positive cooperative ligand binding of estradiol to the ER (5),(6). These studies found a direct correlation between Hill slope and ER concentration, which range from a Hill slope of 1.1 at 0.2 to 0.3nM ER to a Hill slope of 1.58 at 2nM ER in cytosolic preparations. Abrogation of ER dimerization resulted in a shift from positive cooperative to non-cooperative ligand binding at high ER concentrations (5). Despite these results, some controversy exists as to the ability of the GR to bind ligand cooperatively as the binding studies of Sheppard *et al.* (7) displayed non-cooperative ligand binding in both whole cell as well as cytosolic saturation binding assays with GR concentrations as high as 277 fmol GR per mg protein.

Theoretically, cooperative ligand binding implies ligand independent dimerization of the GR, which effectively creates two ligand binding sites where the association of the first ligand facilitates the binding of the second in a more energetically favourable reaction and thus increases the affinity of the receptor for the ligand (8). However, Cho *et al.* (2) made no comment as to whether ligand affinity was influenced by the change in GR concentration and concomitant shift in binding characteristics to cooperative ligand binding. Neither did they calculate the specific GR concentrations required to elicit non-cooperative and positive cooperative ligand binding. The literature relating concentration of GR to ligand affinity shows considerable variation regarding effects of GR concentration on ligand binding affinity. For example, saturation binding studies by Chrousos *et al.* (9) on cytosolic fractions of cultured skin fibroblasts expressing varying concentrations of GR show an increase in ligand binding affinity in cells expressing high GR concentrations. Davidson *et al.* (10) in whole mouse skin cytosol showed a similar increase in ligand binding affinity in cells with high GR concentrations. While whole cell saturation binding assays by Elakovic *et al.* (11) demonstrate the exact opposite, namely a correlation between an increase in GR concentration in peripheral blood mononuclear cells (PBMC) and a decrease in ligand binding affinity reflected in an increase in the dissociation constant (K_d). In contrast to the previous studies, saturation binding studies performed by Sun *et al.* (12) on rat muscle cytosol expressing varying levels of GR found no change in ligand affinity at differing GR concentrations.

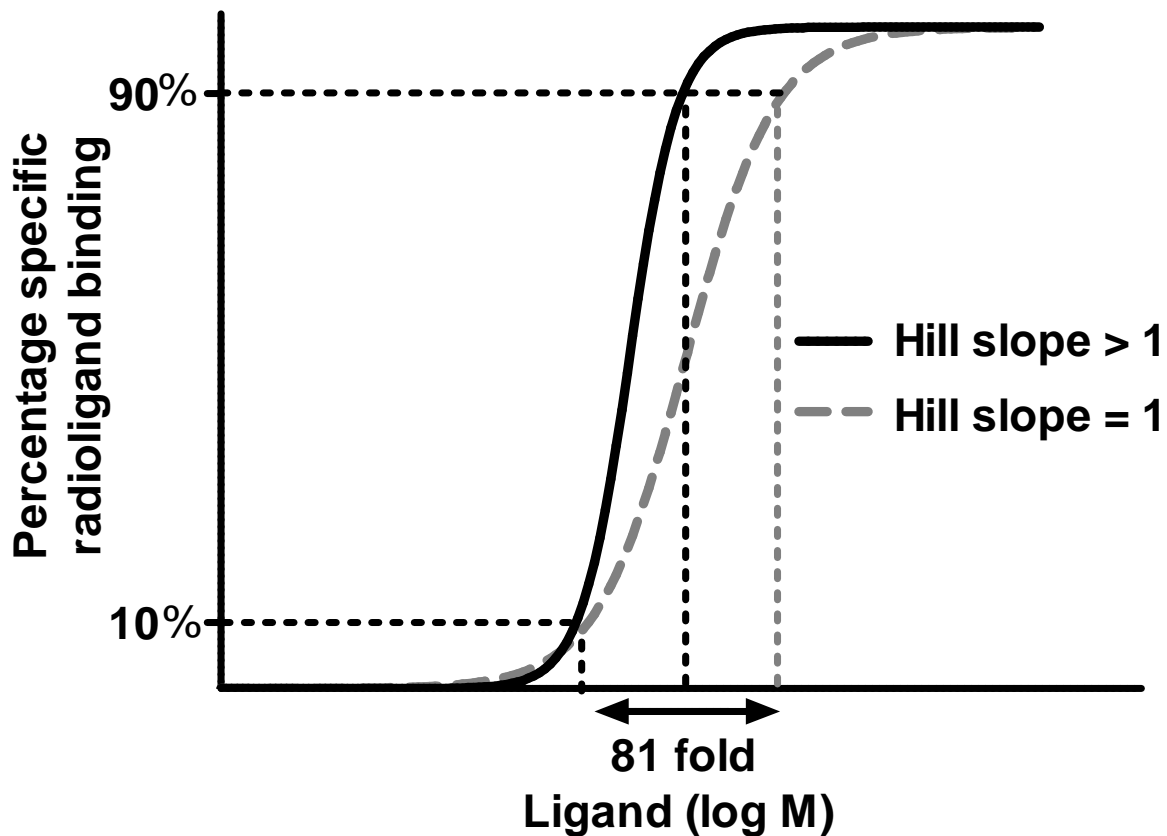


Figure 3.2. **Saturation binding curves.** Representative graph demonstrating non-cooperative ligand binding (grey dashed line) where an 81-fold increase in ligand concentration results in a shift from 10% to 90% ligand binding and a Hill slope equal to 1. Positive cooperative ligand binding (black solid line) where less ligand is required to shift binding from 10% to 90% and the Hill slope is greater than 1.

Tantalising as these results are they have been carried out under decidedly non-physiological conditions. For example the radioactive binding assays of Cho *et al.* (2) were performed on cytosolic fractions diluted at least 3-fold in a solution of sodium molybdate which functions to stabilize the GR (13). Ligand binding affinity, defined by the K_d , was shown to be 3-fold lower in whole cells versus cytosolic fractions (7), which is believed to be as a result of the differences in the cellular *milieu*. The presence of 11β HSD ((14),(15)), GR concentration and its phosphorylation state (16), ligand binding proteins such as CBG (17) and co-modulators of the receptor such as Hsp90 (18), FKBP52 (3) and Ubc9 (2) are all known to influence ligand binding affinity and would be altered in cytosolic versus whole cell binding assays. In addition, no study explicitly examined the relationship between GR concentration and both cooperative ligand binding and affinity.

We thus aim to replicate the difference in GR concentration which Cho *et al.* (2) demonstrated as sufficient to elicit a shift from non-cooperative to positive cooperative ligand binding. Once established we will test whether these different GR concentrations result in the same shift to cooperative ligand binding and if this can be correlated with a change in ligand binding affinity in whole cell saturation

binding assays. In addition we will use the GR dimerization deficient mutant (GRdim) to investigate the prerequisite for GR dimerization in cooperative ligand binding. We hypothesize that a GR concentration dependent change from non-cooperative to positive cooperative ligand binding will result in an increase in ligand binding affinity with the GRwt but not the GRdim mutant.

Results

3.1 Establishing a viable model in which to compare the effects of glucocorticoid receptor concentrations

In order to establish whether ligand binding to the GR is cooperative at high levels in whole cells and whether this affects ligand binding affinity we sought to conduct whole cell saturation binding studies on cells expressing varying concentrations of GR. As the ligand binding affinity of the GR is known to vary between cells (11, 19, 20), which may be due to the influence of co-modulators such as the TPR, FKBP52, and Hsp90 which are differentially expressed in tissues and have been shown to affect ligand binding to the GR (3, 18), we decided to work in a single cell line. We selected COS-1 cells, which are immortalised monkey kidney fibroblast cells, as they contain little to no endogenous GR (21) (Fig.3.3) and could act as a “blank slate” for our GR concentration studies. Ideally we would have liked to have created stable cell lines which have integrated transfected plasmid DNA into their genomes. These cell lines would be derived from a single clone and each cell would have the same GR concentration and make up a homogenous population. However, of the numerous clones created over a 6 month period none resulted in a stable introduction of the GR expressing plasmid and would consistently express less and less GR as determined through whole cell binding. After considerable effort devoted to this endeavour, with no success, we had to compromise. As a result all of our experiments were conducted in COS-1 cells which were transiently transfected with varying amounts of GR plasmid. The cells were pooled and replated after transfection to minimize differences in transfection efficiency within experiments. Between experiments the expressed GR levels were monitored either directly through radioactive ligand binding assays (Fig.3.3) or by monitoring fluorescence intensity of fluorescently labelled GR (Fig.4.5) and indirectly through Western blots (Fig.6.1).

As our study aimed to elucidate the effects of GR concentration on ligand binding and its downstream consequences we chose to focus on the ligand binding of the transcriptionally active GR α as opposed to the non-ligand binding and dominant negative GR β isoform (22, 23). Furthermore we decided to focus solely on the human GR as its behaviour has been found to differ from that of rodent GR (24).

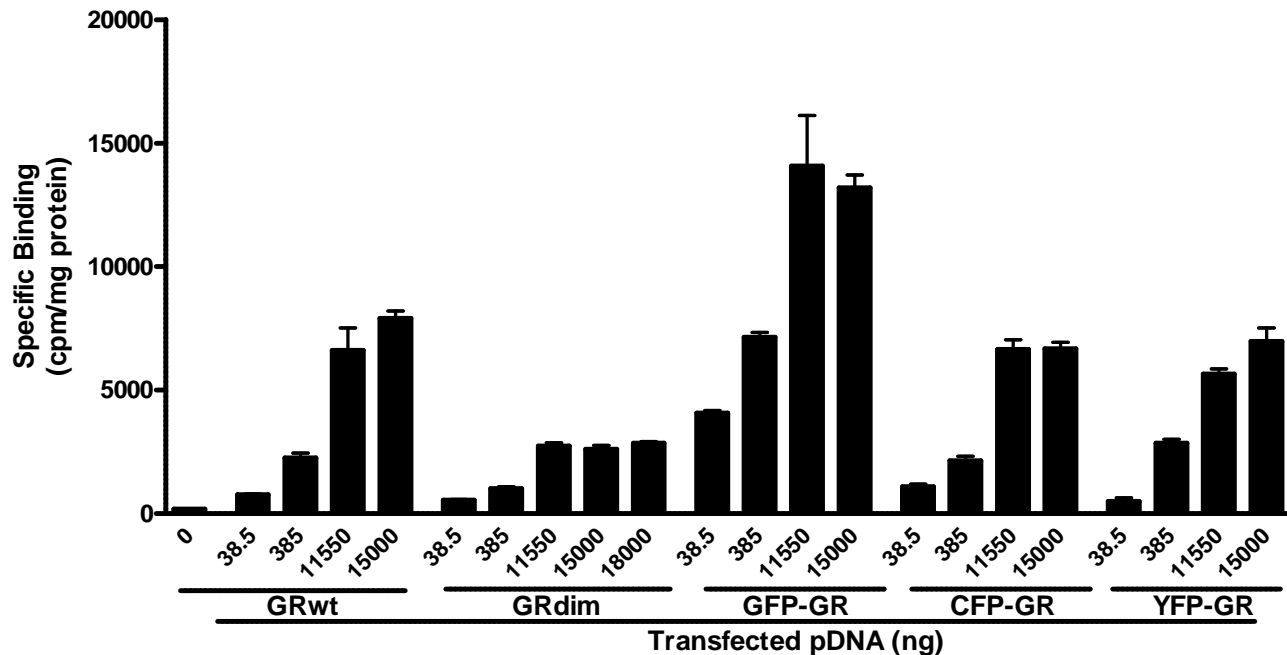


Figure 3.3. **Relative expression levels of GR plasmids.** Whole cell binding was carried out on COS-1 cells DEAE-Dextran transfected with the indicated amounts of plasmid DNA as described in *materials and methods*. Total binding and non-specific binding were normalized to protein concentration (Bradford assay). Specific binding (total binding - nonspecific binding) was plotted and represents a single experiment performed in triplicate (\pm SEM).

Our first task was to establish the maximal and minimal GR expression levels possible through a variety of GR plasmids using transient transfections in COS-1 cells. The relationship between the amount of plasmid DNA transfected and GR expressed is not linear and varies considerably between vectors. What was clear from our radioactive binding study on expression levels of GR plasmids is that GR expression levels plateau at 11550ng plasmid DNA per 10cm tissue culture plate forty eight hours after DEAE-Dextran transfection (Fig.3.3). We thus chose this plasmid level as our maximal transfected GR plasmid level. To represent our lowest GR concentration we selected the 38.5ng plasmid amount as it results in GRwt expression levels which are roughly a fourth of the maximum. Finally the 385ng plasmid level was included as its GR expression level falls roughly half way between the two extremes.

The GR wild type (GRwt), D-loop dimerization domain mutant GR (GRdim) and the green fluorescent protein tagged GR (GFP-GR) expression levels differ due to the fact that their genes are contained in different vectors. In hindsight it would have been optimal for them to have been expressed in a single vector but effort has been made through direct and indirect methods to only compare GR concentrations that are similar.

We do detect trace amounts of endogenous COS-1 cell GR (Fig.3.3), however, these levels are at least 10-fold lower than those expressed at the lowest GRwt plasmid concentration and as a result may be considered negligible.

Prior to performing competitive and saturation binding assays it was necessary to perform time course experiments for each receptor type and concentration in order to establish the incubation time required for ligand binding equilibrium (Fig.3.4). In each case ligand binding reached its plateau at or before four hours. We therefore selected this as the time of incubation for our binding studies.

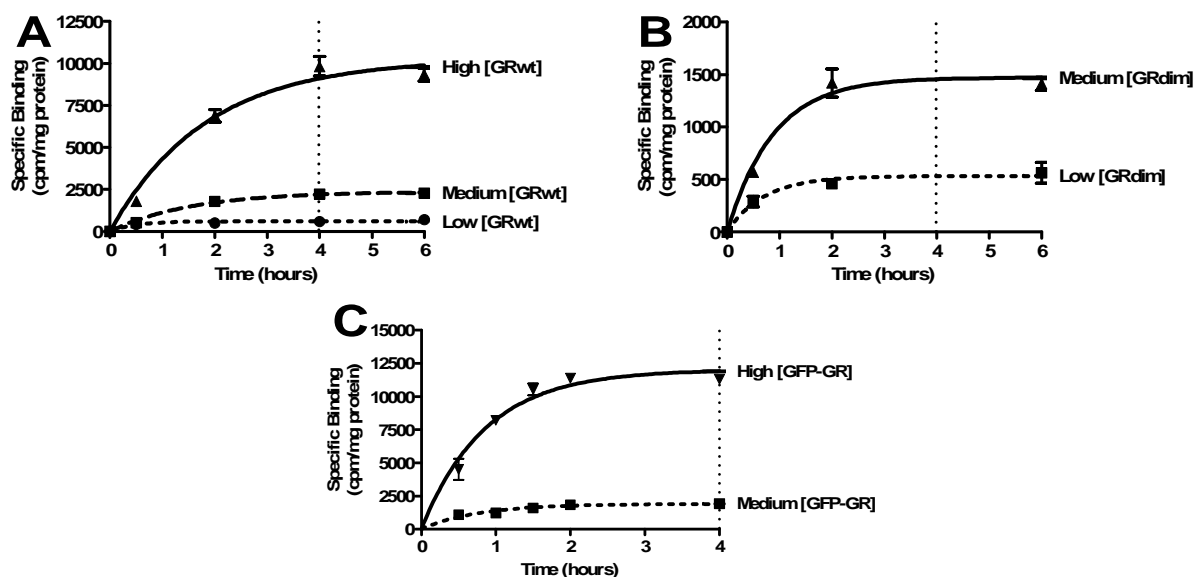


Figure 3.4. **Time courses of GRwt, GRdim and GFP-GR radioactive ligand binding.** COS-1 cells were transfected with (A) low, medium or high levels of GRwt, (B) low or medium GRdim levels or (C) medium or high GFP-GR levels and filled to 11550ng total plasmid DNA/10cm plate with empty vector. Time courses to determine binding equilibrium were performed as described in *materials and methods*. Total binding and non-specific binding were normalized to protein concentration (Bradford assay) and specific binding (total binding - nonspecific binding) was plotted using one phase exponential association curves and represents a single experiment performed in triplicate (\pm SEM).

Due to the expense of radioactive ligand and the high concentrations of ligand required for saturation binding studies we first investigated whether competitive ligand binding assays could be used in order to establish a shift in the Hill slope and in ligand binding affinity. Another advantage of competitive binding is that a range of ligands can be tested as the affinity of the unlabeled ligand can be determined indirectly by measuring its ability to compete with the binding of a radioactive ligand. In these assays varying concentrations of unlabeled ligand compete with a fixed concentration of [3 H]-labelled ligand. As the concentration of unlabeled ligand increases so the amount of [3 H]-labelled ligand bound to the receptor decreases (Fig.3.5A). The binding parameter obtained from competitive binding curves is the concentration of unlabeled ligand that inhibits the binding of the radioactive

ligand by 50 percent, this is called the IC_{50} (25). Unfortunately neither the $\log IC_{50}$ nor the Hill slope was influenced by the concentration of GFP-GR expressed (Fig.3.5B,C). In addition, although the $\log IC_{50}$ varied significantly between test compounds the pattern of binding affinity was not altered by GR concentration (Fig.3.5D). From these results we concluded that competitive binding assays were not an effective way to test for variances in Hill slope or ligand binding affinity because of the existence of two confounding processes as the competitive ligand binding assay evaluates not only the binding of the unlabeled ligand but also that of the [3 H]-labelled ligand as well.

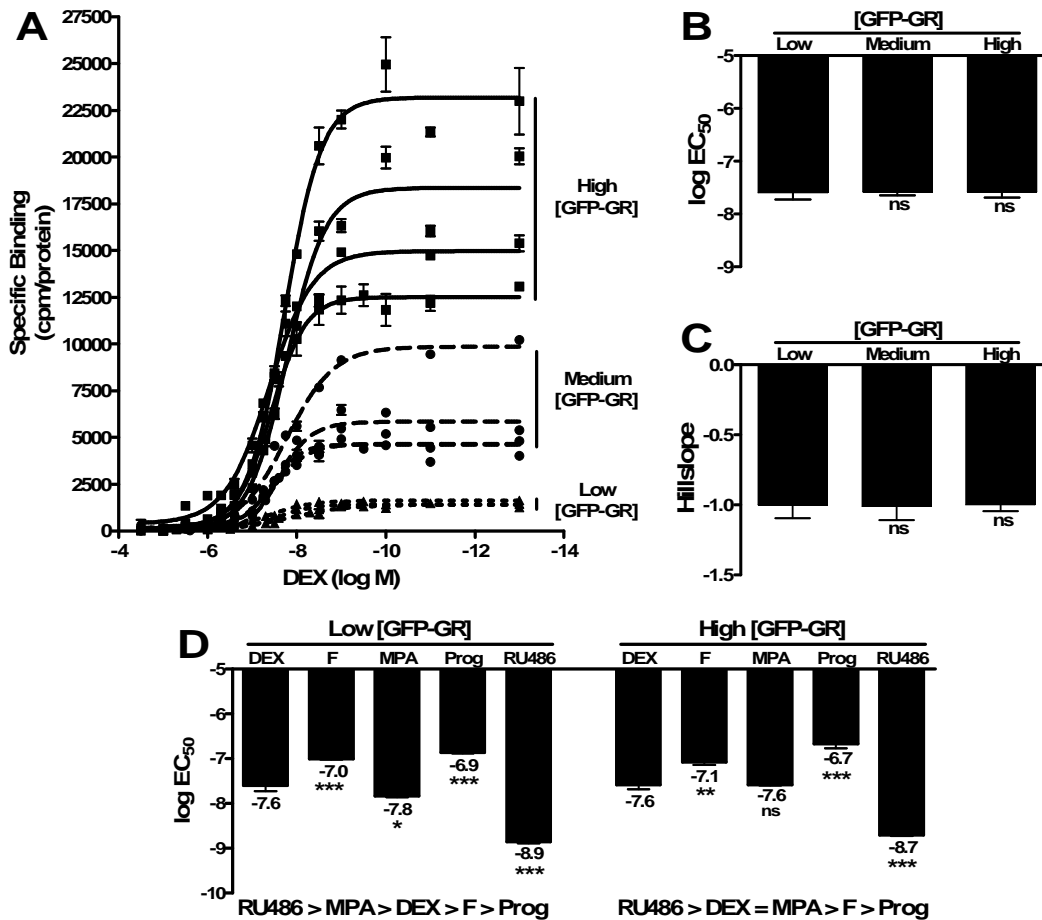


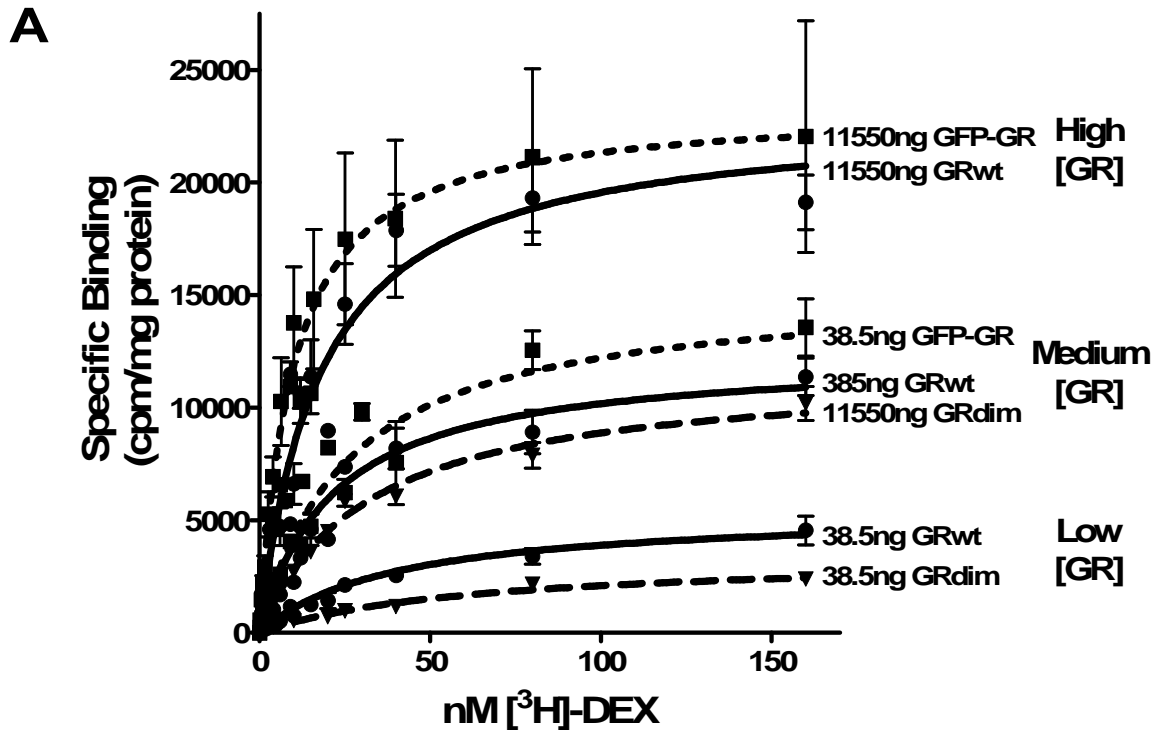
Figure 3.5. Competitive binding assays do not show any change in $\log IC_{50}$ or Hill slope as a result of differences in GR concentration. COS-1 cells (2×10^6 cells/10cm plate) were transfected with low (38.5ng), medium (385ng) or high (11550ng) GFP-GR levels and competitive whole cell binding was carried out as described in *materials and methods* using 20nM [3 H]-DEX and varying concentrations of unlabeled DEX, F, MPA, Prog or RU486. Total binding was normalized to protein concentration (Bradford assay) and the baseline plateau representing non-specific binding was subtracted from all data points. **(A)** The specific binding was fit to a sigmoidal dose-response curve with a variable slope which generates **(B)** $\log IC_{50}$ as well as **(C)** Hill slope values. Statistical analysis on both was carried out using one-way analysis of variance followed by Bonferroni's multiple comparison test. **(D)** Statistical analysis of the $\log IC_{50}$ values of various test compounds within the low and high GFP-GR populations were carried out using one-way analysis of variance followed by Dunnett's post test against DEX stimulation (* $P < 0.05$, ** $P < 0.01$, *** $P < 0.001$). All results represent a minimum of three independent experiments performed in triplicate (\pm SEM).

3.2 Saturation binding was used to designate low, medium and high glucocorticoid receptor concentrations

Saturation binding revealed expressed GR concentrations which fell into three statistically different groups (Fig.3.6A,B). GR levels ranging from 41.8 to 67.0 fmol GR per mg protein were designated as our low GR concentration population, 144.1 to 189.7 fmol GR per mg protein as our medium GR concentration population and 283.9 to 292.3 fmol GR per mg protein as our high GR concentration population. These reflect GR per cell levels ranging from 16300 to 114000 and GR concentration in nM from 6.7 to 47.1 (Fig.3.6B).

All our experiments were carried out in COS-1 cells which were transiently transfected with GR using the DEAE-Dextran method. Fluorescence microscopy revealed that there is a considerable variation in transfection efficiency and resultant expressed GR levels from cell to cell within a population (Fig.3.7). Furthermore fluorescence microscopy showed that roughly 20 percent of cells in a population were transfected. In order to acknowledge this fact we have included an average theoretical prediction of the fmol GR per mg protein in transfected cells only, assuming a transfection efficiency of 20 percent (Fig.3.6B).

Having corrected for transfection efficiency, the GR concentrations studied range from 209 to 1462 fmol GR per mg protein or 81500 to 570000 GR per cell. Although these levels are higher than most GR concentrations reported in human tissue culture cell lines and tissue biopsies (Table 1.1), there are certain tissues and pathological states which lead to the expression of GR at similar levels to our model system. For example, the concentration of GR reported in mononuclear leukocytes, a form of white blood cells, was 191 fmol GR per mg protein (9), while another study revealed GR levels as high as 893 fmol GR per mg protein in healthy skin, rising to 2777 fmol GR per mg protein in the skin of AIDS patients (26). Cytotrophoblasts (epithelial stem cells) have been shown to contain GR concentrations as high as 16200 fmol GR per mg protein (27). We can therefore argue that our medium and high GR concentrations reflect physiological GR levels particularly when compared to GR levels in skin (26) and epithelial stem cells (27).



B

	Transfected plasmid (ng)	Bmax CPM/mg protein \pm SEM	[GR] fmol/mg protein \pm SEM	GR/cell	[GR] (nM)	fmol GR/mg protein (assuming 20% transfection)	[GR] Designation
GRwt	38.5	5437 \pm 503 ^a	67.0 \pm 6.2 ^a	26200	10.8	335	Low
	385	12382 \pm 965 ^b	152.6 \pm 11.9 ^b	59600	24.6	763	Medium
	11550	23036 \pm 1363 ^c	283.9 \pm 16.8 ^c	111000	45.8	1420	High
GRdim	38.5	3394 \pm 199 ^a	41.8 \pm 2.5 ^a	16300	6.7	209	Low
	11550	11691 \pm 428 ^b	144.1 \pm 5.3 ^b	56300	23.2	721	Medium
GFP-GR	38.5	15390 \pm 1277 ^b	189.7 \pm 15.7 ^b	74100	30.6	949	Medium
	11550	23718 \pm 2179 ^c	292.3 \pm 26.8 ^c	114000	47.1	1462	High

Figure 3.6. **Saturation binding establishes three distinct and statistically different populations of GR namely, low, medium and high.** COS-1 cells were transiently transfected with GRwt (low, medium or high), GRdim (low or medium) or GFP-GR (medium or high) and filled to 11550ng total plasmid DNA/10cm tissue culture plate with the empty vector pGL2-basic. After replating cells were serum starved for 24 hours and saturation binding was carried out according to *materials and methods*. (A) Specific binding was plotted against nM $[^3\text{H}]\text{-DEX}$ and curves fit using one site binding hyperbola to obtain Bmax values. (B) Summary table of expressed GR from saturation binding results. GR/cell, nM GR concentration and fmol GR/mg protein have all been derived from the maximal binding (Bmax) value as described in *materials and methods*. Statistical analysis on maximal binding (Bmax) and fmol GR per mg protein was carried out using ANOVA followed by Newman-Keuls multiple comparison post test, where conditions with different letters are statistically different from one another ($P < 0.01$). All results represent a minimum of two independent experiments performed in triplicate (\pm SEM).

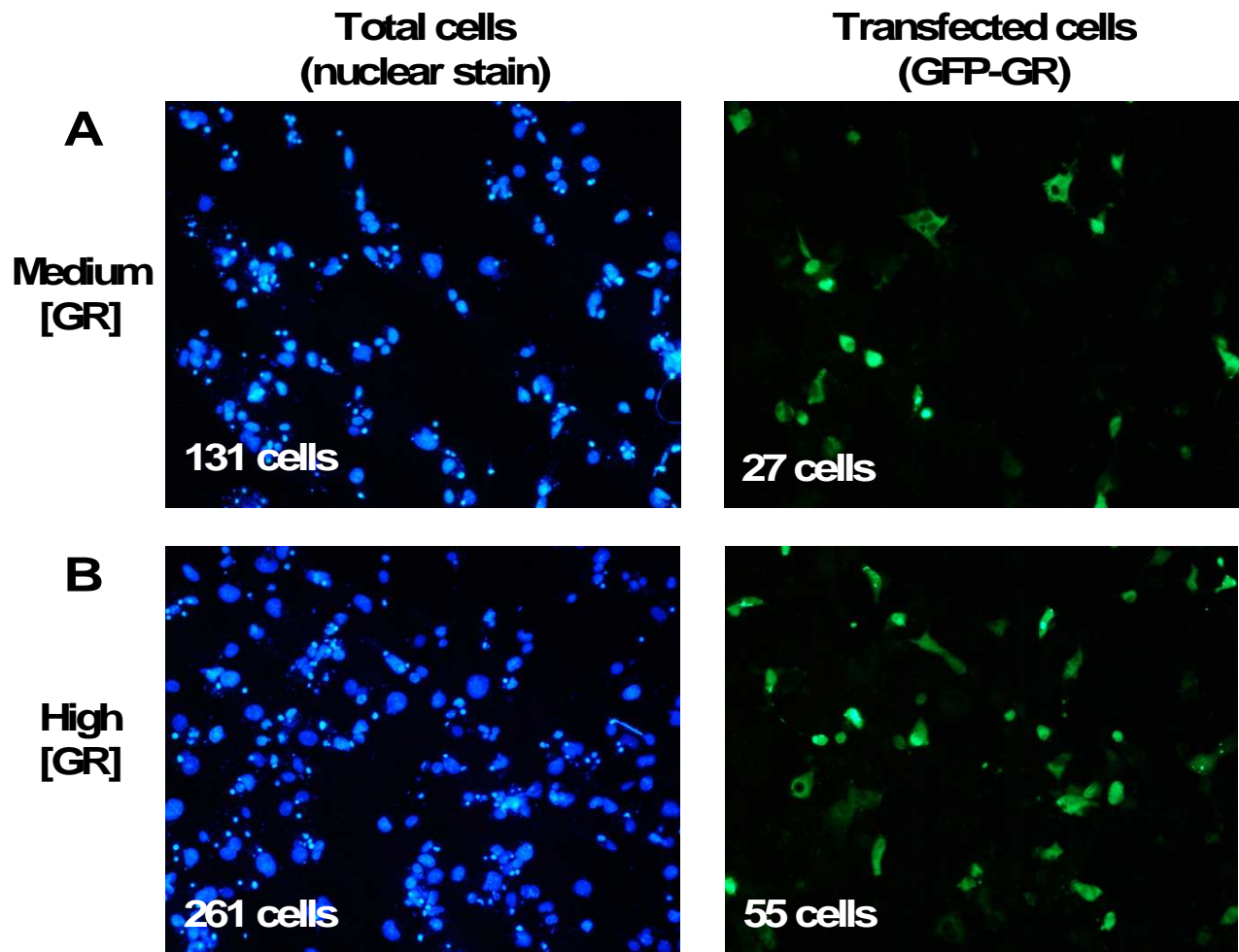


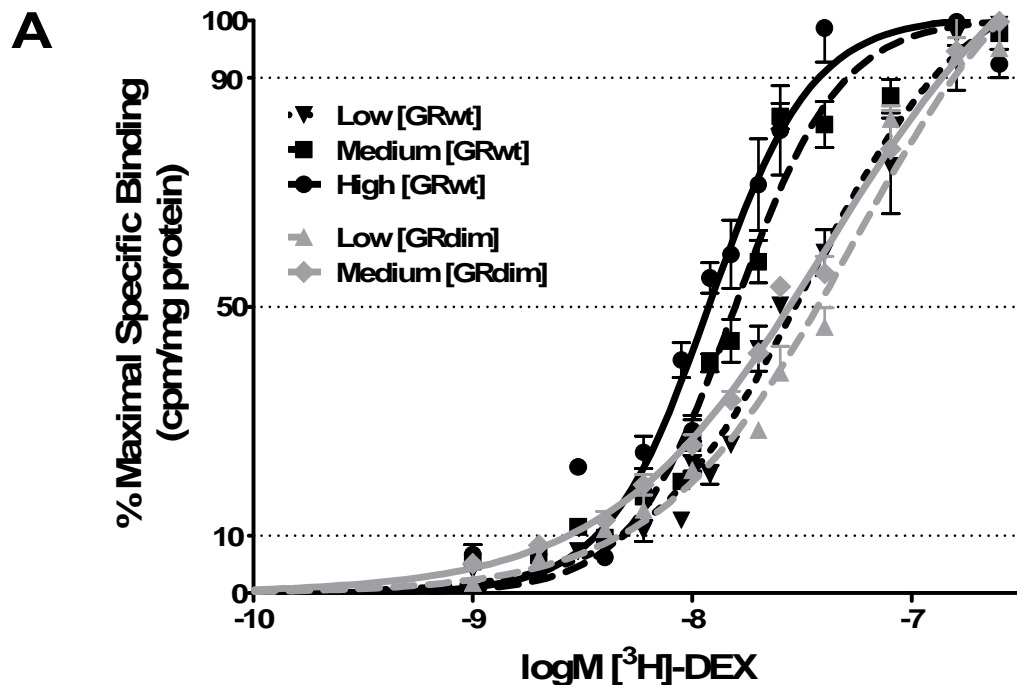
Figure 3.7. The transfection efficiency of COS-1 cells through the DEAE-Dextran method is ~20 percent. COS-1 cells transiently transfected with (A) medium or (B) high concentrations of GFP-GR. The Hoechst nuclear stain is used to visualize the total number of cells present while the GFP signal is only detected in cells expressing the GFP-GR plasmid.

Although the expression of GR has been analysed in a comprehensive study of major tissues of the human body this was only at the level of GR mRNA (28). The majority of studies which have looked at the expression of the GR protein in a single tissue have done so through radioactive binding assays in cell lysates (29-32) or through Western blotting (28, 33) neither of which are optimal in terms of quantifying GR concentration due to the qualitative nature of Western blot experiments and the altered behaviour of GR binding *in vitro* (19). In addition, in experiments where GR concentration has been accurately quantified, values are primarily given in terms of GR per cell which in itself is problematic. A more practical measurement for the expression of GR concentration would be in molar. This is also the most useful measurement of GR concentration for mathematical modelling. There is a need for a systematic study of GR concentrations, expressed in molar and performed through whole cell binding assays, in a wide variety of tissue types.

3.3 Positive cooperative ligand binding is GR concentration and dimerization dependent

Having established which amounts of GR plasmid would yield 3 statistically different populations of GR we set out to determine the effect of GR concentration on cooperative ligand binding and K_d using whole cell saturation binding. When specific binding of GRwt and GRdim concentrations was plotted against $\log M$ [3H]-DEX concentrations and curves fit using sigmoidal dose-response with variable slope (Fig.3.8A), there is a clear left shift of the medium and high GRwt concentration curves, but not of the GRdim medium concentration curve. This implies that concentration of ligand required to shift binding from 10 to 90 percent receptor occupancy is reduced at medium and high GRwt concentrations. Specifically, the fold increase in ligand concentration required to shift receptor occupancy from 10 to 90 percent is 60-fold at the low GRwt concentration, 11-fold at the medium GRwt concentration and 10-fold at the high GRwt concentration. Calculation of Hill slopes indicate that ligand binding at low GR concentrations was non-cooperative for all GR types but shifted significantly to positive cooperative ligand binding (Hill slope >1) at medium and high GRwt and high GFP-GRwt concentrations (Fig.3.8B). The Hill slope at the low GRwt level was 1.08, which is similar to the 0.995 value Cho *et al.* (2) found with their low GR concentration, while our medium GRwt concentration's Hill slope of 1.57 is comparable to that of Cho *et al.*'s high GR concentration of 1.479. We showed a further receptor concentration dependent increase in Hill slope at our high GR concentration to 1.72, while the high GFP-GR concentration displayed a Hill slope more in line with the medium GRwt concentration (Fig.3.8B). Positive cooperative ligand binding at the medium GRwt as well as the high GRwt and high GFP-GR concentrations are noteworthy as it represents the first evidence in whole cell binding assays of positive cooperative ligand binding to the GR.

Binding to the medium concentration of GRdim (34) remained non-cooperative (Fig.3.8A,B) despite the fact that the GR concentrations of medium GRwt and medium GRdim were statistically the same (Fig.3.6B). The fact that the medium concentration of GRwt displayed positive cooperative ligand binding while that of the medium concentration of GRdim was non-cooperative implies that loss of cooperative ligand binding is due to the single point mutation in the D-loop of the GRdim receptor. We can thus conclude that the impaired dimerization brought about by this mutation rendered the GRdim incapable of positive cooperative ligand binding and that the ability to bind ligand in a positive cooperative manner was indeed dependent on the ability of GR to dimerize.



B

	[GR] designation	Hill slope \pm SEM	Cooperative binding	K_d (nM) \pm SEM	K_d change vs. low [GRwt]
GRwt	Low	1.08 \pm 0.06 ^a	No	49.1 \pm 6.7	-
	Medium	1.57 \pm 0.03 ^b	Yes	23.9 \pm 1.2*	Yes
	High	1.72 \pm 0.02 ^b	Yes	16.8 \pm 5.8*	Yes
GRdim	Low	1.00 \pm 0.09 ^a	No	52.3 \pm 2.9	-
	Medium	0.88 \pm 0.02 ^a	No	33.2 \pm 4.1	-
GFP-GRwt	Medium	0.78 \pm 0.10 ^a	No	28.4 \pm 9.0	-
	High	1.44 \pm 0.17 ^b	Yes	10.9 \pm 3.0**	Yes

Figure 3.8 **Saturation binding reveals the extent of GR concentration dependent differences in cooperative ligand binding (Hill slope) and ligand binding affinity (K_d).** Saturation binding was carried out according to *materials and methods*. (A) Specific binding of GRwt (low, medium or high) or GRdim (low or medium) was plotted against logM [3 H]-DEX and curves fit using sigmoidal dose-response (variable slope) to obtain Hill slopes. (B) Summary table of saturation binding results. Statistical analysis on Hill slope was carried out using ANOVA followed by Newman-Keuls multiple comparison post test, where conditions with different letters are statistically different from one another ($P < 0.01$). Statistical analysis of K_d values was through a one tailed unpaired t test against the low GRwt concentration (* $P < 0.05$, ** $P < 0.01$). All results represent a minimum of two independent experiments performed in triplicate (\pm SEM).

The theoretical maximum Hill slope for binding to a receptor with a single binding site is 1, which increases to 2 when two binding sites are present. Our GRwt Hill slope values fell between 1.08 and 1.72, which indicates a shift in ligand binding from binding predominantly to the receptor monomer at

low GR concentrations to binding predominantly to the GR dimer at high GR concentrations. The fact that the Hill slope approaches but does not reach its theoretical maximum of 2 is to be expected as the Hill slope coefficient is known to provide a minimum estimate of the number of binding sites involved (1).

From the graph representing specific binding of GRwt and GRdim concentrations plotted against $\log M$ [^3H]-DEX concentration (Fig.3.8A), it is possible to visualize not only the increase in the steepness of the slope between 10 and 90 percent ligand binding, which determines the Hill slope, but also the decrease in the concentration of ligand required for 50 percent of maximal binding or K_d . Our results suggest that there is a correlation between increased positive cooperative ligand binding and a decreased K_d compared to the non-cooperatively bound low GRwt concentration (Fig.3.8B). This also held true for the high GFP-GR concentration, which displayed positive cooperative ligand binding and had a significantly lower K_d than the non-cooperative ligand binding at low GRwt concentration. This supports the theory that positive cooperative ligand binding and increased ligand binding affinity are linked. The slight and not significant variations in K_d between the GR types (GRwt versus GFP-GR or GRdim) may be ascribed to conformational differences resulting from the mutation in the second zinc finger of the DBD in GRdim and the large fluorescent protein tag in GFP-GR, respectively.

The K_d of the GR for DEX in cytosolic preparations has been shown to vary between 3.7nM (35) and 7.6nM (36). While whole cell saturation binding studies performed on COS-1 cells transiently transfected with high levels of GRwt through the highly effective lipofectamine based reagent Fugene display a [^3H]-DEX binding K_d of 12.6nM (37), which is similar to the 16.8 to 10.9nM ligand binding affinity displayed at our high GR concentrations.

Once corrected for 20 percent transfection efficiency the minimum concentration of GRwt at which we demonstrate positive cooperative ligand binding and a concomitant increase in ligand binding affinity (K_d) is 763 fmol GR per mg protein or 298000 GR per cell (Fig3.6B, Fig3.8B). This may explain why Sheppard *et al.* (7) showed non-cooperative ligand binding in both whole cell as well as cytosolic saturation binding assays with GR concentrations of 277 fmol GR per mg protein and casts further doubt on the results of Elakovic *et al.* (11) who demonstrated a shift in K_d from 2.5nM at only 1391 GR per cell to a K_d of 98.6nM at 15133 GR per cell in PBMC from a healthy human population. Although the study by Chrousos *et al.* (9) supports our results in terms of showing an increase in affinity (decrease in K_d) at higher concentrations of GR, this increase occurred between 53 and 191 fmol GR per mg protein, which is much lower than the level we found. The discrepancy regarding the level of GR through which an increase in K_d is observed may be explained by the fact that this saturation binding study was conducted on cytosolic fractions and not in whole cells or by the fact that Chrousos

et al. was investigating patients with primary cortisol resistance who may have had mutated GR receptors.

We have demonstrated that positive cooperative ligand binding occurs at high concentrations of GRwt and GFP-GR, that this is GR dimerization dependent and that it results in an increase in ligand binding affinity. We thus postulate that as receptor concentrations increase so will the prevalence of ligand binding to GR dimer. In order for this to occur there must be a GR concentration dependent increase in ligand independent dimerization of the GR. The next step in our study was then to test this possible mechanism for positive cooperative ligand binding, notably ligand independent dimerization of the GR at GR concentrations that elicit cooperative ligand binding.

3.4 Bibliography

1. Weiss JN (1997) The hill equation revisited: Uses and misuses. *FASEB J* 11: 835-841.
2. Cho S, Kagan BL, Blackford JA, Jr, Szapary D & Simons SS, Jr (2005) Glucocorticoid receptor ligand binding domain is sufficient for the modulation of glucocorticoid induction properties by homologous receptors, coactivator transcription intermediary factor 2, and Ubc9. *Mol Endocrinol* 19: 290-311.
3. Davies TH, Ning YM & Sanchez ER (2005) Differential control of glucocorticoid receptor hormone-binding function by tetratricopeptide repeat (TPR) proteins and the immunosuppressive ligand FK506. *Biochemistry* 44: 2030-2038.
4. Hidalgo P, *et al* (2001) Recruitment of the transcriptional machinery through GAL11P: Structure and interactions of the GAL4 dimerization domain. *Genes Dev* 15: 1007-1020.
5. Notides AC, Lerner N & Hamilton DE (1981) Positive cooperativity of the estrogen receptor. *Proc Natl Acad Sci U S A* 78: 4926-4930.
6. Sasson S & Notides AC (1982) The inhibition of the estrogen receptor's positive cooperative [3H]estradiol binding by the antagonist, clomiphene. *J Biol Chem* 257: 11540-11545.
7. Sheppard KE (1998) Decreased apparent affinity of corticosterone for colonic crypt glucocorticoid receptors is dependent on the cellular milieu and is distinct from corticosterone metabolism. *J Steroid Biochem Mol Biol* 64: 35-42.
8. Franco R, *et al* (2006) The two-state dimer receptor model: A general model for receptor dimers. *Mol Pharmacol* 69: 1905-1912.
9. Chrousos GP, *et al* (1982) Primary cortisol resistance in man. A glucocorticoid receptor-mediated disease. *J Clin Invest* 69: 1261-1269.
10. Davidson KA & Slaga TJ (1983) Glucocorticoid receptor levels in mouse skin after repetitive applications of 12-O-tetradecanoylphorbol-13-acetate and mezerein. *Cancer Res* 43: 3847-3851.

11. Elakovic I, Perisic T, Cankovic-Kadijevic M & Matic G (2007) Correlation between glucocorticoid receptor binding parameters, blood pressure, and body mass index in a healthy human population. *Cell Biochem Funct* 25: 427-431.
12. Sun X, Fischer DR, Pritts TA, Wray CJ & Hasselgren PO (2002) Expression and binding activity of the glucocorticoid receptor are upregulated in septic muscle. *Am J Physiol Regul Integr Comp Physiol* 282: R509-18.
13. Hutchison KA, Stancato LF, Jove R & Pratt WB (1992) The protein-protein complex between pp60v-src and hsp90 is stabilized by molybdate, vanadate, tungstate, and an endogenous cytosolic metal. *J Biol Chem* 267: 13952-13957.
14. Low SC, *et al* (1994) Sexual dimorphism of hepatic 11 beta-hydroxysteroid dehydrogenase in the rat: The role of growth hormone patterns. *J Endocrinol* 143: 541-548.
15. Seckl JR & Walker BR (2001) Minireview: 11beta-hydroxysteroid dehydrogenase type 1- a tissue-specific amplifier of glucocorticoid action. *Endocrinology* 142: 1371-1376.
16. Webster JC, *et al* (1997) Mouse glucocorticoid receptor phosphorylation status influences multiple functions of the receptor protein. *J Biol Chem* 272: 9287-9293.
17. Pusch L, Wegmann S, Caldwell JD & Jirikowski GF (2009) Expression of corticosteroid-binding globulin in human astrocytoma cell line. *Cell Mol Neurobiol* 29: 583-588.
18. Caamano CA, Morano MI, Dalman FC, Pratt WB & Akil H (1998) A conserved proline in the hsp90 binding region of the glucocorticoid receptor is required for hsp90 heterocomplex stabilization and receptor signaling. *J Biol Chem* 273: 20473-20480.
19. Chriguier RS, *et al* (2005) Glucocorticoid sensitivity in young healthy individuals: In vitro and in vivo studies. *J Clin Endocrinol Metab* 90: 5978-5984.
20. Grasso G, Lodi L, Lupo C & Muscettola M (1997) Glucocorticoid receptors in human peripheral blood mononuclear cells in relation to age and to sport activity. *Life Sci* 61: 301-308.
21. Gougat C, *et al* (2002) Overexpression of the human glucocorticoid receptor alpha and beta isoforms inhibits AP-1 and NF-kappaB activities hormone independently. *J Mol Med* 80: 309-318.
22. Leung DY, de Castro M, Szeffler SJ & Chrousos GP (1998) Mechanisms of glucocorticoid-resistant asthma. *Ann N Y Acad Sci* 840: 735-746.
23. Webster JC, Oakley RH, Jewell CM & Cidlowski JA (2001) Proinflammatory cytokines regulate human glucocorticoid receptor gene expression and lead to the accumulation of the dominant negative beta isoform: A mechanism for the generation of glucocorticoid resistance. *Proc Natl Acad Sci U S A* 98: 6865-6870.
24. Rogatsky I, Waase CL & Garabedian MJ (1998) Phosphorylation and inhibition of rat glucocorticoid receptor transcriptional activation by glycogen synthase kinase-3 (GSK-3). species-specific differences between human and rat glucocorticoid receptor signaling as revealed through GSK-3 phosphorylation. *J Biol Chem* 273: 14315-14321.
25. Motulsky HJ & Mahan LC (1984) The kinetics of competitive radioligand binding predicted by the law of mass action. *Mol Pharmacol* 25: 1-9.

26. Guo WX, *et al* (1996) Expression and cytokine regulation of glucocorticoid receptors in kaposi's sarcoma. *Am J Pathol* 148: 1999-2008.
27. Driver PM, *et al* (2001) Expression of 11 beta-hydroxysteroid dehydrogenase isozymes and corticosteroid hormone receptors in primary cultures of human trophoblast and placental bed biopsies. *Mol Hum Reprod* 7: 357-363.
28. Pujols L, *et al* (2002) Expression of glucocorticoid receptor alpha- and beta-isoforms in human cells and tissues. *Am J Physiol Cell Physiol* 283: C1324-31.
29. Beattie CW, Hansen NW & Thomas PA (1985) Steroid receptors in human lung cancer. *Cancer Res* 45: 4206-4214.
30. Paoletti P, *et al* (1990) Characteristics and biological role of steroid hormone receptors in neuroepithelial tumors. *J Neurosurg* 73: 736-742.
31. Yu ZY, *et al* (1981) A study of glucocorticoid receptors in intracranial tumors. *J Neurosurg* 55: 757-760.
32. Voutsas IF, *et al* (2007) A novel quantitative flow cytometric method for measuring glucocorticoid receptor (GR) in cell lines: Correlation with the biochemical determination of GR. *J Immunol Methods* 324: 110-119.
33. Li LB, Leung DY, Hall CF & Goleva E (2006) Divergent expression and function of glucocorticoid receptor beta in human monocytes and T cells. *J Leukoc Biol* 79: 818-827.
34. Heck S, *et al* (1994) A distinct modulating domain in glucocorticoid receptor monomers in the repression of activity of the transcription factor AP-1. *EMBO J* 13: 4087-4095.
35. Hellal-Levy C, *et al* (1999) Specific hydroxylations determine selective corticosteroid recognition by human glucocorticoid and mineralocorticoid receptors. *FEBS Lett* 464: 9-13.
36. Lu NZ, Collins JB, Grissom SF & Cidlowski JA (2007) Selective regulation of bone cell apoptosis by translational isoforms of the glucocorticoid receptor. *Mol Cell Biol* 27: 7143-7160.
37. Dong DD, Jewell CM, Bienstock RJ & Cidlowski JA (2006) Functional analysis of the LXXLL motifs of the human glucocorticoid receptor: Association with altered ligand affinity. *J Steroid Biochem Mol Biol* 101: 106-117.

Chapter 4

Results: Ligand independent dimerization of the glucocorticoid receptor

Introduction

Positive cooperative ligand binding presupposes the existence of more than one binding site. Based on the work of Cho *et al.* (1) and our own findings in whole cell saturation binding studies (Chapter 3) we hypothesized that ligand independent dimerization at high GR concentrations is responsible for the existence of two ligand binding sites which allows for positive cooperative ligand binding to the GR at high, but not at low, GR concentrations.

It has been established through glycerol gradient centrifugation of purified GR (2) as well as through FRET experiments in live cells (3) that the activated GR exists as a homodimer independently of DNA binding. Two areas of the GR have been identified as influential in GR dimerization namely, the D-loop of the DBD and the LBD. Specifically, it was shown that GR dimerization is stabilized through the second zinc finger of the DBD (4), which is termed the D-loop, while dimerization can also be achieved through the LBD alone (5). Segard-Maurel *et al.* (6) determined the K_d of activated GR dimerization independent of DNA binding as 3.9nM in cell cytosol, while Bledsoe *et al.* (7) demonstrated that dimerization of activated GR LBD has a K_d of 1.5 μ M under similar conditions, implying that affinity of the full length GR is higher than the LBD alone.

Ligand independent dimerization has been demonstrated in the ER (8) but we have not been able to find a study which specifically focuses on levels of ligand independent dimerization of the GR. Some studies have, however, implicitly investigated ligand independent dimerization. For example, Dewint *et al.* (9) show ligand independent dimerization of the GR in a Co-IP experiment, which was roughly 90% of DEX induced dimerization. The explanation they offered was that in transient transfections of GR the heightened concentrations of receptor outnumber that of heat shock protein chaperones which are required to maintain the monomeric GR conformation. Interestingly, they also reveal CpdA's ability to disrupt GR dimerization in a dose dependent manner. In a follow up article on CpdA, Robertson *et al.* (Addendum B) (10) reported the same finding, namely ligand independent pull down of a differentially tagged GR and CpdA induced abrogation of dimerization in a Co-IP experiment. They went on to demonstrate the same phenomena in a live cell FRET experiment where the addition of CpdA reduced the ligand independent association of CFP tagged and YFP tagged GR. This was reflected in a decrease in the FRET signal following CpdA addition. Both these studies as well as a myriad of others demonstrate dimerization of the GR as a result of stimulation by the potent synthetic GC, DEX (2, 3, 6, 11, 12). In fact, dimerization of the GR following ligand binding is a well known characteristic of the receptor.

Armed with the Co-IP and FRET techniques and the knowledge that ligand independent dimerization of the GR was detectable both *in vitro* and in whole cells, we set about testing our hypothesis that ligand independent dimerization increases at GR levels shown to exhibit positive cooperative ligand binding. As DEX is known to result in maximal dimerization of the GR, while CpdA abrogates dimerization we used these ligands as a positive and negative, respectively, control for dimerization.

Results

4.1 Demonstrating ligand independent dimerization using Co-IP

The Co-IP technique we have used relies on Flag anti-body tagged beads which will associate with the Flag protein, a short sequence of 8 amino acids (N-DYKDDDDK-C (1012 Da) (13). When incubated with the cell lysate, these beads trap Flag-tagged proteins and any particles associated to them. We have used a Flag-GR (molecular mass, 96 kDa), which has a Flag tag, and a GFP-GR (molecular mass, 128.5 kDa), which is larger than the Flag-GR due to its fluorescent protein tag. Where we have immunoprecipitated the Flag-GR using the Flag anti-body tagged beads we expect to co-precipitate GFP-GR if it has dimerized with the Flag-GR. Thus if GFP-GR is visualized in the pull down it implies dimerization of the differentially tagged GRs. As visualization of the Co-IP pull down is done on a Western blot using a primary anti-body against the GR it is necessary that the two tagged GR's used have a large size difference in order to differentiate between the two. We expect to see the 128.5 kDa GFP-GR migrate considerably slower than the smaller 96kDa Flag-GR through the acrylamide gel which allows for easy differentiation between the two.

For optimal association and pull down equal concentrations of these tagged GRs is required. A radioactive binding experiment revealed vastly different expression levels from the two vectors (Fig.4.1). It was therefore necessary to transfect the two plasmids in a ratio of 1:8 of GFP-GR to Flag-GR. Westerns run on the Co-IP inputs illustrate similar expression levels of the two plasmids at this transfection ratio (Fig.4.2B,C). We transfected three populations of GR, which mirror the low, medium and high GRwt levels defined through saturation binding studies (Fig.3.6B). Along with the pairing of Flag-GRwt and GFP-GRwt we examined the Flag-GRwt and GFP-GRdim pair in parallel. As the name suggests GFP-GRdim consists of a GFP tagged dimerization D-loop mutant GR. We have included the GFP-GRdim in order to confirm the significance of dimerization in our pull down study and to gain a better insight into this mutation. Much work has been done on this specific D-loop mutation (11, 14-16) and it is generally assumed to be incapable of dimerization, however, its ability to dimerize has never been tested directly.

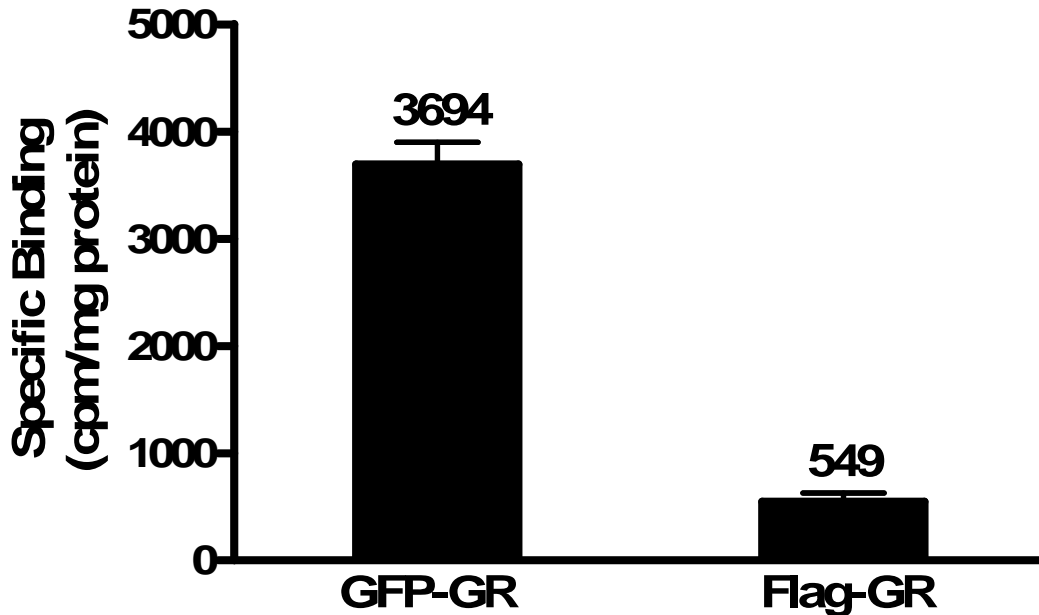


Figure 4.1. **Flag-GR and GFP-GR expression levels differ considerably.** COS-1 cells (2×10^6 cells/10cm plate) were transfected with 5775ng GFP-GR or 5775ng Flag-GR and filled to 11550ng total plasmid DNA/10cm plate with empty vector. Whole cell binding was carried out as described for the determination of expression levels of GR plasmids in *materials and methods*. Total binding and non-specific binding was normalized to protein concentration (Bradford assay). Specific binding (total binding - nonspecific binding) was plotted and represents a single experiment performed in triplicate (\pm SEM).

As Co-IP controls (Fig.4.2A) we transfected Flag-GR, GFP-GRwt or GFP-GRdim only at concentrations that represent half the total GR levels expressed at the low, medium or high GR concentrations. This was done to demonstrate that no non-specific pull down of either GFP-GRwt or GFP-GRdim occurs at any of the three GR concentrations studied. As can be seen in the first column at each GR concentration (Fig.4.2A), where Flag-GR was transfected alone and the Co-IP experiment was carried out, there is a single band which corresponds to the size of the Flag-GR. This result confirms that the Flag-GR is effectively pulled down by the Flag-anti-body containing beads. The next two columns at each receptor level represent the Co-IP pull down from cells expressing GFP-GRwt or GFP-GRdim only. No bands are visible in these columns, which confirm that there is no non-specific pull down of either of the GFP-tagged GRs. We have run the inputs of these Co-IP experiments in the columns to the right of the Co-IP controls. There is a single distinct band at the Flag-GR size where Flag-GR has been transfected. However, the band that can be seen running at the same level as the Flag-GR in the GFP-GRwt and GFP-GRdim lanes represent break down products of these receptors and are not as a result of incorrect loading or transfection. This is supported by the fact that Co-IP of these samples results in no Co-IP pull down, which would have occurred if they contained any Flag-GR.

4.1.1 Co-IP studies show GFP-GR pull down independent of ligand stimulation, which increases as GRwt levels do.

COS-1 cells were transfected with low, medium or high levels of GRwt or GRdim and treated with solvent to determine the effect of GR concentration on ligand independent dimerization. The inputs of each Co-IP experiment were run (Fig.4.2B,C) in order to monitor for transfection efficiency and all GFP-GR pull down was normalized against its respective Flag-GR band in order to correct for differences in loading and anti-body concentration between the GR concentrations. Due to the differences in expressed GR between the three GR concentrations it was necessary to alter the primary and secondary anti-body concentrations used as described in *materials and methods*.

At the low level of GFP-GRwt (Fig.4.2B) as well as GFP-GRdim (Fig.4.2C) we saw little to no GFP-GR pull down following solvent (EtOH) induction, which implies almost no ligand independent dimerization. However, at the medium GR concentrations there was clear ligand independent GFP-GR pull down of both GFP-GRwt and the GFP-GRdim. Results at the high GR concentrations follow a similar trend to those at the medium concentration although ligand independent GFP-GR pull down was stronger through the GFP-GRwt. Clearly ligand independent dimerization is GR concentration dependent with even the GFP-GRdim tending toward it at medium and high GR concentrations. Pooled analysis of the ligand independent GFP-GRwt and GFP-GRdim pull down of three independent Co-IP experiments at the low, medium and high GR concentrations (Fig.4.3A) indicates marginal ligand independent dimerization at the low GR concentrations. This increases significantly at the medium and high GFP-GRwt concentrations, similarly to the saturation binding results of GRwt, which displayed positive cooperative ligand binding at medium and high GRwt concentrations. GFP-GRwt, however, only displayed cooperative ligand binding at the high, but not the medium, GR concentration (Fig.3.8B). A possible explanation for the discrepancy between the dimerization results (Fig.4.3A) and the saturation binding results (Fig.3.8B) is that for the Co-IP GFP-GR was dimerised to a Flag-GR partner and thus saturation binding of these partners should be done to definitively establish the correlation between dimerization and cooperative ligand binding. Although GFP-GRdim pull down showed a trend towards increased ligand independent dimerization at medium and high levels (Fig.4.3A) it was significantly ($P < 0.05$) lower than that of the GFP-GRwt pull down. It is also important to note that although GFP-GRdim has the dimerization impairing mutation in its D-loop the Flag-GR used in this study retains complete ability to dimerize. As dimerization requires the D-loops of both receptors the wild type Flag-GR may impart some dimerization ability to the GFP-GRdim. Constructing a Flag-GRdim in order to better elucidate the dimerization capacity of the GRdim mutant is a future study option.

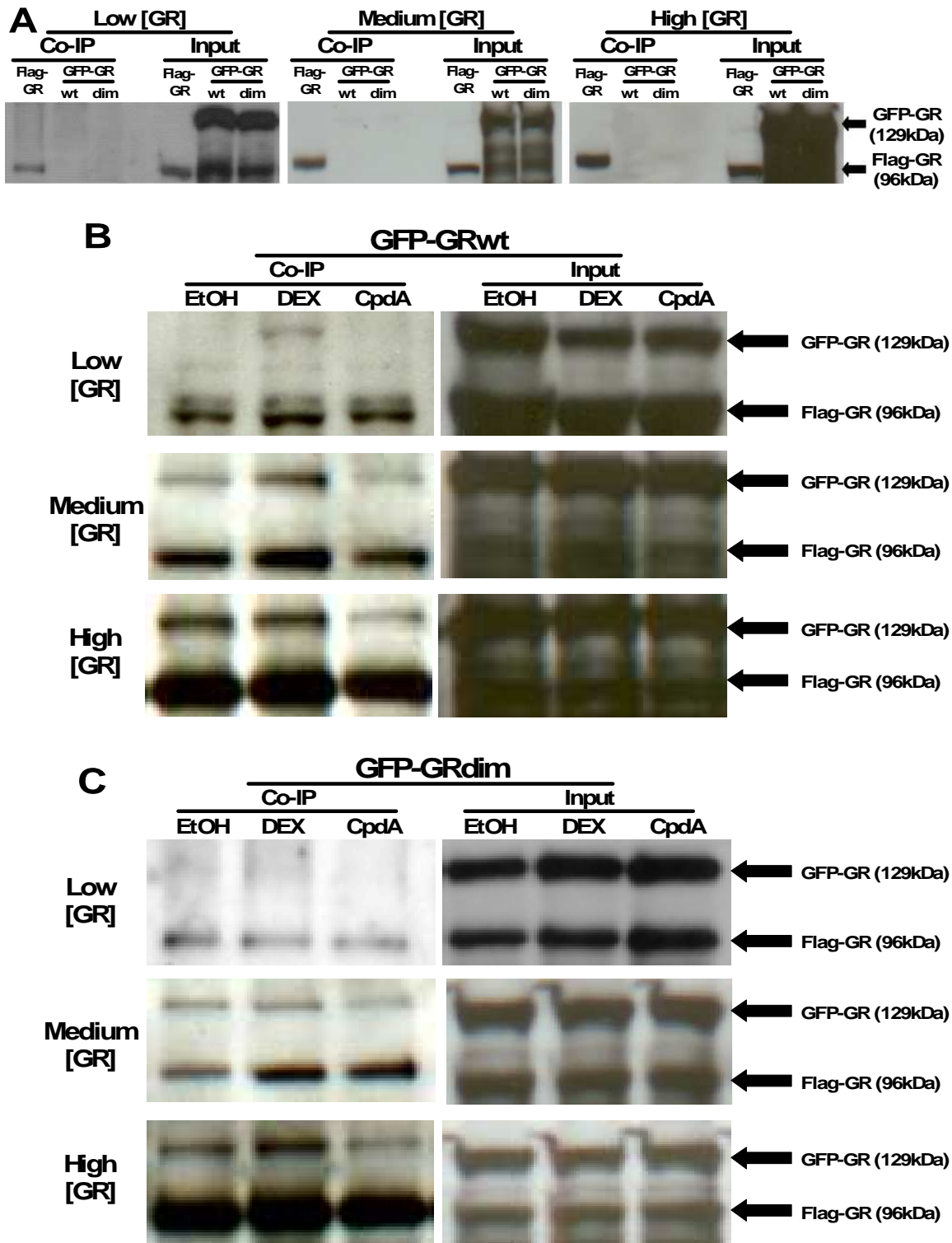


Figure 4.2. **Co-IP reveals ligand independent dimerization of the GR at high concentrations.** (A) Representative Western blots of Co-IP controls. Cells were transfected with low levels (38.5ng) of GR (34.22ng Flag-GR or 4.28ng GFP-GRwt or 4.28ng GFP-GRdim), medium levels (385ng) of GR (342.2ng Flag-GR or 42.8ng GFP-GRwt or 42.8ng GFP-GRdim) or high (11550ng) GR levels (10266ng Flag-GR or 1284ng GFP-GRwt or 1284ng GFP-GRdim). Representative Western blots of GFP-GRwt (B) and GFP-GRdim (C) Co-IP experiments were carried out as described in *materials and methods*.

4.1.2 DEX increases dimerization at the low GRwt concentration while CpdA addition abrogates dimerization at the medium and high GRwt concentrations

The addition of DEX at the low GR concentration (Fig.4.2B,C) resulted in dimerization of the Flag-GR and GFP-GRwt, which was seen as a GFP-GRwt band in the Co-IP column. No such band appears for GFP-GRdim at the low GR concentration supporting the theory that the mutation in the D-loop of the DBD impairs dimerization. The addition of CpdA had no influence on the Co-IP at the low GR concentrations as ligand independent dimerization at these levels is minimal (Fig.4.2B,C, Fig.4.3A). At medium GR concentrations where there was ligand independent GFP-GR pull down of both the GFP-GRwt and the GFP-GRdim, addition of DEX had a minimal effect on increasing dimerization while CpdA reduced the level of dimerization (Fig.4.2B,C). Pull down at the high GR concentrations follow a similar trend to those at the medium GR concentration. Ligand independent GFP-GR pull down was stronger through the GFP-GRwt and thus the addition of DEX resulted in a greater increase in GFP-GRdim pull down (Fig.4.2B,C).

In order to compare the pull down of GFP-GR across experiments and GR concentration levels we normalized GFP-GR levels from three independent experiments induced by EtOH, DEX or CpdA relative to the maximal level of GFP-GRwt pull down at each receptor concentration following the addition of DEX. Maximal dimerization is achieved through DEX stimulation of GFP-GRwt and because of this we set its level of pull down as 100 percent dimerization and compared EtOH, CpdA and all three GFP-GRdim conditions at each GR concentration to this condition (Fig.4.3B). At the low GFP-GRwt concentration DEX stimulation caused a significant 2.3-fold increase in GFP-GRwt pull down over EtOH stimulation. However, DEX stimulation caused no increase in the GFP-GRwt pull down at the medium and high GFP-GRwt concentrations (Fig.4.3B). This suggests that ligand independent GR dimerization at medium and high GRwt levels is already so high prior to DEX stimulation that addition of DEX does not significantly change the observed level of GRwt dimerization in this assay. This result is similar to that seen by Dewint *et al.* (9) as they showed ligand independent dimerization which was 90 percent of the DEX stimulated dimerization. At medium and high GRwt concentrations CpdA addition resulted in a significant decrease in GFP-GRwt pull down when compared to the ligand independent dimerization levels at these GR concentrations (Fig.4.3B). This indicates considerable ligand independent dimerization of the GRwt at the medium and high GRwt concentrations which is abrogated by CpdA.

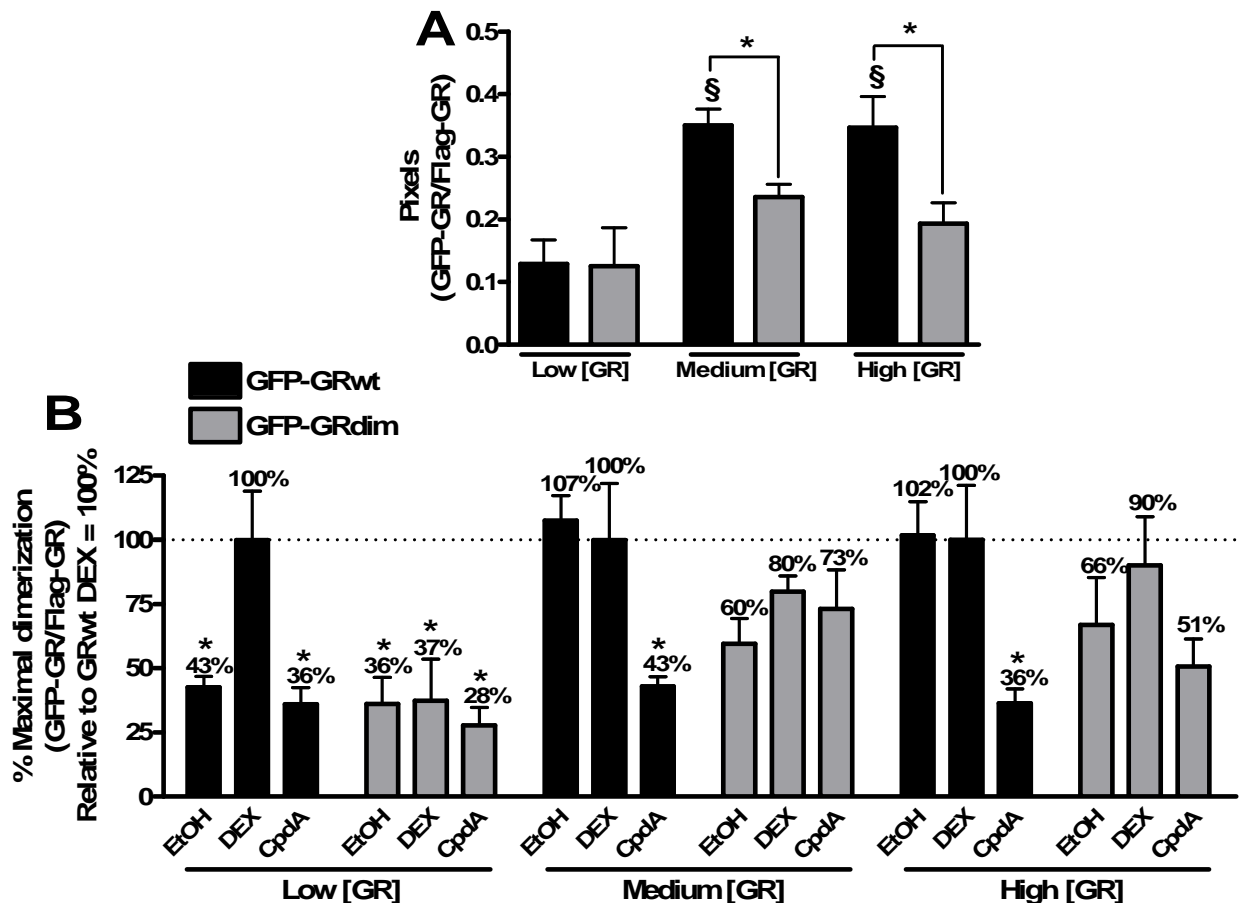


Figure 4.3. **Ligand independent dimerization of the GRwt and GRdim increases as their concentration does.** Co-IP was performed as described in *materials and methods*. (A) Low, medium or high GRwt or GRdim concentrations exposed to EtOH stimulation. Flag-GR and GFP-GR concentrations were quantified using UN-SCAN-IT software. GFP-GR pull down was then normalized over Flag-GR levels. Statistical analysis was through one tailed unpaired t tests of GRwt against GRdim (* $P < 0.05$) and ANOVA followed by Dunnett's post test against low GR concentration within GRwt or GRdim populations ($^{\S}P < 0.05$). (B) GR levels were quantified using UN-SCAN-IT software, GFP-GR pull down was normalized over Flag-GR and expressed relative to DEX GRwt set at 100 percent, at each receptor level. Statistical analysis was carried out using ANOVA followed by Dunnett's post test against DEX stimulation of GRwt at each receptor level ($P^* < 0.05$, $P^{**} < 0.01$). All results are representative of three independent experiments (\pm SEM).

The GFP-GRdim shows a significant increase, from 36 to 66 percent, in ligand independent dimerization as receptor levels increase from low to high GR concentration (Fig.4.3B). DEX addition also results in a trend toward increased dimerization at the medium and high GRdim concentrations, which peaks at 90 percent of that of DEX stimulated GRwt at the high GRdim concentration (Fig.4.3B), while CpdA addition at the high GRdim concentration results in a decrease in dimerization, from 66 percent through EtOH to 51 percent following CpdA stimulation (Fig.4.3B). These results imply that the GRdim is capable of considerable levels of dimerization at medium and high GR concentrations. As discussed earlier this is most probably enhanced by binding to the wild type Flag-GR. Optimally a Flag-GRdim should have been used in conjunction with the GFP-GRdim. The high levels of GFP-

GRdim ligand independent pull down, notably 60 percent of the GFP-GRwt at medium GR concentrations and 66 percent of GFP-GRwt at the high GR concentration, indicate at most an impairment of dimerization by the D-loop mutation in the GFP-GRdim and not abrogation of dimerization. It would be useful to expand on this assay by including a full D-loop mutant pair (Flag-GRdim/GFP-GRdim) in order to definitively evaluate the dimerization capacity of GRdim. We hypothesize that ligand independent dimerization of GRdim to GRdim at medium and high GR concentrations would be considerably reduced as saturation binding remains non-cooperative at these GR concentrations.

Finally these Co-IP experiments have demonstrated that ligand independent dimerization of the GFP-GRwt to Flag-GRwt increases from 43 percent at the low GR concentration to ~100 percent at the medium and high GR concentrations (Fig.4.3B). The medium and high GR concentrations are also the GR concentrations that demonstrate positive cooperative ligand binding in GRwt (Chapter 3). Ligand independent dimerization of GR at these elevated levels is thus a promising explanation for positive cooperative ligand binding although positive cooperative ligand binding is only seen at the high GFP-GR concentration. To further strengthen our argument we evaluated GR dimerization in live cells using the FRET technique.

4.2 Demonstrating ligand independent dimerization using FRET

The FRET technique is often termed a molecular ruler. Excitation of a donor fluorophore when in close proximity (typically < 10nm) to its acceptor fluorophore will result in a nonradiative, long-range dipole-dipole energy transfer (Fig.4.4). This energy transfer from stimulated donor to the acceptor molecule may be detected as an increase in the emission level of the acceptor fluorophore (17). CFP and YFP make up a robust FRET donor and acceptor pair. They are resistant to photo bleaching and have excitation and emission wavelengths which are far enough apart to minimize spectral crosstalk (18, 19). Some crosstalk into the FRET channel (excitation at 430nm, emission at 535nm) was detected from the YFP channel (excitation at 500nm, emission at 535nm) as well as from the CFP channel (excitation at 430nm, emission at 470nm). The signals measured in the FRET channel were corrected for cross-talk from the YFP and CFP channels using the following equation:

$$\mathbf{nFRET = FRETsignal - (\alpha \times YFPsignal) - (\beta \times CFPsignal)}$$

Where n is normalized FRET and α and β were determined by measuring the crossover into the FRET channel of the YFP and CFP signals, respectively, in cells expressing either CFP-GR or YFP-GR on its own. In our system, 2.6% of the YFP signal (α) and 59% of the CFP signal (β) were detected in the FRET channel. Trinkle-Mulcahy *et al.* (20) demonstrated similar levels of crossover, notably 67% of

the CFP signal and 19% of the YFP signal. The crosstalk correction we used was devised by Trinkle-Mulcahy *et al.* and is based on previous FRET studies by Tron *et al.* (21).

The yellow fluorescent protein tagged GR (YFP-GR) we used as our acceptor fluorophore has been shown to be transcriptionally active (22). It occurs in the same vector as the CFP-GR and they have equal expression levels (Fig.3.3). As their expression levels match one another as well as that of the GRwt we transfected equal amounts of each fluorescently tagged GR at the same total levels of plasmid DNA as for the low, medium and high GRwt concentrations in the whole cell saturation binding assay.

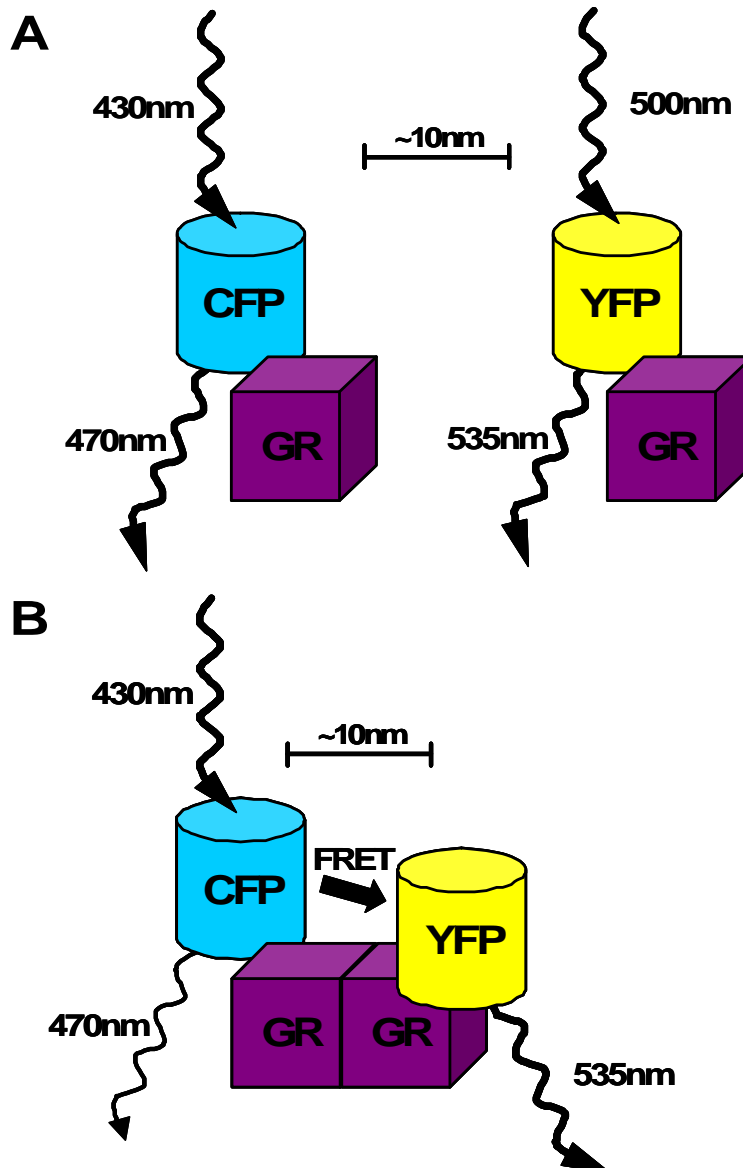


Figure 4.4. **Diagram illustrating FRET energy transfer when donor (CFP) and acceptor (YFP) molecules are in close association.** (A) When the CFP-GR and YFP-GR occur as monomers, excitation of CFP will result in an emission at 470nm while YFP excitation results in an emission at 535nm. (B) Dimerization of CFP-GR and YFP-GR brings their fluorophores into close association. Excitation of CFP results in a lowered emission at 470nm and an energy transfer (FRET) to YFP causing its excitation and emission at 535nm.

Due to the inherent variation in transfection efficiency within transient transfections it was necessary to monitor the relative GR expression levels within each cell analysed. The F-don signal (CPF) was used to monitor the transfection efficiency of each cell using an exposure time of 1500ms at 100 percent light intensity. These F-don values reflect the CFP signal after 30 minutes of DEX stimulation measured in a region of interest (ROI) in the nucleus of each individual cell (Fig.4.5). As the shape and size of COS-1 cells vary considerably we found that the normalization was most effective following DEX stimulation as this resulted in nuclear import of the CFP-GR and the concentration of its signal within the nucleus. Of course it also meant that selection of cells could only be made following the 30 minute FRET time course. Cells with an F-don emission of 0-600 (arbitrary units) were selected to represent the low GR concentration population, cells with F-don signals between 600-1200 to represent the medium GR concentration population and cells with F-don signals of >1200 for the high GR concentration population (Fig4.5).

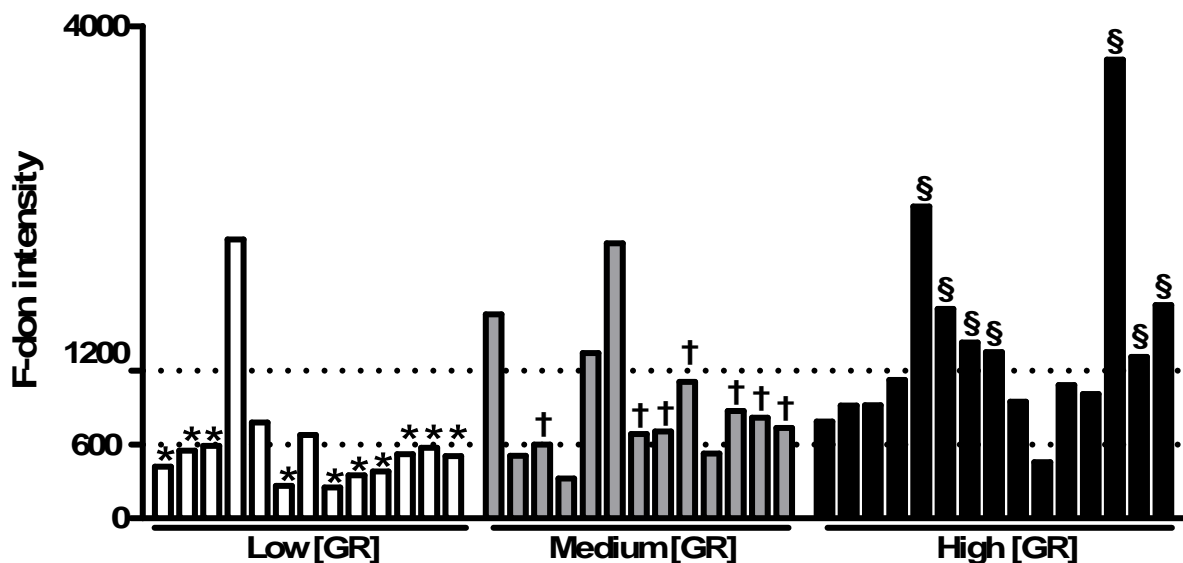


Figure 4.5. **Relative CFP-GR (F-don) expression levels in individual cells within low, medium and high GR concentration populations.** FRET was carried out as described in *materials and methods*. Exposure time of 1500ms at 100% light intensity was used. F-don values reflect the CFP signal after 30 minutes of DEX stimulation measured in a region of interest in the nucleus of each individual cell. Cells with an F-don emission of 0-600 were selected for the low [GR] concentration (*, n=10), F-don signals between 600-1200 for the medium [GR] population (†, n=7) and F-don of >1200 for the high [GR] population (§, n=7).

4.2.1 Ligand independent dimerization of the GR occurs in the cytoplasm at high GR concentrations

As has been demonstrated for GFP-GR (23, 24) there is rapid import into the nucleus of the CFP-GR (F-don) and YFP-GR (F-acc) following DEX stimulation (Fig.4.6A,B,C). As dimerization levels of the heterodimer pair CFP-GR and YFP-MR have been shown to be influenced by ligand concentration (25), we decided to use 10^{-6} M DEX to induce complete dimerization as this is a saturating concentration of the ligand (26).

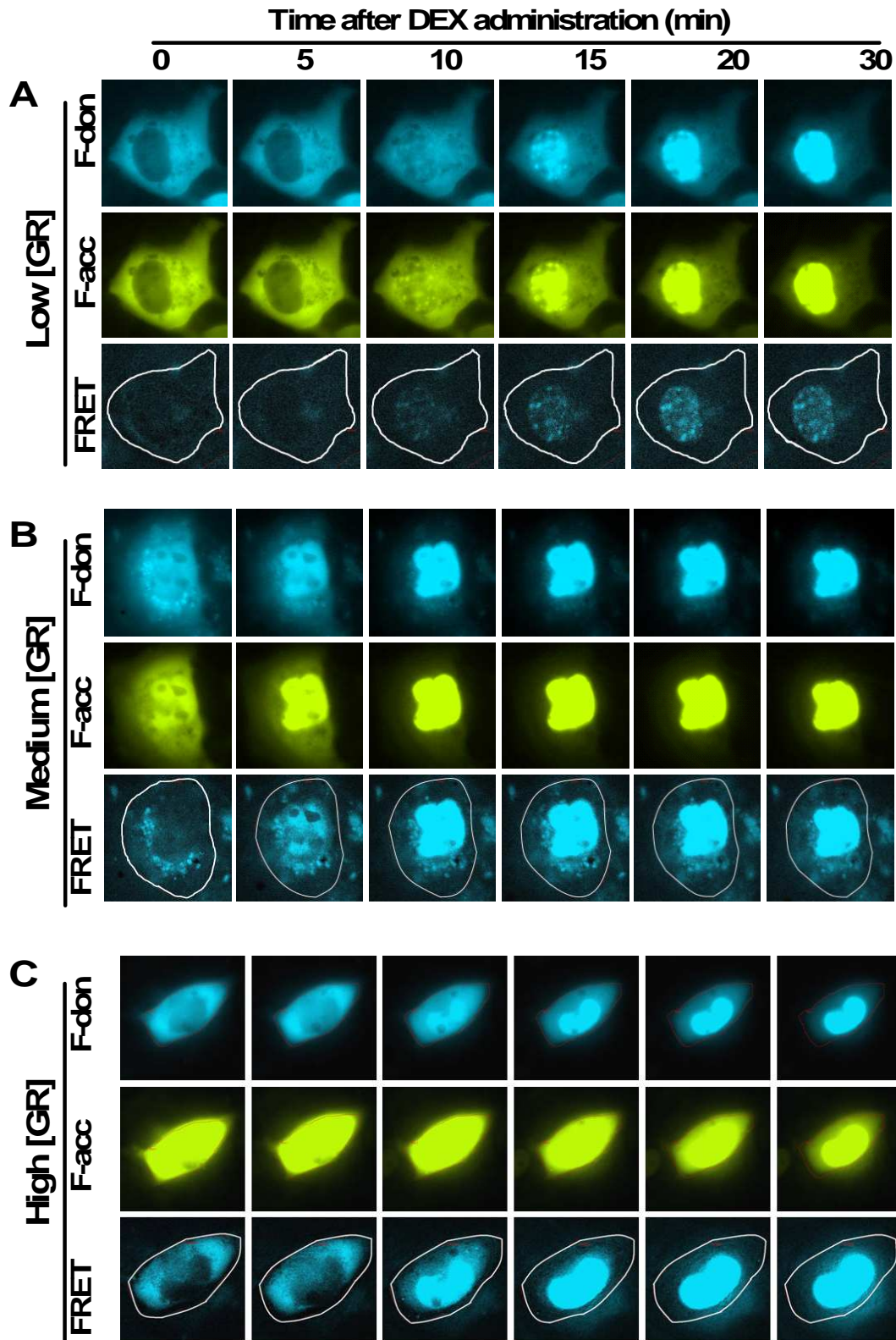


Figure 4.6. **Representative F-don, F-acc and FRET signals over time.** FRET was carried out as described in *materials and methods*. Cells were transfected with **(A)** low levels of GR, **(B)** medium levels of GR or **(C)** high levels of GR and treated with 10^{-6} M DEX for 30 minutes while F-don, F-acc and FRET intensity was monitored on an Olympus IX 81 motorized inverted microscope at 37°C . The white lines in the FRET images designate the cellular membrane which has been used as the ROI.

The corrected FRET signal is indicated by the blue fluorescent signal below the yellow F-acc images (Fig.4.6). The corrected FRET signal will only appear where there is interaction of the CFP-GR and YFP-GR, it therefore indicates areas of dimerization of the CFP-GR and YFP-GR. At the low GR concentration the corrected FRET signal increases over time following DEX stimulation (Fig.4.6A) with very little initial dimerization of the GR that gradually increases after DEX stimulation. There is a low level of ligand independent GR dimerization in the perinuclear space at the medium GR concentration which migrates to the nucleus and increases following DEX addition (Fig.4.6B). The level of ligand independent dimerization prior to DEX stimulation at the high GR concentration is considerable and clearly cytoplasmic (Fig.4.6C). Following DEX induction at the high GR concentration there is nuclear import as for the low and medium GR concentrations (Fig.4.6A,B). Ligand independent dimerization of the GR as indicated by the corrected FRET signal, occurs in the cytoplasm as is demonstrated at the medium and high GR concentrations. We have therefore selected the cellular membrane (as indicated by the white line) to represent our region of interest (ROI) for FRET analysis (Fig.4.6A,B,C). Arguments have been made that the GR dimerizes once bound to glucocorticoid response elements (GRE) (27, 28). However, these results as well as those of Savory *et al.* (3) indicate both ligand independent and ligand dependent dimerization of the GR in the cytoplasm.

With the assistance of J. Rohwer (Department of Biochemistry, Stellenbosch University) we developed a mathematic model which calculates the level of ligand independent GR dimerization prior to DEX administration (refer to *materials and methods*) (Fig.4.7). The model indicates a significant shift from 37 percent ligand independent dimerization at low GR concentrations to 60 and 63 percent ligand independent dimerization at medium and high GR concentrations, respectively. Roughly two thirds of the low GR concentration is monomeric, which changes to roughly one third at the medium and high GR concentrations (Fig.4.7).

Although the level of ligand independent dimerization of the FRET technique calculated by the mathematic model (Fig.4.7) is lower than the ~100 percent demonstrated at the medium and high GFP-GRwt concentrations in the Co-IP experiment (Fig.4.3B), the calculated ligand independent dimerization of the low GR concentration closely matches the 43 percent displayed by the low GFP-GRwt concentration in the Co-IP results. The difference at the medium and high GR concentrations may be symptomatic of the *in vitro* versus the whole cell nature of the Co-IP and FRET experiments. Despite this fact, both experiments indicate a similar trend namely, predominantly monomeric fluorescent protein tagged GRwt at the low GR concentration, which shifts to predominantly dimeric at the high GR concentrations.

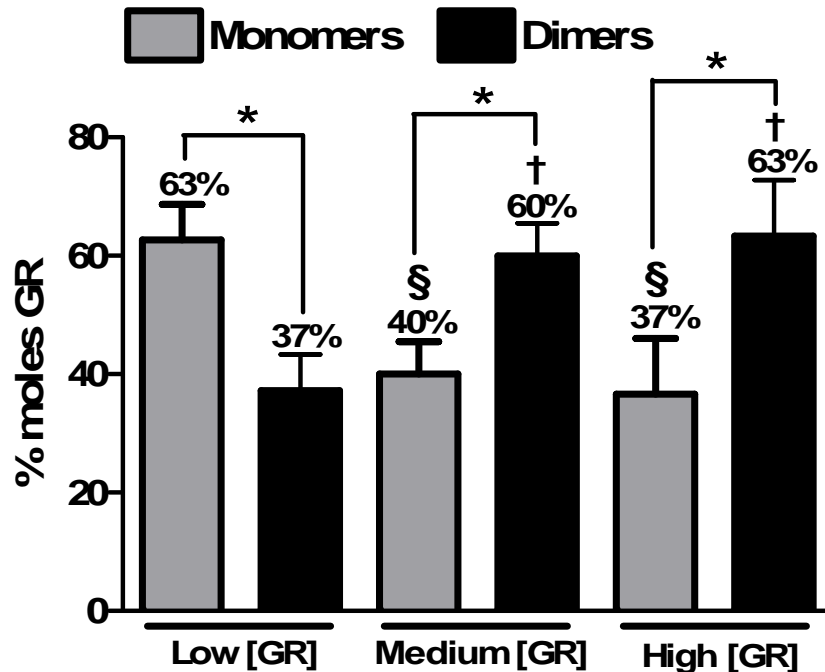


Figure 4.7. **Mathematic derivation of CFP, YFP and FRET signal indicate that ligand independent dimerization of the GR increases as GR concentration increases.** FRET was carried out as described in *materials and methods*. Mathematical derivation as described in *materials and methods* was carried out on the corrected FRET, F-don and F-acc fluorescence and reveals the percentage moles of GR occurring as either monomers or homodimers prior to ligand stimulation. Statistical analysis was through ANOVA followed by Dunnett's post test against low GR concentration within medium and high GR concentration monomers (§ $P < 0.05$) or dimers († $P < 0.05$) and one tailed unpaired t tests comparing percentage monomers against percentage dimers at each GR concentration (* $P < 0.05$). Results represent a minimum of four independent experiments (\pm SEM).

4.2.2 The fold induction of DEX induced maximal FRET decreases as GR levels increase

There are obvious differences in the levels of corrected FRET between the three GR concentrations; ligand induced as well as uninduced FRET levels increase as GR concentration increases (Fig. 4.8A). It is also clear that FRET levels plateau well before the 30 minutes time point of DEX stimulation and remain constant from roughly the 20th minute of DEX stimulation onwards. This differs from the findings of Nishi *et al.* (25) who demonstrate GR and MR heterodimerization peaking after 60 minutes and only in the nucleus.

Due to the nature of our studies, direct comparison of FRET levels between the three receptor concentrations can not be made without first normalizing for differences in GR expression (Fig.4.8B). Even if we assumed an equal degree of dimerization across these GR populations we would still demonstrate higher FRET at the high GR concentration than at the low GR concentration simply as a result of its greater levels of GR. In order to correct for this, the raw corrected FRET data for each cell

was normalized over its ligand uninduced FRET value (Fig.4.8B). This gives curves which represent the fold increase in FRET at each of the three GR concentrations (Fig.4.8B). By fitting sigmoidal dose-response variable slope curves to this normalized FRET data, maximal fold induction of FRET (Fig.4.8C) may be generated for each of the three GR concentrations.

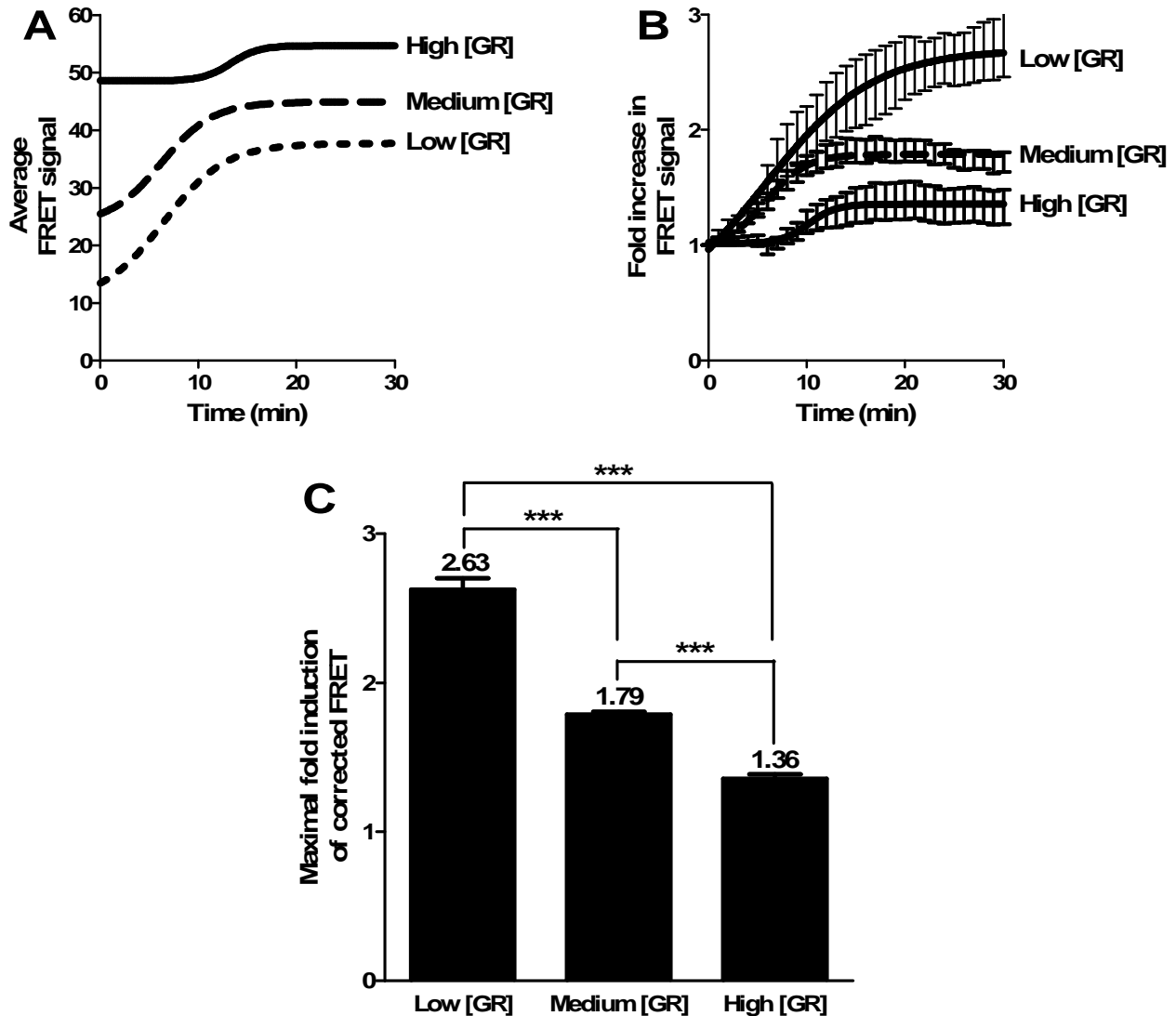


Figure 4.8. Ligand induced dimerization decreases as GR concentration increases reflecting a higher uninduced dimer percentage. FRET was carried out as described in *materials and methods*. Cells were treated with 10^{-6} M DEX for 30 minutes while F-don, F-acc and FRET intensity was monitored on an Olympus IX 81 motorized inverted microscope at 37°C. (**A**) Average FRET signal plotted against time and fit to a sigmoidal dose-response variable slope curve. (**B**) Fold increase in FRET response was calculated by normalizing each experiment to its unstimulated FRET signal and fit to a sigmoidal dose-response variable slope curve which generates (**C**) maximal fold induction of FRET. Statistical analysis was carried out using one-way analysis of variance followed by Bonferroni's multiple comparison test (** $P < 0.001$). The figure is representative of seven independent experiments (\pm SEM).

The levels of maximal fold FRET induction following DEX stimulation decrease significantly as GR concentration increases (Fig.4.8C). This reflects the increase in ligand independent FRET values we see as GR concentrations increases (Fig.4.7, Fig.4.8A). Similarly to the DEX induced 2.3-fold increase in GFP-GRwt pull down seen at the low GRwt concentration in our Co-IP experiments (Fig.4.3B) there is a DEX induced 2.63-fold increase in dimerization at the low GR concentration in the FRET assay (Fig.4.8C). Reassuringly the calculated theoretical increase in dimerization derived from the mathematical model at low GR concentrations, from the 37 percent ligand independent dimerization to 100 percent after DEX addition is a similar 2.7-fold (Fig.4.7). The fold increase in DEX induced dimerization drops to 1.79 and 1.36 at the medium and high GR concentrations, respectively (Fig.4.8C). Again these reflect the theoretical maximal fold increase in dimerization at the medium (1.67) and high (1.59) GR concentrations calculated by our mathematical model (Fig.4.7). The low GR concentration undergoes a 1.5-fold greater increase in dimerization relative to the medium GR concentration following DEX administration, which rises to a 1.9-fold greater increase in dimerization at the low GR concentration relative to the high GR concentration. In order for the DEX induced fold induction of dimerization to decrease as receptor levels increase there must be an increase in the amount of ligand independent dimerization as receptor levels increase. This is an indirect proof which demonstrates a statistically significant increase in ligand independent dimerization at the medium and high GR concentrations when compared to the low GR concentration.

In summary, both the Co-IP and FRET results demonstrate a significant increase in ligand independent dimerization at the high fluorescent protein tagged GRwt concentrations, which does display cooperative ligand binding (Fig.3.8). Although saturation ligand binding was not carried out on the specific CFP-GR/YFP-GR or Flag-GR/GFP-GR pairs used in the Co-IP and FRET assays, but rather on GFP-GR alone (Fig.3.8), we suggest that this GR concentration dependent increase in ligand independent dimerization may be the mechanism whereby positive cooperative ligand binding is elicited. However, definitive correlation between cooperative ligand binding and ligand independent dimerization awaits saturation binding of the specific GR pairs used in the Co-IP and FRET assays.

Having demonstrated that cooperative ligand binding results at medium and high levels of GRwt (Chapter 3) and that it may be correlated to ligand independent dimerization (Chapter 4) we have focused our further research on the implications of cooperative ligand binding. The first characteristic we studied is the translocation of the GR, focusing on its rate of ligand dependent import into the nucleus, distribution once nuclear and rate of export following the withdrawal of stimulating ligand.

4.3 Bibliography

1. Cho S, Kagan BL, Blackford JA, Jr, Szapary D & Simons SS, Jr (2005) Glucocorticoid receptor ligand binding domain is sufficient for the modulation of glucocorticoid induction properties by homologous receptors, coactivator transcription intermediary factor 2, and Ubc9. *Mol Endocrinol* 19: 290-311.
2. Wrange O, Eriksson P & Perlmann T (1989) The purified activated glucocorticoid receptor is a homodimer. *J Biol Chem* 264: 5253-5259.
3. Savory JG, *et al* (2001) Glucocorticoid receptor homodimers and glucocorticoid-mineralocorticoid receptor heterodimers form in the cytoplasm through alternative dimerization interfaces. *Mol Cell Biol* 21: 781-793.
4. Dahlman-Wright K, Wright A, Gustafsson JA & Carlstedt-Duke J (1991) Interaction of the glucocorticoid receptor DNA-binding domain with DNA as a dimer is mediated by a short segment of five amino acids. *J Biol Chem* 266: 3107-3112.
5. De Kloet ER, Vreugdenhil E, Oitzl MS & Joels M (1998) Brain corticosteroid receptor balance in health and disease. *Endocr Rev* 19: 269-301.
6. Segard-Maurel I, *et al* (1996) Glucocorticosteroid receptor dimerization investigated by analysis of receptor binding to glucocorticosteroid responsive elements using a monomer-dimer equilibrium model. *Biochemistry* 35: 1634-1642.
7. Bledsoe RK, *et al* (2002) Crystal structure of the glucocorticoid receptor ligand binding domain reveals a novel mode of receptor dimerization and coactivator recognition. *Cell* 110: 93-105.
8. Tamrazi A, Carlson KE, Daniels JR, Hurth KM & Katzenellenbogen JA (2002) Estrogen receptor dimerization: Ligand binding regulates dimer affinity and dimer dissociation rate. *Mol Endocrinol* 16: 2706-2719.
9. Dewint P, *et al* (2008) A plant-derived ligand favoring monomeric glucocorticoid receptor conformation with impaired transactivation potential attenuates collagen-induced arthritis. *J Immunol* 180: 2608-2615.
10. Robertson S, *et al* (2010) Abrogation of glucocorticoid receptor dimerization correlates with dissociated glucocorticoid behavior of compound a. *J Biol Chem* 285: 8061-8075.
11. Adams M, Meijer OC, Wang J, Bhargava A & Pearce D (2003) Homodimerization of the glucocorticoid receptor is not essential for response element binding: Activation of the phenylethanolamine N-methyltransferase gene by dimerization-defective mutants. *Mol Endocrinol* 17: 2583-2592.
12. Newton R (2000) Molecular mechanisms of glucocorticoid action: What is important?. *Thorax* 55: 603-613.
13. Terpe K (2003) Overview of tag protein fusions: From molecular and biochemical fundamentals to commercial systems. *Appl Microbiol Biotechnol* 60: 523-533.
14. Reichardt HM, *et al* (1998) DNA binding of the glucocorticoid receptor is not essential for survival. *Cell* 93: 531-541.

15. Reichardt HM, *et al* (2001) Repression of inflammatory responses in the absence of DNA binding by the glucocorticoid receptor. *EMBO J* 20: 7168-7173.
16. Frijters R, *et al* (2010) Prednisolone-induced differential gene expression in mouse liver carrying wild type or a dimerization-defective glucocorticoid receptor. *BMC Genomics* 11: 359.
17. Sekar RB & Periasamy A (2003) Fluorescence resonance energy transfer (FRET) microscopy imaging of live cell protein localizations. *J Cell Biol* 160: 629-633.
18. Hink MA, Borst JW & Visser AJ (2003) Fluorescence correlation spectroscopy of GFP fusion proteins in living plant cells. *Methods Enzymol* 361: 93-112.
19. Zhang J, Campbell RE, Ting AY & Tsien RY (2002) Creating new fluorescent probes for cell biology. *Nat Rev Mol Cell Biol* 3: 906-918.
20. Trinkle-Mulcahy L, Sleeman JE & Lamond AI (2001) Dynamic targeting of protein phosphatase 1 within the nuclei of living mammalian cells. *J Cell Sci* 114: 4219-4228.
21. Tron L, *et al* (1984) Flow cytometric measurement of fluorescence resonance energy transfer on cell surfaces. quantitative evaluation of the transfer efficiency on a cell-by-cell basis. *Biophys J* 45: 939-946.
22. Schaaf MJ & Cidlowski JA (2003) Molecular determinants of glucocorticoid receptor mobility in living cells: The importance of ligand affinity. *Mol Cell Biol* 23: 1922-1934.
23. Htun H, Barsony J, Renyi I, Gould DL & Hager GL (1996) Visualization of glucocorticoid receptor translocation and intranuclear organization in living cells with a green fluorescent protein chimera. *Proc Natl Acad Sci U S A* 93: 4845-4850.
24. Galigniana MD, *et al* (1998) Heat shock protein 90-dependent (geldanamycin-inhibited) movement of the glucocorticoid receptor through the cytoplasm to the nucleus requires intact cytoskeleton. *Mol Endocrinol* 12: 1903-1913.
25. Nishi M, Tanaka M, Matsuda K, Sunaguchi M & Kawata M (2004) Visualization of glucocorticoid receptor and mineralocorticoid receptor interactions in living cells with GFP-based fluorescence resonance energy transfer. *J Neurosci* 24: 4918-4927.
26. Ronacher K, *et al* (2009) Ligand-selective transactivation and transrepression via the glucocorticoid receptor: Role of cofactor interaction. *Mol Cell Endocrinol* 299: 219-231.
27. Dahlman-Wright K, Siltala-Roos H, Carlstedt-Duke J & Gustafsson JA (1990) Protein-protein interactions facilitate DNA binding by the glucocorticoid receptor DNA-binding domain. *J Biol Chem* 265: 14030-14035.
28. Ong KM, Blackford JA, Jr, Kagan BL, Simons SS, Jr & Chow CC (2010) A theoretical framework for gene induction and experimental comparisons. *Proc Natl Acad Sci U S A* 107: 7107-7112.

Chapter 5

Results: The influence of dimerization on GR nuclear import, export and distribution

Introduction

Having established the GR levels at which non-cooperative and positive cooperative ligand binding takes place (Chapter 3), we demonstrated that ligand independent dimerization of the GR at high concentrations may account for cooperative ligand binding (Chapter 4). In the current results chapter we report on the investigation of the influence of GR concentration, the ability to dimerize and positive cooperative ligand binding on the rate of nuclear import, nuclear distribution and the rate of nuclear export of the GR.

Upon ligand binding the GR undergoes a ligand dependant conformational change which results in its rapid and active nuclear import (1, 2). There is clear evidence that the nuclear import rate is ligand dependent (3) and that the degree of GR nuclear localization is a critical factor in determining the level of GR function (4). The rate of nuclear import of the GFP tagged GR in live cell fluorescent studies has also been shown to be cell type (5) and ligand concentration dependant (6). In addition, previous research demonstrated that once imported nuclear mobility (7) and the pattern of GR distribution (8) in the nucleus are differentially affected by ligands and ligand concentration. Nuclear mobility is primarily influenced by the association of the activated GR with DNA or other transcription factors, thus the greater the capacity for transcription the slower the mobility and the more particulate (or non-random) the distribution of the GR in the nucleus. Finally, following the withdrawal of ligand, the GR undergoes passive nuclear export (9, 10) where the GR diffuses from the nucleus back into the cytoplasm.

In order to quantify nuclear import and export we have used either direct fluorescence labelling where a GFP tagged GR was used in live cell experiments or indirect fluorescence labelling of the GR where a fluorescent secondary anti-body was used to visualize a GR specific primary anti-body complexed with the GR in fixed and permeabilized cells. The advantage of using direct fluorescent labelling is that nuclear import and export may be monitored in an individual live cell in real time. However, we were concerned that the large protein tag may in some way impede GR movement and have thus also conducted indirect immunofluorescent studies on the unlabeled GR. Another difference between these two assays lies in the quantification method employed. Where as the direct fluorescence procedure directly measures the accumulation of fluorescence either in the nucleus or in the cytoplasm of an individual cell, depending on whether import or export is being studied, the immunofluorescent technique requires manual counting of a population of cells where the average localization of fluorescence within the population of cells, either in the nucleus or in the cytoplasm, is determined.

Results

5.1 Nuclear import of the glucocorticoid receptor

Following exposure to ligand, the rate of activated GR nuclear import exceeds receptor export, resulting in high concentrations of GR in the nucleus (11). The active process of nuclear import of the GR occurs quickly and relies on the association of the GR with Hsp90 (12), FKBP52 (13) and importin- α (14). This complex is actively shuttled into the nucleus by dynein (15, 16) along the cytoskeleton (12) through the nuclear pore complex (17). The nuclear import of GFP-GR in transiently transfected COS-7 cells has been shown to be both ligand and ligand concentration dependent, displaying greater differences in import rate at low ligand concentrations (18).

5.1.1 The $t_{1/2}$ of live cell nuclear import of GFP-GR decreases as receptor concentrations increase.

Live cell nuclear translocation assays were conducted in COS-1 cells transiently transfected with medium and high GFP-GR concentrations, receptor levels which demonstrated non-cooperative and positive cooperative ligand binding (Chapter 3), respectively.

Following the induction of test compound, live cell images of nuclear import were taken every minute over a 60 minutes period (Fig.5.1, Fig.5.2A). Nuclear import was quantified as the increase in GFP fluorescence in the nucleus over the period of stimulation, taking the zero time point as 0% and the maximal fluorescence as 100%. The entire nuclear area was selected as the ROI and is indicated by the interior of a white border (Fig.5.1). A one phase exponential association curve was fit to this data which generated a half time ($t_{1/2}$) to maximal nuclear localization.

Increasing GFP-GRwt concentration from medium to high resulted in a significant decrease in the $t_{1/2}$ of nuclear import through DEX (Fig.5.2B). This was also the case for DEX induction through the dimerization impaired D-loop mutant GFP-GRdim (Fig.5.2B). Although GFP-GRwt had a significantly faster rate of nuclear import than GFP-GRdim at both GR concentrations, the difference in GR import $t_{1/2}$ decreased from 2.8-fold longer for GFP-GRdim at the medium GR concentration to 1.9-fold longer for the GFP-GRdim at the high GR concentration. GFP-GRdim import at the high GR concentration is identical to the nuclear import rate of the medium GFP-GRwt concentration. Based on our Co-IP results which demonstrate a high degree (90 percent of GRwt levels) of ligand dependent dimerization of the high GR concentration GFP-GRdim (Fig.4.3B) we hypothesize that at this saturating concentration of DEX the high concentration of GFP-GRdim starts to display ligand dependent

dimerization similar to that of the GFP-GRwt. Although the significantly increased rate of import for the GRwt as compared to the GRdim could suggest a role for cooperative ligand binding that requires the ability to dimerize, the fact that the GFP-GRdim also displays a shift in import rate at high concentrations excludes any influence that positive cooperative ligand binding may have on this parameter as saturation ligand binding demonstrated that the GRdim is incapable of positive cooperative ligand binding (Fig.3.8B). It is thus more likely that the observed phenomena of increased nuclear import rate at increased GR levels is due to the laws of mass action namely, a faster reaction rate at increased concentration of GR and that loss of GR dimerization may play a role in enhancing the rate of nuclear import and in nuclear retention (to be discussed in section 5.3).

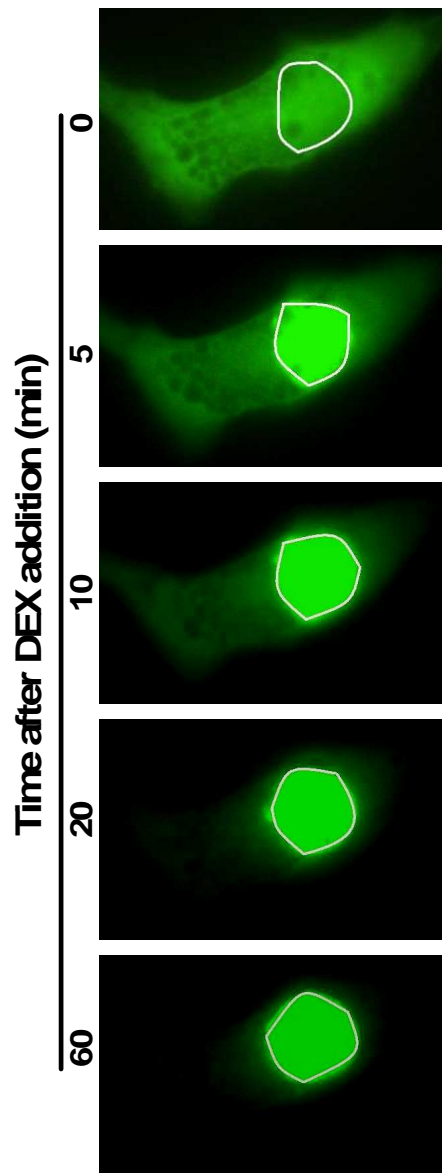


Figure 5.1. **Live cell nuclear import studies** were carried out as described in *materials and methods*. A single cell was induced with 10^{-6} M DEX and GFP images were taken every minute over a 60 minute period. The white circle around the nucleus represents the region of interest.

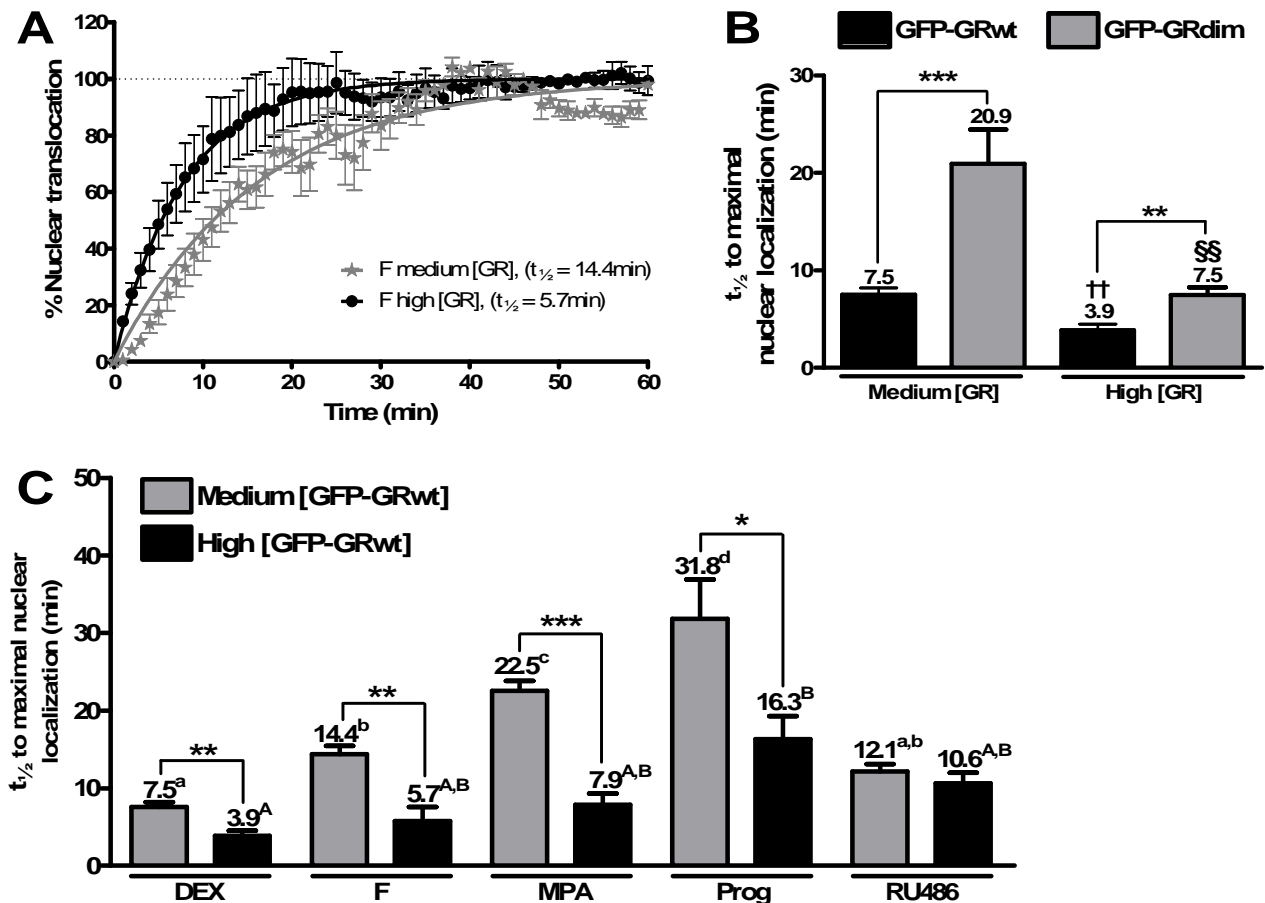


Figure 5.2. Higher GR concentrations decrease the nuclear import half-time ($t_{1/2}$) of a range of test compounds. (A) Representative graph depicting nuclear import following 10^{-6} M F induction at medium and high GFP-GRwt concentrations which was quantified as the increase in GFP fluorescence in the nucleus over the period of stimulation, taking the zero time point as 0% and the maximal fluorescence as 100%. A one phase exponential association curve was fit to this data which generated a $t_{1/2}$ to complete nuclear localization. (B) Live cell nuclear import of 10^{-6} M DEX stimulated cells expressing medium and high GFP-GRwt or GFP-GRdim. Statistical analysis of $t_{1/2}$ to maximal nuclear localization was through one tailed unpaired t tests, GFP-GRwt against GFP-GRdim (** $P < 0.01$, *** $P < 0.001$) and medium against high GFP-GRwt concentration ($^{\dagger}P < 0.01$) and medium against high GFP-GRdim concentration ($^{\S\S}P < 0.01$). (C) Cells were induced with 10^{-6} M DEX, F, MPA, Prog or RU486. Statistical analysis of $t_{1/2}$ to maximal nuclear localization comparing medium to high GFP-GR concentrations was carried out using one tailed unpaired t test (* $P < 0.05$, ** $P < 0.01$, *** $P < 0.001$). ANOVA followed by Newman-Keuls post test was used to compare ligands within the medium GFP-GR concentration (lower case letters) or high GFP-GR concentration (capital letters). Conditions with different letters are statistically different from one another ($P < 0.01$). Results represent a minimum of five cells, each from independent experiments (\pm SEM).

We show that the nuclear import rate decreases significantly as GFP-GR concentration increases for DEX, cortisol (F), MPA and Prog and that the import rate stimulated by these test compounds varies significantly at the medium GFP-GR concentration, while RU486 does not display the same behaviour (Fig.5.2C). Although the sequence of ligand import rates at the medium GFP-GR concentration (DEX > RU486 > F > MPA > Prog) does not match any of the order of potency parameters tested by

Ronacher *et al.* (19), a general trend does emerge in that DEX, which they show to be the most potent ligand in GR binding, GRE driven transactivation and NF κ B driven transrepression, resulted in the fastest GR import rate, while Prog, which is the least potent ligand in these assays, had the slowest GR import rate. At the high GFP-GR concentration there is less variation in the import rates between test compounds with only DEX and Prog demonstrating significantly different import times (Fig.5.2C). Although at the medium GR concentration the import rates of DEX, F, MPA and Prog are all significantly different from one another, at the high GR concentration the statistical differences are decreased. For example, the difference between DEX and Prog induced nuclear import $t_{1/2}$ falls from 24.3 minutes at the medium GR concentration to 12.4 minutes at the high GR concentration. We propose that increasing the receptor level sufficiently will decrease all ligand import rates to a theoretical minimum where the import machinery required for this active process becomes limiting.

Results in the literature suggest that the $t_{1/2}$ of GFP-GR import following the addition of 10^{-6} M DEX is ~5 minutes (12), while maximal nuclear localization of GFP-GR is achieved 30 minutes after 10^{-7} M DEX stimulation (20). Our live cell nuclear import results are similar to those seen in the literature, namely nuclear import $t_{1/2}$ of GR following 10^{-6} M DEX stimulation of between 7.5 and 3.9 minutes, depending on the concentration of GFP-GRwt studied. We also tested the nuclear import following stimulation with a non-saturating, 10^{-9} M, DEX concentration, which displayed a significantly reduced nuclear import rate of 11.1 minutes compared to the 3.9 minutes following stimulation with 10^{-6} M DEX in the high GR concentration population (Fig.5.3). In order to ensure a plateau in the level of nuclear import after 60 minutes and to minimize the differences in receptor occupation due to differing ligand affinities we, however, decided to conduct most of our further studies at saturating (10^{-6} M) ligand concentrations.

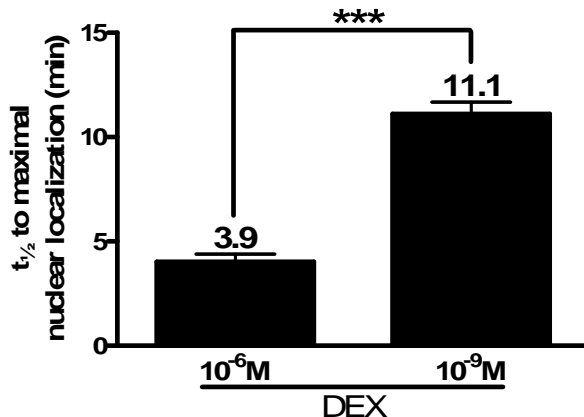


Figure 5.3. **Nuclear import is ligand concentration dependent.** Live cell nuclear import was carried out as described in the *materials and methods* on COS-1 cells transfected with the high concentration of GFP-GRwt following either 10^{-6} M or 10^{-9} M DEX stimulation. Statistical analysis was carried out using two tailed unpaired t test (***) $P < 0.001$). Results represent a minimum of three cells, each from independent experiments (\pm SEM).

5.1.2 The ability to dimerize influences both maximal nuclear localization as well as the $t_{1/2}$ of nuclear import in immunofluorescent nuclear import assays

Where as the live cell nuclear translocation assay illustrates the mobility of GFP-GR within a single live cell in real time, immunofluorescent analysis relies on anti-body directed fluorescent labelling of the GR in cells fixed and permeabilized at specific time points. Nuclear import was quantified by double blind counting of cells in a population of 50 cells per time point and per condition. Cells were classified as nuclear when they displayed distinct nuclear localization of the GR (60 percent nuclear and above), where GR concentration was clearly higher in the nucleus than that in the cytoplasm (Fig.5.4A). The percentage nuclear cells were calculated as the ratio of nuclear over total cells counted. Hoechst staining of the nucleus of cells which was detected through the DAPI-signal, aided in nuclear quantification (Fig.5.4A). Although, this method of classification is commonly used (18), it is important to note that what is measured is in fact not absolute nuclear or cytoplasmic GR localization, but rather greater than 60 percent nuclear distribution.

COS-1 cells were transiently transfected with low and medium levels of GRwt or GRdim. To reiterate, whole cell saturation binding assays showed positive cooperative ligand binding to the medium GRwt concentration but was non-cooperative at the low GRwt concentration and at both low and medium GRdim concentrations (Fig.3.8B). The maximal percentage of cells displaying nuclear localization following DEX induction is significantly higher for the low and medium GRwt concentrations (~95 percent) than for that of GRdim (~76.5 percent) (Fig.5.4C). This effect is independent of positive cooperative ligand binding, which occurs at the medium GRwt concentration but not at the low GRwt concentration, as both GRwt concentrations display roughly equal levels of nuclear import. However, maximal nuclear import is clearly influenced by dimerization as induction with the dimerization abrogating dissociative GC, CpdA, results in similar levels of nuclear import through both the GRwt and the GRdim (Fig.5.4B,C). What a decrease in the percentage of cells displaying nuclear GR localization signifies in this assay is that within the populations counted not all cells reach 60 percent nuclear localization of GR. Therefore, the ability to dimerize although not an absolute requirement for nuclear import, does play a role in the extent of GR import. These results are similar to those presented by Robertson *et al.* (Addendum B) (21) for DEX or CpdA induced nuclear import of the mouse GRwt (mGRwt) and mouse GRdim (mGRdim), where DEX stimulation of the mGRwt resulted in 93 percent nuclear import and CpdA stimulation of mGRwt resulted in 66 percent nuclear import. Both the study by Robertson *et al.* as well as these results (Fig.5.4C) demonstrate similar behaviour for DEX through the dimerization impaired GRdim as for CpdA through the GRwt. We therefore hypothesize that the dimerization abrogating CpdA results in a similar conformation of the GRwt as exists for the dimerization impaired GRdim mutant following DEX stimulation.

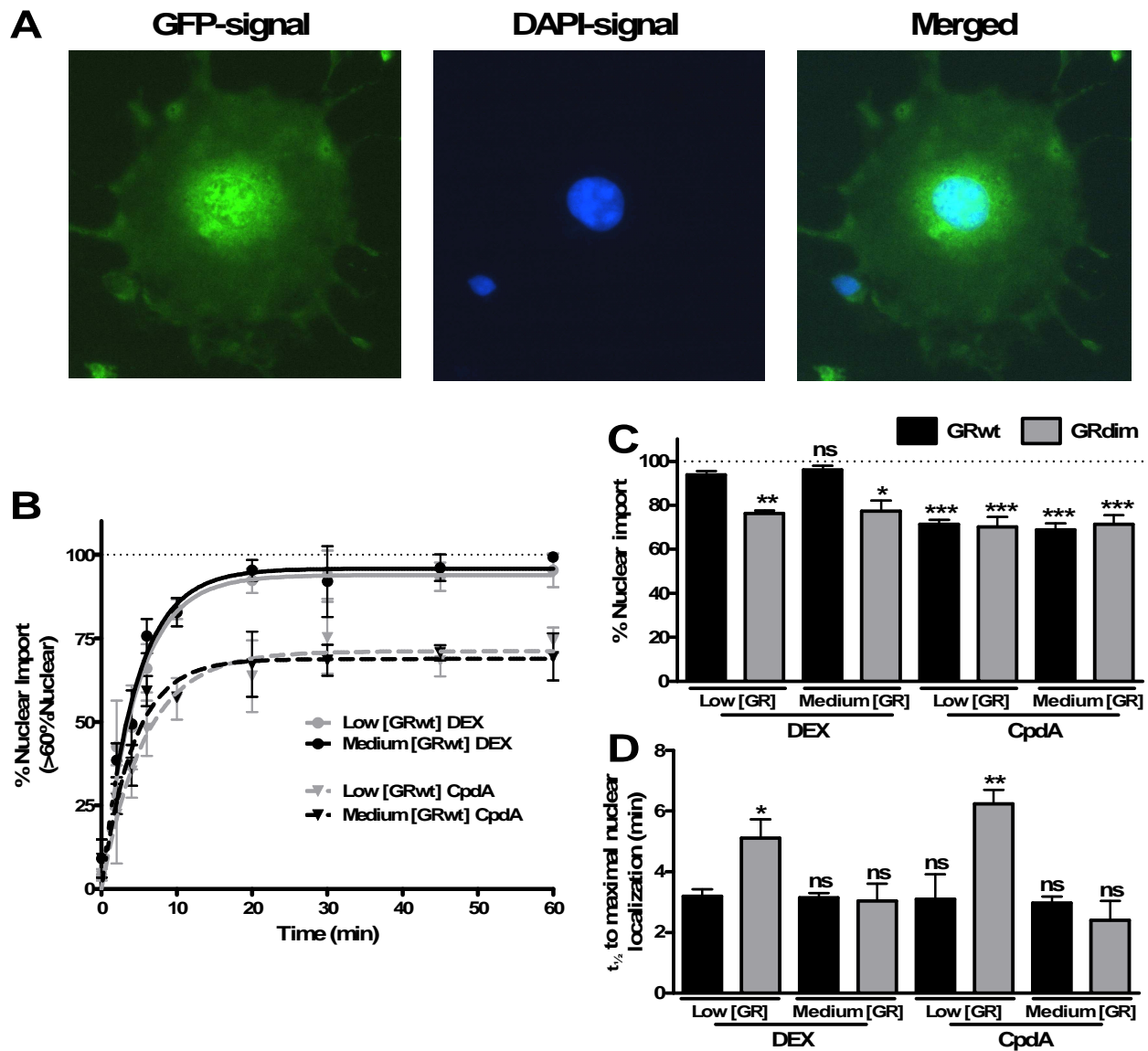


Figure 5.4. **The ability to dimerize influences $t_{1/2}$ and extent of nuclear import.** Immunofluorescent analysis of nuclear import was performed as described in *materials and methods*. (A) Representative images of a single cell displaying 60% nuclear GRwt localization. The GFP-signal depicts the position of the GR and the DAPI-signal detects the nuclear Hoechst stain, while the merged image is a combination of the two. (B) Representative graph of low and medium GRwt concentrations stimulated with 10^{-6} M DEX or 10^{-5} M CpdA. Statistical analysis was carried out on (C) percentage maximal nuclear localization and (D) $t_{1/2}$ to maximal nuclear localization using ANOVA followed by Dunnett's post test against DEX stimulated low GRwt concentration (* $P < 0.05$, ** $P < 0.01$ *** $P < 0.001$). Results represent 50 cells counted per condition and time point from three independent experiments (\pm SEM).

We demonstrate a significantly slower rate of nuclear import through the low GRdim concentration following either DEX or CpdA stimulation (Fig.5.4D). What is noteworthy is that the medium concentration of GRdim behaves in a more similar manner to the GRwt in terms of nuclear import rate than the low concentrations of GRwt and GRdim do, which is the same trend we saw in the live cell nuclear import assays (Fig.5.2B). Our Co-IP results suggest that the medium concentration of GRdim

displays a degree of ligand independent dimerization (Fig.4.3), albeit significantly lower than that of the GRwt. We therefore conclude that the medium concentration GRdim approaches wild type like behaviour, which results in an increase in its nuclear import rate to a level that is similar to the GRwt, despite displaying insufficient ligand independent dimerization for positive cooperative ligand binding to be observed (Fig.3.8B). Where as the live cell nuclear import assay demonstrated clear GR type and concentration dependent differences in the $t_{1/2}$ of nuclear import (Fig.5.2B), the indirect immunofluorescent analysis of nuclear import does not show a difference in the nuclear import rate between low and medium GRwt concentrations or between medium concentrations of GRwt and GRdim (Fig.5.4D) and only mimics the live cell analysis at the low GR concentration where GRdim results in a slower rate of import. However, as the immunofluorescent analysis represents a population of cells and not the import within a single cell it is inherently a less accurate means of measuring the $t_{1/2}$ of nuclear import and may simply not be sensitive enough to detect the differences in nuclear import rate. In a similar assay Robertson *et al.* (Addendum B) (21) also demonstrated no differences in the nuclear import rate when studying DEX or CpdA induced import of mGRwt or mGRdim.

It is important to note that the import rate reflects both the rate of nuclear import as well as the rate of nuclear export. As nuclear export is primarily through passive diffusion it is an on going process which occurs even during ligand stimulation and therefore primary nuclear import. A possible cause for the reduced nuclear import rate at the low GRdim concentration (Fig.5.4D) and incomplete nuclear localization at both low and medium GRdim concentrations (Fig.5.4C) may be faster nuclear export. An increase in nuclear export rate is associated with a reduced ability to bind to Hsp90 in the nucleus (9, 10) and may be linked to increased nuclear mobility as a result of a decrease in DNA affinity as revealed by agonist bound YFP-GR (3),(9, 10). It is enticing to speculate that the significant increase in nuclear import rate and significant decrease in nuclear localization of the GRdim is as a result of an increased nuclear export rate. We will explore this possibility in Section 5.3.

As immunofluorescent analysis of nuclear import measures the $t_{1/2}$ to 60% or greater nuclear import and not the time to maximal nuclear import as the live cell study does, this results in a reduced $t_{1/2}$ of nuclear import when compared to the live cell nuclear import assay. This is best illustrated at the medium GRwt concentration where DEX stimulation results in a nuclear import $t_{1/2}$ of 3.2 minutes (Fig.5.4D) in the immunofluorescent assay and an import $t_{1/2}$ of 7.5 minutes in the live cell assay (Fig.5.2B). Our study demonstrates similar import rates to results in the literature, which show indirect immunofluorescent studies of GR import $t_{1/2}$ of 4 to 5 minutes following 10^{-6} M DEX addition (3, 7).

The fact that the GRwt concentration shows no influence on nuclear import may be a short coming of the assay itself. When compared to the live cell import assay the time points analyzed are greatly

reduced and represent the average import of a wide variety of cells. Due to the fact that the quantification of nuclear localization is performed by physical human observation at 20-fold magnification and not by the Cell[®] imaging software at 60-fold magnification it is highly likely that cells with low GR and therefore reduced fluorescent labelling are simply not accounted for. As described in *materials and methods* we actively selected cells with low GR expression from our low GFP-GRwt and low GFP-GRdim concentration populations for live cell import analysis. They therefore represent cells with a truly reduced GR level. Unfortunately the rather blunt instrument of indirect immunofluorescent labelling relies on human observation of a population of cells where those expressing the very lowest GR concentrations are most likely undetectable to the human eye. This technique is simply not sensitive enough due to the short comings of the human optical threshold which are exposed by the indirect labelling technique and which can not hope to match the efficiency of direct fluorophore labelling and the increased level of magnification. It must also be noted that the level of background fluorescence is vastly increased in the immunofluorescent assay due to the nature of this assay further hampering the detection of cells expressing low GR concentrations.

5.2 Nuclear distribution is ligand as well as dimerization dependent

Results in the literature indicate that induction with the potent GR agonist, DEX, results in discrete nuclear foci, areas within the nucleus where the activated GR aggregates, while induction with the GR antagonist RU486 leads to diffuse nuclear localization of the activated GR (3, 6, 9). It has been demonstrated that GFP-GR mobility within the nucleus, which is an active process, is determined by ligand concentration and affinity for GRE binding. For example, in transiently transfected COS-1 cells binding of ligands with high affinity for the GR results in a clear decrease in GR nuclear mobility (22). Furthermore, increasing the concentration of GFP-AR in transiently transfected cells also leads to 5-fold decrease in its nuclear mobility, which may be as a result of enhanced HRE binding at increased receptor concentration (23). It is hypothesized that conformational changes of the GR following ligand binding enable it to transiently bind nuclear structures or domains that are slow moving and that this is reflected in decreased receptor mobility in the nucleus as demonstrated by fluorescence recovery after photobleaching (FRAP) of GFP-GR (9). Furthermore, nuclear mobility has been shown to be slower in areas of high GR concentration than in areas of low GR concentration (8). The theory that receptor mobility is slowed by associations with transcription machinery and through direct binding to DNA is consistent with RNA fluorescence in situ hybridization (FISH) studies that have demonstrated active transcription close to receptor nuclear foci (24-26), which is ligand dependent (27, 28). As nuclear distribution is an important factor for predicting the level of transcriptional activation we have investigated the influence of positive cooperative ligand binding and GR dimerization on nuclear distribution.

We have based our study of nuclear distribution of the GFP-GRwt and GFP-GRdim on those performed by Schaaf *et al.* (8) who quantified nuclear distribution in terms of the variation in fluorescent intensity along a line drawn through the nucleus. The resulting quotient of variation (CV) along this nuclear line represents the distribution of fluorescently labelled GR. A high CV (typically >17 percent) (8) signifies a non-random nuclear distribution where discrete foci or speckles of fluorescence are visible. A low CV indicates random nuclear distribution typified by a diffuse distribution of fluorescence. Our results demonstrate a quotient of variation (CV) value of ~18 percent following 10^{-6} M DEX stimulation (Fig.5.5C), which is very similar to the ~19 percent shown by Schaaf *et al.* at the same concentration of DEX in COS-1 cells expressing YPF-GRwt.

Our nuclear distribution assay displays similar results to those of Schaaf *et al.* (8) despite the fact that we have not used a confocal microscope but have relied on the deconvoluting capability of the Cell® imaging software of an IX-81 inverted fluorescence microscope (Olympus Corp., Japan). Initial studies prior to the use of the deconvoluting software generated fluorescent intensity profiles through the nucleus which were bell shaped. This was as a result of the three dimensional structure of the nucleus. When viewed in its entirety the spherical nucleus has a greater concentration of GFP-GR in its centre than at its periphery. By taking images above and below the chosen focal plane the software can deconvolute the influence of this intensity to generate an image which is in effect the fluorescent profile of a single focal plane. The graphs of our deconvoluted nuclear fluorescence intensity have a linear axis (Fig.5.5B) as is demonstrated for those using the confocal imaging (8).

Distribution of activated GR in the nucleus has been shown to be influenced by ligand. Previous studies from the literature demonstrate that stimulation with the agonist DEX results in a non-random particulate distribution of the GR in the nucleus while stimulation with the antagonist RU486 leads to a random distribution of the GR in the nucleus (3, 6, 9). Our studies demonstrate that stimulation with the dissociated GC, CpdA, results in random nuclear distribution of the GR, which is reflected in a lower percentage CV than the potent agonist DEX (Fig.5.5C). A high percentage CV equates to non-random nuclear distribution, which indicates the formation of discrete foci within the nucleus where the GR is sequestered (Fig.5.5A,C). These foci have been shown to correspond with areas of the nucleus where active transcription takes place (24, 25). CpdA induces random nuclear distribution through both the GFP-GRwt and the GFP-GRdim, which supports the evidence that CpdA is incapable of inducing transactivation (29) via the GR.

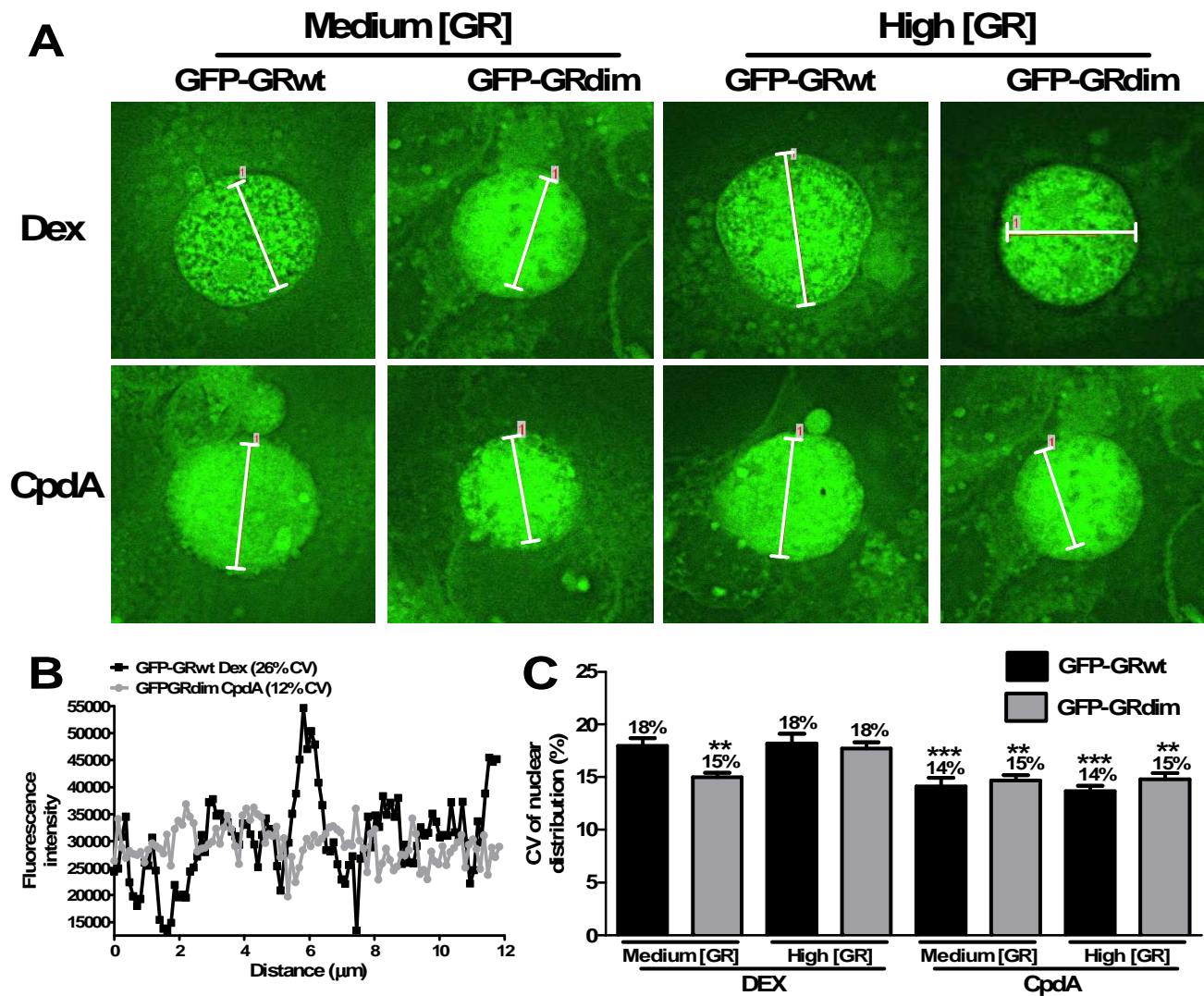


Figure 5.5. **CpdA stimulation results in the random nuclear distribution of GR while DEX stimulation results in a non-random distribution of GRwt and high concentrations of GRdim.** The nuclear distribution assay was performed as described in *materials and methods*. Cells expressing medium or high GFP-GRwt or medium or high GFP-GRdim were induced with 10^{-6}M DEX or 10^{-5}M CpdA for 1 hour. Z-stack images of the nuclei were taken at various focal planes and these were used to deconvolute a single nuclear image. As long a line as possible was selected in each nuclei avoiding nucleoli and the Cell[®] imaging software was used to quantify the coefficient of variation (CV) of GFP fluorescence intensity along this line in 5 cells per condition from 4 separate experiments ($\pm\text{SEM}$). **(A)** Representative deconvoluted nuclear images of either 10^{-6}M DEX or 10^{-5}M CpdA stimulated cells. **(B)** Representative graph of fluorescent intensity from two cells demonstrating fluorescent intensity along two nuclear lines with a CV of 12% and 26%, respectively. **(C)** Statistical analysis of CV of nuclear distribution was carried out using ANOVA followed by Dunnett's post test against DEX stimulated medium GFP-GRwt concentration (* $P < 0.05$, ** $P < 0.01$ *** $P < 0.001$).

The pattern of GFP-GRwt nuclear distribution following DEX induction was not influenced by receptor concentration. We therefore conclude that positive cooperative ligand binding to the GR does not affect this parameter (Fig.5.5A,C). However, the random distribution of the DEX induced low GFP-GRdim concentration as well as that elicited through CpdA induction (Fig.5.5C) indicates a role of

dimerization in nuclear sequestering. Dimerization impaired GR mutants have been shown to bind to DNA with a reduced capacity relative to the wild type receptor (30-33), which would explain the random distribution demonstrated by the low concentration of GFP-GRdim. Interestingly DEX induced nuclear distribution of the GFP-GRdim shifts from a random to a non-random pattern as the receptor concentration increases (Fig.5.5A,C). This is similar to our nuclear import results which demonstrate wild type like behaviour at the high GFP-GRdim concentration. Again we hypothesize that at high concentrations the GFP-GRdim is capable of a degree of ligand induced dimerization which affords it a degree of wild type behaviour which, however, is not sufficient to elicit positive cooperative ligand binding.

5.3 Nuclear export of the glucocorticoid receptor

The export of GR from the nucleus upon ligand withdrawal occurs over a time period of hours and is a passive process (34). Indirect immunofluorescence studies by Hache *et al.* of GR export from the nucleus following the washout of 10^{-6} M cortisol (F) show a $t_{1/2}$ of 8-9 hours and that the GR remains predominantly nuclear 48 hours after 10^{-6} M RU486 washout in GrH2 cells (7). Carrigan *et al.* saw no nuclear export of the GR 24 hours after washout of 10^{-6} M F in transiently transfected COS-7 cells (35). Export of endogenous GR from isolated thymocytes was shown to have a $t_{1/2}$ of 12 hours following the washout of 10^{-6} M DEX (3). The nuclear export of GFP-GR in a live cell assay 5 hours after the washout of 5×10^{-8} M DEX demonstrated predominant nuclear localization (10). Retention of the GR in the nucleus has been shown to be linked to GR association with nuclear Hsp90 (10). Due to the rapid rate of GR dissociation from DNA following ligand withdrawal of 30 to 60 minutes (36) and the subsequent localization of GR to transcriptionally inactive areas of the nucleus (34) it is unlikely that the export rate of GR plays a major role in GR function.

5.3.1 The $t_{1/2}$ of live cell nuclear export is dimerization dependent

In order to represent nuclear export of the GR in terms of both the level of GFP-GR diffusion out of the nucleus and the level of its concomitant accumulation in the cytoplasm we quantified nuclear export as the ratio of GFP in the centre of the nucleus divided by that in the mid point of the cytoplasm (Fig.5.6, Fig.5.7A).

Our initial studies on the GFP-GRwt following induction and washout of 10^{-6} M DEX revealed protracted nuclear export rates ($t_{1/2}$ ~20 hours) (Fig.5.7A), which is similar to results shown in the literature where export studies on transiently transfected GFP-GR in COS-7 cells demonstrated ligand dependent export rates as well as 75 percent nuclear distribution 24 hours after 10^{-6} M DEX washout

(18). In order to visualize complete nuclear export of the GR from the nucleus we thus stimulated with 10^{-9} M DEX where the average $t_{1/2}$ of nuclear export was reduced to ~4 hours (Fig.5.8B). These findings indicate that nuclear export is ligand concentration dependent.

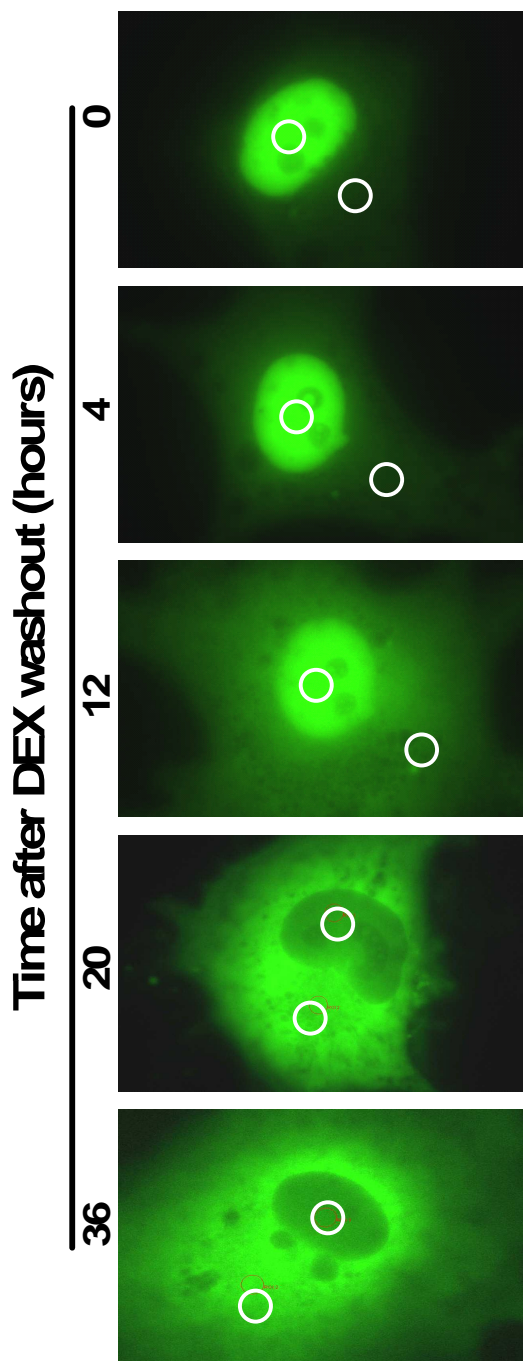


Figure 5.6. **Live cell nuclear export studies.** COS-1 cells were transiently transfected with pEGFP-C2-GR (GFP-GR) using the DEAE-Dextran method. A single cell was induced with 10^{-6} M DEX for 1 hour after which it was rinsed 4 times with sterile PBS and stripped DMEM was added. Nuclear export was analyzed at 0, 4, 12, 20 and 36 hours after washout. The small white circles represent the ROIs, situated at the mid point of the nucleus and the mid point between nuclear membrane and cellular membrane. As the cell is alive and moves considerably over the 36 hour period, ROIs must be redrawn for each time point.

As the live cell nuclear export study was carried out over a 36 hour period we were concerned that a build up of GFP-GR in the cytoplasm may have been as a result of new protein expression and not of GFP-GR export into the cytoplasm. We therefore ran an experiment where cycloheximide or solvent was incubated along with the cells during the assay. Cycloheximide blocks translational elongation and is therefore an inhibitor of protein biosynthesis, furthermore Avenant *et al.* (37) have demonstrated that the same cyclohexamide treatment is capable of blocking protein biosynthesis in COS-1 cells. We found no difference between the export time of medium concentrations of GFP-GRwt or GFP-GRdim with or without cycloheximide (Fig.5.7B). It is therefore possible to assume that the build up of GFP-GR in the cytoplasm is as a result of nuclear export and not due to significant effects attributable to the synthesis of new GFP-GR over the 36 hour assay.

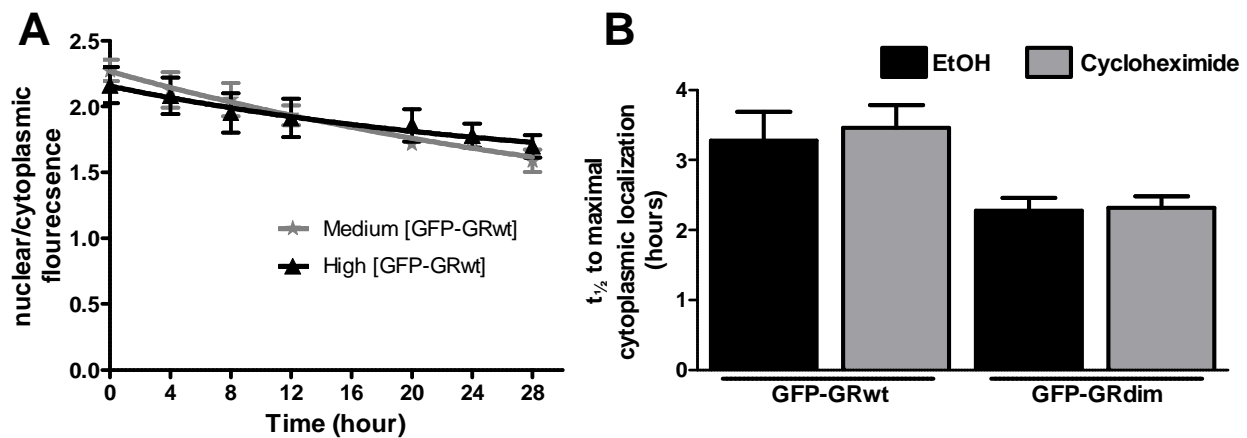


Figure 5.7. Induction with 10^{-6} M DEX results in protracted export rates while administration of cycloheximide does not influence the live cell nuclear export rate. Live cell nuclear export was performed as described in *materials and methods*. **(A)** Protracted nuclear export ($t_{1/2}$ ~20 hours) following induction with 10^{-6} M DEX. **(B)** COS-1 cells expressing medium concentrations of either GFP-GRwt or GFP-GRdim were induced with 10^{-9} M DEX for 1 hour after which they were rinsed 4 times with sterile PBS and stripped DMEM containing either EtOH or 1μ M cycloheximide (Sigma). Nuclear export was quantified as the ratio of GFP fluorescence in the mid point of the nucleus over that in the midpoint between nuclear membrane and cellular membrane. Data was fit to a one phase exponential decay curve which generates a $t_{1/2}$ to maximal cytoplasmic localization. Statistical analysis was carried out using one tailed unpaired t test. Results represent three individual cells from one experiment (\pm SEM).

There was no statistical difference in nuclear export rate between the medium or high GFP-GRwt or medium and high GFP-GRdim (Fig.5.8B). However, nuclear export studies do offer a possible explanation for the slower nuclear import rate and lower maximal localization levels of GFP-GRdim when compared to that of GFP-GRwt (Fig.5.2B,C,D), as there is a significant trend towards faster nuclear export of the GFP-GRdim (Fig.5.8A,B). To reiterate, the nuclear import rate comprises both the rate of import as well as that of export. We therefore propose that the faster rate of nuclear export demonstrated by GFP-GRdim contributes to its reduced nuclear import rate (Fig.5.2B). Furthermore,

the diffuse pattern of nuclear distribution elicited by stimulation with dimerization abrogating CpdA and demonstrated by the low concentration of GFP-GRdim following DEX stimulation (Fig.5.5C), suggest that dimerization is necessary to retain the GR in the nucleus. We thus propose that the reduced levels of nuclear localization shown by GRdim as well as CpdA stimulated GRwt (Fig.5.4C) may be linked to the increased nuclear export rate displayed by dimerization impaired GR (Fig.5.8A,B), which is possibly caused by a decrease in nuclear retention reflected by the random pattern of nuclear distribution (Fig.5.5C).

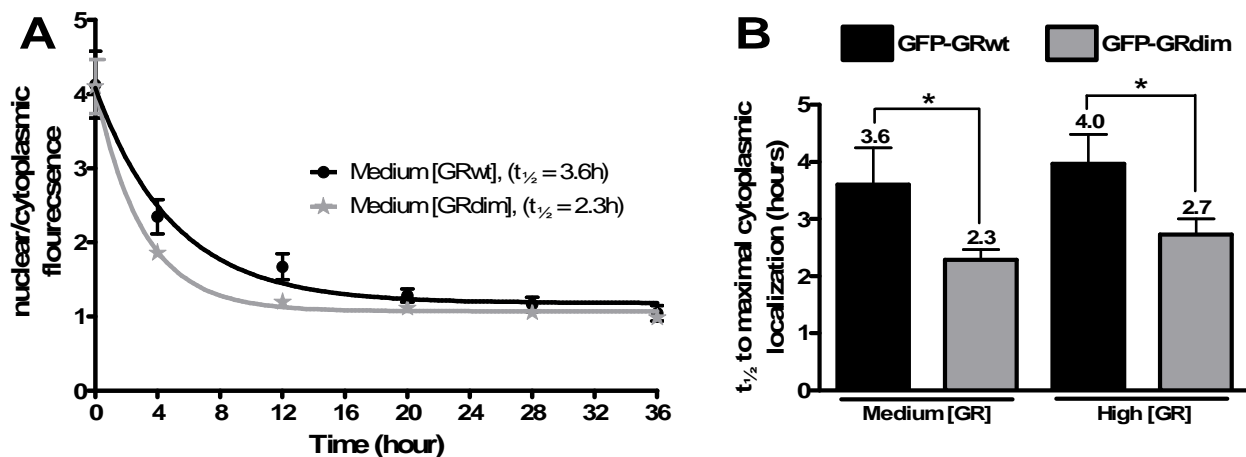


Figure 5.8. GR dimerization decreases the rate of nuclear export. (A) A representative graph depicting nuclear export in cells expressing medium GFP-GRwt or GFP-GRdim following the washout of 10^{-9} M DEX quantified as the ratio of GFP fluorescence in the nucleus over that in the cytoplasm. A one phase exponential decay curve was fit to the data which generated a $t_{1/2}$ to maximal cytoplasmic localization. (B) Nuclear export rates of medium and high GFP-GRwt or GFP-GRdim. Statistical analysis was carried out using one tailed unpaired t test (* $P < 0,05$). All results represent a minimum of six individual cells from independent experiments (\pm SEM).

5.3.2 Increased ligand binding affinity of the medium GRwt concentration results in protracted nuclear retention following the washout of 10^{-6} M DEX

Immunofluorescence has been used to quantify nuclear export in much the same way it was for nuclear import. Low and medium concentrations of GRwt or GRdim were stimulated for one hour with 10^{-6} M DEX after which the DEX was washed out and cells were fixed, permeabilized and fluorescently labelled at time points following the washout from 0 to 28 hours. Figure.5.9 depicts representative cells expressing the medium GRwt concentration.

Immunofluorescent analysis of nuclear export was conducted following the washout of either 10^{-6} M DEX or 10^{-5} M CpdA. The export $t_{1/2}$ value reflects the half time to less than 60 percent nuclear GR localization (Fig5.10). Our live cell nuclear export studies revealed a dramatically faster rate of nuclear

export (Fig.5.8B) as compared to immunofluorescent results (Fig.5.10). However, this is to be expected due to the lowered concentration of DEX used to induce nuclear import (10^{-9} M versus 10^{-6} M).

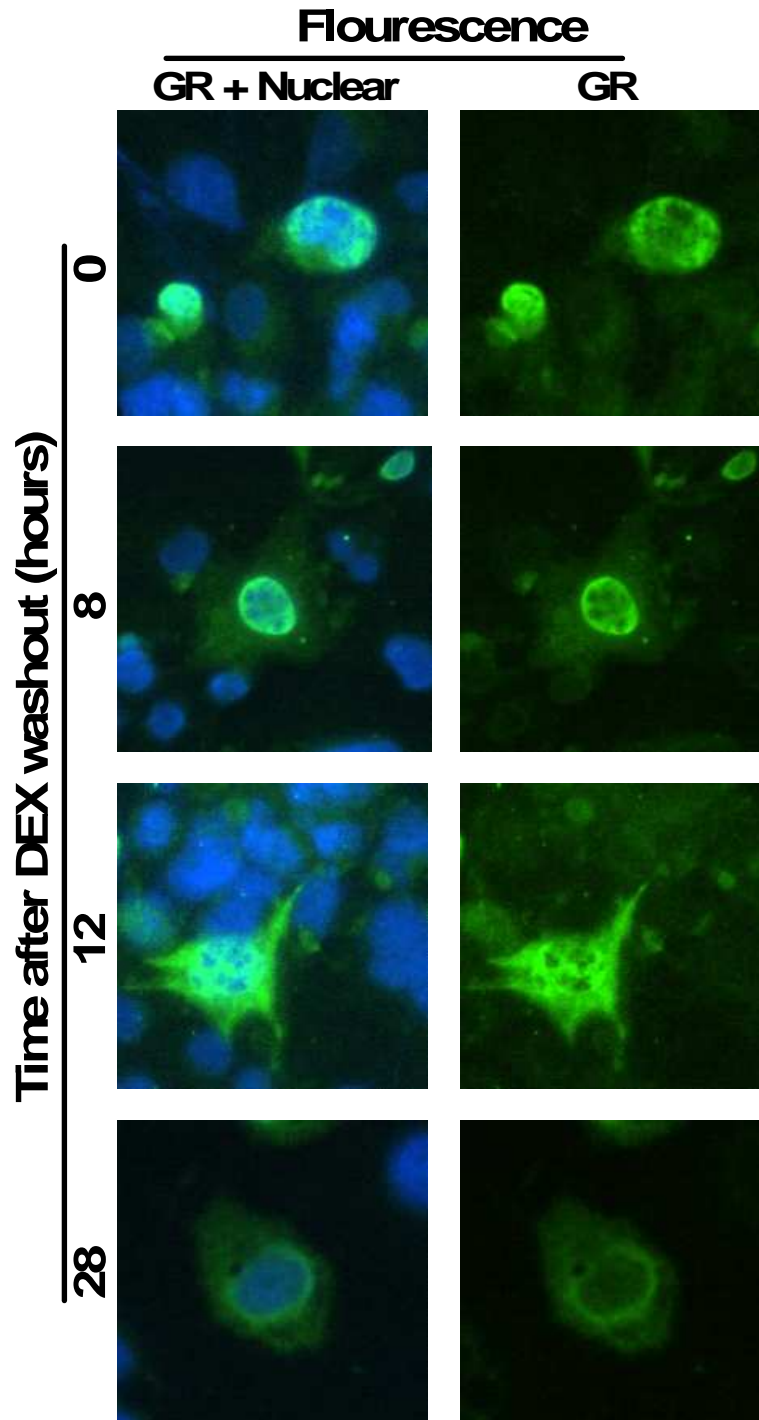


Figure 5.9. **Immunofluorescent analysis of nuclear export.** Immunofluorescence analysis of nuclear export was performed as described in *materials and methods*. Representative images at varying time points following the washout of 10^{-6} M DEX at medium concentrations of GRwt. The GR and nuclear overlay depict the Hoechst nuclear stain and GFP signal which indicates the position of the GR. The GR images demonstrate the GFP-signal.

The medium GRwt concentration following DEX stimulation and washout (Fig.5.10A,B) is the only export $t_{1/2}$ which significantly differs from the other DEX induced GR levels and constructs. Demonstrating an increase in nuclear export $t_{1/2}$ from 13.3 hours at the low GRwt concentration following DEX withdrawal to 21.4 hours at the medium GRwt concentration. Furthermore the nuclear export rate of the low and medium GRwt concentrations following CpdA washout is similar and non-significantly different from the DEX stimulated low GRwt concentration in the immunofluorescent assay (Fig.5.10B). Although it is tempting to attribute the increase in export rate at the medium GRwt concentration to cooperative ligand binding, the fact that live cell nuclear export of GFP-GR displayed no such receptor concentration dependent difference in nuclear export rate (Fig.5.8B) cautions against this interpretation. Rather, the explanation we offer for this phenomenon is that ligand independent dimerization of the medium GRwt concentration increases its sensitivity to DEX and thus the thousand fold greater concentration of stimulating DEX in the immunofluorescent assay versus the live cell export assay may result in trace amounts of DEX remaining in the cell after washout which only the ligand independent dimerized GR can bind due to its increased ligand binding affinity as revealed by saturation binding assays (Fig.3.8B), thus prolonging its nuclear export. This is not observed with CpdA as CpdA abrogates dimerization of the GR and export rates following its washout remain the same for both receptor types and concentrations.

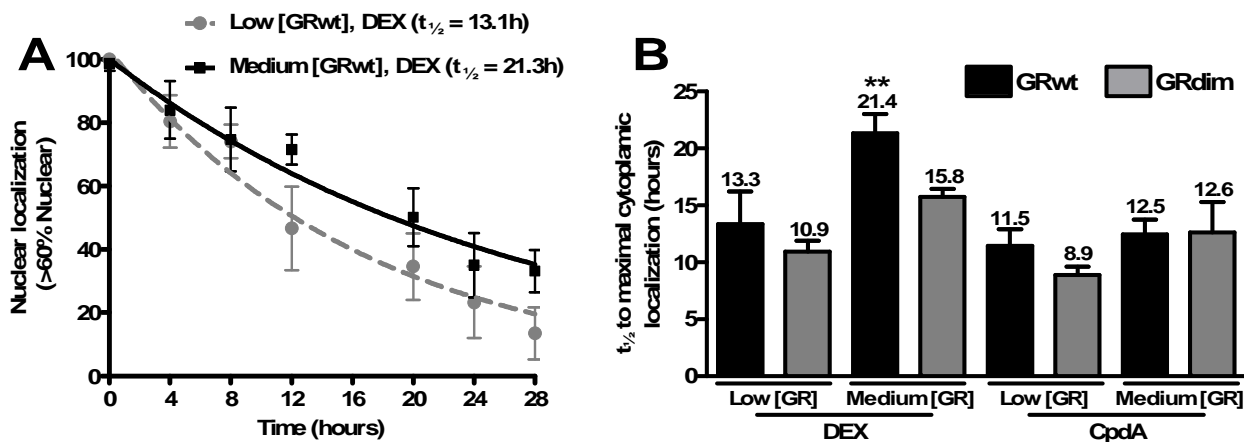


Figure 5.10. Immunofluorescent analysis of nuclear export shows an increased $t_{1/2}$ at medium GRwt following DEX stimulation only. Immunofluorescent nuclear export studies were carried out as described in *materials and methods*. Cells were stimulated with $10^{-6}M$ DEX or $10^{-5}M$ CpdA for 1 hour, rinsed three times with sterile PBS at $37^{\circ}C$ and incubated for 0, 4, 8, 12, 20, 24 and 28 hours in stripped DMEM. The percentage nuclear of total cells counted was fit to a one phase exponential decay curve, (A) graph of low and medium GRwt concentrations exposed to DEX, (B) which generates a $t_{1/2}$ to maximal cytoplasmic localization. Statistical analysis was carried out on $t_{1/2}$ to maximal nuclear localization, percentage maximal nuclear localization and $t_{1/2}$ to maximal cytoplasmic localization using ANOVA followed by Dunnett's post test against DEX stimulated low GRwt concentration (* $P < 0.05$, ** $P < 0.01$ *** $P < 0.001$). All results represent 50 cells per condition from three independent experiments (\pm SEM).

5.4 Overview of Chapter 5 results

Our results in this chapter demonstrate significant variation in the rates of GR nuclear import and export as well as nuclear distribution at varying GR concentrations, with different constructs and following DEX or CpdA stimulation. However, it is not obvious whether these differences arise due to cooperative ligand binding at the high GRwt concentrations or because of GR concentration and dimerization effects. One may argue that if cooperative ligand binding was the cause for differences in GR mobility and distribution then DEX stimulation would alter the behaviour of only the concentration of GRwt, which displays cooperative ligand binding. GRwt concentrations that display non-cooperative ligand binding should behave similarly to all GRdim concentrations. Furthermore, CpdA stimulation should result in a difference in behaviour compared to DEX stimulation at GRwt concentrations that elicit cooperative ligand binding.

The arguments for the influence of cooperative ligand binding on nuclear import include an increase in the live cell nuclear import rate at high GFP-GRwt concentration, which was significantly faster than that of the high concentration of GFP-GRdim (Fig.5.2), the decrease in the DEX induced maximal nuclear localization of the medium concentration of GRdim as compared to GRwt (Fig.5.4C) and the fact that stimulation with CpdA decreased the maximal nuclear localization of GRwt to parity with DEX stimulated GRdim (Fig.5.4C). However, the case against the influence of cooperative ligand binding on nuclear import is stronger. The live cell assay revealed a GRdim concentration dependent increase in nuclear import rate (Fig.5.2), while nuclear import quantified through immunofluorescence demonstrated no difference in the DEX stimulated nuclear import rate or maximal nuclear localization through low and medium GRwt concentrations (Fig5.4). Furthermore, the nuclear import rate following DEX stimulation at medium GRwt and GRdim concentrations is also similar (Fig.5.4). These counter arguments against the influence of cooperative ligand binding on GR nuclear import suggest that the ability of GR to dimerize and increased GR concentration, rather than cooperative ligand binding, promote an increase in GR nuclear import rate and maximal nuclear localization at saturating ligand concentrations. Intriguingly, immunofluorescent import studies at subsaturating DEX concentrations suggest an influence of cooperative ligand binding. Although the nuclear import rate of the low and medium GRwt concentrations are statistically the same following 10^{-6} M DEX stimulation, there is a significant difference in their import rates at lower DEX concentrations (Fig.5.11). Where as the nuclear import rate of the medium concentration of GRwt following the stimulation with 10^{-6} M, 10^{-9} M or 10^{-10} M DEX remains statistically similar, that of the low concentration of GRwt decreases significantly as stimulating DEX concentrations decrease (Fig5.11). Thus, cooperative ligand binding may enhance nuclear import of the GR, but only at subsaturating GC concentrations.

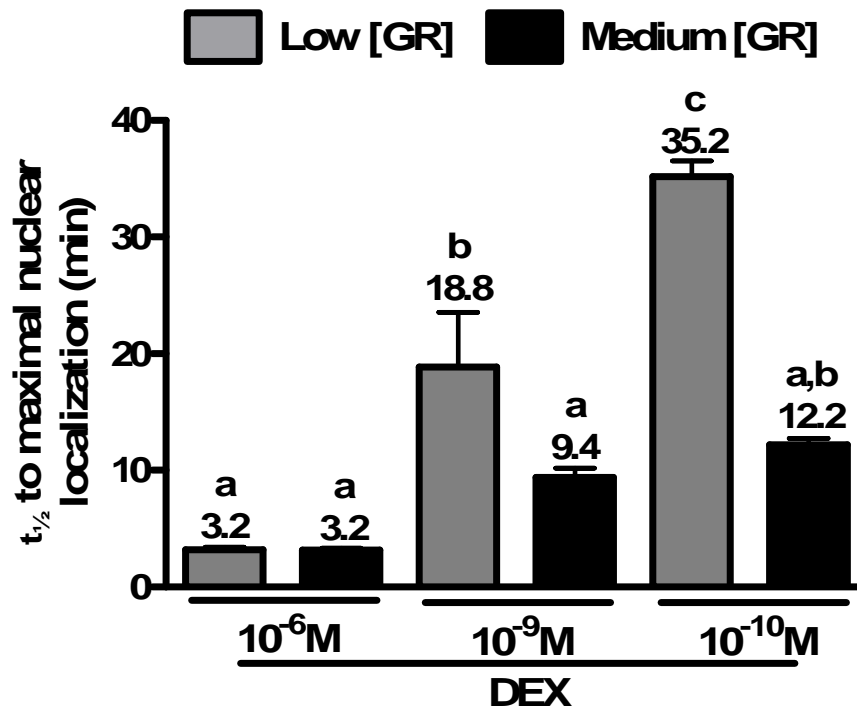


Figure 5.11. **Immunofluorescent nuclear import stimulated by various DEX concentrations.** Immunofluorescent analysis of nuclear import stimulated by $10^{-6}M$, $10^{-9}M$ or $10^{-10}M$ DEX was performed as described in *materials and methods* on COS-1 cells expressing low or medium concentrations of GRwt. Statistical analysis was carried out on $t_{1/2}$ to maximal nuclear localization using ANOVA followed by Newman-Keuls post test. Conditions with different letters are statistically different from one another ($P < 0.01$). Results represent 50 cells counted per condition and time point from three independent experiments (\pm SEM).

The fact that CpdA stimulation resulted in uniform nuclear distribution through both the GFP-GRwt and GFP-GRdim supports an influence of cooperative ligand binding on this parameter (Fig.5.5). However, GFP-GRwt concentration has no influence on nuclear distribution and DEX stimulated high GFP-GRdim concentration behaves similarly to the high GFP-GRwt concentration (Fig.5.5). These results thus rather suggest an influence of GR dimerization on nuclear distribution.

The fact that the live cell nuclear export rate of high GFP-GRdim concentration is significantly faster than high GFP-GRwt concentration supports an influence of cooperative ligand binding on this parameter. However, the same behaviour is also observed at the medium GFP-GR concentrations (Fig.5.8). Also arguing against the influence of cooperative ligand binding on nuclear export following the washout of subsaturating DEX concentrations is the fact that GFP-GRwt concentration does not significantly affect the nuclear export rate (Fig.5.8). The immunofluorescent analysis of nuclear export following the washout of saturating concentrations of ligand, revealed behaviour suggestive of an influence of cooperative ligand binding.

The nuclear export rate was significantly slower at the medium GRwt concentration than at the low GRwt concentration, while GRdim, at both low and medium concentrations, behaves like the low GRwt concentration. Furthermore, stimulation with CpdA results in a uniform rate of nuclear export (Fig.5.10). Taken together the results suggest that dimerization enhances nuclear retention following the washout of subsaturating DEX concentrations, while cooperative ligand binding may result in enhanced nuclear retention following the washout of saturating DEX concentrations.

Having established the influence of GR concentration, dimerization and positive cooperative ligand binding on GR translocation and nuclear distribution we next focused our study on the effects these parameters may have on the ability of the GR to transactivate and transrepress genes and specifically, the consequence of positive cooperative ligand binding on GR's role as a transcription factor.

5.5 Bibliography

1. DeFranco DB (2002) Navigating steroid hormone receptors through the nuclear compartment. *Mol Endocrinol* 16: 1449-1455.
2. Shahin V (2006) Route of glucocorticoid-induced macromolecules across the nuclear envelope as viewed by atomic force microscopy. *Pflugers Arch* 453: 1-9.
3. Vicent GP, Pecci A, Ghini A, Piwien-Pilipuk G & Galigniana MD (2002) Differences in nuclear retention characteristics of agonist-activated glucocorticoid receptor may determine specific responses. *Exp Cell Res* 276: 142-154.
4. Hayashi R, Wada H, Ito K & Adcock IM (2004) Effects of glucocorticoids on gene transcription. *Eur J Pharmacol* 500: 51-62.
5. Nishi M, Ogawa H, Ito T, Matsuda KI & Kawata M (2001) Dynamic changes in subcellular localization of mineralocorticoid receptor in living cells: In comparison with glucocorticoid receptor using dual-color labeling with green fluorescent protein spectral variants. *Mol Endocrinol* 15: 1077-1092.
6. Htun H, Barsony J, Renyi I, Gould DL & Hager GL (1996) Visualization of glucocorticoid receptor translocation and intranuclear organization in living cells with a green fluorescent protein chimera. *Proc Natl Acad Sci U S A* 93: 4845-4850.
7. Hache RJ, Tse R, Reich T, Savory JG & Lefebvre YA (1999) Nucleocytoplasmic trafficking of steroid-free glucocorticoid receptor. *J Biol Chem* 274: 1432-1439.
8. Schaaf MJ, Lewis-Tuffin LJ & Cidlowski JA (2005) Ligand-selective targeting of the glucocorticoid receptor to nuclear subdomains is associated with decreased receptor mobility. *Mol Endocrinol* 19: 1501-1515.
9. Schaaf MJ & Cidlowski JA (2003) Molecular determinants of glucocorticoid receptor mobility in living cells: The importance of ligand affinity. *Mol Cell Biol* 23: 1922-1934.

10. Tago K, Tsukahara F, Naruse M, Yoshioka T & Takano K (2004) Regulation of nuclear retention of glucocorticoid receptor by nuclear Hsp90. *Mol Cell Endocrinol* 213: 131-138.
11. Liu J & DeFranco DB (2000) Protracted nuclear export of glucocorticoid receptor limits its turnover and does not require the exportin 1/CRM1-directed nuclear export pathway. *Mol Endocrinol* 14: 40-51.
12. Galigniana MD, *et al* (1998) Heat shock protein 90-dependent (geldanamycin-inhibited) movement of the glucocorticoid receptor through the cytoplasm to the nucleus requires intact cytoskeleton. *Mol Endocrinol* 12: 1903-1913.
13. Banerjee A, *et al* (2008) Control of glucocorticoid and progesterone receptor subcellular localization by the ligand-binding domain is mediated by distinct interactions with tetratricopeptide repeat proteins. *Biochemistry* 47: 10471-10480.
14. Tanaka M, Nishi M, Morimoto M, Sugimoto T & Kawata M (2003) Yellow fluorescent protein-tagged and cyan fluorescent protein-tagged imaging analysis of glucocorticoid receptor and importins in single living cells. *Endocrinology* 144: 4070-4079.
15. Harrell JM, *et al* (2004) Evidence for glucocorticoid receptor transport on microtubules by dynein. *J Biol Chem* 279: 54647-54654.
16. Davies TH, Ning YM & Sanchez ER (2002) A new first step in activation of steroid receptors: Hormone-induced switching of FKBP51 and FKBP52 immunophilins. *J Biol Chem* 277: 4597-4600.
17. Pemberton LF & Paschal BM (2005) Mechanisms of receptor-mediated nuclear import and nuclear export. *Traffic* 6: 187-198.
18. Yoshikawa N, *et al* (2002) Distinct interaction of cortivazol with the ligand binding domain confers glucocorticoid receptor specificity: Cortivazol is a specific ligand for the glucocorticoid receptor. *J Biol Chem* 277: 5529-5540.
19. Ronacher K, *et al* (2009) Ligand-selective transactivation and transrepression via the glucocorticoid receptor: Role of cofactor interaction. *Mol Cell Endocrinol* 299: 219-231.
20. Usuku T, *et al* (2005) Visualization of glucocorticoid receptor in the brain of green fluorescent protein-glucocorticoid receptor knockin mice. *Neuroscience* 135: 1119-1128.
21. Robertson S, *et al* (2010) Abrogation of glucocorticoid receptor dimerization correlates with dissociated glucocorticoid behavior of compound a. *J Biol Chem* 285: 8061-8075.
22. Elbi C, *et al* (2004) Molecular chaperones function as steroid receptor nuclear mobility factors. *Proc Natl Acad Sci U S A* 101: 2876-2881.
23. Marcelli M, *et al* (2006) Quantifying effects of ligands on androgen receptor nuclear translocation, intranuclear dynamics, and solubility. *J Cell Biochem* 98: 770-788.
24. van Royen ME, *et al* (2007) Compartmentalization of androgen receptor protein-protein interactions in living cells. *J Cell Biol* 177: 63-72.
25. Wrangé O, Eriksson P & Perlmann T (1989) The purified activated glucocorticoid receptor is a homodimer. *J Biol Chem* 264: 5253-5259.

26. Stavreva DA, Muller WG, Hager GL, Smith CL & McNally JG (2004) Rapid glucocorticoid receptor exchange at a promoter is coupled to transcription and regulated by chaperones and proteasomes. *Mol Cell Biol* 24: 2682-2697.
27. Meijsing SH, Elbi C, Luecke HF, Hager GL & Yamamoto KR (2007) The ligand binding domain controls glucocorticoid receptor dynamics independent of ligand release. *Mol Cell Biol* 27: 2442-2451.
28. Voss TC, John S & Hager GL (2006) Single-cell analysis of glucocorticoid receptor action reveals that stochastic post-chromatin association mechanisms regulate ligand-specific transcription. *Mol Endocrinol* 20: 2641-2655.
29. De Bosscher K, *et al* (2005) A fully dissociated compound of plant origin for inflammatory gene repression. *Proc Natl Acad Sci U S A* 102: 15827-15832.
30. Dahlman-Wright K, Siltala-Roos H, Carlstedt-Duke J & Gustafsson JA (1990) Protein-protein interactions facilitate DNA binding by the glucocorticoid receptor DNA-binding domain. *J Biol Chem* 265: 14030-14035.
31. Drouin J, *et al* (1992) Homodimer formation is rate-limiting for high affinity DNA binding by glucocorticoid receptor. *Mol Endocrinol* 6: 1299-1309.
32. Tanner TM, *et al* (2010) A 629RKLKK633 motif in the hinge region controls the androgen receptor at multiple levels. *Cell Mol Life Sci* 67: 1919-1927.
33. Adams M, Meijer OC, Wang J, Bhargava A & Pearce D (2003) Homodimerization of the glucocorticoid receptor is not essential for response element binding: Activation of the phenylethanolamine N-methyltransferase gene by dimerization-defective mutants. *Mol Endocrinol* 17: 2583-2592.
34. Yang J, Liu J & DeFranco DB (1997) Subnuclear trafficking of glucocorticoid receptors in vitro: Chromatin recycling and nuclear export. *J Cell Biol* 137: 523-538.
35. Carrigan A, *et al* (2007) An active nuclear retention signal in the glucocorticoid receptor functions as a strong inducer of transcriptional activation. *J Biol Chem* 282: 10963-10971.
36. Reik A, Schutz G & Stewart AF (1991) Glucocorticoids are required for establishment and maintenance of an alteration in chromatin structure: Induction leads to a reversible disruption of nucleosomes over an enhancer. *EMBO J* 10: 2569-2576.
37. Avenant C, Ronacher K, Stubsrud E, Louw A & Hapgood JP (2010) Role of ligand-dependent GR phosphorylation and half-life in determination of ligand-specific transcriptional activity. *Mol Cell Endocrinol* 327: 72-88.

Chapter 6

Results: Transactivation and transrepression of genes is influenced by positive cooperative ligand binding to the GR

Introduction

The human GR α is a potent ligand dependent transcription factor, which has been shown to directly influence the expression of 2978 out of 41079 genes monitored in human osteosarcoma U2OS bone cells after 6 hours of induction with 10^{-7} M DEX (1). Of these genes 1522 were repressed while 1456 were induced by DEX stimulated GR α . Chromatin immunoprecipitation-microarray work in A549 human lung cells following 1 hour stimulation with 10^{-7} M DEX demonstrated that of the 548 known or potentially GC responsive genes studied, 68 percent were regulated through direct GR binding to GRE, which suggests that 32 percent of GR responsive promoters in this system function through tethering of the GR to other transcription factors (2) and not through direct interaction of the GR with DNA. Thus the activated GR influences gene transcription in two distinct ways (3),(4),(5). Through direct binding to GREs and nGRE, which up or down regulate transcription, respectively, or via tethering to DNA bound transcription factors such as NF κ B, AP-1 or signal transduction and activation of transcription-5 (STAT5) (4).

Direct binding of the GR to DNA occurs predominantly through the GRE, which consists of two palindromic 6bp half-sites that are separated by a 3bp spacer (5'-GGTACAnnnTGTTCT-3') (6). While most GREs contain this sequence, whether conserved or degenerate, their orientation, distance from transcription start site (TSS) and number vary greatly from gene to gene. This is of great importance as GRE occupancy is a primary determinant of GC responsiveness (2) and is known to vary from gene to gene (7). It has been shown that each GRE half-site binds one subunit of the GR homodimer (8). Drouin *et al.* (9) demonstrated that the affinity of GR homodimers for the GRE are 5-fold higher than that of GR monomers ($K_d = 0.2$ nM for dimers versus 1nM for monomers) and that GR dimers bind to DNA more stably *in vitro* than GR monomers (9). Furthermore, they demonstrated that GR dimerization was a rate limiting step in high affinity GRE binding by the GR and that dimerization of the GR occurred before association with the GRE. Results from Segard-Maurel *et al.* (10) that indicate an increased affinity of the GRE for GR dimer relative to monomer as well as greater stability of the GRE dimer binding support these findings and suggest that GR dimerization precedes GRE binding.

The question of whether GR binds to GREs as a preformed dimer or dimerizes following binding of two GR monomers to each of the two half-sites within the GRE is controversial. Our Co-IP (Fig.4.2B) and FRET results (Fig.4.6, Fig.4.7) indicate ligand independent dimerization of the GR, which is independent of DNA binding, while the work of Savory *et al.* (11) demonstrate ligand dependent dimerization of the GR in the cytoplasm. A recent article by Ong *et al.* (12) has questioned the influence of dimerization prior to DNA binding in first-order Hill dose-response curves (FHDC). Furthermore, they claim that the majority of GR association with DNA is through monomeric GR, the

evidence is based on theoretical considerations as well as transactivation assays which demonstrate FHDC for both the GRwt and a range of dimerization defective GR mutants. Although the dimerization mutants display weaker efficacy than the GRwt their capacity to induce transactivation reflects the fact that GR monomer binding to DNA is possible and results in activation of the GRE driven promoter reporter. In support of their theory they site binding of one retinoid X receptor (RXR) to its DNA half-site which induces a conformational change in the dimer interface of this receptor which facilitates binding of the second RXR at the neighbouring half-site (13). However, the same conformational change has not been shown for the complete GR and has only been demonstrated in studies performed on the DBD of the GR (14). A further argument they offer is a study which sites ligand dependent as well as ligand independent binding of the ER monomer to the estrogen response element (ERE) (15), which is also controversial in light of evidence which indicates ligand dependent as well as independent homodimerization of the ER-LBD, which shows a K_d of less than 0.1nM independent of ERE binding (16). Ong *et al.* (12), however, concede that dose-response curves which do not demonstrate FHDC behaviour may arise due to binding of the preformed GR dimer, a theory we will examine in Section 6.3.1.

McNally *et al.* (17) were the first to demonstrate the dynamic behaviour of GR binding to GREs. In cells expressing GFP-GR as well as an array of 200 copies of the mouse mammary tumour virus (MMTV) promoter, recruitment and occupancy of the GFP-GR could be visualized directly in live cells. Incredibly the receptor bound the GRE for only 10 to 20 seconds at a time before dissociating, which gave rise to the 'hit and run' theory of transcription where the initial transient binding of the GR is sufficient to recruit a secondary set of transcription factors that form a stable complex, which initiates transcription (18, 19). This 'hit and run' behaviour leaves the GR free to form further associations with the promoter that can initiate the next wave of transcription.

In contrast to dimer mediated transactivation via GREs there is mounting evidence that the GR's ability to repress inflammatory and immune genes is primarily through tethering of the GR monomer to proinflammatory transcription factors such as NF κ B and AP-1 (20-22). Research conducted in mice expressing only the D-loop dimerization mutant, GRdim, indicate that, despite drastically impaired transactivation via the GRdim, these mice are still viable due to the capacity of the GRdim to transrepress pro-inflammatory genes (23). The GRdim has been shown to be capable of repressing NF κ B driven transcription both *in vivo* as well as *in vitro* (24). Although initial studies questioned the ability of the GRdim to induce transactivation of genes (23), recent studies have demonstrated that the GRdim transactivates more strongly than the GRwt through multiple (two or more) GRE's (25). The capacity of both GRwt and GRdim to transactivate depends on the promoter in question, where as most promoters favour transactivation through the GRwt, there are a few that favour the GRdim (7).

The dissociative GC, CpdA, is capable of transrepression via NF κ B and AP-1 (26),(27) but does not induce transactivation (28),(29). This dissociative behaviour has been linked to CpdA's ability to abrogate dimerization of the GR (Addendum B) (30, 31). There is clearly a link between dimerization of the GR and transactivation.

Having shown that increasing GR concentration results in ligand independent dimerization of the GR (Chapter 4) and positive cooperative ligand binding to the GR (Chapter 3), we were interested in exploring the effects of GR concentration on both transactivation and transrepression. In order to test the influence of positive cooperative ligand binding on the transcriptional capacity of the GR we selected three promoter reporters representing either repression of an NF κ B driven gene (32) or activation of a composite GR promoter containing either one or two GRE's from the tyrosine amino transferase gene (TAT) (33). As GR's ligand dependent ability to transrepress NF κ B is a primary function of its anti-inflammatory nature and the fact that GRE's are known to elicit a robust transactivation response, these were natural choices for our promoter reporter assays. Furthermore, we also studied the level of GR induced mRNA production of the endogenous GILZ gene in COS-1 cells. The GILZ protein is a potent anti-inflammatory transcription factor (34) whose promoter is known to contain multiple GRE's (35), which has been shown to be under the direct control of activated GR (36),(37). As the promoter reporter assays are a relatively artificial transactivation system we have included the endogenous GR responsive GILZ gene in order to replicate a more physiologically relevant test of transactivation within the context of genomic DNA and complete promoter structure. Although the GILZ gene has not been characterized in monkey cells, such as COS-1 (green monkey), Avenant et al. (36) have demonstrated GC dependent up regulation of GILZ mRNA in COS-1 cells using commercially available primers for the human GILZ gene. A similar strategy has been employed in this study in order to allow for direct comparison with the rest of the assays performed in the same cell line.

There are three parameters through which ligand induced transcription may be quantified namely, the maximal level of agonist induced gene activation or repression (efficacy), the concentration of agonist required to illicit half of the maximal response (potency), and the amount of agonist activity elicited by partial agonists when compared to the response of a potent agonist (biocharacter) (38). Increasing GR concentration has been shown to increase the efficacy and potency of DEX as well as to shift the biocharacter of the weak GR agonists, RU486 and MPA, towards full agonist behaviour in transrepression promoter reporter assays (39-41). Similarly, increasing GR concentrations in transactivation promoter reporter assays has resulted in an increase in DEX induced efficacy and potency and a shift from weak agonist to full agonist behaviour of dexamethasone 21-mesylate (Dex-Mes), RU486 and Prog (41-44). To our knowledge, however, no studies have explicitly investigated

the connection between GR concentration, cooperative ligand binding and the three parameters of ligand induced transcription. Thus we aim to test whether the differences in GR concentration shown to shift ligand binding from non-cooperative to positive cooperative will also result in a shift in efficacy, potency and biocharacter in transactivation.

Results

6.1 Establishing promoter reporter assay conditions

In the majority of reporter promoter assays involving transient transfections plasmids which constitutively express β -galactosidase or renilla luciferase are transfected along with the reporter promoter constructs. This is done in order to normalize for differences in transfection efficiency and non-specific squelching between individual conditions within experiments and between experiments themselves. The most popular of these transfection normalization constructs are the commercially available pSV- β -gal (Promega) (40, 45, 46) and pCMV- β -gal (Invitrogen) (41, 47-49). Optimization assays using either of these constructs revealed a significant ligand independent decrease in β -galactosidase expression as the level of transfected GR increased (results not shown). Due to this fact normalization by the different β -galactosidase levels would result in skewed results and we thus decided to forgo this form of transfection control. Instead we transfected large populations of cells, pooled them and replated them for each reporter promoter assay and then normalized by protein concentration to correct for differences in plating (we have done so for all experimental techniques). This ensures uniform transfection efficiency within experiments. We have confirmed that changes in GR concentration do not result in non-specific squelching of transcription through induction of the NF κ B driven promoter reporter (Fig.6.3A,B) and monitoring of the expression of the endogenous GAPDH gene (Fig.6.17) are low, medium and high GR concentrations.

In order to monitor GR levels between experiments we ran lysates from each transfection condition of each promoter reporter assay on Western blots. Experiments that displayed aberrant transfection rates of GR (GR levels which fell outside of their respective population concentration) were excluded (Fig.6.1A,C). Pixels from digitized Western blots was used to compare the expression levels of transiently transfected GR to levels determined in saturation binding assays (fmol GR per mg protein) and revealed a good correlation ($R^2 = 0.97$) between the two methods of determining GR concentration (Fig.6.1B). Although saturation binding was not carried out on the 385ng GRdim transfection level we have used pixel intensity from Western blots and the GR correlation curve (Fig.6.1B) to derive its concentration in fmol GR per mg protein (Fig.6.1C). We estimate the GR concentration at this transfection condition to be 65.5 fmol GR per mg protein, which shows no

statistical difference to the low concentration of GRwt (67.0 fmol GR per mg protein). We have therefore compared these two populations directly and term them both low GR concentrations (Fig.6.1C). This method of quantifying GR concentration is in accordance with a comparative study by O'Donnell (50), which compares Western blots and radioactive ligand binding as means of GR quantification. Western blots have been run on the lysates from all promoter reporter assays as well as from the RT-PCR assay in order to monitor GR concentration levels between experiments.

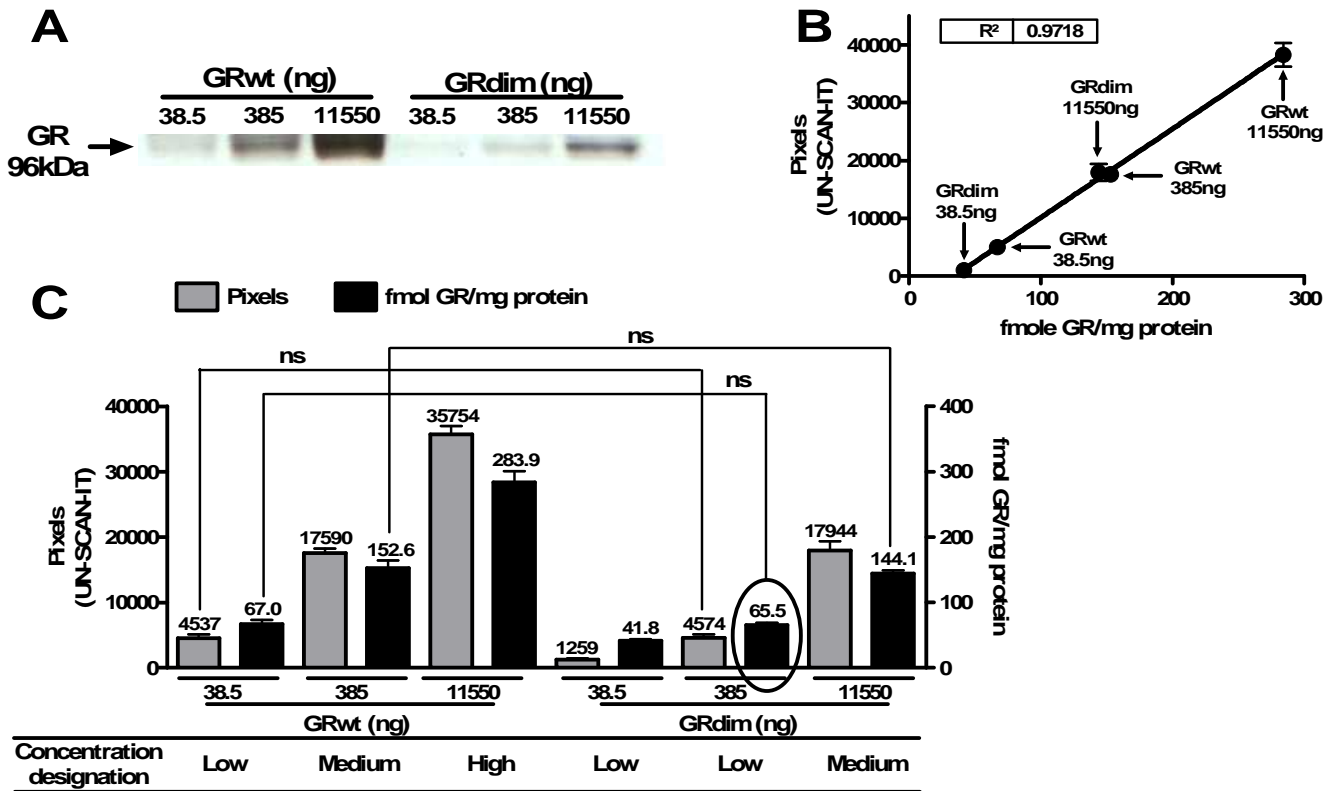


Figure 6.1. **The use of Western blots to monitor and determine GR levels.** Cells were DEAE-Dextran transfected with GRwt (38.5ng, 385ng or 11550ng) or GRdim (38.5ng, 385ng or 11550ng). Replated 24 hours later into 24 well plates (4×10^5 cells/plate) in stripped DMEM. **(A)** Representative Western blotting, carried out 24h after replating on all transfections. 20 μ g of protein was loaded and separated on a 10% SDS-PAGE gel. Following electrophoresis, proteins were electroblotted and transferred to Hybond-ECL nitrocellulose membrane (Amersham Biosciences), which were probed for GR with H-300 anti-GR (Santa Cruz Biotechnology) diluted 1:3000 in 5% (w/v) casein in TBST buffer followed by ECL peroxidase-labeled anti-rabbit anti-body (AEC-Amersham Biosciences) diluted 1:10000 in 5% (w/v) casein in TBST buffer. Blots were visualized with ECL Western blotting detection reagents (GE Healthcare) on Hyperfilm (Amersham Biosciences). Densitometric analysis of the immunoblots was carried out using UN-SCAN-IT gel 6.1 software (Silk Scientific). **(B)** Correlation between GR concentrations in fmol GR per mg protein derived from saturation binding carried out 48h after transfection on the 38,5ng, 385ng and 11550ng GRwt as well as 38.5ng and 11550ng GRdim transient transfections and their respective densitometric values from Westerns. Using this curve the GR concentration of the 385ng GRdim population was estimated to be 65.5fmol GR/mg protein. **(C)** Comparison between transfected GR plasmid and GR concentration (right axis) or pixels (left axis). The derived 385ng GRdim concentration is indicated with a circle. Statistical analysis was through one tailed unpaired t tests. All results represent a minimum of two independent experiments performed in triplicate (\pm SEM).

6.2 Transrepression of a NF κ B containing promoter construct is influenced by cooperative ligand binding to the GR

To investigate the effects of GR concentration and cooperative ligand binding on transrepression we chose a reporter promoter which contains three copies of the NF κ B transcription factor binding site from the IL-6 cytokine gene promoter. The promoter of this potent pro-inflammatory cytokine contains the binding sequence for NF κ B (5'-GGGATTTTCC-3') and is activated by direct binding of the NF κ B protein (32). A constant concentration of the p(IL6 $\kappa\beta$)₃50h.IL6P-luc promoter reporter was transfected along with either the GRdim or GRwt expressing plasmid at levels that produce either low or medium GR concentrations. The low GR concentration reflects the level of GRwt at which ligand binding is non-cooperative, while the medium GRwt concentration is the receptor level at which the GRwt starts to display positive cooperative ligand binding (Fig3.8B). Ligand binding to the GRdim remains non-cooperative at both GR concentrations. We have stimulated the activation of NF κ B with phorbol 12-myristate 13-acetate (PMA), which leads to the downstream release of the inhibitory protein κ B (I κ B) from NF κ B (51), which then binds to the p(IL6 $\kappa\beta$)₃50h.IL6P-luc promoter leading to the transcription of luciferase protein (Fig.6.2A).

The ability of activated GR to repress NF κ B transcription has been shown to be dependent on a direct interaction between the two transcription factors and is independent of GR binding to DNA (3, 5). The repression of NF κ B driven interleukin-8 (IL-8) expression by the GR was shown to be ligand dependent due to differential recruitment of co-factors to the GR following ligand binding. This in turn influences the ability of GR to bind to the p65 subunit of NF κ B, the primary mechanism through which GR represses NF κ B (45, 52). Induction of GR with either DEX or CpdA results in interaction between the activated GR and the p65 subunit of NF κ B resulting in repression of luciferase transcription (Fig.6.2B). Reichardt *et al.* (23, 24) have demonstrated that transrepression of an NF κ B responsive gene occurs equally well through the GRwt as through the GRdim, suggesting that binding to the p65 subunit is possible by both the GR monomer as well as the GR dimer.

Stimulation with PMA results in maximal luciferase transcription that is not significantly different at any receptor concentration of either the GRwt or GRdim constructs (Fig.6.3A,B). These results are similar to results seen by Zhao *et al.* (40). In other words there is no ligand independent influence of GR concentration on the level of NF κ B driven transcription at levels of GR, which have been shown to result in non-cooperative as well as positive cooperative ligand binding (Chapter 3).

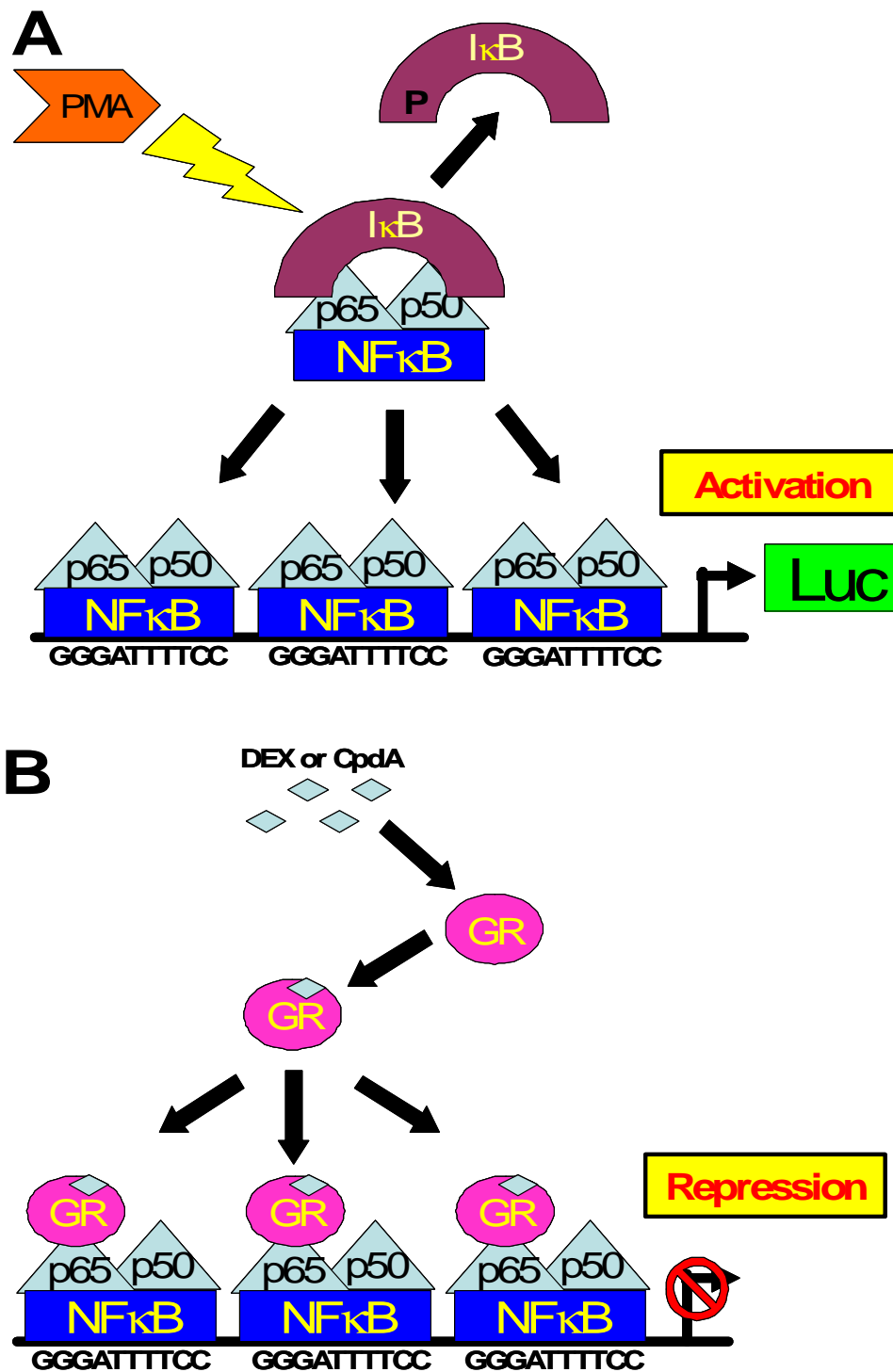


Figure 6.2. **Repression by the activated GR of the transcription of an NFκB driven promoter reporter.** (A) PMA stimulation results in the down stream phosphorylation of inhibitory protein-κB (IκB) and its subsequent degradation. This frees the NFκB heterodimer which consists of p50 and p65 proteins. NFκB then migrates to the nucleus where it binds to the three NFκB binding elements of the p(IL6κβ)₃50hu.IL6P-luc promoter reporter stimulating the transcription of luciferase. (B) Activation of the GR by either DEX or CpdA results in its migration into the nucleus where it binds directly to the p65 subunit of NFκB, repressing expression.

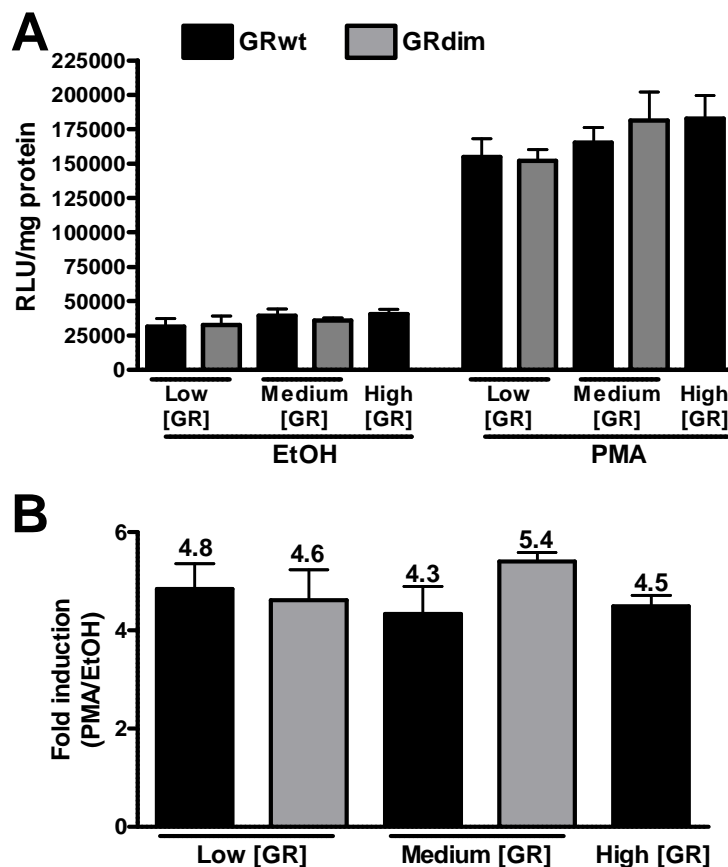


Figure 6.3. PMA induction is unaffected by variation in receptor concentration. Cells expressing low, medium or high concentrations of GRwt or low or medium concentrations of GRdim and the promoter reporter p(IL6κβ)₃50hu.IL6P-luc were induced with PMA or EtOH as described for transrepression in *materials and methods*. **(A)** Induction and **(B)** maximal fold induction representing maximal induction by PMA normalized to EtOH induction for each transfection condition was plotted. Statistical analysis was carried out using ANOVA followed by Newman-Keuls post test within the EtOH and PMA stimulated as well as maximal fold induction populations. Results represent four independent experiments performed in triplicate (±SEM).

We have chosen to compare the ability of the potent GR agonist, DEX, and the dissociative GC, CpdA, in our transrepression assay as DEX stimulation has been shown to result in GR dimerization while CpdA impairs it (Chapter 4). This strategy, together with the use of varying GR concentrations of GRwt and GRdim, should allow for elucidation of the role of GR dimerization and cooperative ligand binding in transrepression. The maximal induction achieved through PMA stimulation alone (Fig.6.3) is repressed by GR activated by either DEX or CpdA (Fig.6.2B, Fig.6.4A). In order to better interpret our data we firstly converted the relative light units (RLU) of luciferase normalized to protein concentration (Fig.6.4A) to percentage induction, where we set the top plateau (PMA and EtOH induction) as 100 percent induction (Fig.6.4B). Finally, we subtracted the percentage induction values from 100 percent to generate percentage repression data (Fig.6.4C), which we fit to sigmoidal dose-response curves in order to generate maximal percentage repression (efficacy) and the log EC₅₀ (potency) of transrepression.

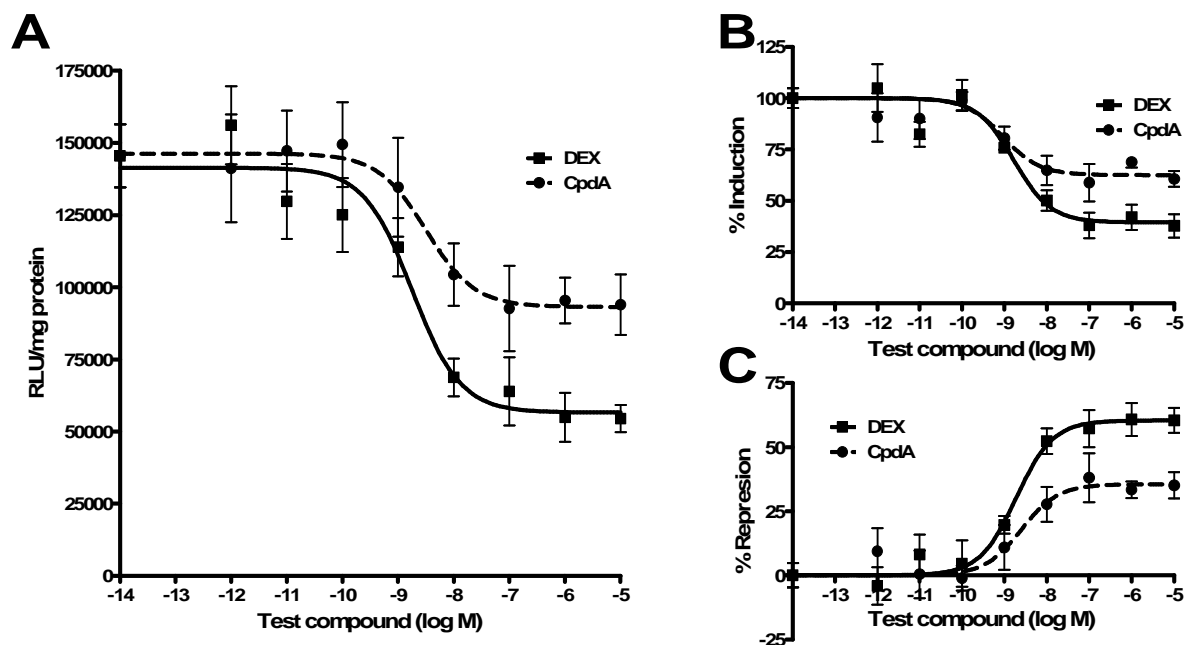


Figure 6.4. **Percentage repression is derived from induction results.** The transrepression promoter reporter assay using p(IL6 $\kappa\beta$)₃50hu.IL6P-luc was carried out as described in *materials and methods* in COS-1 cells expressing the medium concentration of GRwt. (A) Luciferase activity was determined and normalized against protein concentrations. (B) RLU/mg protein values are expressed as a percentage of the maximal response (PMA and EtOH = 100%) and finally subtracted from 100% producing percentage repression (C). Sigmoidal dose-response curves were fit to the percentage repression data to generate potency (log EC₅₀) and maximal repression results. Results represent four independent experiments performed in triplicate (\pm SEM).

6.2.1 Potency of transrepression

The potency (log EC₅₀) of repression through DEX induced GRwt was significantly reduced by an increase in GR concentration (Fig.6.5A). A trend is visible, where increasing GRwt concentrations result in decreasing levels of potency culminating in a significant difference between the EC₅₀ at the low GRwt concentration (1nM) and the high GRwt concentration (5nM). The potency of DEX induced transrepression through GRdim is not significantly different between the low and medium concentrations (Fig.6.5A). The medium concentration of GRdim displays statistically greater potency as reflected by an EC₅₀ of 0.40nM compared with an EC₅₀ of 2.0nM at the medium concentration of GRwt. The fact that GRdim displays a similar transrepression potency as compared to GRwt at the low GR concentration, where both receptors show non-cooperative ligand binding, while at medium GR concentrations, where GRwt shows cooperative ligand binding, we see a significant difference in potency suggests that cooperative ligand binding influences the potency of transrepression. We thus demonstrate that a shift to cooperative ligand binding may result in a decrease in the potency of transrepression. We hypothesize that the high affinity GR dimer, which predominates at the medium and high GRwt concentrations, binds ligand preferentially resulting in fewer activated GR monomers at

subsaturating ligand concentrations. The greater potency reflected by the GRdim suggests that repression of NF κ B favours the activated GR monomer, which would explain why cooperative ligand binding results in a decrease in transrepression potency. The potency of CpdA induced transrepression within each concentration of GR and between the two constructs is statistically not significantly different (Fig.6.5A). This is most likely due to the fact that CpdA is known to abrogate GR dimerization (Chapter 4) creating an essentially monomeric population of activated GR through either the GRdim or the GRwt.

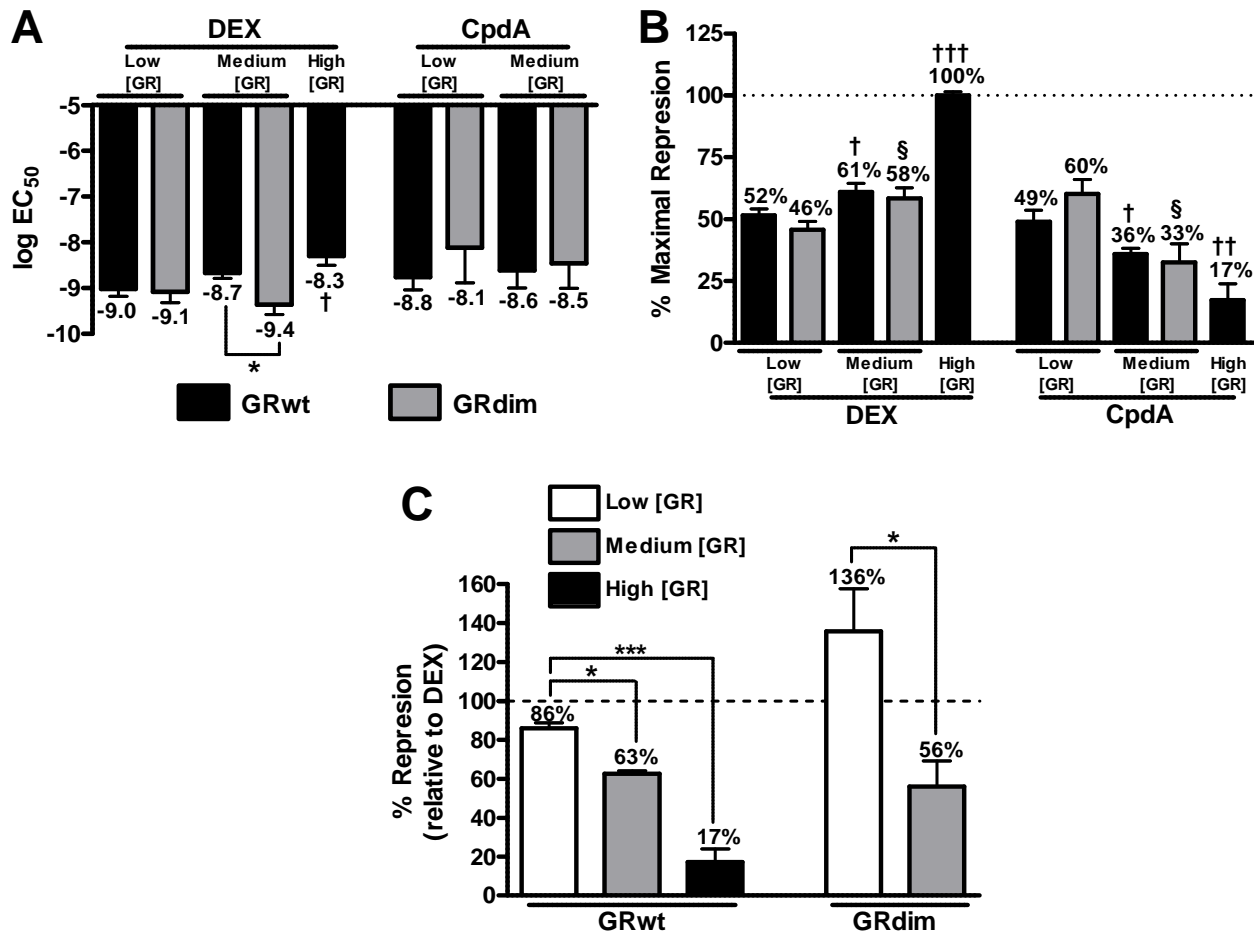


Figure 6.5. DEX displays reduced potency of transrepression through the GRwt and greater efficacy (maximal repression) as GR levels increase, while CpdA's ability to repress transcription decreases as GR levels increase. Cells were transiently transfected with low, medium or high GRwt or low or medium GRdim and 12000ng p(IL6 κ)₃50hIL6 β -luc and transrepression was carried out as described in *materials and methods*. Statistical analysis of (A) log EC₅₀ and (B) percentage repression was through two tailed unpaired t tests of GRwt against GRdim (*P<0.05), low GRwt against medium GRwt or high GRwt concentration ([†]P<0.05, ^{††}P<0.01, ^{†††}P<0.001) and low GRdim against medium GRdim concentration ([§]P<0.05). (C) Percentage repression by CpdA representing maximal repression relative to that of DEX repression (set to 100 percent and indicated with a dotted line) within the same GR concentration and type. Statistical analysis for GRwt was with ANOVA followed by Dunnett's post test against the low GRwt concentration (*P<0.05, ***P<0.001) while a two tailed unpaired t test of low GRdim against medium GRdim was carried out (*P<0.05). Results represent four independent experiments performed in triplicate (\pm SEM).

Contrary to our results, it has been reported that increasing the levels of GRwt transfected into COS-7 cells has led to an increase in potency, reflected in a decrease in the EC_{50} of DEX induced NF κ B repression from 2.2nM at low GR concentrations to 0.1nM at high GR concentrations (40). However, it was not made clear whether this was a statistically significant observation. While our EC_{50} values for DEX fall within a similar range namely, 1nM at the low GRwt concentration and 5nM at the high GRwt concentration, we do not see the same 22-fold increase in potency as GR concentrations increase. Instead we demonstrate a 5-fold decrease in potency as GRwt concentration increases from a level at which non-cooperative ligand binding occurs to a level where positive cooperative ligand binding occurs. We can also not be sure whether the results of Zhoa *et al.* (40) reflect similar GR concentrations to those tested by us and if ligand independent dimerization of the GR occurred at their increased GR concentration. It may be that their levels of GR are not sufficiently high enough to result in positive cooperative ligand binding to ligand independent GR dimers and that the increase in GR concentration in their system simply results in a greater population of GR monomers and therefore a larger pool of activated GR once DEX stimulation has occurred. In addition, the promoter reporter construct they used differs from ours in terms of the copies of the NF κ B-site (Zhoa *et al.* 5 copies versus our construct with 3 copies). It is possible that promoter architecture modulates responses to GR concentration.

6.2.2 Efficacy of transrepression

We saw no significant difference between GRwt and GRdim at the same concentrations of receptor when comparing the efficacy for transrepression elicited by DEX or CpdA (Fig.6.5B). Positive cooperative ligand binding occurs at the medium concentration of GRwt, but not at the medium concentration of GRdim. Thus the fact that these two conditions elicit the the same efficacy implies that positive cooperative ligand binding has no influence on the efficacy of transrepression at the saturating concentrations of ligand required to elicit maximal repression. There is, however, a significant increase in maximal repression via DEX as GR concentrations increase, which reflects the basic premise that an increase in transcription factor concentration will result in an increase in response (Fig.6.5B) and has been shown in previous studies with the GRwt (39, 40). The high GRwt concentration shows a significantly elevated efficacy despite displaying the weakest potency of the DEX induced population (Fig.6.5B). This may seem counter intuitive, however, it is important to note that the concentration of ligand required to elicit maximal efficacy (1 μ M) (Fig.6.4) is 200-fold higher than the potency (5nM) at the high GRwt concentration. Where as a subsaturating concentration of ligand will bind almost exclusively to the dimerized GRwt due to its high affinity, at the saturating ligand concentration there will be sufficient ligand available to activate GR monomers as well.

The similar levels of DEX efficacy demonstrated by the two GR constructs at the low and medium GR concentration (Fig.6.5B) do suggest that repression can occur through the GR dimer. This is supported by previous work by Reichardt *et al.* (23, 24) in mouse tissue expressing GRdim, where dimerization impaired GR was shown to be as capable of repressing transcription as the wild type receptor. In addition, a GRdim was shown to repress an AP-1 driven promoter reporter with the same efficacy as the GRwt (21) following DEX stimulation.

6.2.3 Biocharacter shift of CpdA

Having explored the capacity of DEX to induce transrepression we moved onto the efficacy of CpdA induced transrepression of our promoter reporter. Previous studies have shown mixed results for CpdA repression. De Bosscher *et al.* (26) demonstrated dose dependent CpdA repression on the same promoter reporter construct as the one we used, while Yemelyanov *et al.* (28) also displayed CpdA induced repression of a promoter reporter containing 3 NFkB elements. Contrary to these findings Avenant *et al.* (47) demonstrated no transrepression by CpdA of a promoter reporter containing 5 NFkB elements.

Our own findings demonstrate that, contrary to the behaviour of DEX, CpdA displays a significant decrease in efficacy as GR concentration increases (Fig.6.5B). When expressed relative to DEX repression at each GR type and concentration, where DEX efficacy is set at 100 percent, CpdA efficacy falls from 86 percent of that of DEX at the low GRwt level to only 17 percent of that of DEX at the high GRwt concentration. GRdim displays a similar trend (Fig.6.5C). Unlike previous work on RU486 and MPA, which displayed a biocharacter shift from weak or partial agonist to full agonist behaviour relative to DEX as GR concentration increased in a PMA induced NFkB promoter reporter assay (40), our results indicate that CpdA demonstrates a shift from full agonist to weak agonist behaviour as receptor levels increase (Fig.6.5C).

Although CpdA has been shown to abrogate ligand independent dimerization of the GR (30, 31), its capacity to bind to the medium and high concentrations of GRwt, which display positive cooperative ligand binding, is drawn into question by competitive binding assays in the current study (Fig.6.6). We demonstrated that the ability of CpdA to displace [³H]-DEX decreased as GR concentration increased, dropping from a high of 97 percent displacement at the low GR concentration (Fig.6.6A) to 15 percent displacement at the high GR concentration (Fig.6.6C). Previous results demonstrated a similar trend in cell lines expressing disparate levels of GR. For example, in the L929sA cell line, which expresses GR at a low level, De Bosscher *et al.* (26) demonstrate 81 percent [³H]-DEX displacement, while results shown in Addendum B (30, 31) using BWTG3 cells that have high GR expression levels, show only a

47 percent displacement of [³H]-DEX. Clearly GR concentration influences the ability of CpdA to bind to the GR and thus impairs its ability to cause repression at GR concentrations which display positive cooperative ligand binding (Fig.6.5C, Fig.3.8B). Furthermore, the competitive whole cell binding results in the L929sA cell line (26) demonstrated an IC₅₀ of CpdA which was 4-fold lower than that of DEX, indicating greater affinity than DEX for the GR in this cell line, while in the BWTG3 cells (30, 31) CpdA displayed a K_d which was 63-fold higher than for DEX. This shift from a higher affinity for CpdA than DEX at low GR concentrations in the L929sA cell line to a lower affinity than DEX in the BWTG3 cells with a higher GR concentration is not displayed by our results where CpdA maintains a greater affinity than DEX at all three GR concentrations. What is, however, tantalizing is the fact that the IC₅₀ of CpdA rises from 13.6nM at the low GRwt concentration to 32.1nM at the medium GRwt concentration, peaking at 57.4nM at the high GRwt concentration (Fig.6.6), which indicates a decrease in CpdA's binding affinity to the GR as GR concentrations increase.

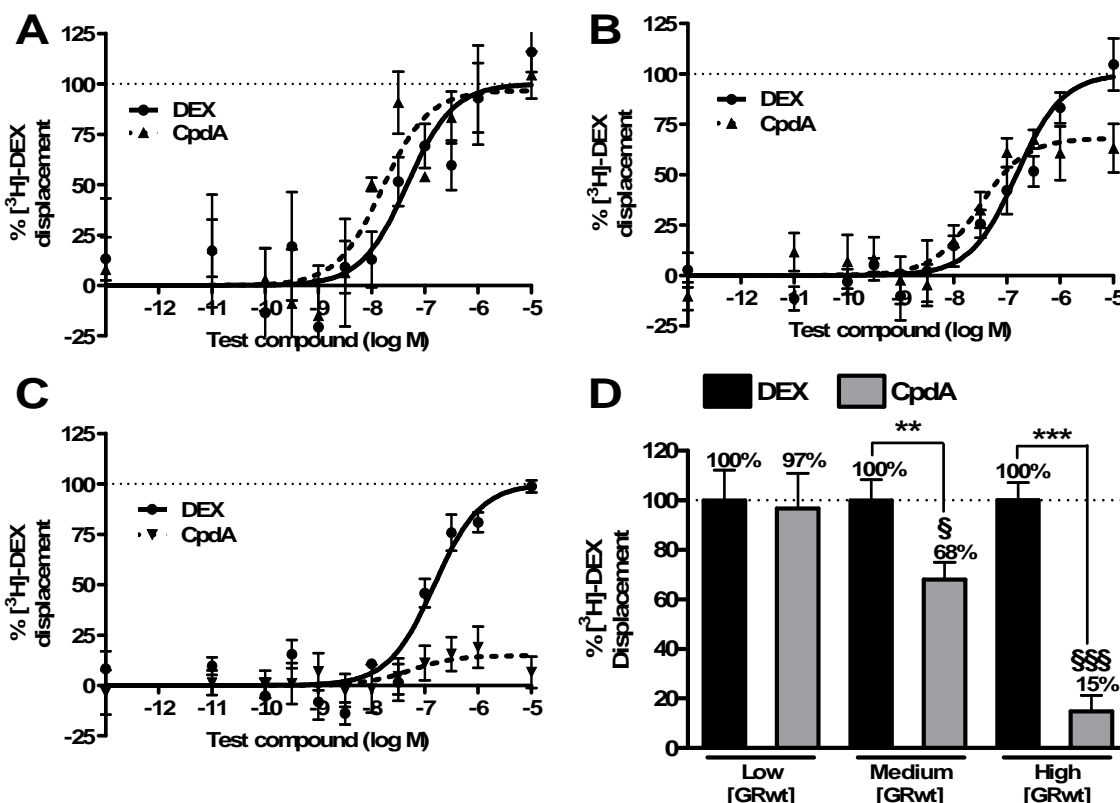


Figure 6.6. As GR levels rise CpdA displaces less [³H]-DEX from the GRwt. Cells were transfected with (A) low GRwt, (B) medium GRwt or (C) high GRwt and competitive whole cell binding was carried out as described in *materials and methods*. Total binding was normalized to protein concentration and expressed as percentage displacement (bottom plateau for maximal labelled DEX displacement designated as 100% displacement and top plateau where no displacement took place as 0% displacement). Sigmoidal dose-response curves were fit to this data which generated maximal percentage displacement results. (D) Maximal percentage [³H]-DEX displacement by DEX or CpdA at low, medium and high GR concentrations. Statistical analysis was through two tailed unpaired t tests of DEX or CpA stimulated low [GR] against medium [GR] or high [GR] (§P<0.05, §§§P<0.001) and DEX against CpdA stimulation (**P<0.01, ***P<0.001). All results represent two independent experiments performed in triplicate (±SEM)

We suggest that ligand independent dimerization of the GR at high receptor concentrations leads to a conformational change in the ligand binding pockets of the dimerized GR, which increases the affinity of the GR for DEX (reflected by both a decreased DEX binding K_d and positive cooperative DEX binding (Fig.3.8B)), which would make it harder for the CpdA to displace DEX from the receptor at high GR concentrations. In addition, as CpdA has a vastly different and non-steroidal chemical structure from that of the steroidal potent synthetic agonist, DEX (Fig.1.1), it is quite possible that ligand independent dimerization of the GR, which has been shown to result in positive cooperative DEX binding, may result in a reduction in CpdA's binding affinity. This is supported by the fact that the DEX independent effects of GR concentration on CpdA's repression efficacy indicate that CpdA has a lowered capacity to interact with GR at concentrations, which display ligand independent dimerization (Fig.6.5C).

However, the fact that we have shown CpdA's ability to abrogate ligand independent dimerization at the medium and high GR concentrations to levels seen at the low GR concentration (Fig.4.3B) is a difficult point to resolve and one which requires greater attention. Future competitive binding studies of CpdA's ability to displace [3 H]-DEX at the low and medium concentration of GRdim may help us to unravel this conundrum. The discovery that CpdA has a greatly reduced capacity to induce repression at high GR concentrations may explain why Avenant *et al.* (47), who performed their transrepression assays in transiently transfected COS-1 cells expressing a high GR level, saw no activity through CpdA.

6.3 Transactivation of GRE containing promoter reporters is influenced by ligand independent dimerization as well as the dimerization status of the GR

We chose to investigate the activation of a multiple GRE containing promoter reporter, namely pTAT-GRE2-Elb-luc (Fig.6.7) as this form of promoter represents the majority of direct GR DNA interactions (53) and provides a robust transactivation response. The promoter of this construct consists of two copies of the GRE from the tyrosine amino transferase gene (TAT) as well as the TATA box from the E1b promoter, which serves as a generic docking site for secondary transcription factors (54, 55).

Similarly to the transrepression assay we transfected a constant amount of promoter reporter plasmid while varying the levels of GRwt or GRdim plasmid in order to achieve GR concentrations that match those defined in our saturation binding assays (Fig.3.6B). The medium and high GRwt concentrations have been shown to display positive cooperative ligand binding (Fig.3.8B) as a result of ligand independent dimerization of the GR at these concentrations (Chapter 4). The low GRwt concentration and both low and medium GRdim concentrations display non-cooperative ligand binding (Fig.3.8B)

and greatly reduced ligand independent dimerization (Chapter 4). It is important to note that the low GRwt and low GRdim receptor levels as well as the medium GRwt and medium GRdim receptor concentrations have been demonstrated to be statistically the same through whole cell binding and through Western blotting, respectively (Fig.6.1).

Representative dose response curves of transactivation illustrates the large differences in maximal response (efficacy) and log EC₅₀ (potency) brought about by changes in GRwt and GRdim concentration (Fig.6.8). We will discuss these differences, as well as biocharacter shifts of a range of test compounds compared to the potent synthetic agonist DEX.

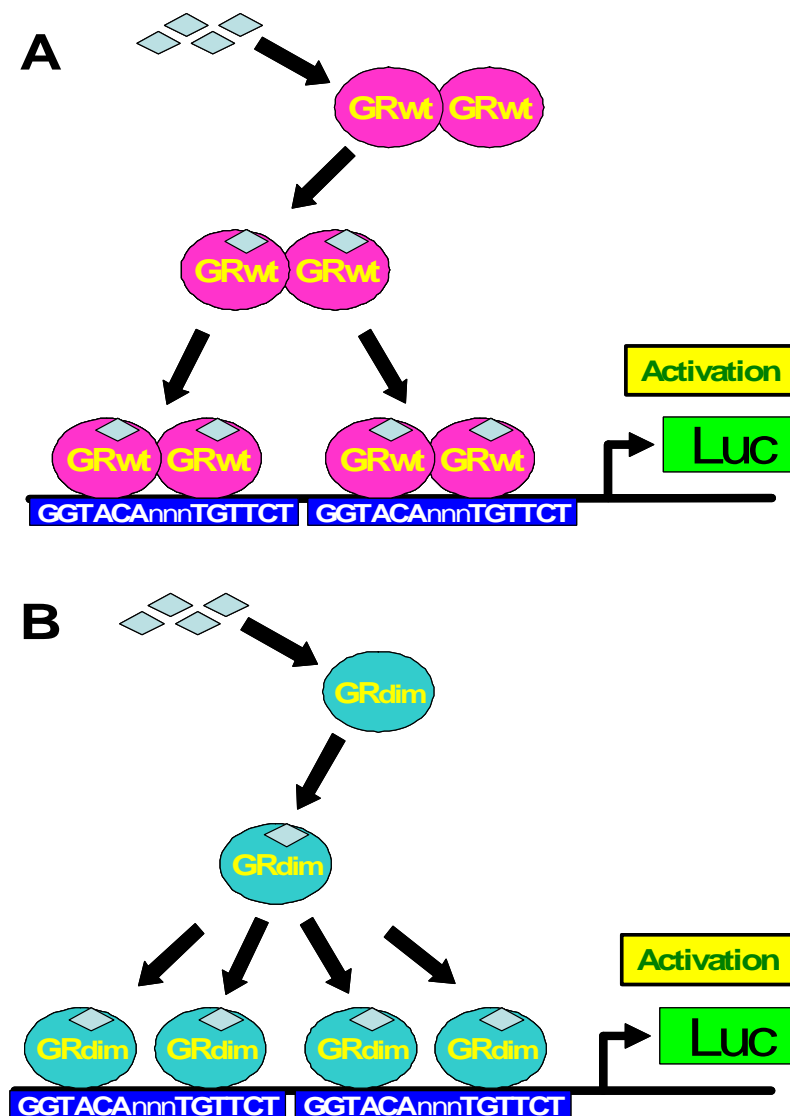


Figure 6.7. **Activation by the GR of the multiple GRE driven pTAT-GRE2-Elb-luc promoter reporter.** (A) Ligand binding to the GRwt results in association of the activated dimer to each of the two GRE's stimulating the transcription of luciferase. (B) Ligand binding to the GRdim results in its association as a monomer to each of the two GRE half-sites within the two GREs stimulating the expression of luciferase.

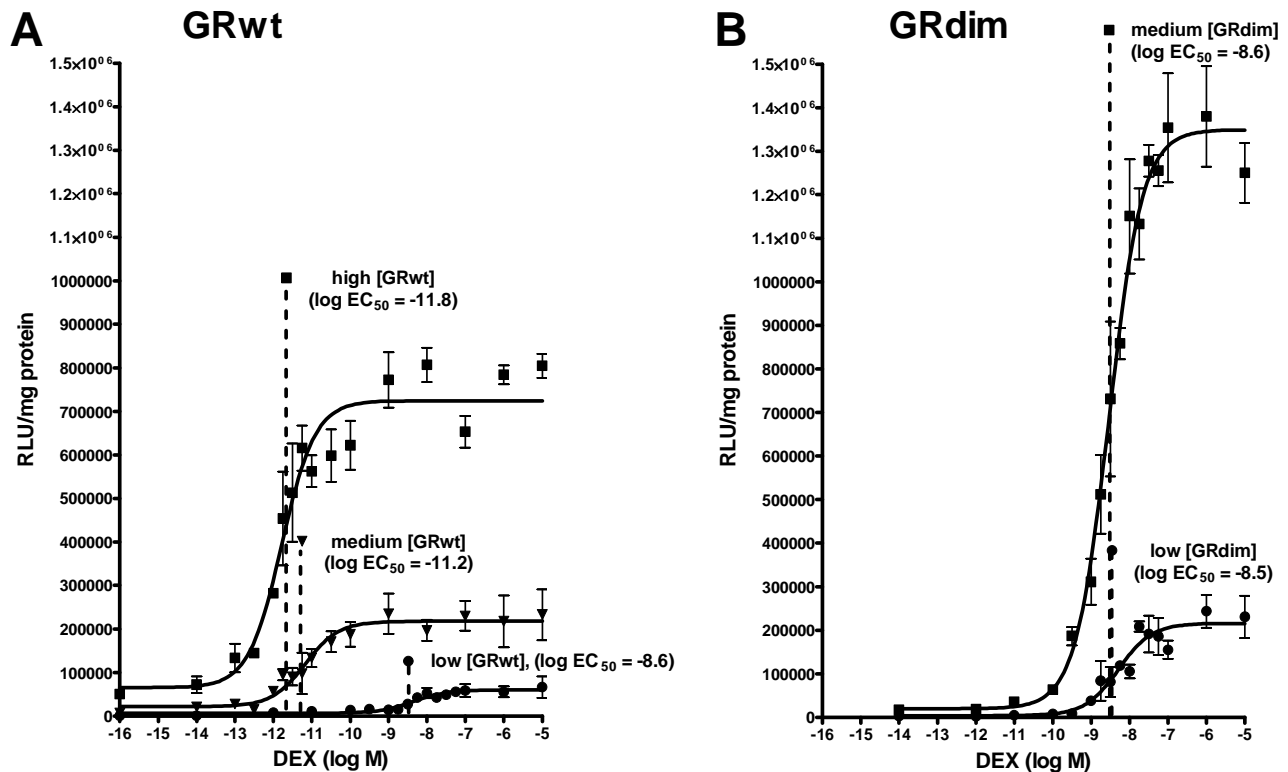


Figure 6.8. **GR levels and the ability to dimerize influence potency (log EC₅₀) and efficacy (maximal induction) in transactivation assays.** Representative dose response curves of transactivation, which represent a single experiment performed in triplicate (\pm SEM). Cells were DEAE Dextran transfected with (A) low, medium or high GRwt or (B) low or medium GRdim and 3000ng pTAT-GRE2-Elb-luc and the transactivation assay using DEX as test compound was carried out as described in *materials and methods*. Average potency (log EC₅₀) for each condition from a minimum of three independent experiments performed in triplicate is indicated with the dotted lines

6.3.1 Potency of transactivation

The characteristic of transactivation we will analyse first is potency, namely the concentration of ligand required to elicit 50 percent of the maximal response. Results in the literature suggest an influence of GR concentration on potency. For example, Szapary *et al.* (44) demonstrated a shift for 1nM DEX induced promoter reporter activation from 41.6 percent to 77.7 percent of 1 μ M DEX activation as GR concentration increased. This implies greater sensitivity to ligand as the receptor level increases. In more thorough examinations by the Simons group where dose response curves were generated, a clear increase in DEX potency was demonstrated as a left shift in the dose response curves as GR concentration increased (43, 56). All of these studies were conducted with a promoter reporter which contained 2 GREs. Unfortunately, none have defined the actual GR concentration studied or specified EC₅₀ values, nor have they made an explicit connection to cooperative ligand binding and ligand independent dimerization of the GR.

Representative dose response curves from our DEX induced promoter reporter assays demonstrate a clear left shift as GRwt concentration increases (Fig.6.8A). The same can not be said for GRdim, which displays basically the same log EC₅₀ value at both low and medium GRdim concentrations (Fig.6.8B). When these potency values were statistically compared a clear trend emerges, namely significantly increased potency at GRwt concentrations which were shown to display positive cooperative ligand binding, namely the medium and high GRwt concentrations (Fig.6.9A). Despite having the same receptor concentration as the medium GRwt, the medium GRdim concentration has the same potency as the low levels of GRwt and GRdim. In addition, GRdim in contrast to GRwt, shows no significant change in potency as its concentration increases from low to medium levels (Fig.6.9A). These GR populations (low GRwt concentration, low GRdim concentration and medium GRdim concentration) have all been shown to display non-cooperative ligand binding (Fig.3.8B) in whole cell saturation binding. Thus, there is a direct correlation between increased potency in transactivation and positive cooperative ligand binding, both of which occur at the medium and high GRwt concentrations only.

The potency values expressed in log EC₅₀ units represent vastly different levels of sensitivity to DEX stimulation as the EC₅₀ values of DEX induced GRwt drop from 2.5nM at the low, to 0.006nM at the medium and to 0.002nM at the high GRwt concentration. This equates to a 417 and 1250-fold increase in potency at the medium and high GRwt concentrations, respectively. The physiological relevance of this massive increase in potency at GR concentrations which display positive cooperative ligand binding is that in tissues with high enough GR concentrations genes with GRE containing promoters will be maximally activated by even low concentrations of GC. Even the lowest levels of endogenous or pharmacologically administered GC will be enough to induce maximal induction in tissues with high enough GR concentrations. To illustrate, exposure to 1 mg of DEX, a common pharmacological dosage, results in plasma DEX levels ranging from 1 to 10nmol per litre 24 hours later (57). Where as a concentration of 1nM DEX would result in roughly 10 percent of maximal induction in cells expressing low levels of GR, cells expressing GR levels above the medium GR concentration of 763 fmol GR per mg protein (Fig.3.6B) would display maximal levels of transactivation. When DEX levels drop further to 0.1nM, cells expressing low levels of GR would essentially not respond at all, while those expressing GR levels at which positive cooperative ligand binding occurs would still respond at their maximal level. Even at a concentration of 0.006nM DEX, 167-fold lower than the 1nM shown at physiological concentrations, cells expressing the medium GR level would respond with 50 percent of their maximal efficacy, while tissue with GR levels displaying non-cooperative ligand binding would show no transactivation at all. Cells with GR concentrations high enough to result in positive cooperative ligand binding would therefore be hypersensitive to DEX and would exist in a state of maximal transactivative response once exposed to DEX were it not for ligand

induced down regulation of the GR. It is important to stress that the medium to high GRwt concentrations reflect a GR concentration range of 763 to 1420 fmol GR/mg protein or 298000 to 555000 GR/cell. Although some tissues do express GR at these elevated levels, as demonstrated in Tables 1.1 and 1.2, the majority of healthy cells within the human body will retain the capacity to respond to changes in GC concentration due to their relatively low GR levels.

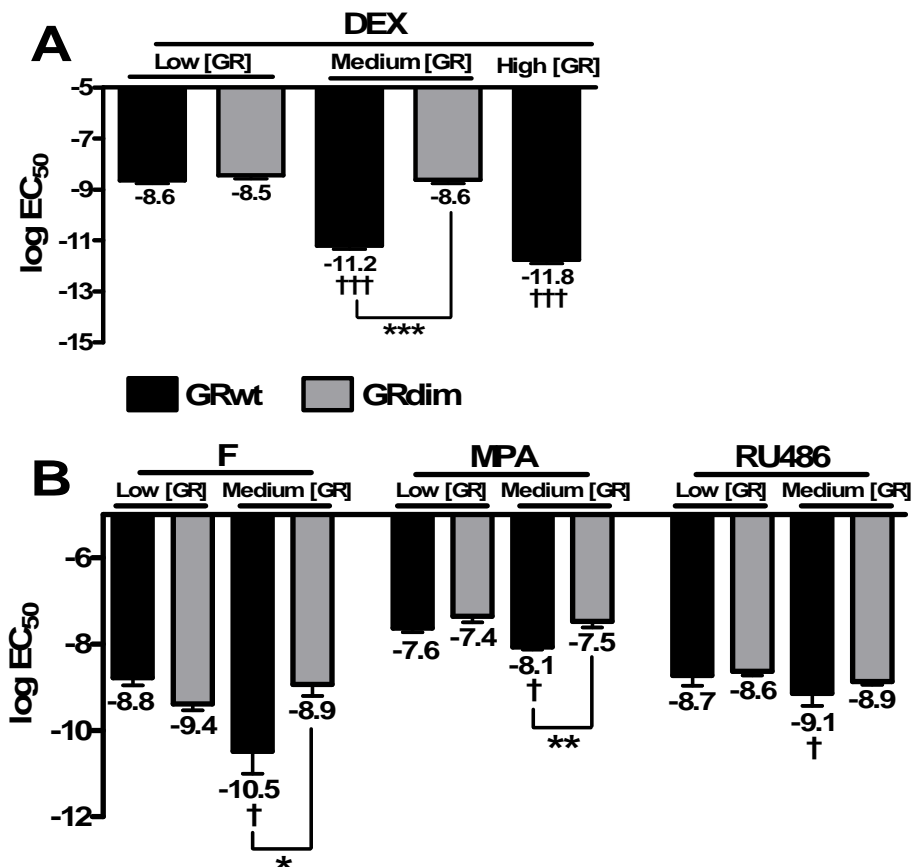


Figure 6.9. **Potency (log EC₅₀) increases due to positive cooperative ligand binding.** Transactivation assays using low, medium or high GRwt and low or medium GRdim concentrations were performed as described in *materials and methods*. Sigmoidal dose-response curves were fit to the experimental data which generated log EC₅₀ values for (A) DEX as well as for (B) F, MPA and RU486. Statistical analysis was through two tailed unpaired t test of low GRwt concentration against medium GRwt or high GRwt concentrations (†P<0.05, ††P<0.001), low GRdim concentration against medium GRdim concentration or GRwt against GRdim at the same GR concentration (*P<0.05, **P<0.01, ***P<0.001). All results represent a minimum of three independent experiments performed in triplicate (±SEM).

The t_{1/2} of unstimulated GR following incubation with cycloheximide has been shown to be 44 hours, while the t_{1/2} of GR drops to 10 hours following stimulation with 10⁻⁵M DEX and cycloheximide (47). Thus down regulation of the GR would eventually result in GR levels low enough to no longer result in positive cooperative ligand binding, although this would probably take longer than the t_{1/2} quoted in a system that was not exposed to cycloheximide. A decrease in GR concentration would blunt the hypersensitivity of cells expressing GR concentrations, which result in positive cooperative ligand

binding, however, our results clearly indicate that this blunting of response has not occurred following 24 hours of DEX exposure. Furthermore, it has been demonstrated in binding assays conducted on human tissue biopsies that elevated GR levels are maintained despite exposure to physiologically basal GC levels (58, 59).

Although their potency shifts are less extreme, we see the same trend emerging for F, MPA and RU486 as for DEX (Fig.6.9B). A significant increase in potency occurs at the medium GRwt concentration, which has been shown to display positive cooperative ligand binding (Fig.3.8B). The fold-increase in potency from low to medium GRwt concentrations for these ligands is 53, 3.2 and 2.5-fold for F, MPA and RU486, respectively, which is less than that seen with DEX. The concentration of free F in the blood varies from ~18.7nM in the morning to ~3.3nM at night (60), which would mean that the increased EC_{50} value from 1.6nM at low GRwt concentrations to 0.03nM at medium GRwt concentrations for F would entail a shift from a varying circadian influence of endogenous F on cells expressing GR at the low concentration to a maximal response in cells expressing the medium GR concentration. The lower increase in EC_{50} seen with MPA and RU486 as a result of increased GR concentration suggests that positive cooperative ligand binding and the potency increase it elicits may be ligand specific. The potent synthetic agonist, DEX, and the potent endogenous agonist, F, respond more strongly (417-fold increase for DEX and 53-fold increase for F) to the increase in ligand independent dimerization at the medium GR level than the partial agonists, MPA and RU486 (3.2-fold increase for MPA and 2.5-fold increase for RU486). To clarify this issue it would be of great interest to test whether these test compounds also bind to the medium and high GR concentrations in a positive cooperative fashion.

Transactivation assays performed using the same promoter reporter but at the medium and high GFP-GR concentrations revealed similar results to those seen for the GRwt (Fig.6.10). Although the high GFP-GR concentration displays similar potency to high GRwt, medium GFP-GR displays consistently higher potency than low GRwt. The discrepancy between low GRwt and medium GFP-GR potencies may reflect effects due to GR concentration that are unrelated to cooperative ligand binding as the concentrations of these two GR species are significantly different (Fig.3.6) while their Hill slopes both indicate non-cooperative ligand binding (Fig.3.8). In contrast for the high GRwt and high GFP-GR levels both GR concentrations and Hill slopes are comparable. There was a significant increase in potency for DEX, F and RU486 at the high GFP-GR concentration, which displays positive cooperative ligand binding for DEX (Fig.3.8B). Although MPA and Prog did not show a significant change in potency they displayed the same trend as the other test compounds. Prog and RU486 display potency's similar to that of the potent agonist, DEX, at the high GFP-GR concentration which may suggest a difference in the behaviour of the GFP-tagged receptor compared to that of the wild type as

with GRwt this was not observed (Fig.6.9A,B). The increase in potency as we shift from medium to high GFP-GR concentration is 32-fold for DEX, 40-fold for F, 53-fold for MPA, 160-fold for Prog and 75-fold for RU486. The increase in potency we saw between low and medium GRwt concentrations was 397-fold for DEX, 53-fold for F, 3.2-fold for MPA and 2.5-fold for RU486. Thus there is considerable difference in the fold potency changes demonstrated for MPA and RU486 between the GRwt and GFP-GR, when moving from GR concentration that display non-cooperative to cooperative ligand binding. In addition the rank order of potency increases change from DEX > F > MPA > RU486 for GRwt to Prog > RU486 > MPA > F > DEX for GFP-GR. Again it would be of interest to test whether these test compounds display a greater or lesser disposition for positive cooperative ligand binding through the high GFP-GR concentration than through the medium GRwt concentrations. For DEX, for example, we have shown that positive cooperative ligand binding is elicited at a higher GR concentration for GFP-GR than for GRwt (Fig.3.6B, Fig.3.8B).

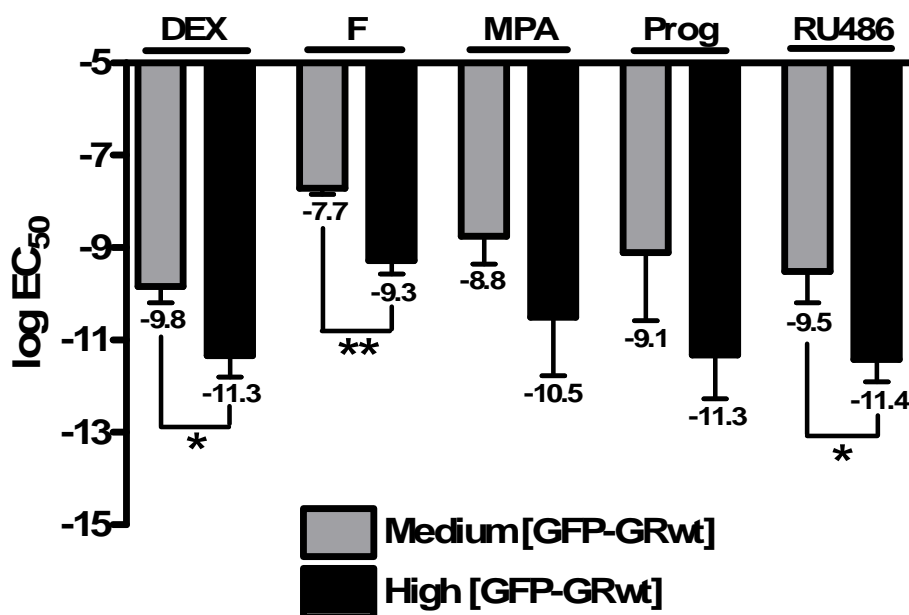


Figure 6.10. **Positive cooperative ligand binding to GFP-GR increases potency (log EC₅₀).** Cells were transfected with medium (38.5ng) or high (11550ng) GFP-GR levels and 3000ng pTAT-GRE2-Elb-luc and induced with EtOH or a range of 10⁻⁵ M to 10⁻¹¹M of DEX, F, MPA, Prog or RU486 in stripped DMEM for 24 hours. Transactivation assays were performed as described in *materials and methods*. Sigmoidal dose-response curves were fit to the experimental data which generated log EC₅₀. Statistical analysis was through one tailed unpaired t test (*P<0.05, **P<0.01). Results represent three independent experiments performed in triplicate (±SEM).

Zhang *et al.* (42) show a 2.1-fold increase in transactivation potency for DEX but not for RU486, as GRwt levels increase, in the same system. As the increase in fold potency at our medium GRwt concentration for MPA and RU486 (3.2 and 2.5-fold, respectively) differs so markedly from the 417-fold seen with DEX, it raises the question of whether positive cooperative ligand binding, which was

only demonstrated for DEX, occurs for partial agonists and antagonists. Interestingly, while MPA displays lower potency than DEX at both low and medium GRwt levels, RU486 displays similar potency as DEX at the low GR concentration. It is therefore not as simple as relating the potency values at GR concentrations which display non-cooperative DEX binding to relative increases in potency at GR levels, which display positive cooperative DEX binding. Positive cooperative binding would first have to be established for the partial agonists as well. This is an avenue which may be explored in follow up research.

A recent paper by Ong *et al.* (12) describes a mathematical model which predicts the FHDC of steroid hormone induced protein product. This model aims to clarify how, despite changes in the potency and maximum activity of dose response curves due to the influence of cofactors or GR concentration, dose response curves retain a first order Hill coefficient. As can be seen in Figs.6.8 & 6.11, our dose response curves maintain FHDC characteristics, which are not influenced by positive cooperative ligand binding at medium and high GRwt concentrations. Despite displaying positive cooperative ligand binding at the medium and high GRwt concentrations, the Hill slope for transactivation dose response curves remains non-cooperative. This result is consistent with the model of Ong *et al.* (12) which predicts that GR dimerization is not a necessary step for gene induction.

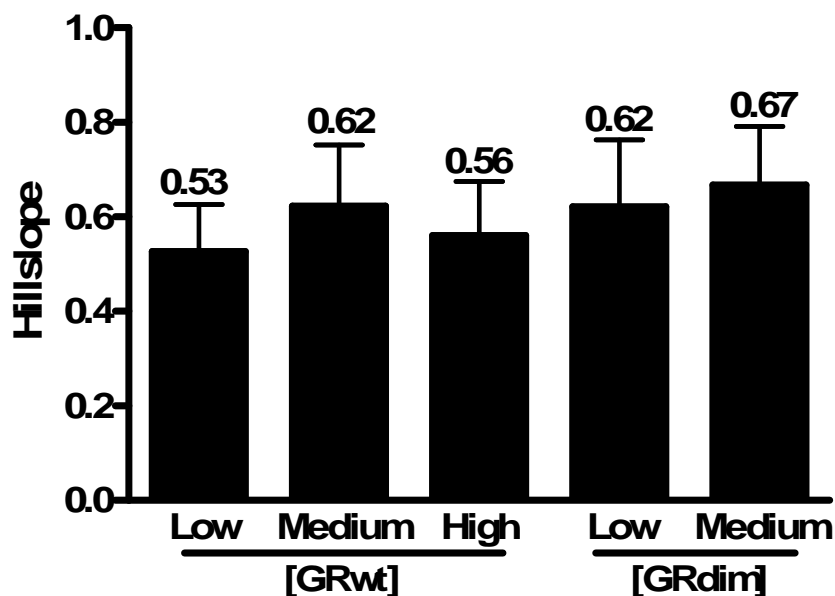


Figure 6.11. **The Hill slope of dose response curves remains FHDC and is not influenced by positive cooperative ligand binding.** Transactivation assays were performed as described in *materials and methods* on COS-1 cells expressing low, medium or high GRwt or low or medium GRdim concentrations. Log (agonist) plotted against response was analyzed using variable slope curves. This generated Hill slope values for DEX stimulation. Statistical analysis was through ANOVA followed by Newman-Keuls multiple comparison post test. All results represent a minimum of three independent experiments performed in triplicate (\pm SEM).

However, Ong *et al.* (12) do raise the question of whether GR binding to DNA occurs via preformed dimers or through the sequential binding and subsequent dimerization of GR monomers. Their mathematical model suggests that to retain FHDC, DNA binding must occur via the sequential binding of GR monomers. However, our FRET results (Chapter 4) confirm GR dimerization in the cytoplasm, independent of DNA binding. Furthermore, the electro mobility shift studies of Drouin *et al.* (9) are direct confirmation that DNA binding by preformed GR dimers does occur. Although DNA independent GR dimerization does not preclude the binding of GR monomers to the DNA and their subsequent dimerization, it would suggest that where DNA independent GR dimerization does occur it would lead to a decrease in potency due to the reduced availability of monomers. Tellingly, however, Ong *et al.* (12) as well as our own results display far greater potency through the GRwt than via the GRdim.

To summarize, the increase in potency seen at medium and high GRwt and high GFP-GR concentrations, but not with GRdim, support our observation that ligand independent dimerization of the GR at high concentrations allows for positive cooperative ligand binding, which results in increased potency through transactivation of a range of test compounds. Generally an overview of the literature confirms our findings that an increase in GR concentration results in an increase in transactivation potency (42-44, 61), however, none of these studies correlated the increase in potency with cooperative ligand binding to the GR, as we have done.

6.3.2 Ligand independent transactivation

Ligand independent activation of promoter reporter constructs is an often encountered characteristic of the assay and constructs which display a high level are termed leaky vectors. It is common practice to normalize activation results against the ligand independent transactivation in order to generate specific fold induction by test compounds. Ligand independent transactivation is generally considered a non-specific function, however, our results indicate that increasing the concentration of GRwt or GRdim leads to an increase in ligand independent transactivation through both a multiple GRE containing construct (Fig.6.12A) as well as a single GRE containing promoter construct (Fig.6.12B).

We will discuss the multiple GRE (pTAT-GRE2-Elb-luc a 2 x GRE promoter reporter) first. Although we see a significant difference in ligand independent transactivation at the low GR concentration between GRwt and GRdim we do not see any at the medium GR concentration (Fig.6.12A). We therefore exclude positive cooperative ligand binding as the cause for this behaviour because both the low GRwt and GRdim concentrations display non-cooperative ligand binding, while the medium concentration of GRwt, but not the medium GRdim concentration, displays positive cooperative ligand binding (Fig.3.8B). Although increasing the concentration of a transcription factor, in this case GR, is

expected to result in an increase in transactivation this should propose a linear relationship between GR concentration and ligand independent transactivation. However, the relationship we see is an exponential rise in transcription. While the GRwt concentration increases 2.3 and 4.2-fold above the low GR concentration at the medium and high GRwt concentrations, respectively, they result in a fold increase in ligand independent transcription of 4.7 and 22.2, respectively. The relatively modest increase in ligand independent transcription from low to medium GR concentration is followed by a steep increase in ligand independent transactivation at the high GR concentration. Although this behaviour can not be linked to ligand independent dimerization of the GRwt at the medium GR concentration it may be that at the high GR concentration the equilibrium shifts towards even greater ligand independent activation of transactivation. Intriguingly in MCF-7 cells over expressing ER α 8-fold, ligand independent endogenous promoter occupancy and gene expression has been documented (48). Thus, increasing GR concentrations may result in more non-specific associations of the GR with the promoter resulting in an increase in ligand independent transactivation.

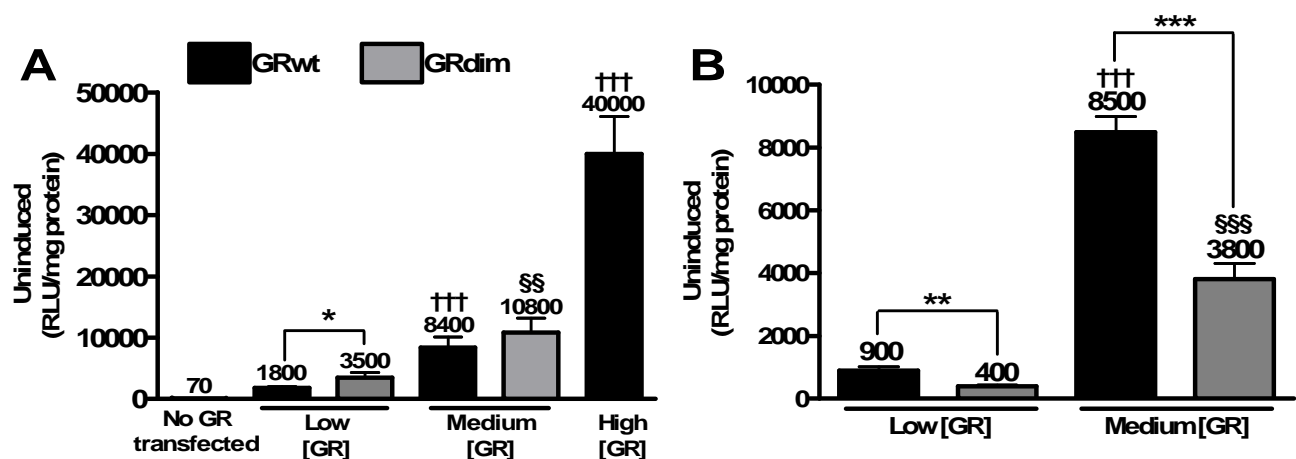


Figure 6.12. Ligand independent transactivation increases as receptor concentration does. Transactivation assays were performed on cells were transfected with (A) 3000ng pTAT-GRE2-Elb-luc (2 x GRE promoter reporter) or (B) 3000ng p Δ ODLO (1 x GRE promoter reporter) as described in *materials and methods* in a minimum of two independent experiments performed in triplicate (\pm SEM). Results are expressed as uninduced (EtOH) RLU/mg protein values following 24 hours EtOH stimulation. Statistical analysis was through two tailed unpaired t tests of low GRwt concentration against medium GRwt or high GRwt concentrations ($^{\dagger\dagger\dagger}P < 0.001$), low GRdim concentration against medium GRdim concentration ($^{\$ \$}P < 0.01$, $^{\$ \$ \$}P < 0.001$) and GRwt against GRdim ($^*P < 0.05$, $^{**}P < 0.01$, $^{***}P < 0.001$).

As for the multiple GRE containing promoter reporter construct (Fig.6.12A), both the GRwt and GRdim also display significant ligand independent transactivation via the single GRE containing promoter reporter construct (Fig.6.12B). However, with the single GRE containing promoter reporter, in contrast to the multiple GRE containing promoter reporter, the GRwt displays significantly higher levels of ligand uninduced transactivation than the GRdim. We have to rule out the influence of ligand

independent dimerization on this behaviour as uninduced transactivation is 2.3-fold higher through the GRwt than through the GRdim at the low GR concentrations, which is similar to the 2.4-fold greater ligand uninduced transactivation through the medium GRwt concentration compared to the medium GRdim concentration. This despite the fact that the medium GRwt concentration, but not the medium GRdim concentration, displays positive cooperative ligand binding due to ligand independent dimerization. However, the significant difference between ligand uninduced transactivation between GRwt and GRdim does suggest that at the single GRE containing promoter reporter construct, but not the multiple GRE containing construct, the ability to dimerize may play a role.

6.3.3 Efficacy, fold induction and biocharacter shift

As has been stated earlier, the concentration of transcription factor is closely linked to the transcription response as has been demonstrated in numerous GR concentration studies (42-44, 56, 62). Our findings support this assumption for both the GRwt as well as the GRdim for all test compounds analyzed (Fig.6.13A, Fig.6.14A) through the multiple GRE promoter construct. Similarly to ligand independent transactivation (Fig.6.12A), we find that the effect of GR concentration on transactivation efficacy becomes larger the more GR is present with a 3.7 to 12.3-fold increase in DEX induced efficacy at medium and high GRwt concentrations, respectively, reflecting a 2.3 and 4.2-fold increase in GRwt concentration (Fig.6.13A). Where as when GRdim concentration increases 2.2-fold from low to medium GR concentration we see a 5.5-fold increase in transactivation efficacy via DEX (Fig.6.13A).

Intriguingly we demonstrated significantly higher efficacy of transactivation via the multiple GRE containing promoter reporter through the GRdim than through the GRwt at both low as well as at medium receptor concentrations for all ligands tested (Fig.6.13A, Fig.6.14A). Specifically, for DEX at the low GR concentration the increased efficacy due to GRdim is 5.1-fold, while at the medium GR concentration it was 7.7-fold, relative to GRwt. Early work with a similar D-loop dimerization impaired GRdim mutant displayed greatly reduced transactivation relative to the wild type receptor through a promoter reporter containing two GREs (21, 23, 63). It was therefore assumed that this mutation attenuated transactivation. However, more recent studies have contradicted this assumption. For example, Adams *et al.* (64) using an analogous D-loop GRdim demonstrated that DEX transactivation efficacy of the phenylethanolamine N-methyltransferase (PNMT) promoter, which contains at least two GREs, was roughly 3 fold greater than that of the GRwt, while this fell to roughly 0.4-fold through a single GRE containing promoter reporter. They also show that the GRdim binds directly to DNA although with a lower affinity than the GRwt. In addition, Liu *et al.* (25) demonstrated that the GRdim fold DEX activation of transcription through a promoter containing 3 GREs is 79.4-fold higher than

through a single GRE containing promoter. The GRwt also favoured transcription through the multiple GRE but only produces a 7.2-fold difference in DEX transactivation fold induction of the multiple GRE containing promoter relative to the single GRE containing promoter in their system. They also demonstrated enhanced GRdim efficacy through a promoter containing 2 GREs from the TAT gene, which is similar to our promoter reporter.

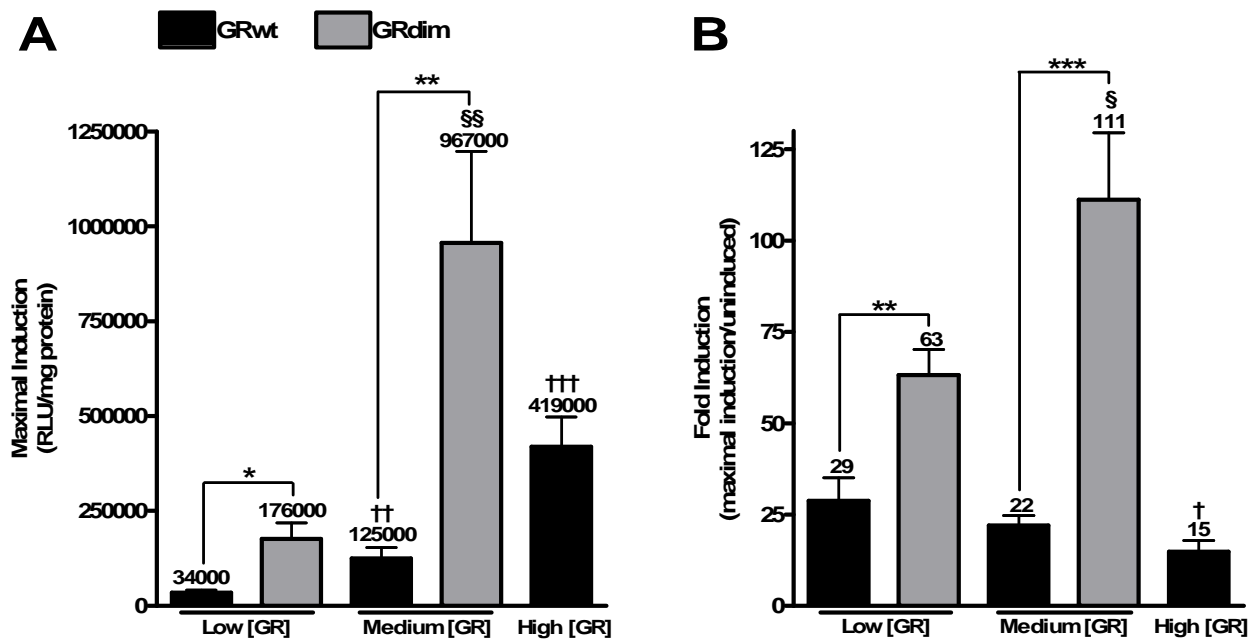


Figure 6.13. DEX efficacy (maximal induction) increases as receptor levels increase as does GRdim fold induction while GRwt fold induction decreases. Transactivation assays of the multiple GRE containing pTAT-GRE2-E1b-luc induced with DEX were performed as described in *materials and methods*. Sigmoidal dose-response curves were fit to the experimental data which generated (A) maximal induction. (B) Fold induction was calculated as maximal induction normalized to ligand uninduced induction. Statistical analysis was through two tailed unpaired t tests of low GRwt concentration against medium GRwt or high GRwt concentrations ($^{\dagger}P<0.05$, $^{\ddagger}P<0.01$, $^{\dagger\dagger\dagger}P<0.001$), low GRdim concentration against medium GRdim concentration ($^{\S}P<0.05$, $^{\S\S}P<0.01$) and GRwt against GRdim ($^*P<0.05$, $^{**}P<0.01$, $^{***}P<0.001$). Results represent a minimum of three independent experiments performed in triplicate (\pm SEM).

The efficacy of transactivation through F, MPA and RU486 of the multiple GRE containing promoter reporter showed similar trends to that of DEX (Fig.6.14A). Efficacy increased significantly as the concentration of both GRwt, as well as GRdim, increased, while GRdim demonstrated a significantly greater efficacy than the GRwt at both low and medium GR concentrations for most compounds. Although the levels of maximal induction differ between ligands the major trends towards enhanced efficacy at increased GR concentrations and through the GRdim seem universal.

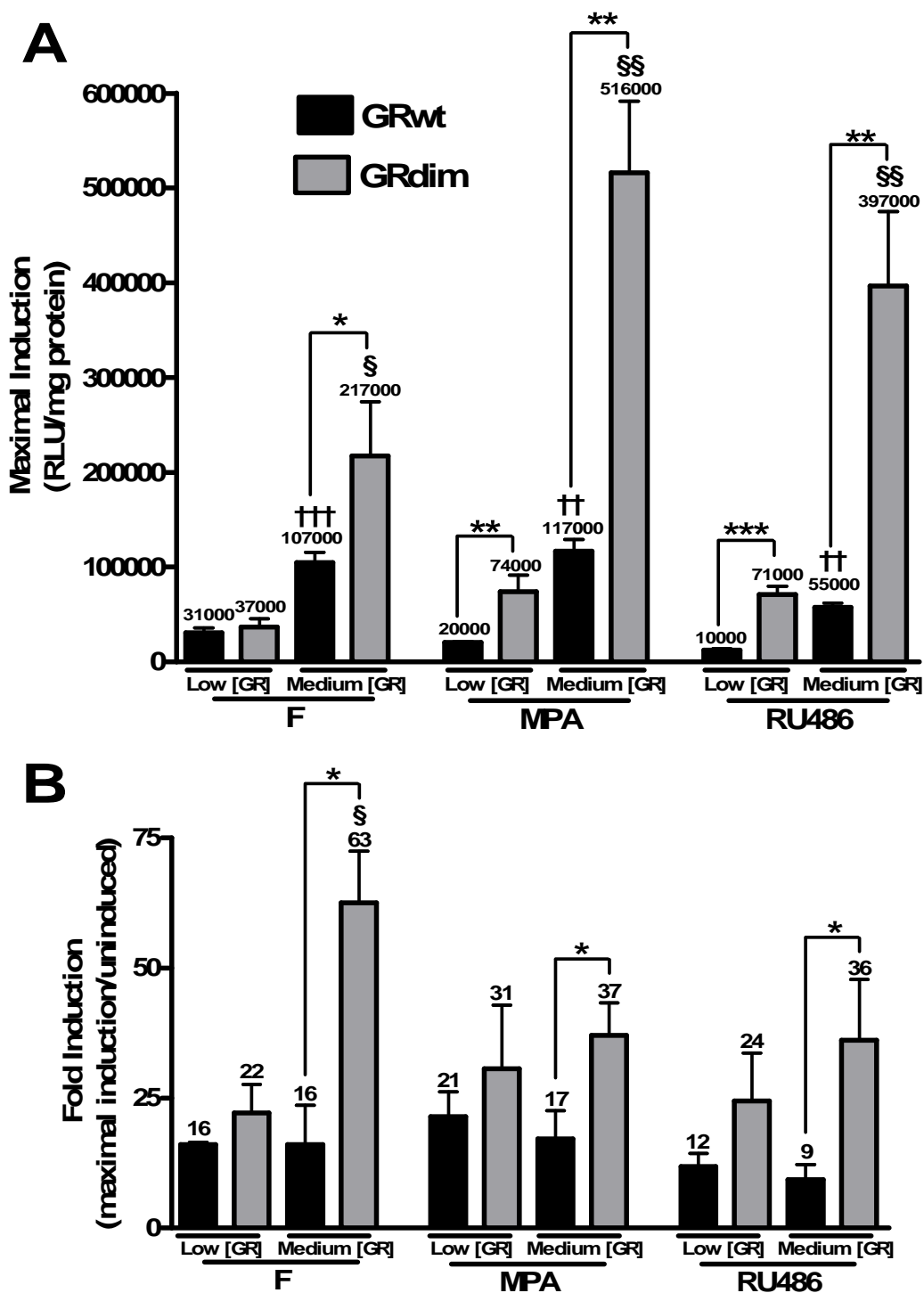


Figure 6.14. **Efficacy (maximal induction) increases as receptor levels increase as does GRdim fold induction for a range of test compounds.** Transactivation assays on the multiple GRE containing pTAT-GRE2-Elb-luc were performed as described in *materials and methods*. Sigmoidal dose-response curves were fit to the experimental data which generated (A) maximal induction. (B) Fold induction was calculated as maximal induction normalized to ligand uninduced induction. Statistical analysis was through two tailed unpaired t test of low GRwt concentration against medium GRwt concentration ($^{++}P<0.01$, $^{+++}P<0.001$), low GRdim concentration against medium GRdim concentration ($^{\$}P<0.05$, $^{\$\$}P<0.01$) and GRwt against GRdim ($^*P<0.05$, $^{**}P<0.01$, $^{***}P<0.001$). Results represent a minimum of three independent experiments performed in triplicate (\pm SEM).

Transactivation efficacy through the single GRE containing promoter reporter was also investigated. We transiently transfected the same concentration as for our multiple GRE promoter reporter assays of a promoter reporter containing only a single GRE from the GR responsive TAT gene ($p\Delta ODLO$) along with low and medium GRwt or GRdim concentrations. As the literature suggests we saw no ligand induced activation through the GRdim and transactivation efficacy generally increased with an increase in GRwt concentration, as was seen with the multiple GRE containing promoter reporter (Fig.6.15A).

As a matter of interest we converted the maximal induction (efficacy) results of the multiple GRE containing promoter construct (Fig.6.13A, Fig.6.14A) to fold induction (Fig.6.13B, Fig.6.14B) by normalizing them to the ligand uninduced induction values (Fig.6.12A). Due to the exponential increase in ligand uninduced transactivation at the medium and high GRwt concentrations our fold induction values decrease statistically as GRwt levels increase (Fig.6.13B). We did not see the same trend through the GRdim, which maintained an increase in fold induction as GRdim concentration increases. This may be due to the fact that the ligand independent transactivation for the GRdim is smaller relative to ligand induced transactivation with the multiple GRE containing promoter reporter construct. Fold induction of the single GRE containing promoter reporter through GRwt was also seen to decrease at the medium GRwt concentration relative to low GR concentration (Fig.6.15B). Once again this was due to an increase in ligand uninduced activation at the medium GRwt concentration (Fig.6.12B, Fig.6.15A).

The disparity between maximal induction and fold induction results for the GRwt highlight the effect elicited by ligand independent transactivation on the analysis of transactivation results. Are we to believe that increasing GRwt concentrations result in an increase or a decrease in efficacy via the GRE containing constructs? Based on the maximal response data it would look as though increasing GRwt concentration leads to an increase, while fold induction implies the opposite. Most researchers present transactivation results in the form of fold induction (2, 48), however, where differences in GR concentration or the transfection levels of GR co-factors are being studied efficacy is almost always presented as a percentage of the maximal response of a positive control such as a saturating concentration of DEX (41-44, 56, 65). As changes in the level of GR (43) and GR cofactors, such as TIF2 (44), SRC-1 (44) and SMRT (44), result in large changes in maximal response (efficacy) as well as the level of ligand independent transactivation of promoter reporter assays, presenting these results as a percentage of a control makes for easier comparison. It is clear that where changes have been made to the level of expressed transcription factors, presenting maximal transactivation as fold induction is avoided. The reason for this, as our results indicate (Fig.6.12), is the large difference in ligand independent transactivation that is seen through variances in transcription factor concentration

(44). We suggest no hard or fast rules to govern the presentation of transactivation efficacy results, however, it is advisable for the researcher to be aware of the impact variances in uninduced transcription could make on fold induction results. It would also be useful if the levels of ligand uninduced transcription are acknowledged in order to better interpret fold induction data, which may be misleading where differences in transcription factor concentrations exist.

Previous work indicates that mutations in the D-loop of the GR result in a loss of cooperative binding by the receptor to the GRE (66), which is reflected by a 5-fold lower affinity for DNA binding by the GR monomer relative to the GR dimer (9). Work by Tanner *et al.* (67) on the AR suggests a possible explanation for enhanced transcription at multiple HREs by DNA binding impaired receptors. Their research suggests that mutations in the hinge region of the AR, which result in weaker association of the activated mutant AR to HREs and a shorter residence time, results in enhanced transactivation. They ascribe this to the 'hit and run' theory of transcription (18, 19) where faster cycling of transcription factors at response elements results in higher activity. In defense of this theory Meijising *et al.* (7) demonstrated that the TAT promoter, despite having the lowest GR binding affinity of a range of GREs, also had the highest fold transactivation, while the PAL promoter, which had the highest GR binding affinity, displayed the lowest fold transactivation.

One may envisage a scenario where dimerization of the GR results in the effective halving of potential transcription factors, which may explain the reduced efficacy seen through the GRwt, however, it has been demonstrated that transactivation can not occur through binding to a GRE half-site alone (68). Therefore, two monomers of the GRdim would be necessary to activate a GRE in the same way as a single GR dimer would (Fig.6.7). Thus the most plausible explanation for the observed enhanced efficacy of the GRdim over the GRwt in our study is the 'hit and run' theory. While the primarily dimeric activated GRwt forms more stable longer lasting associations with the promoter, the primarily monomeric GRdim shuttles on and off the promoter more rapidly. However, as each association by either the GRwt or the GRdim has the capacity to elicit a round of transcription, the increased cycling by the GRdim results in greater maximal transcription through the GRdim.

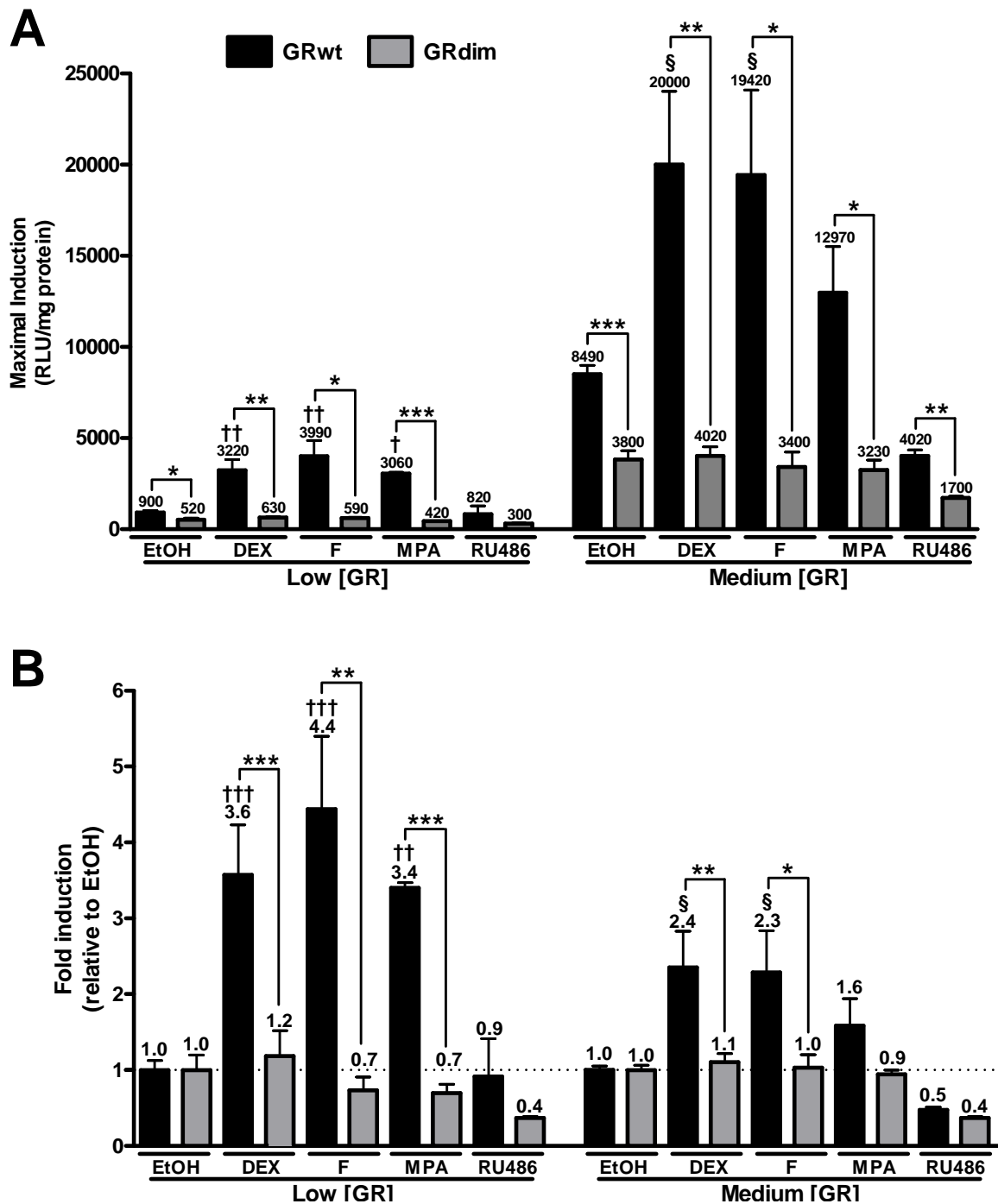


Figure 6.15. **GRdim shows no ligand induced transactivation through a single GRE, however, ligand uninduced transactivation increases with GRdim concentration.** Cells were transfected with low or medium GRwt or GRdim and 3000ng p Δ ODLO filled to 14550ng total plasmid. Induction was with EtOH, 10^{-6} M DEX, F, MPA or RU486 in stripped DMEM for 24 hours. Transactivation assays were performed as described in *materials and method*. **(A)** Maximal induction and **(B)** fold induction calculated as maximal induction normalized to ligand uninduced induction were plotted. Statistical analysis was through ANOVA followed by Dunnett's post test comparing uninduced (EtOH) conditions to the ligand induced conditions within the low ($^{\dagger}P<0.05$, $^{\dagger\dagger}P<0.01$, $^{\dagger\dagger\dagger}P<0.001$) or medium ($^{\S}P<0.05$) concentration populations of GRwt or GRdim and two tailed unpaired t tests of GRwt against GRdim ($^*P<0.05$, $^{**}P<0.01$, $^{***}P<0.001$). Results represent two experiments performed in triplicate (\pm SEM).

Maximal induction occurs at saturating concentrations of test compound, unlike potency, which is determined at sub-saturating levels. We thus hypothesize that variations in ligand affinity brought about by positive cooperative ligand binding will be less apparent for efficacy (maximal induction) than it was for potency. Furthermore, the analysis of the influence of positive cooperative ligand binding on efficacy is complicated by the inherent differences in the capacity of GRwt and GRdim to transactivate, as well as the non specific tendency for increased transcription at increased concentrations of GR (44, 56, 65). As a result it is not possible to ascertain any clear influence of positive cooperative ligand binding on the efficacy of transactivation, whether expressed as maximal induction or fold induction. However, when comparing the biocharacter of the range of test compounds investigated in our study against that of DEX we can discern an influence of positive cooperative ligand binding on individual ligands in comparison to that of DEX. MPA and RU486 both display significant increases in efficacy via the multiple GRE containing promoter reporter at GRwt as well as GFP-GR concentrations, which display positive cooperative ligand binding, while no such shift is evident with the GRdim (Fig.6.16A,B). This is unlike the biocharacter shift displayed through the single GRE containing promoter reporter (Fig.6.15B). For example, the biocharacter of MPA displayed a shift from full agonist behaviour displaying 95 percent of the DEX fold induction at the low GRwt concentration to partial agonist behaviour displaying 65 percent of the DEX fold induction at the medium GRwt concentration through the single GRE containing promoter reporter (Fig.6.15A). Conversely, MPA shifted from a partial agonist to a supra-agonist via the multiple GRE containing promoter, while the weak agonist RU486 shifted to partial agonist behaviour with GRwt and GFP-GR (Fig.6.16). However, we see no significant change in the biocharacter of the endogenous agonist F through the multiple GRE containing promoter reporter. GR concentration dependent biocharacter shifts from weak to partial agonist behaviour normalized to DEX have previously also been presented for RU486 (42, 43), Prog (42-44, 56) and dexamethasone 21-mesylate (Dex-Mes) (43, 44, 56). However, no previous study has correlated this behaviour with cooperative ligand binding and ligand uninduced GR dimerization.

We demonstrated no significant biocharacter shift in F, MPA or RU486 through an increase in the GRdim concentration from low to medium concentration (Fig.6.16A). As the ligand binding to the GRdim remains non-cooperative, even at the medium GR concentration, the fact that no biocharacter shifts are elicited through the GRdim, strengthens our argument for cooperative ligand binding induced biocharacter shifts in the GRwt. Interestingly, it was demonstrated that the shift from partial to full agonist behaviour (56) as well as receptor dependent increases in potency (62) are saturatable. Voss *et al.* (62) suggest that GR co-factors and non-specific transcription machinery start to become limiting which impairs any further rise in efficacy.

Our results suggest that the efficacy of MPA and RU486 increase via the multiple GRE containing promoter reporter construct at GR concentrations which show positive cooperative ligand binding for DEX. Ligand independent dimerization of the receptor may prime its response and shift the biocharacter towards that of a more potent agonist. The biocharacter of the agonist F does not demonstrate the same shift and we hypothesize that its transcription response already demonstrates a theoretical maximum, which is similar to that of DEX. We propose that it is only weak or partial agonists that are affected by positive cooperative ligand binding at saturating ligand concentrations. It would be beneficial to test the capacity of these test compounds to induce GR dimerization at GRwt concentrations which display non-cooperative as well as positive cooperative ligand binding in order to correlate ligand independent dimerization with the shift in biocharacter.

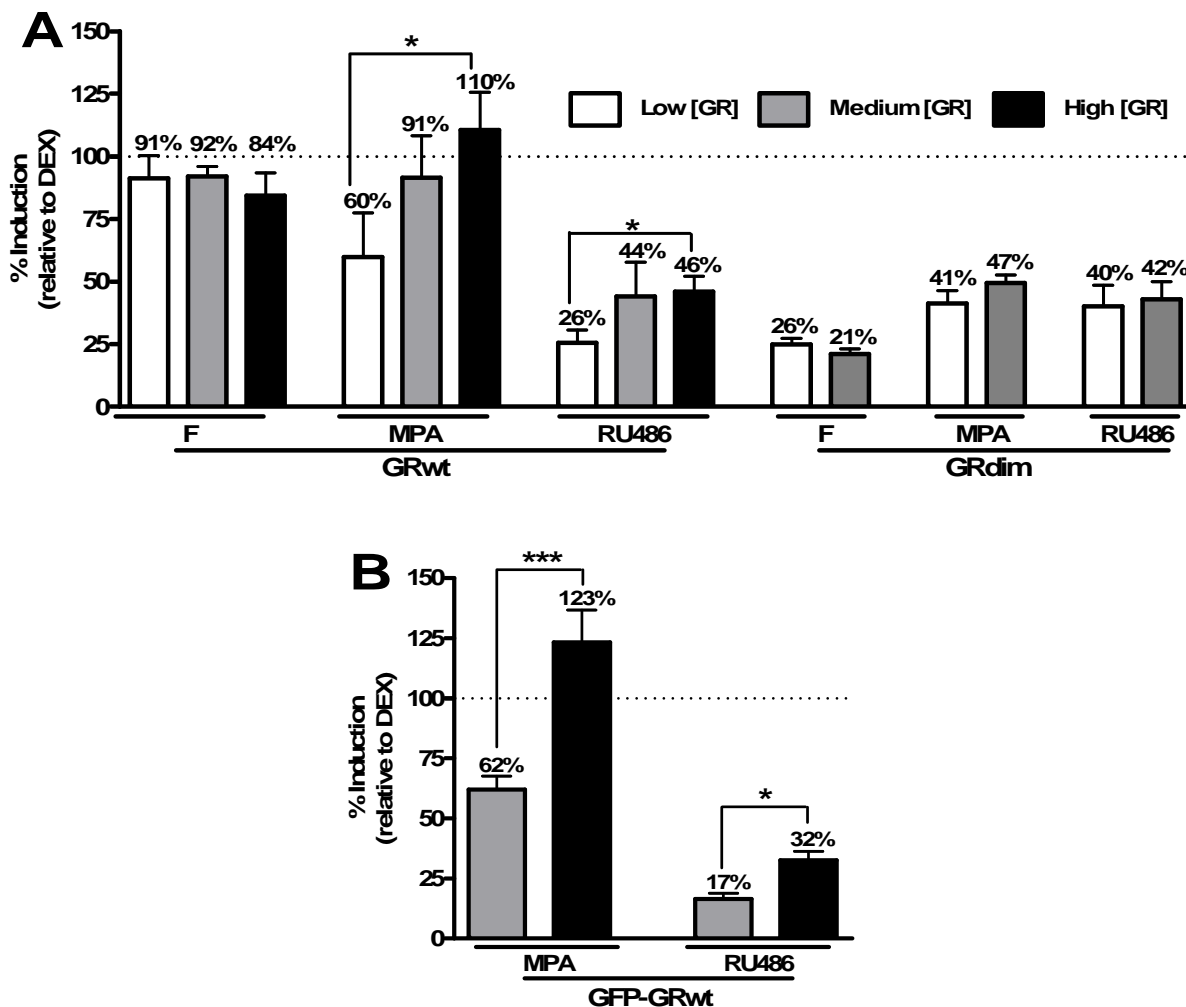


Figure 6.16. **The ability to cooperatively bind ligands influences the biocharacter of MPA and RU486 in transactivation assays.** Transactivation assays on the pTAT-GRE2-Elb-luc were performed as described in *materials and methods* in COS-1 cells expressing (A) low, medium or high GRwt or low or medium GRdim or (B) medium or high GFP-GR. Percentage induction of F, MPA or RU486 representing maximal induction of each of these test compounds relative to that of DEX (set at 100 percent) at the same GR concentration and GR construct either GRwt or GRdim. Statistical analysis was through two tailed unpaired t tests (* $P < 0.05$, *** $P < 0.001$). Results represent three independent experiments performed in triplicate (\pm SEM).

In summary, efficacy is GR concentration dependent, displaying a promoter specific sensitivity to GR dimerization. The single GRE containing promoter reporter construct requires GR dimerization in order to facilitate ligand dependent transactivation, while the transactivation of the multiple GRE is actually enhanced by the reduced capacity of GRdim to dimerize. It is unlikely that cooperative ligand binding influences the efficacy of transactivation through either the single or multiple GRE containing promoter reporter constructs. On the other hand the biocharacter shifts of MPA and RU486 through the multiple GRE containing promoter reporter may be attributed to the influence of cooperative ligand binding.

6.4 Transactivation of the endogenous GILZ gene

Having established the relevance of dimerization and receptor concentration in ligand independent transactivation as well as ligand induced potency and efficacy with promoter reporter assays we sought to compare these characteristics in a more endogenous system. We used transiently transfected COS-1 cells expressing low, medium or high GRwt concentrations as well as the low or medium GRdim concentrations. Following an 8 hour induction with either EtOH or 10^{-6} M DEX we determined the relative mRNA expression levels of the GR-responsive endogenous GILZ gene (33, 34, 37) through RT-PCR. In order to correct for cDNA loading we determined the concentration of GAPDH mRNA within each sample. As has been recently demonstrated by Visser *et al.* (69) as well as by Burkhart *et al.* (70), the ubiquitously expressed house keeping gene, GAPDH is not influenced by DEX stimulation. Our own raw data confirms that DEX did not affect GAPDH levels and also indicates that GAPDH expression is not significantly affected by the transfection of varying GR concentrations either (Fig.6.17).

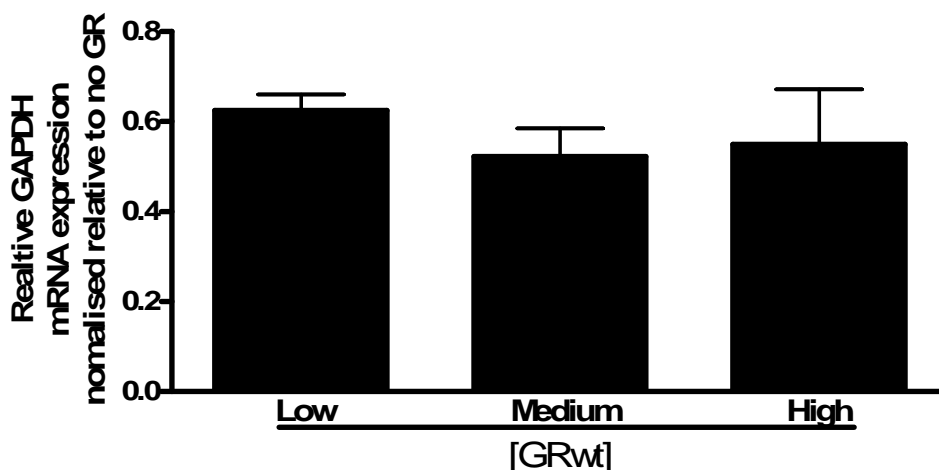


Figure 6.17. **The relative expression of GAPDH is not affected by varying concentrations of transfected GR.** RT-PCR on the GAPDH gene was carried out on cells expressing low, medium or high concentrations of GRwt as described in *materials and methods*. Statistical analysis was carried out using ANOVA followed by Newman-Keuls multiple comparison post test. Results represent a minimum of two independent experiments performed in quadruplicate (\pm SEM).

As a necessary control, melting curves were run on all GILZ and GAPDH RT-PCR products (Fig.6.18A,B). A single peak per sample confirmed that only one product was amplified in the PCR reaction and that no primer dimers were formed. Standard curves of a range of cDNA concentrations were created in order to determine the cycle threshold (CT) of the GILZ and GAPDH primers (Fig.6.18C,D) and to calculate the efficiency (E) of amplification. The E of the GILZ primers was calculated as 2.08 while the E of the GAPDH primers was 1.89. These values indicate a high degree of E for both primers as they are close to 2, which is the theoretical maximum for E (71). These efficiencies were calculated from the slope of the standard curves:

$$E = 10^{[-1/\text{slope}]}$$

The efficiencies were applied to subsequent CT values in order to quantify the relative expression ratio of the target gene (GILZ) relative to that of the reference gene (GAPDH) using the Pfaffl (71) mathematical model:

$$\text{Relative expression ratio} = \frac{(E_{\text{target}})^{\Delta\text{CP}_{\text{target}}(\text{control} - \text{sample})}}{(E_{\text{reference}})^{\Delta\text{CP}_{\text{reference}}(\text{control} - \text{sample})}}$$

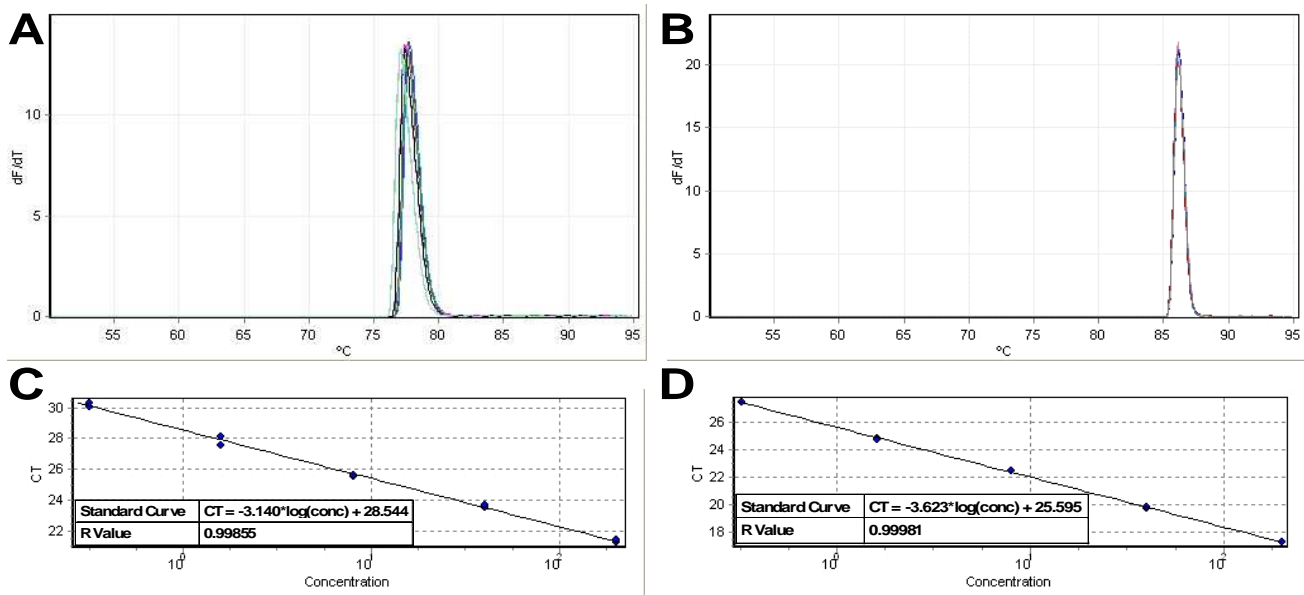


Figure 6.18. **Melting and standard curves of GILZ and GAPDH.** RT-PCR was carried out as described in *materials and methods* using primers for GILZ and GAPDH cDNA. Melting curves for (A) GILZ and (B) GAPDH. Standard curves of (C) GILZ and (D) GAPDH. Amplification efficacy was generated using Rotor-Gene 6000 Series Software 1.7 (Corbett) to determine primer efficiency.

6.4.1 Ligand independent transactivation of GILZ

Our results indicate that ligand independent transactivation of the endogenous GILZ gene increases significantly as GR concentrations increase (Fig.6.19A). Unlike the ligand independent transactivation of the multiple GRE containing promoter reporter (Fig.6.12A), the medium concentration of GRdim displays significantly reduced ligand independent induction compared to the medium GRwt concentration. However, these results are more in line with the single GRE promoter reporter studies (Fig.6.12B) that also showed significantly less ligand uninduced transactivation via GRdim at the medium GR concentration. Ligand independent induction also seems to plateau at the GRwt levels which display positive cooperative ligand binding with no significant difference between medium and high GRwt concentrations (Fig.6.19A). This is in sharp contrast to the promoter reporter studies with the multiple GRE containing promoter construct where ligand uninduced transactivation sharply and significantly increased between medium and high GRwt concentrations (Fig.6.12A). The level of ligand independent transactivation of the endogenous GILZ gene is far less than that seen through the multiple GRE containing promoter reporter. The maximal ligand independent induction of the GILZ gene displayed by the high GRwt concentration is only 2.5-fold greater than where no GR was transfected. This is in sharp contrast to the 571-fold increase in ligand independent transactivation of the multiple GRE containing promoter reporter at the high GRwt concentration (Fig.6.12A). Furthermore, the difference between ligand uninduced transactivation between the low and medium GRwt concentrations is also greatly reduced in the endogenous assay with only a 1.4-fold difference for the GILZ gene versus a 4.7-fold difference for the multiple GRE and a 9.4-fold difference for the single GRE containing construct.

The literature suggests that the GILZ promoter is a weak inducer of transcription with activity roughly 10-fold lower than that of the single GRE containing TAT promoter (7). In line with the 'hit and run' theory of transcription, Meijnsing *et al.* (7) demonstrate higher levels of transcription through promoters that bind the GR weakly. Although the GILZ promoter has a relatively low affinity for the GR it is still considerably higher than that of the TAT promoter (7). The fact that one of our reporter promoter constructs contains two TAT GRE's may further enhance its capacity for transactivation relative to that seen for the endogenous GILZ gene.

A further difference may lie at the level of quantification or transcription in each of these systems. Where as the concentration of the stable protein luciferase produced over a 24 hour period is measured in the promoter reporter assay the transactivation of the endogenous GILZ gene is quantified as the level of mRNA produced after 8 hours of stimulation. Recent research has shown that following stimulation, the level of mRNA produced by GR responsive genes may either peak

rapidly and remain constant for a 24 hour period, peak rapidly and decrease quickly or increase slowly over a 24 hour period (72), which suggests that mRNA does not necessarily accumulate in the way that the luciferase protein does. Our own time studies to optimise for the maximal level of GILZ mRNA transcription following DEX stimulation ranged from 2 to 24 hours and revealed that the 8 hour time point was optimal in our system (data not shown). The time period of 24 hour induction for the promoter reporter allows for a greater build up of transactivation product, namely luciferase. On the whole, measurements of endogenous transactivation which rely on mRNA detection are known to display lower fold induction and maximal response than promoter reporters containing multiple GREs (33, 36). Our findings are thus in line with those reported in the literature.

6.4.2 Efficacy of GILZ transactivation

6.4.2.1 Maximal induction

Maximum induction by DEX of the GILZ gene (Fig.6.19B) normalizes DEX induced GILZ induction to the GILZ levels of the uninduced no GR transfected population. This is comparable to the maximal induction of promoter reporter transactivation (Fig.6.13A, Fig.6.15A) as induction is not normalized to the specific levels of ligand independent transactivation, but rather represents the total ligand induced as well as ligand uninduced transcription. Stimulation of the GRwt results in a significant GR concentration dependent increase in GILZ expression, which is similar to what is demonstrated by the GRwt in the single and multiple GRE containing promoter reporter construct assays (Fig.6.13A, Fig.6.15A).

Interestingly, there is a 1.4-fold increase in GILZ maximal induction through the endogenous GR in COS-1 cells, indicated as the cells where no GR has been transfected (Fig.6.19B) and suggests the presence of low levels of endogenous GR in COS-1 cells. Maximal DEX induction of GILZ mRNA production by the GRdim was not significantly different from that of the corresponding GRwt concentration. This is in sharp contrast to the significantly heightened response displayed by GRdim in the multiple GRE containing promoter reporter assay (Fig.6.13A) and the significantly decreased response seen with the single GRE promoter reporter assay (Fig.6.15A). Furthermore, the low and medium GRdim maximal DEX induced GILZ inductions are not significantly different from one another. Increasing GRdim concentration from low to medium GR levels results in a 1.3-fold increase in maximal induction of the endogenous GILZ gene, while the same increase in GRdim concentration results in a 5.5-fold increase in maximal induction of the multiple GRE containing promoter reporter (Fig.6.13A). This highlights the decreased transactivation efficacy displayed by GRdim in the endogenous assay and is supported by results from a recent paper which studied the GC,

prednisolone's ability to induce endogenous gene transcription in a GRdim expressing mouse model that revealed that while 347 genes were upregulated in GRwt expressing mice only 29 were upregulated in the GRdim mice (73).

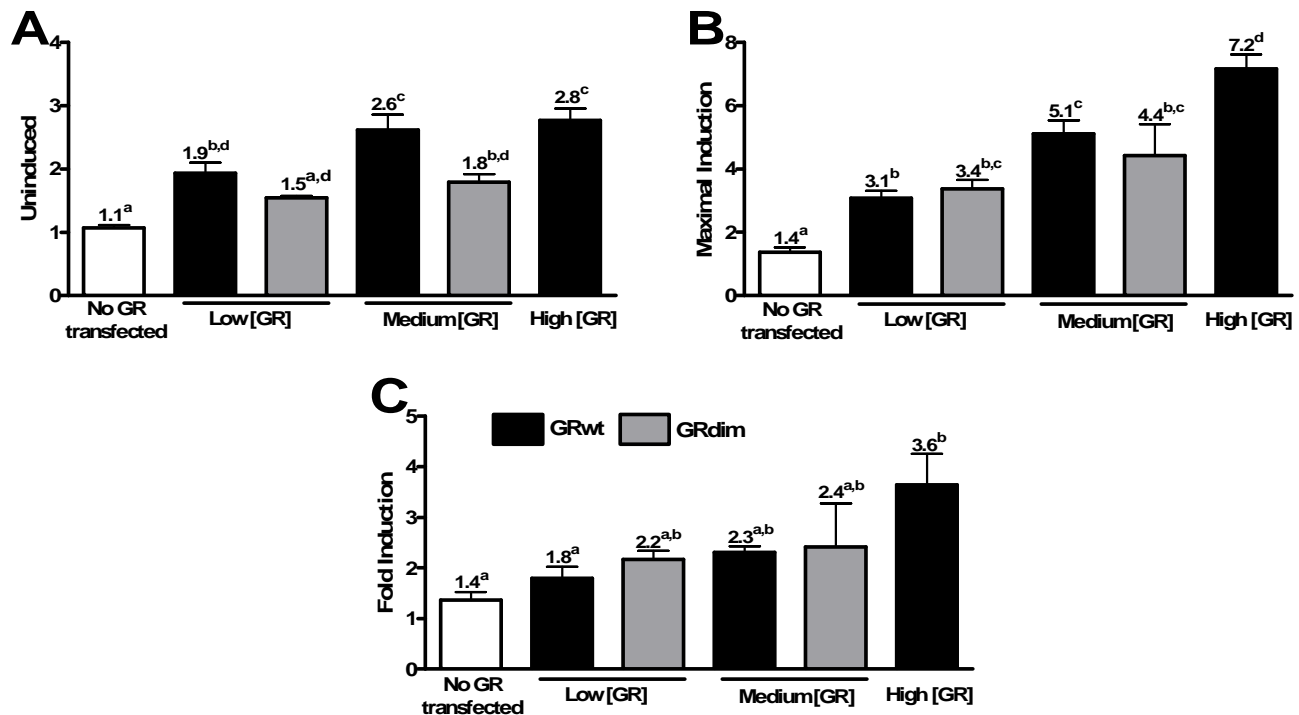


Figure 6.19. Real time PCR quantification of endogenous GILZ gene expression. RT-PCR was carried out as described in the *materials and methods* on cells induced for 8 hours with either EtOH or 10^{-6} M DEX. GILZ expression was calculated relative to GAPDH for each condition. **(A)** Uninduced GILZ expression was calculated from EtOH induced GILZ expression at the indicated levels of transfected GR normalized to EtOH induced GILZ expression where no GR was transfected. **(B)** Maximum GILZ expression where 10^{-6} M DEX at each GR condition was normalized to EtOH induced GILZ expression where no GR was transfected. **(C)** Fold induction induced by 10^{-6} M DEX relative to EtOH for each transfection condition. Statistical analysis was carried out using ANOVA followed by Newman-Keuls multiple comparison post test, where conditions with different letters are statistically different from one another ($P < 0.01$). Results represent a minimum of two independent experiments performed in quadruplicate (\pm SEM).

6.4.2.2 Fold induction

When results are converted to fold induction (Fig.6.19C) by normalizing the maximal induction to the specific ligand independent induction at each GR concentration (Fig.6.19A) we see minimal increases in fold induction at the low and medium GRwt and GRdim concentrations. Only the high concentration of GRwt results in significantly raised fold induction when compared to that of the no GR transfected population. Fold induction of both the multiple and single GRE containing promoter reporters displayed the inverse, namely significant decreases in fold induction as GRwt concentrations increased (Fig.6.13B, Fig.6.15B). These disparate results reflect the 22.2-fold and 9.4-fold increases in ligand

independent transactivation of the multiple and single GRE containing promoter reporters, respectively, when moving from low to maximal GRwt concentrations (Fig.6.12A,B) as compared to the 1.5-fold increase in ligand independent transactivation of the GILZ gene when moving from the low to the high GRwt concentration (Fig.6.19A). The GRdim demonstrated a significant increase in fold induction as its concentration increased in the multiple GRE containing promoter reporter assay (Fig.6.13B), a similar trend emerges for GRdim driven GILZ transactivation, however, the increase in levels was not significant.

The 3.6-fold induction we see at the high GRwt concentration is comparable to previous work using the same primers. Avenant *et al.* (36) achieved 4.5-fold induction of GILZ in COS-1 cells transiently transfected with high levels of GR and stimulated with a saturating DEX concentration. Fold induction of the endogenous GILZ gene has been shown to increase from 3.6 to 6 in U2OS cells transfected with increasing amounts of GRwt (74), which again reflects the significant shift we demonstrate from 1.8-fold induction at the low GRwt concentration to 3.6-fold induction at the high GRwt concentration.

6.4.3 Summary of endogenous GILZ transactivation

Meijsing *et al.* (7) demonstrated that a D-loop dimerization impaired GR mutant, similar to the one we have used, can activate the GILZ promoter at roughly 80 percent of the GRwt levels in a promoter reporter assay, while Rogatsky *et al.* (74) show GRdim induction of the endogenous GILZ in U2OS cells to be only 20 percent of the GRwt induction. At our low GR concentration we demonstrate that the GRdim is capable of 110 percent of the maximal induction achieved by the GRwt (Fig.6.19B), which falls to 86 percent of the maximal induction achieved by the GRwt at the medium GR concentration (Fig.6.19B). This decrease in maximal induction demonstrated by the GRdim relative to the GRwt may reflect positive cooperative ligand binding to the GRwt at the medium GR concentration. However, once corrected for the increased ligand independent induction seen through the GRwt, the GRdim displays better fold induction than the GRwt at both the low and medium GR concentrations (Fig.6.19C). It would be of great interest to us to place the GRdim gene in the same vector as the GRwt in order to test the behaviour of the GRdim at GR levels similar to that of the high GRwt. As yet we can not conclusively conclude whether the difference we see in maximal induction between the medium concentration of GRwt and GRdim is due to positive cooperative ligand binding or as a result of the enhanced ligand independent transactivation displayed by the GRwt in general. To definitively establish the effect of cooperative ligand binding on maximal induction it would be useful to compare the maximal induction of high GRdim to high GRwt to ascertain whether positive cooperative ligand binding causes an increase in transactivation of the endogenous GILZ gene.

To conclude, we have demonstrated that increased GRwt concentrations result in increased ligand independent transactivation of the endogenous GILZ gene and an increase in maximal induction. Ligand independent transactivation is significantly higher at the levels of GRwt, which display positive cooperative ligand binding, while they remain statistically similar to the low GRwt concentration, which displays non-cooperative ligand binding, at both low and medium GRdim concentrations. Increasing GRwt concentrations results in a significant increase in maximal DEX induction at each GRwt population, while maximal DEX induction at the low and medium GRdim concentrations are not significantly different from one another. Furthermore, the medium GRwt concentration displays a trend towards greater maximal induction than the medium concentration of GRdim. Only the high concentration of GRwt, which also shows the greatest extent of ligand independent dimerization (Chapter 4) and largest Hill slope (Chapter 3), displays significantly different fold induction relative to COS-1 cells where no GR has been transfected. As the medium GRdim and medium GRwt have similar levels of fold induction we can not conclude that positive cooperative ligand binding is responsible for the increased fold induction at the high GRwt concentration, as the medium GRwt concentration also binds ligand in a positive cooperative fashion. As reflected by the greatly reduced ligand independent induction, maximal induction, and fold induction it is clear that the endogenous GILZ transactivation assay is far less sensitive to the shift in positive cooperative ligand binding than the promoter reporter assay. In the future we would like to investigate the response of the endogenous GILZ gene to subsaturating concentrations of DEX at varying GR concentrations in order to determine whether the increase in potency we see through our promoter reporter assay (Fig.6.9A) is also seen with an endogenous gene.

We offer a summary of all results and a discussion of their relevance when viewed as a whole, in the following chapter.

6.5 Bibliography

1. Lu NZ, Collins JB, Grissom SF & Cidlowski JA (2007) Selective regulation of bone cell apoptosis by translational isoforms of the glucocorticoid receptor. *Mol Cell Biol* 27: 7143-7160.
2. So AY, Chaivorapol C, Bolton EC, Li H & Yamamoto KR (2007) Determinants of cell- and gene-specific transcriptional regulation by the glucocorticoid receptor. *PLoS Genet* 3: e94.
3. De Bosscher K, Vanden Berghe W & Haegeman G (2003) The interplay between the glucocorticoid receptor and nuclear factor-kappaB or activator protein-1: Molecular mechanisms for gene repression. *Endocr Rev* 24: 488-522.
4. Dostert A & Heinzl T (2004) Negative glucocorticoid receptor response elements and their role in glucocorticoid action. *Curr Pharm Des* 10: 2807-2816.

5. Newton R & Holden NS (2007) Separating transrepression and transactivation: A distressing divorce for the glucocorticoid receptor?. *Mol Pharmacol* 72: 799-809.
6. Beato M, Chalepakis G, Schauer M & Slater EP (1989) DNA regulatory elements for steroid hormones. *J Steroid Biochem* 32: 737-747.
7. Meijising SH, *et al* (2009) DNA binding site sequence directs glucocorticoid receptor structure and activity. *Science* 324: 407-410.
8. Tsai SY, *et al* (1988) Molecular interactions of steroid hormone receptor with its enhancer element: Evidence for receptor dimer formation. *Cell* 55: 361-369.
9. Drouin J, *et al* (1992) Homodimer formation is rate-limiting for high affinity DNA binding by glucocorticoid receptor. *Mol Endocrinol* 6: 1299-1309.
10. Segard-Maurel I, *et al* (1996) Glucocorticosteroid receptor dimerization investigated by analysis of receptor binding to glucocorticosteroid responsive elements using a monomer-dimer equilibrium model. *Biochemistry* 35: 1634-1642.
11. Savory JG, *et al* (2001) Glucocorticoid receptor homodimers and glucocorticoid-mineralocorticoid receptor heterodimers form in the cytoplasm through alternative dimerization interfaces. *Mol Cell Biol* 21: 781-793.
12. Ong KM, Blackford JA, Jr, Kagan BL, Simons SS, Jr & Chow CC (2010) A theoretical framework for gene induction and experimental comparisons. *Proc Natl Acad Sci U S A* 107: 7107-7112.
13. Holmbeck SM, Dyson HJ & Wright PE (1998) DNA-induced conformational changes are the basis for cooperative dimerization by the DNA binding domain of the retinoid X receptor. *J Mol Biol* 284: 533-539.
14. Dahlman-Wright K, Siltala-Roos H, Carlstedt-Duke J & Gustafsson JA (1990) Protein-protein interactions facilitate DNA binding by the glucocorticoid receptor DNA-binding domain. *J Biol Chem* 265: 14030-14035.
15. Furlow JD, Murdoch FE & Gorski J (1993) High affinity binding of the estrogen receptor to a DNA response element does not require homodimer formation or estrogen. *J Biol Chem* 268: 12519-12525.
16. Tamrazi A, Carlson KE, Daniels JR, Hurth KM & Katzenellenbogen JA (2002) Estrogen receptor dimerization: Ligand binding regulates dimer affinity and dimer dissociation rate. *Mol Endocrinol* 16: 2706-2719.
17. McNally JG, Muller WG, Walker D, Wolford R & Hager GL (2000) The glucocorticoid receptor: Rapid exchange with regulatory sites in living cells. *Science* 287: 1262-1265.
18. George AA, Schiltz RL & Hager GL (2009) Dynamic access of the glucocorticoid receptor to response elements in chromatin. *Int J Biochem Cell Biol* 41: 214-224.
19. Hager GL, Nagaich AK, Johnson TA, Walker DA & John S (2004) Dynamics of nuclear receptor movement and transcription. *Biochim Biophys Acta* 1677: 46-51.
20. Hayashi R, Wada H, Ito K & Adcock IM (2004) Effects of glucocorticoids on gene transcription. *Eur J Pharmacol* 500: 51-62.

21. Heck S, *et al* (1994) A distinct modulating domain in glucocorticoid receptor monomers in the repression of activity of the transcription factor AP-1. *EMBO J* 13: 4087-4095.
22. Karin M (1998) New twists in gene regulation by glucocorticoid receptor: Is DNA binding dispensable?. *Cell* 93: 487-490.
23. Reichardt HM, *et al* (1998) DNA binding of the glucocorticoid receptor is not essential for survival. *Cell* 93: 531-541.
24. Reichardt HM, *et al* (2001) Repression of inflammatory responses in the absence of DNA binding by the glucocorticoid receptor. *EMBO J* 20: 7168-7173.
25. Liu W, Wang J, Yu G & Pearce D (1996) Steroid receptor transcriptional synergy is potentiated by disruption of the DNA-binding domain dimer interface. *Mol Endocrinol* 10: 1399-1406.
26. De Bosscher K, *et al* (2005) A fully dissociated compound of plant origin for inflammatory gene repression. *Proc Natl Acad Sci U S A* 102: 15827-15832.
27. van Loo G, *et al* (2010) Antiinflammatory properties of a plant-derived nonsteroidal, dissociated glucocorticoid receptor modulator in experimental autoimmune encephalomyelitis. *Mol Endocrinol* 24: 310-322.
28. Yemelyanov A, *et al* (2008) Novel steroid receptor phyto-modulator compound a inhibits growth and survival of prostate cancer cells. *Cancer Res* 68: 4763-4773.
29. Wust S, *et al* (2009) Therapeutic and adverse effects of a non-steroidal glucocorticoid receptor ligand in a mouse model of multiple sclerosis. *PLoS One* 4: e8202.
30. Robertson S, *et al* (2010) Abrogation of glucocorticoid receptor dimerization correlates with dissociated glucocorticoid behavior of compound a. *J Biol Chem* 285: 8061-8075.
31. Dewint P, *et al* (2008) A plant-derived ligand favoring monomeric glucocorticoid receptor conformation with impaired transactivation potential attenuates collagen-induced arthritis. *J Immunol* 180: 2608-2615.
32. Plaisance S, Vanden Berghe W, Boone E, Fiers W & Haegeman G (1997) Recombination signal sequence binding protein jkappa is constitutively bound to the NF-kappaB site of the interleukin-6 promoter and acts as a negative regulatory factor. *Mol Cell Biol* 17: 3733-3743.
33. Ronacher K, *et al* (2009) Ligand-selective transactivation and transrepression via the glucocorticoid receptor: Role of cofactor interaction. *Mol Cell Endocrinol* 299: 219-231.
34. Eddleston J, Herschbach J, Wagelie-Steffen AL, Christiansen SC & Zuraw BL (2007) The anti-inflammatory effect of glucocorticoids is mediated by glucocorticoid-induced leucine zipper in epithelial cells. *J Allergy Clin Immunol* 119: 115-122.
35. Muzikar KA, Nickols NG & Dervan PB (2009) Repression of DNA-binding dependent glucocorticoid receptor-mediated gene expression. *Proc Natl Acad Sci U S A* 106: 16598-16603.
36. Avenant C, Kotitschke A & Hapgood JP (2010) Glucocorticoid receptor phosphorylation modulates transcription efficacy through GRIP-1 recruitment. *Biochemistry* 49: 972-985.

37. Wang JC, *et al* (2004) Chromatin immunoprecipitation (ChIP) scanning identifies primary glucocorticoid receptor target genes. *Proc Natl Acad Sci U S A* 101: 15603-15608.
38. Stoney Simons S,Jr (2003) The importance of being varied in steroid receptor transactivation. *Trends Pharmacol Sci* 24: 253-259.
39. van der Laan S, Lachize SB, Vreugdenhil E, de Kloet ER & Meijer OC (2008) Nuclear receptor coregulators differentially modulate induction and glucocorticoid receptor-mediated repression of the corticotropin-releasing hormone gene. *Endocrinology* 149: 725-732.
40. Zhao Q, Pang J, Favata MF & Trzaskos JM (2003) Receptor density dictates the behavior of a subset of steroid ligands in glucocorticoid receptor-mediated transrepression. *Int Immunopharmacol* 3: 1803-1817.
41. Gougat C, *et al* (2002) Overexpression of the human glucocorticoid receptor alpha and beta isoforms inhibits AP-1 and NF-kappaB activities hormone independently. *J Mol Med* 80: 309-318.
42. Zhang S, Jonklaas J & Danielsen M (2007) The glucocorticoid agonist activities of mifepristone (RU486) and progesterone are dependent on glucocorticoid receptor levels but not on EC50 values. *Steroids* 72: 600-608.
43. Szapary D, Xu M & Simons SS,Jr (1996) Induction properties of a transiently transfected glucocorticoid-responsive gene vary with glucocorticoid receptor concentration. *J Biol Chem* 271: 30576-30582.
44. Szapary D, Huang Y & Simons SS,Jr (1999) Opposing effects of corepressor and coactivators in determining the dose-response curve of agonists, and residual agonist activity of antagonists, for glucocorticoid receptor-regulated gene expression. *Mol Endocrinol* 13: 2108-2121.
45. Adcock IM, Nasuhara Y, Stevens DA & Barnes PJ (1999) Ligand-induced differentiation of glucocorticoid receptor (GR) trans-repression and transactivation: Preferential targeting of NF-kappaB and lack of I-kappaB involvement. *Br J Pharmacol* 127: 1003-1011.
46. Coghlan MJ, *et al* (2003) A novel antiinflammatory maintains glucocorticoid efficacy with reduced side effects. *Mol Endocrinol* 17: 860-869.
47. Avenant C, Ronacher K, Stubsrud E, Louw A & Hapgood JP (2010) Role of ligand-dependent GR phosphorylation and half-life in determination of ligand-specific transcriptional activity. *Mol Cell Endocrinol* 327: 72-88.
48. Fowler AM, *et al* (2004) Increases in estrogen receptor-alpha concentration in breast cancer cells promote serine 118/104/106-independent AF-1 transactivation and growth in the absence of estrogen. *FASEB J* 18: 81-93.
49. Buser AC, *et al* (2007) Progesterone receptor repression of prolactin/signal transducer and activator of transcription 5-mediated transcription of the beta-casein gene in mammary epithelial cells. *Mol Endocrinol* 21: 106-125.
50. O'Donnell D, Francis D, Weaver S & Meaney MJ (1995) Effects of adrenalectomy and corticosterone replacement on glucocorticoid receptor levels in rat brain tissue: A comparison between western blotting and receptor binding assays. *Brain Res* 687: 133-142.

51. Novak U, Cocks BG & Hamilton JA (1991) A labile repressor acts through the NFkB-like binding sites of the human urokinase gene. *Nucleic Acids Res* 19: 3389-3393.
52. Garside H, *et al* (2004) Glucocorticoid ligands specify different interactions with NF-kappaB by allosteric effects on the glucocorticoid receptor DNA binding domain. *J Biol Chem* 279: 50050-50059.
53. Heitzer MD, Wolf IM, Sanchez ER, Witchel SF & DeFranco DB (2007) Glucocorticoid receptor physiology. *Rev Endocr Metab Disord* 8: 321-330.
54. Sui X, *et al* (1999) Specific androgen receptor activation by an artificial coactivator. *J Biol Chem* 274: 9449-9454.
55. Jenster G, *et al* (1997) Steroid receptor induction of gene transcription: A two-step model. *Proc Natl Acad Sci U S A* 94: 7879-7884.
56. Chen S, Sarlis NJ & Simons SS, Jr (2000) Evidence for a common step in three different processes for modulating the kinetic properties of glucocorticoid receptor-induced gene transcription. *J Biol Chem* 275: 30106-30117.
57. Chriguier RS, *et al* (2005) Glucocorticoid sensitivity in young healthy individuals: In vitro and in vivo studies. *J Clin Endocrinol Metab* 90: 5978-5984.
58. Guo WX, *et al* (1996) Expression and cytokine regulation of glucocorticoid receptors in kaposi's sarcoma. *Am J Pathol* 148: 1999-2008.
59. Driver PM, *et al* (2001) Expression of 11 beta-hydroxysteroid dehydrogenase isozymes and corticosteroid hormone receptors in primary cultures of human trophoblast and placental bed biopsies. *Mol Hum Reprod* 7: 357-363.
60. Charmandari E, *et al* (2001) Joint growth hormone and cortisol spontaneous secretion is more asynchronous in older females than in their male counterparts. *J Clin Endocrinol Metab* 86: 3393-3399.
61. Cho S, Kagan BL, Blackford JA, Jr, Szapary D & Simons SS, Jr (2005) Glucocorticoid receptor ligand binding domain is sufficient for the modulation of glucocorticoid induction properties by homologous receptors, coactivator transcription intermediary factor 2, and Ubc9. *Mol Endocrinol* 19: 290-311.
62. Voss TC, John S & Hager GL (2006) Single-cell analysis of glucocorticoid receptor action reveals that stochastic post-chromatin association mechanisms regulate ligand-specific transcription. *Mol Endocrinol* 20: 2641-2655.
63. Cato AC, Skroch P, Weinmann J, Butkeraitis P & Ponta H (1988) DNA sequences outside the receptor-binding sites differently modulate the responsiveness of the mouse mammary tumour virus promoter to various steroid hormones. *EMBO J* 7: 1403-1410.
64. Adams M, Meijer OC, Wang J, Bhargava A & Pearce D (2003) Homodimerization of the glucocorticoid receptor is not essential for response element binding: Activation of the phenylethanolamine N-methyltransferase gene by dimerization-defective mutants. *Mol Endocrinol* 17: 2583-2592.

65. Szapary D, Song LN, He Y & Simons SS,Jr (2008) Differential modulation of glucocorticoid and progesterone receptor transactivation. *Mol Cell Endocrinol* 283: 114-126.
66. Dahlman-Wright K, Wright A, Gustafsson JA & Carlstedt-Duke J (1991) Interaction of the glucocorticoid receptor DNA-binding domain with DNA as a dimer is mediated by a short segment of five amino acids. *J Biol Chem* 266: 3107-3112.
67. Tanner TM, *et al* (2010) A 629RKLKK633 motif in the hinge region controls the androgen receptor at multiple levels. *Cell Mol Life Sci* 67: 1919-1927.
68. Drouin J, *et al* (1992) Homodimer formation is rate-limiting for high affinity DNA binding by glucocorticoid receptor. *Mol Endocrinol* 6: 1299-1309.
69. Visser K, Smith C & Louw A (2010) Interplay of the inflammatory and stress systems in a hepatic cell line: Interactions between glucocorticoid receptor agonists and interleukin-6. *Endocrinology* 151: 5279-5293.
70. Burkhart BA, Ivey ML & Archer TK (2009) Long-term low level glucocorticoid exposure induces persistent repression in chromatin. *Mol Cell Endocrinol* 298: 66-75.
71. Pfaffl MW (2001) A new mathematical model for relative quantification in real-time RT-PCR. *Nucleic Acids Res* 29: e45.
72. John S, *et al* (2009) Kinetic complexity of the global response to glucocorticoid receptor action. *Endocrinology* 150: 1766-1774.
73. Frijters R, *et al* (2010) Prednisolone-induced differential gene expression in mouse liver carrying wild type or a dimerization-defective glucocorticoid receptor. *BMC Genomics* 11: 359.
74. Rogatsky I, *et al* (2003) Target-specific utilization of transcriptional regulatory surfaces by the glucocorticoid receptor. *Proc Natl Acad Sci U S A* 100: 13845-13850.

Chapter 7

Discussion

Introduction

In this, the final Chapter, we aim to distil the relevance of our diverse findings into a succinct whole. The role of (7.1) dimerization as a method for generating functional diversity will be addressed followed by a (7.2) brief overview of our own results and their (7.3) implications at a molecular, cellular and physiological level (7.4). Finally, strategies for future studies will be presented.

7.1 Dimerization generates functional diversity

The interactions between proteins form part of nearly all biological processes. These protein-protein interactions may be stable or dynamic. The covalent dimerization of the two subunits which make up the anti-body molecule (1) and the interaction between the subunits of haemoglobin (2) are examples of highly stable protein-protein interactions. We will focus our attention on the dynamic interactions, specifically dimerization, which may be defined as the interaction between two related subunits (3, 4).

Dynamic dimerization, refers to the transitory, non-covalent, association of two identical or closely related proteins in response to a particular signal. More often than not dimerization results in an active complex whose formation initiates a signalling process, examples of which include cytokine receptors (5, 6), Bcl-2 proteins (7) and the NR family (8, 9). An obvious consequence of dimerization is the fact that it brings the two subunits into close proximity with one another. In the case of cytokine receptors, their dimerization allows the interaction of kinases, which are bound to each of the cytokine receptors (10). A further manner through which dimerization enhances signalling reaction rates is by the creation of favourable orientations. An example of which is the insulin receptor that despite relatively high concentrations in the cell membrane requires ligand induced dimerization in order to initiate signalling (11).

Many proteins, which are capable of homodimerization, are also capable of forming heterodimers with related proteins (12). The formation of heteromeric complexes allows for a further level of differential regulation as many heterodimers behave differently than the homodimers of their constitutive subunits (13). For example, while homodimerization of the Bax protein promotes apoptotic cell death following apoptotic stimulation, the disruption of Bax-Bax dimerization by the over expression of Bcl-2 has been shown to prevent apoptosis due to the formation of Bax-Bcl-2 heterodimers (14). Similar behaviour has been reported for the GR where over expression of the largely inactive (15) dominant negative GR β isoform results in significantly reduced transcription through the active GR α (16) brought about by heterodimerization between the two GR isoforms (17). Furthermore, an increase in the ratio of GR β /GR α expression has been linked to GC resistance in a number of diseases (18, 19).

Heterodimerization of the GR with MR or AR may result in heterodimer specific transactivation via HREs (13, 20), while GR heterodimerization with the MR leads to impaired transactivation via GREs (21).

Dynamic dimerization is especially prevalent in transcription factors where the formation of a dimer creates twice the number of potential protein-DNA interactions and has been shown to stabilize DNA binding (22). This is reflected in the greater binding affinity that GR dimers display for DNA as compared to GR monomers (23). The fact that GREs consist of two hexameric half-sites, which are each recognized by one GR DBD, is in itself suggestive of the role which dimerization plays in the recognition of and binding to DNA. Considering the 24-fold greater DNA binding affinity shown by the GR dimer than the GR monomer (24) we hypothesize that the 'cooperative' binding of GR to DNA is brought about not through the sequential binding of two GR monomers and their subsequent dimerization as suggested by Ong *et al.* (25) but rather through the sequential association of each GR subunit in the GR dimer. The advantage of closer proximity and favourable orientation elicited by GR dimerization may account for the increase in DNA binding affinity displayed by GR dimers.

The process of dimerization itself may be sufficient to activate a cell surface receptor related to the epidermal growth factor receptor (26, 27). Although primarily ligand activated, studies in this receptor have shown that dimerization induced by antibodies or resulting from naturally occurring mutations results in signalling independent of ligand (26, 27). Another influence of ligand independent dimerization involves its effect on ligand binding affinity and has been documented in SRs. FRET studies of a truncated ER α LBD mutant, which retains the ability to bind ligand, have demonstrated that the ER α LBD exists as a homodimer independently of ligand binding and that the K_d of dimerization of the truncated ER α LBD was 1nM in the absence of ligand and 0.33nM in the presence of 10^{-6} M estradiol (28). As the K_d implies ligand independent dimerization of the ER α LBD is dependent on its concentration, the higher its concentration the greater the level of ligand independent dimerization. An increase in ER concentration has also been linked to a shift from non-cooperative to positive cooperative ligand binding (29), which in turn has been shown to be dependent on the capacity of the ER to dimerize (29). Since positive cooperative ligand binding, which is defined by a Hill slope >1 , implies ligand binding to more than one binding site, these results strongly suggest that ligand independent dimerization at high concentrations of ER facilitates positive cooperative ligand binding. Evidence that ligand independent dimerization of the GR may facilitate cooperative ligand binding was presented by Cho *et al.* (30) who demonstrated that positive cooperative ligand binding to the GR at high but not at low concentrations of receptor, *in vitro* was dependent on GR dimerization.

Considering the ubiquity of dynamic dimerization as a tool for enhancing the functional diversity of proteins and SRs in particular, could it be that ligand independent dimerization of the GR at high concentrations is a mechanism employed physiologically to impart hypersensitivity to cells expressing high GR levels?

7.2 Overview of results

Following the extensive results Chapters 3, 4, 5 and 6 we feel it is advantageous to present an overview of our findings. The most prominent of which are summarized in Tables 7.1 and 7.2. The results discussed below refer to those presented in either of these Tables, unless otherwise indicated.

In Chapter 3 we defined the low, medium and high GR concentration ranges employed in subsequent assays. In so doing we have made it possible to directly compare the influence of these three receptor concentrations on various aspects of GR behaviour. As far as we have been able to ascertain, through exhaustive literature review, this is the first time that a systematic exploration of the influences of GR concentration has been conducted. Where possible we have duplicated our experiments with low and medium concentrations of the D-loop mutant, GR_{dim}, which has a reduced capacity to dimerize. In so doing we have been able to confirm the influence of GR dimerization in many of our assays. Furthermore, CpdA, a GR ligand shown to abrogate GR dimerization (Addendum B, (31)), has been used to further confirm effects due to GR dimerization.

7.2.1 Chapter 3: Ligand binding affinity increases and cooperative ligand binding occurs at medium and high GR_wt concentrations (Table.7.1)

Our saturation binding studies revealed that ligand binding to the GR_wt changed from non-cooperative at the low GR_wt concentration to positive cooperative at the medium and high GR concentrations as demonstrated by the significant increase in Hill slope at these GR levels. The low GR_{dim} concentration was similar to the low GR_wt concentration and displayed non-cooperative ligand binding. Revealingly the medium GR_{dim} concentration also displayed non-cooperative ligand binding, which is not statistically different from either the low GR_wt or low GR_{dim} concentrations, despite the fact that this concentration of GR_{dim} is statistically similar to the medium GR_wt concentration. The increase in ligand binding affinity reflected by positive cooperative ligand binding was mirrored by a significant decrease in the K_d at the medium and high GR_wt concentrations. Once again, at the same medium concentration of GR that resulted in an increase in ligand binding affinity through the GR_wt, the K_d of the medium GR_{dim} concentration remained statistically comparable to the low GR_wt concentration. These results demonstrate that an increase in GR concentration resulted in an increase

in cooperative ligand binding and ligand binding affinity as displayed at the medium and high GRwt concentrations. Furthermore, the behaviour of the GRdim at the medium receptor concentration confirmed the necessity of GR dimerization for the GR concentration induced cooperative ligand binding and increase in ligand binding affinity.

7.2.2 Chapter 4: Ligand independent dimerization occurs at GR concentrations that display positive cooperative ligand binding (Table.7.1)

In order for ligand binding affinity of the GRwt to be altered its conformation would have to change. Since the Hill slopes generated at the medium and high GRwt concentrations approach 2 it is suggestive of a shift from predominant ligand binding to the GR monomer at low GRwt concentrations to predominant ligand binding to the GRwt dimer at medium and high GRwt concentrations. Based on these findings as well as those of Cho *et al.* (30) we predicted that the conformational change required to alter ligand binding affinity was the increased level of ligand independent dimerization of the GR at heightened receptor concentrations.

To test this hypothesis we employed both a live cell as well as an *in vitro* assay as described in Chapter 4. The Co-IP assay was used to visualize the levels of dimerization between a Flag-GRwt and either GFP-GRwt or GFP-GRdim at the low, medium and high GR concentrations. When quantified relative to the maximal dimerization elicited by the administration of DEX at the low, medium or high GRwt concentrations within each of these receptor concentration populations a clear pattern emerged, namely, significantly increased levels of ligand independent dimerization at the medium and high GRwt concentrations. These GRwt levels display equal levels of dimerization independent of potent agonist stimulation. The administration of the dimerization abrogating, dissociative GC, CpdA, significantly decreased the level of ligand independent dimerization of both medium and high GRwt concentrations, without significantly altering the dimerization level of low GRwt or any of the GRdim concentrations (Fig.4.3B). Although the level of ligand independent GRdim dimerization also increases as the receptor level does, the results are not significantly different from the low GRwt population and may reflect the fact that binding between the GRwt and GRdim is being measured and not between the GRdim and GRdim, exclusively. One may conclude that the GRdim although not completely incapable of dimerization, certainly displays a reduced capacity to dimerize particularly at the low GRdim concentration, where even the administration of DEX did not significantly influence the level of dimerization (Fig.4.3B).

Table 7.1. **Summary of results from Chapters 3, 4 and 5.** The effects of GR concentration and the influence of dimerization have been compared in a number of assays. Grey shaded blocks represent results achieved using tagged GRwt or GRdim but who's concentration remains statistically comparable to the non-tagged receptors and falls within the designated concentration range, either low, medium or high. Statistical analysis was through ANOVA followed by Dunnett's post test against the lowest respective GRwt concentration (*P<0.05, **P<0.01, ***P<0.001).

Results Chapters	Figure	GRwt concentration			GRdim concentration			
		Low	Medium	High	Low	Medium	High	
Chapter 3: Cooperative ligand binding	• fmol GR per mg protein ^a 3.6B, 6.1B	335	763***	1420***	328	721***	-	
		-	949***	1462***	-	-	-	
	• Hill slope ^b 3.8B	1.08	1.57**	1.72***	1.00	0.88	-	
		-	0.78	1.44**	-	-	-	
	• K _d (nM) 3.8B	49.1	23.9*	16.8*	52.3	33.2	-	
		-	28.4	10.9*	-	-	-	
Chapter 4: Ligand independent dimerization	• Co-IP (% dimerization) 4.3B	43%	107%*	102%*	36%	60%	66%	
		37%	60%*	63%*	-	-	-	
	• FRET (% dimerization) 4.7	-	-	-	-	-	-	
		-	-	-	-	-	-	
	Ligand induced dimerization	• Co-IP (% dimerization) 4.3B	100%	100%	100%	37%*	80%	90%
			2.63	1.79***	1.36***	-	-	-
• FRET (fold induction) 4.8C	-	-	-	-	-	-		
Chapter 5: Nuclear localization and distribution	Nuclear import rate (t_{1/2} in min)	• Live cell (10 ⁻⁶ M DEX) 5.2B	-	7.5	3.9**	-	20.9***	7.5
		• Immunofluorescence (10 ⁻⁶ M DEX) 5.4D	3.2	3.2	-	5.1*	3.0	-
		• Immunofluorescence (10 ⁻⁹ M DEX) 5.11	18.8	9.4*	-	-	-	-
	Nuclear localization extent (% nuclear)	• Immunofluorescence (10 ⁻⁶ M DEX) 5.4C	94%	96%	-	76%**	77%*	-
		• % CV 5.5C	-	18%	18%	-	15%**	18%
	Nuclear export (t_{1/2} in hours)	• Live cell (10 ⁻⁹ M DEX) 5.8B	-	3.6	4.0	-	2.3*	2.7
		• Immunofluorescence (10 ⁻⁶ M DEX) 5.10B	13.3	21.4**	-	10.9	15.8	-
		-	-	-	-	-	-	

^aassuming 20% transfection efficiency

^bbold numbers indicate GR concentrations where cooperative ligand binding has been demonstrated

We next analysed the dimerization of low, medium and high concentrations of GRwt through a live cell FRET assay where the levels of ligand independent and dependent YFP-GR and CFP-GR association were visualized in real time. Mathematical modelling of our FRET results revealed a significant increase in ligand independent dimerization at the medium and high GR concentrations. When dimerization was induced by the addition of DEX, the fold induction of FRET was significantly lower at both of these GR levels when compared to the low GR concentration. The reduced capacity for ligand dependent dimerization of the medium and high GR concentrations is due to the high levels of ligand independent dimerization, which diminishes the fold induction of dimerization following DEX stimulation.

Our *in vitro* and live cell analysis of GR dimerization in Co-IP and FRET experiments, respectively, both strongly support our hypothesis that cooperative ligand binding at the medium and high GRwt concentrations is facilitated by ligand independent dimerization of the GR.

7.2.3 Chapter 5: Nuclear import, export and distribution are influenced by GR dimerization (Table.7.1)

Live cell nuclear import studies revealed that the $t_{1/2}$ of GFP-GR nuclear import decreased as receptor concentration increased. However, this trend occurred through both the GFP-GRwt and the GFP-GRdim, implying that cooperative ligand binding was not responsible. The rate of nuclear import was influenced by the ability to dimerize as the GFP-GRdim displayed significantly slower rates of nuclear import than the GFP-GRwt. Immunofluorescent analysis showed no difference in the import rate of low and medium GRwt concentrations at saturating DEX concentrations. Tellingly, there was a significant difference in the nuclear import rate of the low and medium GRwt concentrations at subsaturating DEX levels which may reflect the increased affinity and shift to cooperative ligand binding at this GRwt level. At saturating DEX levels the low GRdim condition had a significantly reduced import rate compared to the GRwt, which implies an effect of dimerization. The extent of nuclear import at saturating DEX concentrations as revealed by the immunofluorescent analysis was not affected by GR concentration. However, GR dimerization is clearly required in order to achieve complete nuclear localization. In support of this, GRwt showed similarly reduced levels of maximal nuclear localization following stimulation with dimerization abrogating CpdA (Fig.5.4C). We have speculated that the reduced nuclear import rates seen through the live cell nuclear import assay as opposed to the immunofluorescent assay was as a result of the fact that the immunofluorescent technique quantified what is in effect 60 percent nuclear localization. However, another possibility does exist, namely that the nuclear mobility of the GFP tagged receptor may be reduced due to its large protein tag.

The use of CpdA was instrumental in deciphering our nuclear distribution results. While GFP-GR concentration did not influence this parameter, the medium GRdim concentration displayed significantly more random distribution following DEX stimulation than the medium GFP-GRwt concentration. However, the high GFP-GRdim displayed non-random distribution similar to the GFP-GRwt. Induction with CpdA resulted in random nuclear distribution at all GFP-GR levels and through both constructs, suggesting that the ability to dimerize does in fact influence the pattern of nuclear distribution. We hypothesize that in this assay the high GFP-GRdim was capable of wild type behaviour due to the significant level of DEX induced dimerization it displayed in the Co-IP assay (Fig.4.3B).

The live cell nuclear export of GFP-GR following the washout of subsaturating DEX concentrations revealed no significant GR concentration dependent differences through either the GFP-GRwt or GFP-GRdim. However, there was a significant increase in export rate through the GFP-GRdim at both medium and high receptor levels when compared to the same concentrations of GFP-GRwt (Fig.5.8B). As the rate of nuclear import reflects both import as well as export, the decreased rate of nuclear import displayed by the GFP-GRdim may reflect the increased export rate. However, this observation must come with the disclaimer that subsaturating concentrations of ligand (export) are being compared with saturating concentrations of ligand (import). Finally, although the immunofluorescent study of nuclear export following the washout of saturating DEX concentrations displayed a trend towards decreased export rates through the GRdim they were not significant. There was, however, a significant decrease in the rate of nuclear export through the medium GRwt concentration, an effect which is not seen following the washout of saturating CpdA concentrations (Fig5.10B) and is therefore dimerization dependent. The tendency towards ligand independent dimerization at the medium GRwt concentration may facilitate nuclear retention because of ligand independent association of the GR dimer to DNA or tethering proteins in the nucleus.

Taken as a whole increased GR concentration resulted in reduced nuclear import times, most probably due to the laws of mass action, while dimerization is required for optimal nuclear import levels and rate. In addition, dimerization influences nuclear localization allowing for non-random association and thus suggests that GR dimerization is required for the majority of GR interactions with DNA. Nuclear export occurs faster through the GRdim and appears to be sensitive to cooperative ligand binding but only following the washout of saturating concentrations of ligand.

7.2.4 Chapter 6: Transactivation and transrepression of genes is influenced by positive cooperative ligand binding to the GR (Table.7.2)

Table 7.2. **Summary of results from Chapter 6.** Transactivation and transrepression results have been normalized to the respective low GRwt value in all conditions except the biocharacter shifts of CpdA, MPA and RU486 where the GRdim values have been normalized to the low GRdim value. Statistical analysis was through ANOVA followed by Dunnett's post test against the low GRwt concentration (*P<0.05, **P<0.01, ***P<0.001) except for the GRdim biocharacter shift results of CpdA, MPA and RU486 which have been compared using two tailed unpaired t tests of low against medium GRdim concentration ([†]P<0.05).

	Figure	GRwt concentration			GRdim concentration	
		Low	Medium	High	Low	Medium
Repression of NFκB promoter reporter						
Ligand independent fold induction ^a	6.3B	1	0.9	0.9	1.0	1.1
Potency (DEX)	6.5A	1	0.5	0.2*	1.3	2.5
Efficacy (DEX)	6.5B	1	1.2	1.9***	0.9	1.1
Biocharacter shift: CpdA	6.5C	1	0.7**	0.2***	1	0.4 [†]
Activation of 2 x GRE promoter reporter						
Ligand independent activation	6.12A	1	4.7*	22.2***	1.9	6.0***
Potency (DEX)	6.9A	1	417***	1250***	0.8	1.0
Efficacy (DEX)	6.13A	1	3.7	12.3***	5.2**	28.4***
Biocharacter shift: MPA	6.16A	1	1.5	1.8***	1	1.1
Biocharacter shift: RU486	6.16A	1	1.7	1.8*	1	1.1
Activation of 1 x GRE promoter reporter						
Ligand independent activation	6.12B	1	9.4***	-	0.4	4.2***
Efficacy (DEX)	6.15A	1	5.0***	-	None	None
Activation of endogenous GILZ						
Ligand independent activation	6.19A	1	1.4*	1.5*	0.8	0.9
Efficacy (DEX maximal induction)	6.19B	1	1.6*	2.3***	1.1	1.4
Efficacy (DEX fold induction)	6.19C	1	1.3	2.0*	1.2	1.3

^abold numbers indicate GR concentrations where cooperative ligand binding has been demonstrated

Neither GR concentration nor dimerization significantly influenced ligand independent transrepression of the NF κ B containing promoter reporter construct. However, the multiple GRE (2 x GRE) promoter reporter displayed ligand independent transcription, which is GR concentration dependent, increasing significantly as GR concentration did. As this behaviour was shown by both the GRwt as well as the GRdim, it suggests that cooperative ligand binding does not play a role. Ligand independent activation of the single GRE (1 x GRE) containing promoter reporter also displayed a significant GR concentration dependent increase.

Furthermore, there was a significant difference in the ligand independent transactivation shown by GRwt and GRdim, suggesting an influence of dimerization on ligand independent transactivation through this construct. Ligand independent transactivation of the endogenous GILZ gene displayed a significant increase at the medium and high GRwt concentrations, where cooperative ligand binding occurs, but not at similar concentrations of GRdim. Clearly the ligand independent transactivation of genes is sensitive to GR concentration. However, the effects of dimerization and cooperative ligand binding are more complex. While the multiple GRE containing construct did not discriminate between GRwt and GRdim, the single GRE favoured activation by GRwt and the endogenous GILZ gene was only sensitive to ligand independent transactivation at GR concentrations which displayed positive cooperative ligand binding.

Intriguingly, transrepression showed a significant decrease in potency as GRwt concentration increased, while the potency of the GRdim at low and medium concentrations remained statistically unchanged. Thus cooperative ligand binding influences the potency of transrepression. We hypothesize that the decrease in potency observed at GRwt concentrations favouring cooperative ligand binding suggests that transrepression of NF κ B favours activated GR monomer over the activated dimer. The increased tendency towards dimerization at the medium and high GRwt levels restrict GR monomer availability while the increased ligand binding affinity (Fig.3.8B) of preformed dimers results in greatly reduced numbers of activated monomers at subsaturating ligand concentrations. This in turn results in decreased potency due to decreased activated monomer concentrations. The potency of DEX transactivation via the multiple GRE containing promoter construct showed that there was a significant increase in potency at the medium and high GRwt concentrations, which displayed positive cooperative ligand binding. The potencies of both GRdim concentrations and the low GRwt concentration were, however, not significantly different. As the potency of the high GRwt concentration was 1250-fold greater than that of the low GRwt concentration, we can not simply ascribe this to the 3-fold increase in ligand binding affinity (Fig.3.8B). Positive cooperative ligand binding at this level of GRwt means that a 10-fold increase in ligand concentration shifts receptor occupancy from 10 percent to 90 percent and this may also be a contributing factor. As the potency change is ligand specific (Fig.6.9B), varying from 417-fold for DEX to 53-fold for F and 2.5-fold for RU486 at the medium GRwt concentration, we hypothesize

that a further ligand dependent conformational change to the receptor is required to explain the potency shift of DEX through the multiple GRE promoter reporter. However, other mechanisms such as the association of FKBP52 (32) or Ubc9 (30) with the GR may be involved in the higher than predicted shift in transactivation potency. Whether or not these are directly related to cooperative ligand binding, remains to be explored.

Efficacy of the NF κ B promoter containing construct was not influenced by dimerization, displaying similar levels of maximal repression through GRwt and GRdim at both the low and medium GR concentrations. It was, however, affected by GR concentration, rising significantly at the high GRwt concentration. We noted a high degree of promoter specific behaviour concerning efficacy through our various transactivation assays. The efficacy of DEX induction of the multiple GRE containing construct was affected by GR concentration and dimerization, displaying enhanced efficacy through the GRdim compared to the GRwt. We ascribe this to the 'hit and run' theory of transactivation where the weaker DNA binding of the GRdim results in more rounds of transcription initiation in the same time frame as the high affinity DNA bound GRwt. Recent results from Visser *et al.* (33) suggest another possible reason for this behaviour. They demonstrate significant DEX induced degradation of the GRwt over a 24 hour period, while incubation with CpdA resulted in a significant upregulation of GRwt levels. In unpublished data from our lab, a similar trend emerges, where incubation of the GRdim with DEX results in significant upregulation of GRdim levels. These results suggest that the loss of GR dimerization through the GRdim mutant or dimerization abrogating, CpdA, may protect the GR from degradation and even lead to its upregulation. If this were the case, it would help to explain the 5.2-fold and 7.7-fold higher efficacy we see through the GRdim at the low and medium GR concentrations, respectively. The maximal DEX induced efficacy of the single GRE containing construct and endogenous GILZ gene displayed similar behaviour in terms of GRwt response. As GRwt concentrations increased so too did their efficacy. However, they diverge in terms of their dimerization dependent behaviour. While the single GRE containing construct displayed no ligand dependent transactivation, there is a non-significant trend towards an increase in the DEX induced efficacy of the transactivation of the GILZ via the GRdim as receptor levels increase. As the levels of maximal efficacy of GILZ transactivation by DEX through the GRdim and GRwt were similar, it suggests that cooperative ligand binding does not play a role in this parameter. The fold induction of the GILZ gene seems to support this theory, displaying a similar level of efficacy through the medium GRwt concentration as through the medium GRdim concentration. However, it is important to note that this parameter is influenced by the high degree of ligand independent activation shown by the medium and high GRwt concentrations. The fact that the single GRE displayed significant receptor concentration dependent ligand independent transactivation through the GRdim but no ligand dependent transactivation is worthy of consideration. Could this imply that GRdim is capable of ligand independent dimerization and transactivation, but not of ligand dependent dimerization?

The biocharacter of CpdA, relative to DEX, in the transrepression assay displayed a shift from full agonist to weak agonist behaviour as both GRwt and GRdim concentrations increased. This was quantified as a significant reduction in the percentage repression relative to DEX. As this tendency was shown through both the GRwt and GRdim it is unlikely that cooperative ligand binding was responsible. Intriguingly, competitive ligand binding experiments demonstrated a significantly reduced ability of CpdA to displace [³H]-DEX at the medium and high GRwt levels (Fig.6.6D). However, although it is important to note that this result reflects CpdA's ability to displace [³H]-DEX and is therefore influenced by both the binding characteristics of DEX and its own binding capacity it is suggestive of a receptor concentration dependent influence on CpdA's ability to bind GR.

The biocharacter of MPA and RU486 induced transactivation of the multiple GRE containing construct displayed a shift towards enhanced agonist behaviour relative to that of DEX as GRwt concentrations increased. MPA shifted from partial to supra agonist, while RU486 shifted from weak to partial agonist behaviour. As the GRdim displayed no such shift for either ligand, we conclude that dimerization was necessary for the shift in biocharacter. Furthermore, although the medium GRwt concentration did not demonstrate a significant difference from that of the low GRwt concentration, there was a clear increase in agonist behaviour at this level which plateau at the high GRwt level for both ligands. This suggests that a shift towards cooperative ligand binding is responsible for the biocharacter changes of MPA and RU486.

7.3 Implications of positive cooperative ligand binding and enhanced ligand binding affinity at high GR concentrations

7.3.1 Molecular

The relevance of protein-protein interactions has been studied for years in G-protein coupled receptors. Models such as the two-state receptor activation model have been proposed to explain the behaviour of these receptors (34), which are activated by ligand binding but require binding of G-proteins in order to become productive. The association of G-proteins to G-protein coupled receptors results in a receptor with high ligand binding affinity while the uncoupled receptor has a low ligand binding affinity (35). This behaviour is similar to that which we have demonstrated at medium and high GR concentrations, where ligand independent dimerization of the GR results in increased ligand binding affinity and positive cooperative ligand binding (Fig.3.8B). Intriguingly, the ligand independent association of G-proteins to G-protein coupled receptors causes a degree of ligand independent signalling, termed constitutive activity (36, 37). This is very much in line with our own results that demonstrate a high degree of ligand independent transactivation at GR levels which are known to display ligand independent dimerization (Fig.6.19A, Fig.6.12A).

We propose a model based on the two-state receptor activation model (38) which accounts for the existence of cooperative ligand binding and explains the energetics involved in the two alternate pathways of GR activation (Fig.7.1).

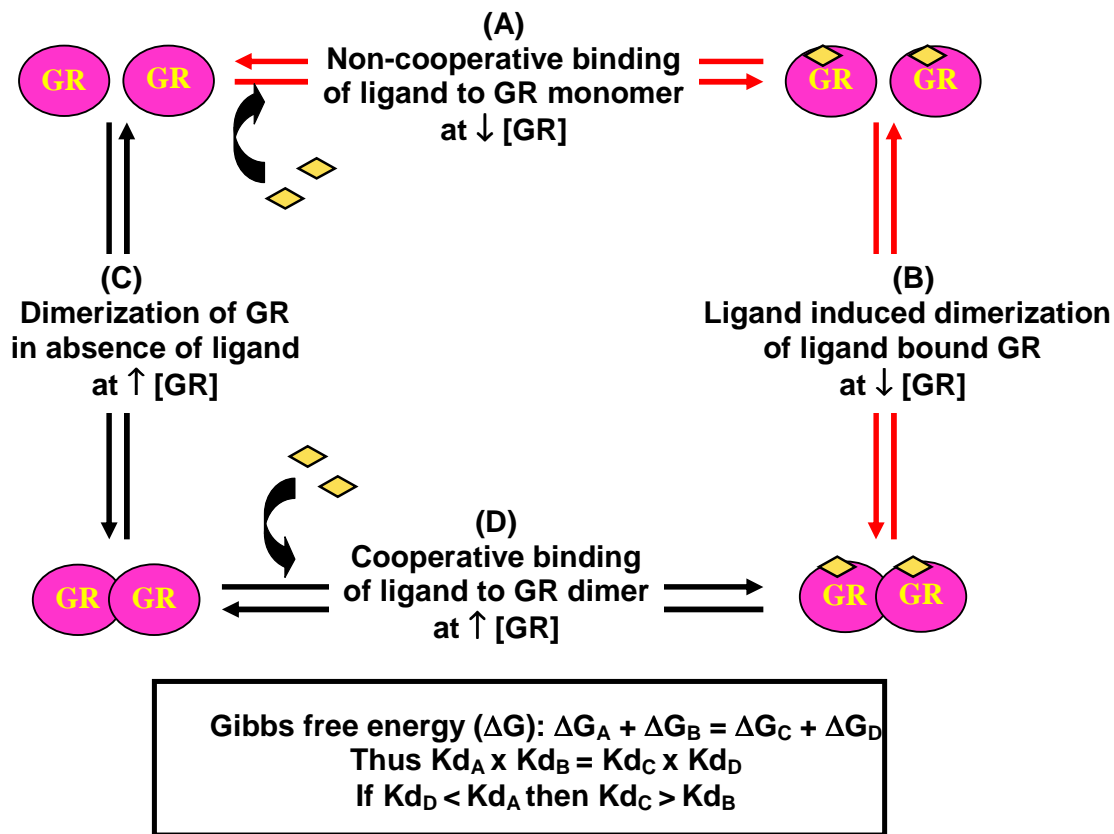


Figure 7.1 **Non-cooperative versus cooperative ligand binding model.** The red arrows denote non-cooperative ligand binding at low GR concentrations. (A) Non-cooperative ligand binding to GR monomers following by (B) ligand dependent dimerization. The black arrows denote cooperative ligand binding at high GR concentrations. (C) Ligand independent dimerization of the GR, followed by (D) cooperative ligand binding.

As hypothesized in Chapter 1, we propose that the formation of an activated ligand-bound GR dimer may occur in one of two ways (Fig.1.11A,B, Fig.7.1). Firstly, via the canonical process of non-cooperative ligand binding to the GR monomer followed by dimerization of two activated GR monomers (Fig.7.1. (A) and (B)). Secondly, by positive cooperative binding of two ligands to the two binding sites of the ligand independently dimerized GR (Fig.7.1. (C) and (D)). As demonstrated by the GR concentration dependent increase in ligand independent GR dimerization (Fig.4.3B, Fig.4.7), the GR exists in equilibrium between monomeric and dimeric form where increasing the GR concentration results in an increase in ligand independent dimerization. As the GR may exist as either a monomer or a dimer and is capable of binding ligand through both conformations, this implies that both pathways of activated GR dimer creation may occur concurrently. As these two pathways share the same substrate (unbound GR and ligand) and convert them to the same product (ligand bound GR dimers) they must share the same total Gibbs free energy (Fig.7.1).

Therefore the Gibbs free energy of reactions A plus B must equal that of reactions C plus D. If one pathway required less energy for the conversion of substrate to product that pathway would come to dominate the entire reaction process. Another way of comparing the energetics of the two reaction pathways is through the K_d , the product of each pathway's constituent reaction's K_d s must be equal in order for the Gibbs free energy requirement of both pathways to remain the same (Fig.7.1). Our results have shown that the K_d of reaction D, namely ligand binding to the preformed GR dimer, is lower than that of ligand binding to the GR monomer, represented by reaction A (Fig.7.1). Thus, in order for the Gibbs free energy to remain equal between the two pathways the K_d of reaction C must be higher than that of reaction B (Fig.7.1). Ligand independent GR dimerization is therefore less energetically favourable than ligand dependent dimerization and will only occur at high concentrations of substrate i.e. GR. Another way of viewing this paradigm is as a means to prime the GR for ligand binding. The fact that the GR dimer is preformed, allows for a protein-protein interaction, which not only forms two ligand binding sites which facilitate cooperative ligand binding, but also increases the GR's affinity for ligand.

7.3.2 Cellular

In a recent review article by Simons (39), he comments on the fact that maximal response (efficacy) of transcription through either transactivation or transrepression can not be correlated with EC_{50} (potency). This is a telling observation as many studies on the response to GCs only look at one subsaturating concentration of ligand (40-42) and do not explore the potency through dose response assays. The growing number of factors, which have been shown to influence the potency of the GC response, including GR concentration (43), highlight the importance of analysing both potency and efficacy.

Having established the molecular consequences of an increase in GR concentration, namely, ligand independent dimerization, which facilitates cooperative ligand binding and an increase in ligand binding affinity, we looked at the effects of these on the mechanism of GR action at a cellular level. While an increase in GR concentration in the live cell import assay resulted in faster import of the GR, this was unrelated to cooperative ligand binding as a similar trend was observed with GRdim (Fig.5.2B). Tellingly, while no GR concentration dependent difference in the rate of GR import was detected at saturating ligand concentrations in the immunofluorescent import assay, a 3-fold difference was detected between low and medium GR concentrations at subsaturating ligand concentrations (Fig.5.3). Thus, the influence of the increased affinity for ligand of the medium GR concentration could only be observed at subsaturating ligand concentrations. The capacity to dimerize increased the rate of nuclear import (Fig.5.2B, Fig5.4D) and its extent in a population of cells (Fig.5.4C), facilitated non-random nuclear distribution (Fig.5.5C), and prolonged nuclear export following the washout of a subsaturating ligand concentration (Fig.5.8B).

Furthermore, the increased ligand binding affinity and capacity for ligand independent dimerization of the medium GR concentration most probably contributed to its significantly prolonged nuclear export, following the washout of a saturating DEX concentration (Fig.5.10B). Thus it appears as if GR concentration and the ability to dimerize, but not cooperative ligand binding to the GR, affects nuclear import, export and distribution.

However, cooperative ligand binding can be directly correlated with a large and significant increase in the potency of DEX transactivation of the multiple GRE containing promoter construct (Fig.6.9A). Furthermore, our results suggest that cooperative ligand binding decreased the potency of transrepression through a promoter reporter construct containing 3 x NF κ B promoter elements (Fig.6.5A). While both the single and multiple GRE containing promoter constructs displayed ligand independent transactivation, which increased as GR concentration did, only the ligand independent transactivation of the endogenous GILZ gene can be ascribed specifically to ligand independent dimerization of the GR at medium and high concentrations and thus cooperative ligand binding.

In general, the efficacy of transcription increased as GR concentration does. This is an observation which has been documented for most transcription factors (44-46) and was also seen in the present study. There was, however, considerable promoter construct specific variation in response to GR dimerization in our study. While efficacy through the multiple GRE containing construct is decreased by GR dimerization (Fig.6.13A), the single GRE containing construct displayed no ligand dependent induction through the GRdim (Fig6.15A), and only the endogenous GILZ gene showed a significant correlation between cooperative ligand binding and an increase in DEX induced efficacy when maximal induction is considered (Fig.6.19B).

The biocharacter of the dissociative GC, CpdA, shifts from a full agonist to a weak agonist in transrepression of a NF κ B containing promoter construct as GR concentration increases (Fig6.5C). This behaviour is not influenced by GR dimerization. On the other hand, cooperative ligand binding influences the biocharacter shift from partial to full agonist behaviour of MPA (Fig.6.16A), as well as the shift from weak to partial agonist behaviour of RU486 (Fig.6.16A) in transactivation of a multiple GRE containing promoter reporter construct.

It is clear that GR concentration and the ability to dimerize have far ranging effects on GC response. This study has attempted to tease apart the cause of these influences and find that cooperative ligand binding and an increased ligand binding affinity, although not particularly influential at saturating ligand concentrations, are especially prominent at subsaturating ligand concentrations. This one may expect considering the enhanced sensitivity to ligand binding that ligand independent dimerization facilitates at high GR concentrations. The medium and high GR levels, which display cooperative ligand binding, result in considerable and significant ligand

independent GILZ induction. The constitutive activity which ligand independent dimerization elicits from this endogenous gene is telling as it implies constant low levels of GR activation in cells exposed to no GC at all. Finally, the high levels of GR concentration dependent, but ligand independent, transcription of the GRE containing promoter constructs serves as a reminder that the highly processed data presented for these assays in many articles may actually result in promising findings being over looked.

7.3.3 Physiological

Although we have not conducted any physiological studies, it is informative to address the ramifications of our cellular observations particularly in light of the observed trends towards GC hypersensitivity at high physiological GR levels (47),(48),(49) and GR resistance at low physiological GR levels (50),(51). Our results stress the numerous influences which GR concentration has on the response to GCs and offer an insight into how increased GR concentrations may result in greater response (efficacy) and sensitivity (potency) to GCs.

An interesting observation from our study is the decrease in the potency of DEX through the NFκB containing promoter construct as GR concentrations increase to levels that display cooperative ligand binding, as apposed to the greatly increased potency of DEX through the multiple GRE containing promoter reporter construct under the same conditions. This would imply a reduced capacity for the anti-inflammatory response and a greater likelihood of side effects in tissues expressing high GR concentrations and exposed to subsaturating concentrations of GCs. It may be that patients who experience greater GC induced side effects also express higher levels of GR in the affected tissues.

Tissues which express GR concentrations within or above the range of our medium GR concentration may furthermore display faster nuclear import of the GR at lower concentrations of GC as well as prolonged nuclear retention following GC withdrawal or no withdrawal at all, considering the ultradian secretion of endogenous GCs. These tissues may have an increased potency for transactivation and a reduced potency for transrepression. In addition, they may display ligand independent activation of GRE containing promoters by the preformed GR dimer. This hypersensitivity to GCs due to ligand independent dimerization of the GR at high GR concentrations may be an important factor in determining the interindividual, tissue-specific and healthy versus diseased state, differences in GC response.

The majority of human tissue biopsies (Table 1.1 and 1.2) display GR concentrations below that of the medium GR concentration of 763 fmol GR/mg protein or 298000 GR/cell tested in this study. They therefore fall outside the range of GR concentration for which positive cooperative ligand

binding has been demonstrated and would retain the capacity to respond to variations in the concentration of endogenous or pharmacologically administered GCs. Only a few healthy tissues, such as skin, and some diseased tissue, like lung cancer tissue and Kaposi's sarcoma in AIDS patients, would be constantly signalling due to their high GR concentrations at physiological GC concentrations.

7.4 Future research

As the association of GCs to GR is the first step in the GR mediated response to GCs (Fig.1.6), the influences of increased ligand binding affinity and cooperative ligand binding are potentially myriad. Having shown that GR concentration and the ability to dimerize directly influences ligand independent dimerization, ligand binding affinity, nuclear import, distribution and localization as well as transrepression and transactivation through GC responsive promoters, we are spoilt for choice in terms of future studies. We have mentioned a number of potential follow up studies within the results chapters and offer the most promising here.

7.4.1 GR dimerization

The construction of a Flag-GRdim or a CFP-GRdim/YFP-GRdim pair would allow us to definitively elucidate the dimerization capacity of the D-loop dimerization impaired GRdim mutant in Co-IP or FRET studies, respectively.

Furthermore, it would be of great interest to us to place the GRdim gene in the same vector as the GRwt in order to test the behaviour of the GRdim at similar levels to that of the high GRwt. As yet we can not predict whether the difference we see in maximal induction of the endogenous GILZ gene between the medium concentration of GRwt and GRdim is due to positive cooperative ligand binding or as a result of the enhanced ligand independent transactivation displayed by the GRwt. The behaviour of the high GRdim concentration would be an acid test as to whether positive cooperative ligand binding is influential in this system.

The ability to induce dimerization of the GR has a prominent affect on the actions of CpdA and DEX, especially on their capacity to induce transactivation. Could the ability to induce GR dimerization be used as a determinant for transactivative function? By testing the ability to induce dimerization of a variety of GCs through either FRET or Co-IP assays and their ability to induce transactivation, we would be able to correlate these parameters.

Our hypothesis for enhanced efficacy of the multiple GRE containing construct through the GRdim rests on its decreased affinity for GREs. This theory could be tested by analysing the DNA

occupancy of the GRdim compared to that of the GRwt using DEX and CpdA stimulation, using the CHIP assay. Furthermore, ligand independent DNA association at high GRwt levels would confirm the capacity for ligand independent GR behaviour.

Vanderbilt *et. al.* (52) established that GR is the primary regulatory factor of GC response by demonstrating a directly proportional relationship between GR concentration and the RNA expression of GRE containing genes following DEX induction. However, recent research has highlighted the importance of GRE structure in GC response (53) Evaluation of a range of GRE's, that differ at times only by one nucleotide, has indicated that their GC responses vary considerably, that GRwt and GRdim have unique transactivation profiles and that GR binding affinity to the GREs does not correspond to the degree of transcription facilitated (53). It would be of interest to examine the influence that GR concentration, the capacity to dimerize as well as ligand independent dimerization have on the ligand dependent as well as ligand independent transactivation of a variety of GREs.

7.4.2 Cooperative ligand binding and increased ligand binding affinity

The comodulators, FKBP51 and FKBP52, are known to influence the localization of the GR (32, 54) as well as its ligand binding affinity (32). FKBP52 association with the GR, via Hsp90, increases the ligand binding affinity of GR as well as stimulating its nuclear import (32), while FKBP51 has the opposite affect on GR action (55-57). It would be of interest to determine whether these comodulators bind preferentially to the GRwt and GRdim through Co-IP assays. Investigating the influence of CpdA or DEX stimulation on the association of either FKBP51 or FKBP52 to the GR would also be advantageous.

The potent synthetic agonist, DEX, and the potent endogenous agonist, F, display greater increases in potency through the multiple GRE containing promoter at the medium GR level than the partial agonists, MPA and RU486. To clarify this issue it would be of interest to test whether all of these test compounds bind to the medium and high GR concentrations in a positive cooperative fashion.

7.4.3 CpdA

Co-incubation of [3H]-estradiol with the antagonist clomiphene abrogates the positive cooperative ligand binding displayed by the ER (58). Considering CpdA's capacity to abrogate dimerization, it would be interesting to show whether it could prevent cooperative ligand binding of the GR, especially in light of its reduced capacity to displace DEX from the GR at high concentrations.

The fact that we have displayed CpdA's ability to abrogate ligand independent dimerization at the medium and high GR concentrations to levels seen at the low GR concentration (Fig.4.3B) is a difficult point to resolve considering the reduced capacity to induce transrepression and displace [³H]-DEX in competitive binding assays. Future competitive binding studies of CpdA's ability to displace [³H]-DEX at the low and medium concentration of GRdim may help us to unravel this conundrum. Furthermore, we could confirm CpdA's ability to compete with DEX for binding through the dimerization elicited by co-incubation of CpdA and DEX in the FRET or Co-IP assays.

7.5 Bibliography

1. Levy Y, Cho SS, Onuchic JN & Wolynes PG (2005) A survey of flexible protein binding mechanisms and their transition states using native topology based energy landscapes. *J Mol Biol* 346: 1121-1145.
2. Kavanaugh JS, Rogers PH & Arnone A (2005) Crystallographic evidence for a new ensemble of ligand-induced allosteric transitions in hemoglobin: The T-to-T(high) quaternary transitions. *Biochemistry* 44: 6101-6121.
3. Klemm JD, Schreiber SL & Crabtree GR (1998) Dimerization as a regulatory mechanism in signal transduction. *Annu Rev Immunol* 16: 569-592.
4. Jones S & Thornton JM (1995) Protein-protein interactions: A review of protein dimer structures. *Prog Biophys Mol Biol* 63: 31-65.
5. Taga T & Kishimoto T (1995) Signaling mechanisms through cytokine receptors that share signal transducing receptor components. *Curr Opin Immunol* 7: 17-23.
6. Horvath CM, Stark GR, Kerr IM & Darnell JE, Jr (1996) Interactions between STAT and non-STAT proteins in the interferon-stimulated gene factor 3 transcription complex. *Mol Cell Biol* 16: 6957-6964.
7. Kim J, Johnson K, Chen HJ, Carroll S & Laughon A (1997) Drosophila mad binds to DNA and directly mediates activation of vestigial by decapentaplegic. *Nature* 388: 304-308.
8. Mangelsdorf DJ & Evans RM (1995) The RXR heterodimers and orphan receptors. *Cell* 83: 841-850.
9. Savory JG, *et al* (2001) Glucocorticoid receptor homodimers and glucocorticoid-mineralocorticoid receptor heterodimers form in the cytoplasm through alternative dimerization interfaces. *Mol Cell Biol* 21: 781-793.
10. Heldin CH (1995) Dimerization of cell surface receptors in signal transduction. *Cell* 80: 213-223.
11. Smith BJ, *et al* (2010) Structural resolution of a tandem hormone-binding element in the insulin receptor and its implications for design of peptide agonists. *Proc Natl Acad Sci U S A* 107: 6771-6776.
12. Jones N (1990) Transcriptional regulation by dimerization: Two sides to an incestuous relationship. *Cell* 61: 9-11.

13. Nishi M, Tanaka M, Matsuda K, Sunaguchi M & Kawata M (2004) Visualization of glucocorticoid receptor and mineralocorticoid receptor interactions in living cells with GFP-based fluorescence resonance energy transfer. *J Neurosci* 24: 4918-4927.
14. Sato T, *et al* (1994) Interactions among members of the bcl-2 protein family analyzed with a yeast two-hybrid system. *Proc Natl Acad Sci U S A* 91: 9238-9242.
15. Oakley RH, Webster JC, Sar M, Parker CR, Jr & Cidlowski JA (1997) Expression and subcellular distribution of the beta-isoform of the human glucocorticoid receptor. *Endocrinology* 138: 5028-5038.
16. Gougat C, *et al* (2002) Overexpression of the human glucocorticoid receptor alpha and beta isoforms inhibits AP-1 and NF-kappaB activities hormone independently. *J Mol Med* 80: 309-318.
17. Oakley RH, Jewell CM, Yudit MR, Bofetiado DM & Cidlowski JA (1999) The dominant negative activity of the human glucocorticoid receptor beta isoform. specificity and mechanisms of action. *J Biol Chem* 274: 27857-27866.
18. Hamid QA, *et al* (1999) Increased glucocorticoid receptor beta in airway cells of glucocorticoid-insensitive asthma. *Am J Respir Crit Care Med* 159: 1600-1604.
19. Sousa AR, Lane SJ, Cidlowski JA, Staynov DZ & Lee TH (2000) Glucocorticoid resistance in asthma is associated with elevated in vivo expression of the glucocorticoid receptor beta-isoform. *J Allergy Clin Immunol* 105: 943-950.
20. Chen S, Wang J, Yu G, Liu W & Pearce D (1997) Androgen and glucocorticoid receptor heterodimer formation. A possible mechanism for mutual inhibition of transcriptional activity. *J Biol Chem* 272: 14087-14092.
21. Liu W, Wang J, Sauter NK & Pearce D (1995) Steroid receptor heterodimerization demonstrated in vitro and in vivo. *Proc Natl Acad Sci U S A* 92: 12480-12484.
22. Renaud JP, *et al* (1995) Crystal structure of the RAR-gamma ligand-binding domain bound to all-trans retinoic acid. *Nature* 378: 681-689.
23. Drouin J, *et al* (1992) Homodimer formation is rate-limiting for high affinity DNA binding by glucocorticoid receptor. *Mol Endocrinol* 6: 1299-1309.
24. Segard-Maurel I, *et al* (1996) Glucocorticosteroid receptor dimerization investigated by analysis of receptor binding to glucocorticosteroid responsive elements using a monomer-dimer equilibrium model. *Biochemistry* 35: 1634-1642.
25. Ong KM, Blackford JA, Jr, Kagan BL, Simons SS, Jr & Chow CC (2010) A theoretical framework for gene induction and experimental comparisons. *Proc Natl Acad Sci U S A* 107: 7107-7112.
26. Schlessinger J (1988) Signal transduction by allosteric receptor oligomerization. *Trends Biochem Sci* 13: 443-447.
27. Weiner DB, Liu J, Cohen JA, Williams WV & Greene MI (1989) A point mutation in the neu oncogene mimics ligand induction of receptor aggregation. *Nature* 339: 230-231.
28. Tamrazi A, Carlson KE, Daniels JR, Hurth KM & Katzenellenbogen JA (2002) Estrogen receptor dimerization: Ligand binding regulates dimer affinity and dimer dissociation rate. *Mol Endocrinol* 16: 2706-2719.

29. Notides AC, Lerner N & Hamilton DE (1981) Positive cooperativity of the estrogen receptor. *Proc Natl Acad Sci U S A* 78: 4926-4930.
30. Cho S, Kagan BL, Blackford JA, Jr, Szapary D & Simons SS, Jr (2005) Glucocorticoid receptor ligand binding domain is sufficient for the modulation of glucocorticoid induction properties by homologous receptors, coactivator transcription intermediary factor 2, and Ubc9. *Mol Endocrinol* 19: 290-311.
31. Robertson S, *et al* (2010) Abrogation of glucocorticoid receptor dimerization correlates with dissociated glucocorticoid behavior of compound a. *J Biol Chem* 285: 8061-8075.
32. Davies TH, Ning YM & Sanchez ER (2005) Differential control of glucocorticoid receptor hormone-binding function by tetratricopeptide repeat (TPR) proteins and the immunosuppressive ligand FK506. *Biochemistry* 44: 2030-2038.
33. Visser K, Smith C & Louw A (2010) Interplay of the inflammatory and stress systems in a hepatic cell line: Interactions between glucocorticoid receptor agonists and interleukin-6. *Endocrinology* 151: 5279-5293.
34. Franco R, *et al* (2006) The two-state dimer receptor model: A general model for receptor dimers. *Mol Pharmacol* 69: 1905-1912.
35. Wong HM, Sole MJ & Wells JW (1986) Assessment of mechanistic proposals for the binding of agonists to cardiac muscarinic receptors. *Biochemistry* 25: 6995-7008.
36. Ann Janovick J & Michael Conn P (2010) Use of pharmacoperones to reveal GPCR structural changes associated with constitutive activation and trafficking. *Methods Enzymol* 485: 277-292.
37. Stoddart LA & Milligan G (2010) Constitutive activity of GPR40/FFA1 intrinsic or assay dependent?. *Methods Enzymol* 484: 569-590.
38. Leff P (1995) The two-state model of receptor activation. *Trends Pharmacol Sci* 16: 89-97.
39. Simons SS, Jr (2008) What goes on behind closed doors: Physiological versus pharmacological steroid hormone actions. *Bioessays* 30: 744-756.
40. Webster JC, Oakley RH, Jewell CM & Cidlowski JA (2001) Proinflammatory cytokines regulate human glucocorticoid receptor gene expression and lead to the accumulation of the dominant negative beta isoform: A mechanism for the generation of glucocorticoid resistance. *Proc Natl Acad Sci U S A* 98: 6865-6870.
41. Reik A, Schutz G & Stewart AF (1991) Glucocorticoids are required for establishment and maintenance of an alteration in chromatin structure: Induction leads to a reversible disruption of nucleosomes over an enhancer. *EMBO J* 10: 2569-2576.
42. Liden J, Delaunay F, Rafter I, Gustafsson J & Okret S (1997) A new function for the C-terminal zinc finger of the glucocorticoid receptor. repression of RelA transactivation. *J Biol Chem* 272: 21467-21472.
43. Chen S, Sarlis NJ & Simons SS, Jr (2000) Evidence for a common step in three different processes for modulating the kinetic properties of glucocorticoid receptor-induced gene transcription. *J Biol Chem* 275: 30106-30117.
44. Jenster G, *et al* (1997) Steroid receptor induction of gene transcription: A two-step model. *Proc Natl Acad Sci U S A* 94: 7879-7884.

45. Spencer TE, *et al* (1997) Steroid receptor coactivator-1 is a histone acetyltransferase. *Nature* 389: 194-198.
46. Heitzer MD, Wolf IM, Sanchez ER, Witchel SF & DeFranco DB (2007) Glucocorticoid receptor physiology. *Rev Endocr Metab Disord* 8: 321-330.
47. Reichardt HM, Umland T, Bauer A, Kretz O & Schutz G (2000) Mice with an increased glucocorticoid receptor gene dosage show enhanced resistance to stress and endotoxic shock. *Mol Cell Biol* 20: 9009-9017.
48. Ho AD, Stojakowits S, Pralle H, Dorner M & Hunstein W (1983) Glucocorticoid receptor level, terminal deoxynucleotidyl transferase activity and initial responsiveness to prednisone and vincristine in leukemia. *Klin Wochenschr* 61: 455-459.
49. Lu YS, *et al* (2006) Glucocorticoid receptor expression in advanced non-small cell lung cancer: Clinicopathological correlation and in vitro effect of glucocorticoid on cell growth and chemosensitivity. *Lung Cancer* 53: 303-310.
50. Reul JM, *et al* (1994) Prenatal immune challenge alters the hypothalamic-pituitary-adrenocortical axis in adult rats. *J Clin Invest* 93: 2600-2607.
51. Costlow ME, Pui CH & Dahl GV (1982) Glucocorticoid receptors in childhood acute lymphocytic leukemia. *Cancer Res* 42: 4801-4806.
52. Vanderbilt JN, Miesfeld R, Maler BA & Yamamoto KR (1987) Intracellular receptor concentration limits glucocorticoid-dependent enhancer activity. *Mol Endocrinol* 1: 68-74.
53. Meijsing SH, *et al* (2009) DNA binding site sequence directs glucocorticoid receptor structure and activity. *Science* 324: 407-410.
54. Davies TH, Ning YM & Sanchez ER (2002) A new first step in activation of steroid receptors: Hormone-induced switching of FKBP51 and FKBP52 immunophilins. *J Biol Chem* 277: 4597-4600.
55. Reynolds PD, Ruan Y, Smith DF & Scammell JG (1999) Glucocorticoid resistance in the squirrel monkey is associated with overexpression of the immunophilin FKBP51. *J Clin Endocrinol Metab* 84: 663-669.
56. Denny WB, Valentine DL, Reynolds PD, Smith DF & Scammell JG (2000) Squirrel monkey immunophilin FKBP51 is a potent inhibitor of glucocorticoid receptor binding. *Endocrinology* 141: 4107-4113.
57. Cheung-Flynn J, Roberts PJ, Riggs DL & Smith DF (2003) C-terminal sequences outside the tetratricopeptide repeat domain of FKBP51 and FKBP52 cause differential binding to Hsp90. *J Biol Chem* 278: 17388-17394.
58. Sasson S & Notides AC (1982) The inhibition of the estrogen receptor's positive cooperative [³H]estradiol binding by the antagonist, clomiphene. *J Biol Chem* 257: 11540-11545.

Addendum A

**Abstracts from public speaking events
Presented by Steven Robertson**

A.1. S. Robertson, A. Louw and J. Haggood (2006), Does receptor concentration affect Glucocorticoid action? *AstraZeneca medical research day, Cape Town, South Africa*

The glucocorticoid receptor (GR) is a ligand-activated transcription factor that is a member of the nuclear receptor family and the target of anti-inflammatory drugs. Upon ligand-binding the GR translocates to the nucleus and the degree of GR nuclear localization is a critical factor in determining the level of GR function. In addition, several reports suggest that GR concentration may modulate the bioactivity of ligands. We propose that exploring the link between GR concentration and ligand-binding parameters, ligand bioactivity and nuclear translocation kinetics will lead to a greater understanding of ligand specificity and the role of GR concentration. COS-1 cells containing very little endogenous GR were transiently transfected with high, medium and low levels of Green Fluorescent Protein-GR (GFP-GR) and exposed to a battery of test compounds that include GR agonists, partial agonists, partial antagonists and a selective GR agonist (SEGRA). Whole cell saturation binding indicates cooperative binding at high GR concentrations (Hill slope > 1) and in accordance, a shift to higher affinity. These findings are mirrored by transactivation studies which demonstrate the impact of GR concentration on bioactivity. We show that increased GR concentration leads to a significant increase in ligand potency (EC₅₀) and efficacy (fold induction). In addition, the bio-character of some compounds change with increased GR concentration. MPA, for example, displays partial agonist activity at lower GR concentrations that shift to supra-agonist activity at high GR concentrations. Fluorescence microscopy reveals that nuclear import of the GR is influenced by the type of ligand, with full agonists displaying the highest rate of import. In addition, increased GR concentration increases the rate of nuclear import. By studying the behaviour of ligands at varying GR concentrations we have shed light on the mechanistic implications of GR-concentration for GR-mediated gene regulation. In addition, our findings may have physiological implications in glucocorticoid resistance or chronic stress.

A.2. S. Robertson, A. Louw and J. Haggood (2008), Does cooperative ligand binding affect glucocorticoid action?, *South African society for biochemistry and molecular biology (SASBMB)*, Grahamstown, South Africa

We examine the implications of cooperative ligand binding for GR-mediated gene regulation by exploring the link between glucocorticoid receptor (GR) concentration and ligand-binding parameters, ligand bio-activity and bio-character, and nuclear translocation kinetics.

COS-1 cells, without endogenous GR, transiently transfected with high, medium and low levels of GR were exposed to a battery of GR ligands. We demonstrate in saturation binding studies that cooperative ligand-binding (Hill slope > 1) with a concurrent significant increase in affinity occurs at high GR concentrations. At GR concentrations that result in cooperative ligand-binding we demonstrate a significant shift in transactivation potency (EC₅₀) and efficacy (fold induction) as measured with promoter reporter assays, a significant decrease in the half time for nuclear localization, as measured by live-cell fluorescent microscopy, and a significant shift in transactivation bio-character for some compounds, such as RU486.

Positive cooperativity has the potential to shift the GR response from a gradual increase in response to increased ligand concentration to a mechanism that resembles a molecular switch. These findings may have physiological implications in that differential gene expression could result in different levels of gene product with the same concentration of steroid.

Keywords: Glucocorticoid receptor, cooperative ligand binding, steroid ligands

A.3. S. Robertson, A. Louw and J. Hapgood (2009), Cooperative ligand binding affects glucocorticoid action, *Experimental biology group (EBG)*, Stellenbosch, South Africa

Won best student speaker of 2009 for this presentation.

It has recently been shown that cooperative ligand-binding to the glucocorticoid receptor (GR) occurs at high, but not low GR concentrations and that increased GR concentrations cause a bio-character switch in ligands in both transrepression and transactivation systems. No investigation has, however, specifically examined the implications of cooperative ligand binding for GR-mediated gene regulation. We have explored the link between GR concentration and ligand-binding parameters, ligand bio-activity and bio-character, and nuclear translocation kinetics in an attempt to evaluate the implications of cooperative ligand binding.

COS-1 cells, containing very little endogenous GR, were transiently transfected with high, medium and low levels of Green Fluorescent Protein-GR (GFP-GR) and exposed to a battery of test compounds that include GR agonists, partial agonists, partial antagonists and a selective GR agonist (SEGRA). We demonstrate in whole cell saturation binding studies that cooperative ligand-binding (Hill slope > 1) with a concurrent significant ($P < 0.05$) increase in affinity occurs at high GR concentrations. Promoter reporter studies show a significant ($P < 0.05$) shift in transactivation potency (EC_{50}) and efficacy (fold induction) at GR concentrations that elicit cooperative ligand-binding. In addition, a significant ($P < 0.05$) shift in transactivation bio-character is demonstrated for some compounds, such as RU486, at GR concentrations that show cooperative ligand-binding. Finally, at GR concentrations that result in cooperative ligand-binding a significant ($P < 0.01$) decrease in the half time for nuclear localization, as measured by live-cell fluorescent microscopy, is observed.

Cooperative ligand-binding presupposes the presence of more than one binding site and as this is only observed at high GR concentrations we hypothesize that binding to GR dimers must be involved and present a model describing our theory. Positive cooperativity in ligand-binding and thus by implication increased levels of GR has the potential to shift the GR response from a gradual increase in response to increased ligand concentration to a mechanism that resembles a molecular switch. These findings may thus have physiological implications in that differential gene expression may result in different levels of gene product with the same concentration of steroid.

Addendum B

ABROGATION OF GLUCOCORTICOID RECEPTOR DIMERIZATION CORRELATES WITH DISSOCIATED GLUCOCORTICOID BEHAVIOUR OF COMPOUND A

Steven Robertson^{1*}, Fatima Allie-Reid^{1*}, Wim Vanden Berghe², Koch Visser¹, Anke Binder¹, Donita Africander¹, Michael Vismer¹, Karolien De Bosscher², Janet Hapgood³, Guy Haegeman² and Ann Louw¹

¹Department of Biochemistry, University of Stellenbosch, Matieland 7602, Stellenbosch, Rep. of South Africa

²Laboratory of Eukaryotic Gene Expression and Signal Transduction (LEGEST), Department of Physiology, Ghent University, K. L. Ledeganckstraat 35, B-9000 Gent, Belgium

³Department of Molecular and Cellular Biology, University of Cape Town, Private Bag X37701, Cape Town, Rep. of South Africa

Address correspondence to: Ann Louw, Department of Biochemistry, University of Stellenbosch, Matieland 7602, Stellenbosch, Rep. of South Africa. Telephone number +27-21-8085873, fax number +27-21-8085863 and email address: al@sun.ac.za

*Steven Robertson and Fatima Allie-Reid contributed equally to the experimentation.

This article has been published by the Journal of Biological Chemistry.

Steven Robertson contributed the following experimental results:

Fig.4C, Fig.5A,B, Fig.6A,B,D,E, Fig.7B, Fig.8A and Fig.S5
